

Investigation on Pavement ME Design Reflective Cracking, Faulting, IRI Prediction Models, Concrete Overlays Design Tool, and Performance Threshold Levels for Iowa Pavement Systems

**Final Report
April 2021**



IOWA STATE UNIVERSITY
Institute for Transportation

Sponsored by
Iowa Department of Transportation
(InTrans Project 18-666)

About the Program for Sustainable Pavement Engineering and Research

The overall goal of the Program for Sustainable Pavement Engineering and Research (PROSPER) is to advance research, education, and technology transfer in the area of sustainable highway and airport pavement infrastructure systems.

About the Institute for Transportation

The mission of the Institute for Transportation (InTrans) at Iowa State University is to save lives and improve economic vitality through discovery, research innovation, outreach, and the implementation of bold ideas.

Iowa State University Nondiscrimination Statement

Iowa State University does not discriminate on the basis of race, color, age, ethnicity, religion, national origin, pregnancy, sexual orientation, gender identity, genetic information, sex, marital status, disability, or status as a US veteran. Inquiries regarding nondiscrimination policies may be directed to the Office of Equal Opportunity, 3410 Beardshear Hall, 515 Morrill Road, Ames, Iowa 50011, telephone: 515-294-7612, hotline: 515-294-1222, email: eooffice@iastate.edu.

Disclaimer Notice

The contents of this report reflect the views of the authors, who are responsible for the facts and the accuracy of the information presented herein. The opinions, findings and conclusions expressed in this publication are those of the authors and not necessarily those of the sponsors.

The sponsors assume no liability for the contents or use of the information contained in this document. This report does not constitute a standard, specification, or regulation.

The sponsors do not endorse products or manufacturers. Trademarks or manufacturers' names appear in this report only because they are considered essential to the objective of the document.

Iowa DOT Statements

Federal and state laws prohibit employment and/or public accommodation discrimination on the basis of age, color, creed, disability, gender identity, national origin, pregnancy, race, religion, sex, sexual orientation or veteran's status. If you believe you have been discriminated against, please contact the Iowa Civil Rights Commission at 800-457-4416 or the Iowa Department of Transportation affirmative action officer. If you need accommodations because of a disability to access the Iowa Department of Transportation's services, contact the agency's affirmative action officer at 800-262-0003.

The preparation of this report was financed in part through funds provided by the Iowa Department of Transportation through its "Second Revised Agreement for the Management of Research Conducted by Iowa State University for the Iowa Department of Transportation" and its amendments.

The opinions, findings, and conclusions expressed in this publication are those of the authors and not necessarily those of the Iowa Department of Transportation.

Technical Report Documentation Page

1. Report No. InTrans Project 18-666	2. Government Accession No.	3. Recipient's Catalog No.	
4. Title and Subtitle Investigation on Pavement ME Design Reflective Cracking, Faulting, IRI Prediction Models, Concrete Overlays Design Tool, and Performance Threshold Levels for Iowa Pavement Systems		5. Report Date April 2021	
		6. Performing Organization Code	
7. Author(s) Leela Sai Praveen Gopiseti (orcid.org/0000-0002-1141-1425), Halil Ceylan (orcid.org/0000-0003-1133-0366), Sunghwan Kim (orcid.org/0000-0002-1239-2350), Bora Cetin (orcid.org/0000-0003-0415-7139), and Orhan Kaya (orcid.org/0000-0001-6072-3882)		8. Performing Organization Report No. InTrans Project 18-666	
9. Performing Organization Name and Address Institute for Transportation Iowa State University 2711 South Loop Drive, Suite 4700 Ames, IA 50010-8664		10. Work Unit No. (TRAIS)	
		11. Contract or Grant No.	
12. Sponsoring Organization Name and Address Iowa Department of Transportation 800 Lincoln Way Ames, IA 50010		13. Type of Report and Period Covered Final Report	
		14. Sponsoring Agency Code	
15. Supplementary Notes Visit https://intrans.iastate.edu/ for color pdfs of this and other research reports.			
16. Abstract <p>The Mechanistic-Empirical Pavement Design Guide (MEPDG) and its accompanying software AASHTOWare Pavement ME Design (PMED) represent major improvements over their predecessors, particularly in their comprehensive coverage of the impact of design inputs on pavement performance.</p> <p>Since PMED's release, numerous updates have been made to the software. Some of the most recent enhancements include the addition of Modern Era Retrospective Analysis for Research and Applications (MERRA) climate data (satellite-based data provided by NASA), a reflective cracking model for overlay performance prediction, and a tool to design bonded concrete overlays on asphalt (BCOA), renamed in PMED as short-jointed plain concrete pavement (SJPCP) over asphalt concrete (AC).</p> <p>A comprehensive evaluation of all the new PMED tools was performed and is presented in this study. The results demonstrate that these updates' significant impact on the distresses predicted by the software compared to predictions using previous versions warrants recalibration. Evaluation of PMED's nationally calibrated models was performed for flexible, rigid, and asphalt concrete over jointed plain concrete pavements for different representative geographical locations, ages, and traffic levels across Iowa. Locally calibrated models were developed for Iowa-specific conditions by determining an appropriate new set of calibration coefficients for use in the PMED software. During this process, multiple advanced optimization approaches were tested, and experiences and recommendations from the entire local calibration process are discussed. Additional analysis was performed to determine recommended layer thicknesses for varying reliability levels using the locally calibrated models.</p> <p>The overall findings from this study will serve as a useful reference and guide for implementing PMED for Iowa pavement design practices. Other states that plan to test and implement PMED for their state design practices will also benefit from this study's complete description of the set of local calibration steps required by PMED.</p>			
17. Key Words AASHTOWare Pavement ME Design—climate—concrete overlays—local calibration—pavement distresses—pavement performance—reflective cracking sensitivity analysis		18. Distribution Statement No restrictions.	
19. Security Classification (of this report) Unclassified.	20. Security Classification (of this page) Unclassified.	21. No. of Pages 233	22. Price NA

INVESTIGATION ON PAVEMENT ME DESIGN REFLECTIVE CRACKING, FAULTING, IRI PREDICTION MODELS, CONCRETE OVERLAYS DESIGN TOOL, AND PERFORMANCE THRESHOLD LEVELS FOR IOWA PAVEMENT SYSTEMS

**Final Report
April 2021**

Principal Investigator

Halil Ceylan, Director

Program for Sustainable Pavement Engineering and Research (PROSPER)
Institute for Transportation, Iowa State University

Co-Principal Investigators

Sunghwan Kim, Associate Director

Program for Sustainable Pavement Engineering and Research (PROSPER)
Institute for Transportation, Iowa State University

Bora Cetin, Associate Professor
Michigan State University

Research Assistant

Leela Sai Praveen Gopiseti

Authors

Leela Sai Praveen Gopiseti, Halil Ceylan, Sunghwan Kim, Bora Cetin, and Orhan Kaya

Sponsored by
Iowa Department of Transportation

Preparation of this report was financed in part
through funds provided by the Iowa Department of Transportation
through its Research Management Agreement with the
Institute for Transportation
(InTrans Project 18-666)

A report from
Institute for Transportation
Iowa State University
2711 South Loop Drive, Suite 4700
Ames, IA 50010-8664
Phone: 515-294-8103 / Fax: 515-294-0467
<https://intrans.iastate.edu/>

TABLE OF CONTENTS

ACKNOWLEDGMENTS	xiii
ACRONYMS, ABBREVIATIONS, AND NOMENCLATURE	xv
EXECUTIVE SUMMARY	xvii
PMED’s New Climate Data Sources	xvii
PMED’s New Reflective Cracking Model	xvii
PMED’s New Short-Jointed Plain-Concrete Pavement Over Asphalt Concrete Model	xviii
Local Calibration Performed for Iowa	xix
Survey Performed on PMED Design Criteria and Reliability	xix
INTRODUCTION	1
Background	1
Research Objectives	2
Report Organization	2
UPDATES AND CHANGES ACROSS VERSIONS OF THE PMED SOFTWARE (AUGUST 2015–AUGUST 2019)	4
Version 2.3.0 – Released on July 1, 2016	4
Version 2.5.0 – Released on July 1, 2018	4
Version 2.5.2 – Released on August 30, 2018	5
Version 2.5.3 – Released on October 16, 2018	5
Version 2.5.4 – Released on April 8, 2019	5
Version 2.5.5 – Released on July 1, 2019	5
EVALUATION OF NASA’S MERRA CLIMATE DATA FOR IOWA PAVEMENT SYSTEMS	6
Background	6
Objective	7
Climate Data Sources	8
Measurement Product Collocation	9
Results	9
Reason for Differences and Use of the Shortwave Radiation Regression Model	29
Summary of Key Findings	34
Recommendations	34
EVALUATION OF PMED’S NEW REFLECTIVE CRACKING MODEL	35
Background	35
Objective	37
PMED’s New Reflective Cracking Model—Overview and Literature Review	37
Methodology	38
Back-Calculation of Reflective Cracking Distress	40
Summary of OAT Sensitivity Analysis Approach	41
Results	44

Summary of Key Findings	53
Recommendations	54
LOCAL CALIBRATION FOR IOWA PAVEMENT SYSTEMS.....	55
Background.....	55
Enhancements in AASHTOWare Pavement ME Design	56
Methodology	57
Local Calibration Results.....	63
Summary of Key Findings	92
EVALUATION OF THE PAVEMENT ME DESIGN CONCRETE OVERLAY DESIGN TOOL.....	96
Background.....	96
Objective	97
Longitudinal Fatigue Cracking—Overview	97
PMED Climate Data – North American Regional Reanalysis (NARR).....	99
Methodology	99
Results.....	101
Summary of Key Findings	107
Recommendations.....	107
DATA-DRIVEN DETERMINATION OF OPTIMAL PAVEMENT THICKNESS BASED ON AASHTOWARE-PAVEMENT-ME-DESIGN-RECOMMENDED DISTRESS CRITERIA AND RELIABILITY LEVELS	108
Background.....	108
Survey Results	109
Summary of Practices – Distress Criteria and Reliability Levels in PMED.....	111
Thickness Determination Based on Achieved Reliability	117
Summary of Key Findings	127
CONCLUSIONS AND RECOMMENDATIONS	129
Conclusions.....	129
Recommendations.....	133
REFERENCES	135
APPENDIX A: MERRA-1 CLIMATE DATA INPUT CHARTS FOR ALL IOWA LOCATIONS	141
APPENDIX B: MERRA-2 CLIMATE DATA INPUT CHARTS FOR ALL IOWA LOCATIONS	157
APPENDIX C: IOWA DOT RECOMMENDED PMED DESIGN INPUTS AND MATERIAL PROPERTIES	173
New AC Pavement Sections	173
New JPCP Sections.....	174
AC over JPCP Sections.....	176
APPENDIX D: SUMMARY OF PMED TRANSFER FUNCTIONS FOR PAVEMENT	

PERFORMANCE PREDICTIONS	179
New AC and AC over JPCP	179
JPCP	184
APPENDIX E: VALIDATION OF LOCAL CALIBRATION RESULTS FOR INDEPENDENT PAVEMENT SECTIONS	187
Flexible/AC Sections	187
Rigid/JPCP Sections	189
AC over JPCP Sections.....	190
APPENDIX F: CALIBRATOR TOOL DEMO FOR LOCAL CALIBRATION	193
Steps Required	193
Advantages of Calibrator Tool.....	200
Limitations of Calibrator Tool.....	200
APPENDIX G: AASHTOWARE PAVEMENT ME DESIGN NATIONAL SURVEY – ADDITIONAL QUESTIONS	201
Threshold Levels and Design Reliabilities for AC over JPCP	201
Data Availability for Pavement Designs.....	203
Local Calibration Approach/Optimization Techniques	206
Additional Design Related Questions.....	208
APPENDIX H: PMED INPUTS FOR RELIABILITY AND THICKNESS DETERMINATION TASK	209
New AC Pavement Sections	209
AADTT Considerations	211
APPENDIX I. LIST OF PROJECT DATA FILES WITH DESCRIPTIONS	213

LIST OF FIGURES

Figure 1. Comparison of flexible/asphalt concrete predictions using GBWS vs. NARR weather data	11
Figure 2. Comparison of flexible/asphalt concrete predictions using GBWS vs. MERRA-1 weather data	12
Figure 3. Comparison of flexible/asphalt concrete predictions using GBWS vs. MERRA-2 weather data	13
Figure 4. Comparison of flexible/asphalt concrete predictions using NARR vs. MERRA-1 weather data	14
Figure 5. Comparison of flexible/asphalt concrete predictions using NARR vs. MERRA-2 weather data	15
Figure 6. Comparison of flexible/asphalt concrete predictions using MERRA-1 vs. MERRA-2 weather data	16
Figure 7. Comparison of rigid/JPCP predictions using GBWS vs. NARR weather data	17
Figure 8. Comparison of rigid/JPCP predictions using GBWS vs. MERRA-1 weather data	18
Figure 9. Comparison of rigid/JPCP predictions using GBWS vs. MERRA-2 weather data	19
Figure 10. Comparison of rigid/JPCP predictions using NARR vs. MERRA-1 weather data	20
Figure 11. Comparison of rigid/JPCP predictions using NARR vs. MERRA-2 weather data	21
Figure 12. Comparison of rigid/JPCP predictions using MERRA-1 vs. MERRA-2 weather data	22
Figure 13. Comparison of AC-over-JPCP predictions using GBWS vs. NARR weather data	23
Figure 14. Comparison of AC-over-JPCP predictions using GBWS vs. MERRA-1 weather data	24
Figure 15. Comparison of AC-over-JPCP predictions using GBWS vs. MERRA-2 weather data	25
Figure 16. Comparison of AC-over-JPCP predictions using NARR vs. MERRA-1 weather data	26
Figure 17. Comparison of AC-over-JPCP predictions using NARR vs. MERRA-2 weather data	27
Figure 18. Comparison of AC-over-JPCP predictions using MERRA-1 vs. MERRA-2 weather data	28
Figure 19. Diurnal variation in percent sunshine based on GBWS, MERRA-1, and MERRA-2 data	29
Figure 20. Comparison of flexible/asphalt concrete predictions for MERRA-1 vs. MERRA-2 using a back-calculated percent sunshine	31
Figure 21. Comparison of rigid/JPCP predictions for MERRA-1 vs. MERRA-2 using a back-calculated percent sunshine	32
Figure 22. Comparison of AC-over-JPCP predictions for MERRA-1 vs. MERRA-2 using a back-calculated percent sunshine	33
Figure 23. PMED output information for AC over JPCP (PMED v2.5.2 screenshot)	41
Figure 24. Overview of two scenarios for reflective cracking considered for sensitivity analysis	44
Figure 25. Comparisons between measured and predicted total rutting distress	65
Figure 26. Comparisons between measured and predicted top-down (longitudinal) cracking distress	66

Figure 27. Comparisons between measured and predicted bottom-up (alligator) cracking distress.....	67
Figure 28. Comparisons between measured and predicted thermal cracking distress.....	69
Figure 29. Comparisons between measured and predicted IRI distress	71
Figure 30. Comparisons between measured and predicted JPCP transverse cracking distress.....	74
Figure 31. Comparisons between measured and predicted mean joint faulting distress	75
Figure 32. Comparisons between measured and predicted IRI distress	77
Figure 33. Comparisons between measured and predicted total rutting distress.....	80
Figure 34. Comparisons between measured and predicted alligator cracking distress.....	82
Figure 35. Comparisons between measured and predicted longitudinal cracking distress.....	83
Figure 36. Comparisons between measured and predicted thermal cracking distress.....	85
Figure 37. Comparisons between measured and predicted reflective cracking distress for Assumption 1: Total transverse length criterion (SciPy optimization).....	86
Figure 38. Comparisons between measured and predicted reflective cracking distress for Assumption 2: Five-year service life criterion (SciPy optimization).....	87
Figure 39. Comparisons between measured and predicted IRI distress based on the total transverse joint length criterion.....	90
Figure 40. Comparisons between measured and predicted IRI distress based on the five-year service life criterion.....	91
Figure 41. PMED v2.5.5 screenshot of performance criteria for SJPCP over AC	98
Figure 42. Summary of the number of agencies using PMED default vs. agency-specific values.....	111
Figure 43. Summary of survey results for flexible pavement distresses: Agency-recommended design criteria and reliability levels.....	114
Figure 44. Summary of survey results for rigid pavement distresses: Agency-recommended design criteria and reliability levels	116
Figure 45. Reliability level versus AC thickness for flexible pavement distresses: (a) IRI, (b) AC layer rutting, (c) total rutting, (d) longitudinal (top-down) cracking, and (e) thermal/transverse cracking (Note that the various colors of solid lines represent various road classifications that in some cases showed exactly the same results and therefore stack on top of one another. Also, the orange line marks 92% reliability and the green line 50% reliability.)	120
Figure 46. Reliability level versus JPCP thickness for the rigid pavement distresses (a) IRI, (b) transverse cracking, and (c) mean joint faulting (Note that the various colors of solid lines represent various road classifications that in some cases showed exactly the same results and therefore stack on top of one another. Also, the orange line marks 92% reliability and the green line 50% reliability.)	122
Figure 47. Effect of joint spacing on reliability and thickness for PMED-predicted IRI (Note that the orange line marks 92% reliability and the green line 50% reliability.).....	124
Figure 48. Effect of joint spacing on reliability and thickness for PMED-predicted transverse cracking (Note that the orange line marks 92% reliability and the green line 50% reliability.).....	125

Figure 49. Effect of joint spacing on reliability and thickness for PMED-predicted mean joint faulting (Note that the solid lines represent various road classifications that in some cases showed exactly the same results and therefore stack on top of one another. Also, the orange line marks 92% reliability and the green line 50% reliability.).....126

Figure A.1. Climate Location ID: 146443 (Ames Municipal Airport).....	141
Figure A.2. Climate Location ID: 145295 (Iowa Regional Airport, Burlington).....	142
Figure A.3. Climate Location ID: 146446 (Eastern Iowa Airport, Cedar Rapids).....	143
Figure A.4. Climate Location ID: 145872 (Davenport Municipal Airport).....	144
Figure A.5. Climate Location ID: 145867 (Des Moines International Airport).....	145
Figure A.6. Climate Location ID: 147024 (Dubuque Regional Airport).....	146
Figure A.7. Climate Location ID: 148169 (Estherville Municipal Airport,.....)	147
Figure A.8. Climate Location ID: 145871 (Iowa City Municipal Airport).....	148
Figure A.9. Climate Location ID: 144715 (Lamoni Municipal Airport).....	149
Figure A.10. Climate Location ID: 146444 (Marshalltown Municipal Airport).....	150
Figure A.11. Climate Location ID: 147596 (Mason City Municipal Airport).....	151
Figure A.12. Climate Location ID: 145293 (Ottumwa Industrial Airport).....	152
Figure A.13. Climate Location ID: 147015 (Sioux Gateway Airport, Sioux City).....	153
Figure A.14. Climate Location ID: 147593 (Spencer Municipal Airport).....	154
Figure A.15. Climate Location ID: 147021 (Waterloo Municipal Airport).....	155
Figure B.1. Climate Location ID: 146443 (Ames Municipal Airport).....	157
Figure B.2. Climate Location ID: 145295 (Iowa Regional Airport, Burlington).....	158
Figure B.3. Climate Location ID: 146446 (Eastern Iowa Airport, Cedar Rapids).....	159
Figure B.4. Climate Location ID: 145872 (Davenport Municipal Airport).....	160
Figure B.5. Climate Location ID: 145867 (Des Moines International Airport).....	161
Figure B.6. Climate Location ID: 147024 (Dubuque Regional Airport).....	162
Figure B.7. Climate Location ID: 148169 (Estherville Municipal Airport).....	163
Figure B.8. Climate Location ID: 145871 (Iowa City Municipal Airport).....	164
Figure B.9. Climate Location Id: 144715 (Lamoni Municipal Airport).....	165
Figure B.10. Climate Location ID: 146444 (Marshalltown Municipal Airport).....	166
Figure B.11. Climate Location ID: 147596 (Mason City Municipal Airport).....	167
Figure B.12. Climate Location ID: 145293 (Ottumwa Industrial Airport).....	168
Figure B.13. Climate Location ID: 147015 (Sioux Gateway Airport, Sioux City).....	169
Figure B.14. Climate Location ID: 147593 (Spencer Municipal Airport).....	170
Figure B.15. Climate Location ID: 147021 (Waterloo Municipal Airport).....	171
Figure D.1. Calibration coefficients of rutting model.....	179
Figure D.2. Transfer function of rutting model: HMA layer.....	180
Figure D.3. Transfer function of rutting model: subgrade layer.....	180
Figure D.4. Calibration coefficients of fatigue cracking model.....	181
Figure D.5. Transfer function of fatigue cracking model: top-down cracking.....	181
Figure D.6. Transfer function of fatigue cracking model: bottom-up cracking.....	182
Figure D.7. Calibration coefficients and transfer function of thermal cracking model.....	182
Figure D.8. Calibration coefficients and transfer function of flexible pavement IRI model.....	183
Figure D.9. Transfer function of reflective cracking model.....	183
Figure D.10. Calibration coefficients and transfer function of JPCP faulting model.....	184
Figure D.11. Transfer function of JPCP transverse cracking model.....	184

Figure D.12. Transfer function of JPCP IRI model	185
Figure G.1. Summary of survey results for AC over JPCP distresses – design criteria and reliability level	203

LIST OF TABLES

Table 1. Ground-based weather stations in Iowa.....	8
Table 2. Overview of PMED design inputs and layer properties	10
Table 3. Layer thicknesses of Iowa pavements investigated	10
Table 4. Overview of locations across the United States considered for sensitivity analysis	39
Table 5. Base cases with varying traffic levels.....	40
Table 6. Overview of PMED design inputs and layer properties	40
Table 7. Test matrix for OAT sensitivity analysis.....	42
Table 8. Sensitivity of design inputs by maximum absolute NSI: PMED inputs to reflective cracking (NSI at 4,000 ft/mile) for LOW traffic cases	45
Table 9. Sensitivity of design inputs by maximum absolute NSI: PMED inputs to reflective cracking (NSI at 4,000 ft/mile) for MEDIUM traffic cases.....	48
Table 10. Sensitivity of design inputs by maximum absolute NSI: PMED inputs to reflective cracking (NSI at 4,000 ft/mile) for HIGH traffic cases	49
Table 11. Sensitivity of design inputs by maximum absolute NSI: PMED inputs to reflective cracking (NSI at 20 years) for LOW traffic cases	50
Table 12. Sensitivity of design inputs by maximum absolute NSI: PMED inputs to reflective cracking (NSI at 20 years) for MEDIUM traffic cases.....	51
Table 13. Sensitivity of design inputs by maximum absolute NSI: PMED inputs to reflective cracking (NSI at 20 years) for HIGH traffic cases.....	52
Table 14. Summary of optimization methods utilized for local calibration	62
Table 15. Summary of global PMED coefficients for flexible pavements.....	64
Table 16. Summary of local calibration results for flexible pavement IRI model using different optimization methods for (a) calibration sites and (b) validation sites	72
Table 17. Summary of global PMED coefficients for rigid pavements	73
Table 18. Summary of local calibration results for rigid pavement IRI model using different optimization methods for (a) calibration sites and (b) validation sites	78
Table 19. Summary of default PMED coefficients for AC over JPCP.....	79
Table 20. Summary of local calibration results for PMED’s AC-over-JPCP IRI model using different optimization methods based on the total transverse joint length criterion for (a) calibration sites and (b) validation sites	88
Table 21. Summary of local calibration results for PMED’s AC-over-JPCP IRI model using different optimization methods based on the five-year service life criterion for (a) calibration sites and (b) validation sites.....	89
Table 22. Summary of PMED v2.5.5’s national vs. recommended local calibration coefficients for Iowa’s flexible pavements	93
Table 23. Summary of PMED v2.5.5’s national vs. recommended local calibration coefficients for Iowa’s rigid pavements.....	94
Table 24. Summary of PMED v2.5.5’s national vs. recommended local calibration coefficients for Iowa’s AC over JPCP	95

Table 25. Input ranges for sensitivity analyses	101
Table 26. NSI summary: 40-year design life and 50% reliability	102
Table 27. NSI summary: 20-year design life and 50% reliability	103
Table 28. NSI summary: 40-year design life and 90% reliability	105
Table 29. NSI summary: 20-year design life and 90% reliability	106
Table 30. Distress criteria and reliability level as displayed on the home screen of the PMED software	108
Table 31. Survey respondent organizations	110
Table 32. Recommended level of reliability for different road classifications.....	117

ACKNOWLEDGMENTS

The authors gratefully acknowledge the Iowa Department of Transportation (DOT) for sponsoring this study. The project technical advisory committee (TAC) members, Chris Brakke and Fereidoon (Ben) Behnami, are gratefully acknowledged for their guidance, support, and direction throughout the research.

Special thanks to Mark Murphy from the Iowa DOT for helping and guiding the research team's use of the measured distress data from the Iowa Pavement Management Information System (PMIS).

ACRONYMS, ABBREVIATIONS, AND NOMENCLATURE

AADTT	annual average daily truck traffic
AASHTO	American Association of State Highway and Transportation Officials
AC	asphalt concrete
ACC	asphalt cement concrete
ACPA	American Concrete Pavement Association
ANN	artificial neural network
API	application programming interface
ARA	Applied Research Associates, Inc.
ASOS	automated surface observing system
AWS	automated weather station
BCOA	bonded concrete overlay of asphalt
BCOA-ME	bonded concrete overlay of asphalt mechanistic-empirical
CCM	cohesive crack model
COOP	Cooperative Observer Program
CRCP	continuously reinforced concrete pavement
CTE	coefficient of thermal expansion
DL	design limit
DOT	department of transportation
ESS	environmental sensing station
FHWA	Federal Highway Administration
GA	genetic algorithm
GBWS	ground-based weather station
GRG	generalized reduced gradient
HCD	hardware configuration definition
HMA	hot-mixed asphalt
IEM	Iowa Environmental Mesonet
InTrans	Institute for Transportation
IRI	International roughness index
JPCP	jointed plain concrete pavement
LCMS	laser crack measuring system
LOE	line of equality
LP	linear programming
LTE	load transfer efficiency
LTPP	long term pavement performance
MAAT	mean annual air temperature
MAPE	mean absolute percentage error
MEPDG	Mechanistic-Empirical Pavement Design Guide
MERRA	Modern-Era Retrospective Analysis for Research and Applications
MOP	manual of practice
MOR	modulus of rupture
MSE	mean square error
NARR	North American Regional Reanalysis
NASA	National Aeronautics and Space Administration
NCCS	NASA Center for Climate Simulation

NCEP	National Centers for Environmental Protection
NCHRP	National Cooperative Highway Research Program
NOAA	National Oceanic and Atmospheric Administration
NSI	normalized sensitivity index
OAT	one-at-a-time
OGFC	open graded friction course
OWS	operating weather station
PCC	Portland cement concrete
PCI	pavement condition index
PCR	pavement condition rating
PMED	Pavement Mechanistic-Empirical Design
PMIS	Pavement Management Information System
PROSPER	Program for Sustainable Pavement Engineering and Research
QCLCD	quality controlled local climatological data
RMSE	root mean square error
RWIS	road weather information system
SEE	standard error estimate
SHA	state highway agency
SIF	stress intensity factor
SJPCP	short-jointed plain-concrete pavement
SJPCP/AC	short-jointed plain-concrete pavement over asphalt concrete
SSR	surface shortwave radiation
TAC	technical advisory committee
UI	user interface
ULCD	unedited local climatological data

EXECUTIVE SUMMARY

The American Association of State Highway and Transportation Officials (AASHTO) AASHTOWare Pavement ME Design (PMED) version 2.5.5, released in June 2019, has numerous enhancements and updates that include the integration of Modern-Era Retrospective Analysis for Research and Applications (MERRA) climate data for the design of flexible pavements and North American Regional Reanalysis (NARR) climate data for the design of rigid pavements. Its previously used ground-based weather station (GBWS) climate data are no longer an available default.

In addition, PMED 2.5.5 adds as state practices new models such as a reflective cracking model (dealing with the most commonly observed distress in asphalt concrete [AC] overlays) and the short-jointed plain-concrete pavement over asphalt concrete (SJPCP/AC) model developed by the University of Pittsburgh. Also, various bugs were resolved and components of performance prediction models within the software were modified to improve its overall performance. This report performs a comprehensive evaluation of all these new PMED tools.

PMED's New Climate Data Sources

Any pavement performance system depends on various factors, such as its structural adequacy, traffic loading, climate conditions, material properties, and construction methods. Unfortunately, variations in ambient temperature and moisture can change material properties and consequently affect the overall pavement performance.

Collecting climate data has been a significant challenge for transportation agencies over the years. This study compares the pavement performance predictions for Iowa pavement systems in the PMED software using four climate data sources: (1) GBWS, (2) NARR, (3) MERRA version 1, and (4) MERRA version 2. Its findings show disagreement among climate data sources for some distresses due to their significant differences in hourly percent sunshine measurements.

To improve pavement performance predictions, a database of “synthetic” percent sunshine measurements was developed using the surface shortwave radiation (SSR) estimates directly provided by MERRA. This eliminated nearly all the observed discrepancies. This study therefore recommends SSR as one of the future inputs in the PMED climate tool.

PMED's New Reflective Cracking Model

One of the main types of distress observed in AC overlays is reflective cracking, and a reflective cracking model has been recently incorporated into the latest released version of the PMED software.

This study documents the sensitivity to various design inputs and material properties on reflective cracking distress as predicted by the PMED software. Six representative locations

distributed across different climate zones of the United States were considered to study the effects of climate extremes on changes in PMED'S predicted reflective cracking distress.

One-at-a-time (OAT) sensitivity analysis was performed for two scenarios to determine the Normalized Sensitivity Index (NSI): (1) the sensitivity of short-term reflective cracking predictions (i.e., the year when predicted distress reached 4,000 ft/mile) and (2) the sensitivity of long-term reflective cracking predictions (i.e., for a 20-year design life).

The overall summary of results shows that the most sensitive PMED inputs with respect to reflective cracking distress are Joint Spacing, Jointed Plain Concrete Pavement (JPCP) Layer Thickness, Transverse Load Transfer Efficiency (LTE), and Alpha and Delta in the AC Sigmoidal Curve, while Annual Average Daily Truck Traffic (AADTT), AC Surface Shortwave Absorption, Effective Binder Content, Air Voids in AC, Tensile Strength, AC Thickness, Ratio of Slabs Distressed before and after Restoration, and Portland Cement Concrete (PCC) Thermal Conductivity are moderately sensitive PMED inputs with respect to reflective cracking distress.

Additional findings are also reported for each traffic level.

PMED'S New Short-Jointed Plain-Concrete Pavement Over Asphalt Concrete Model

A new procedure, Bonded Concrete Overlay of Asphalt Mechanistic-Empirical Design (BCOA-ME), has been developed at the University of Pittsburgh to address the significant limitations of similar procedures that have been used by state highway agencies (SHAs) over the years. A portion of the BCOA-ME procedure, renamed short-jointed plain-concrete pavement over asphalt concrete (SJPCP/AC), was recently added to the PMED software package. The output distress it predicts is longitudinal fatigue cracking calculated in terms of percentage of slabs.

This study reports comprehensive sensitivity results for PMED design inputs with respect to predicted longitudinal fatigue cracking. To help evaluate the impact of climate on PMED'S longitudinal-fatigue-cracking predictions, five climate locations representing different climatic conditions were considered. NSI values were determined by performing OAT sensitivity analysis.

Layer thicknesses were sensitive input parameters in all cases, so careful consideration should be given to performing field surveys to collect information on the existing AC layer and base layer thicknesses to ensure optimization of the SJPCP layer. AADTT, transverse joint LTE, and PCC modulus of rupture were moderately sensitive inputs. Joint spacing and the coefficient of thermal expansion (CTE) were observed to be "insensitive" due to their limited range of input options in the PMED software. In all cases, most input parameters were sensitive to longitudinal fatigue cracking at the International Falls, Minnesota, location, where extreme cold weather and moisture infiltration through cracks result in premature failure of pavement overlays.

Local Calibration Performed for Iowa

Numerous changes in the PMED software warrant recalibration. Local calibration using PMED v2.5.5 was performed for Iowa AC, JPCP and AC-over-JPCP sections. Multiple optimization and resampling approaches such as sensitivity analysis, Microsoft Excel Solver, LINGO, SciPy Optimize, genetic algorithms, bootstrapping, and jackknifing have all been tested for their potential to improve the accuracy of the PMED-predicted vs. measured data comparisons.

Results and experiences from the process of producing a complete set of revised local calibration coefficients are presented and discussed. This is the first study to perform and present the local calibration results for PMED's new reflective cracking model.

The local calibration coefficients recommended for the Iowa DOT to use in design practice as alternatives to their nationally calibrated counterparts are summarized in Table 22 for Iowa's flexible pavements, Table 23 for Iowa's rigid pavements and Table 24 for Iowa's AC over JPCP. (Note that the recommended local calibration coefficients in red in these tables show that these numbers are different from their counterparts in the nationally calibrated models.)

Survey Performed on PMED Design Criteria and Reliability

In an attempt to understand the variations in design criteria and reliability levels recommended for use in the PMED software, a survey addressing this was sent out to state highway agencies (SHAs), pavement engineers, and researchers across the United States and Canada. A total of 26 responses were received, and a summary of respondents' recommendations is presented.

The final pavement design, long-term performance, initial construction costs, and life-cycle costs are greatly affected by the chosen design criteria and reliability levels, so further analysis was performed to determine sensitivity with respect to flexible and rigid pavement thicknesses for a range of distress criteria and reliability levels. A major finding from the PMED design criteria and reliability survey is related to the determination of joint spacing for rigid pavement systems. The majority of responses reflected joint spacings that varied between 15 feet and 20 feet, depending on the local conditions. The impact of joint spacing on the determination of the final thickness and reliability was further evaluated and presented.

INTRODUCTION

Background

The American Association of State Highway and Transportation Officials (AASHTO) AASHTOWare Pavement ME Design (PMED) software is a state-of-the-practice tool for designing new and rehabilitated pavement systems. Since its release, the majority of state highway agencies (SHAs) have already evaluated and implemented it for use in their design procedures, and most of the remaining states are planning to implement it within the next few years.

PMED design and analysis involves an iterative process comprised of three steps:

1. Create a trial design
2. Predict distresses for the trial design by performing PMED runs
3. Review the predicted distresses against the distress criteria considered for the trial design

The trial design is then modified to produce an acceptable design satisfying the relevant distress criteria (AASHTO 2015).

The Mechanistic-Empirical Pavement Design Guide (MEPDG) v1.1 software, after correcting and updating previous research prototypes (i.e., v0.7 to v1.0), was released in 2009 as the official version of the software accompanying the AASHTO *MEPDG Manual of Practice*. This software, enhanced and updated by adding new pavement performance prediction models and by improving existing models, was rebranded in 2011 as DARWin-ME and later marketed as AASHTOWare Pavement ME Design (PMED) in 2013. The MEPDG and its implementation in the PMED software (<http://me-design.com/MEDesign/>) represent a major improvement over their predecessors, particularly in their comprehensive coverage of the impact of design inputs on pavement performance.

The latest available version of PMED is version 2.5.5, released in June 2019. PMED v2.5.5 has numerous enhancements and updates that include the integration of Modern-Era Retrospective Analysis for Research and Applications (MERRA) climate data for the design of flexible pavements and North American Regional Reanalysis (NARR) climate data for the design of rigid pavements. Also, new models such as a reflective cracking model and the short-jointed-plain-concrete-pavement-over-asphalt-concrete (SJPCP/AC) model developed by the University of Pittsburgh have been recently added for use in state practices. In addition, various bugs have been resolved and components of the performance prediction models within the software have been modified to improve its overall performance. The documentation of all the updates and changes can be accessed through the official PMED website (<https://me-design.com/MEDesign/Documents.html>).

The performance prediction models in the PMED software have been globally/nationally calibrated based on NCHRP 1-37A. To achieve intended results, local calibration of these

models based on the assessment of local conditions is recommended. The local calibration concept in MEPDG procedures implies the use of a mathematical process of minimizing the bias and standard error between field-observed pavement distresses and PMED-predicted pavement performance (AASHTO 2010).

Most SHAs using the PMED software have performed local calibration at least once for their respective states since its initial release. However, Ceylan et al. (2015) performed multiple local calibration studies using MEPDG v1.1, DARWin-ME, PMED v2.1.24, and PMED v2.2 and observed differences in predictions resulting from using different versions. Similarly, Haider et al. (2020) verified performance predictions for rigid pavements in Michigan using PMED v2.2 and v2.3, and their findings exhibited significant changes across versions in transverse cracking and International Roughness Index (IRI) prediction. Additional findings from that study reflect significant decreases in slab thicknesses using the same local calibration coefficients obtained from their studies previously performed using PMED v2.0. The results from these studies emphasize the urgent need for recalibration with the latest version (v2.5.5) to enhance SHA confidence in PMED pavement designs.

Research Objectives

The main research objective of this study is to evaluate the major new tools recently added to the PMED software, including a climate tool, a reflective cracking model, and the SJPCP/AC model. A complete in-detail review of modifications across PMED versions made to performance prediction models, emphasizing the need for local recalibration using PMED v2.5.5, is also presented.

A total of 130 pavement sections (flexible, rigid, and AC over JPCP combined) were selected for use in local calibration. A comprehensive measured distress database summarizing these pavement sections' historical data, extracted from Iowa's Pavement Management Information System (PMIS), was included in the calibration process. A number of optimization tools—such as Microsoft Excel Solver, LINGO, genetic algorithms, SciPy Optimize, bootstrapping, and jackknifing—were tested to evaluate local calibration models and determine a new set of local calibration coefficients.

The detailed background, methodologies, and complete findings for each task are presented in the individual chapters of this report.

Report Organization

Chapter 1 presents the background, motivation, objectives, and general approach of this study. Chapter 2 presents a summary of updates and changes made to the PMED software since 2015. Chapter 3 presents the impact of the climate models recently added to the PMED software with respect to Iowa pavement systems. Chapter 4 presents comprehensive sensitivity analysis results for the new reflective cracking model added to the PMED software. Chapter 5 presents the complete local calibration process, study methods, and results with respect to Iowa's flexible,

rigid, and composite pavement systems. Chapter 6 presents comprehensive sensitivity analysis results for the new SJPCP/AC (bonded concrete overlay of asphalt mechanistic-empirical or BCOA-ME) model added to the PMED software. Chapter 7 presents its study's national survey results and associated recommendations for the Iowa DOT to determine optimal pavement thicknesses based on distress criteria and reliability levels. Chapter 8 concludes the report with a summary, conclusions, and recommendations.

The seven appendices at the end of this report include historical variations in climate data for Iowa locations based on MERRA sources (Appendices A and B), a summary of PMED inputs based on Iowa DOT recommendations (Appendix C), a summary of distress transfer functions used internally in the PMED software (Appendix D), validation of the local calibration results for independent pavement sections across Iowa (Appendix E), a demonstration of PMED's new tool for assisting local calibration (Appendix F), additional survey results (Appendix G), PMED inputs for reliability and the thickness determination task (Appendix H), and a list of all the raw and other data files used in the project for accomplishing its various tasks (Appendix I).

UPDATES AND CHANGES ACROSS VERSIONS OF THE PMED SOFTWARE (AUGUST 2015–AUGUST 2019)

Updates to the software before August 2015 (PMED v2.2) are summarized in the Institute for Transportation (InTrans) report titled Investigation of AASHTOWare Pavement ME Design/DARWin-ME Performance Prediction Models for Iowa Pavement Analysis and Design (Ceylan et al. 2015). The updates added in v2.3.0 and later are as follows:

Version 2.3.0 – Released on July 1, 2016

- Inclusion of short-jointed plain concrete pavement over asphalt concrete (SJPCP/AC) based on evaluation of the bonded-concrete overlay of asphalt mechanistic-empirical model developed at the University of Pittsburgh to improve the software’s ability to predict bonded concrete overlay distress as a part of a Federal Highway Administration (FHWA) transportation pooled-fund study, TPF-5(165), Development of Design Guide for Thin and Ultrathin Concrete Overlays of Existing Asphalt Pavements.
- Update of the climate database based on the NARR dataset model, as an extension of the National Centers for Environmental Prediction (NCEP) global reanalysis that included the North American region. Use of the NARR dataset resulted in substantial improvement over previous datasets with respect to accuracy of temperature, winds, and precipitation.
- Incorporation of Map-ME (<http://www.me-design.com/MapME>) with an updated climate dataset from NARR for SJPCP/AC analysis that can pull data from several government datasets for use in designs.
- Recalibration and revision of rigid pavement coefficients in performance prediction models.
- Various other software issues and bugs that were resolved.

Version 2.5.0 – Released on July 1, 2018

- Integration of a manual of practice (MOP) in the software’s Help section to provide a direct reference for users.
- Development of modulus application programming interface (API) for researchers interested in working directly with the modulus analysis module in the software that allows users to access data, such as master curve coefficients, asphalt binders’ viscosity temperature susceptibility (A-VTS), and standard error reports.
- Development of a MasterTCModel file API with access to thermal cracking outputs in the software, including input and output intermediate files.
- Customization of report and enhanced-project comparison allowing users to check and uncheck performance criteria for final display in the output files and to enter a filter mode to compare findings between two projects.
- Inclusion of maintenance strategy tools for “non-structural” designs, adding the capability for including specific surface treatments for flexible and rigid pavement design analysis.
- Integration of National Aeronautics and Space Administration (NASA)-based MERRA climate data for flexible pavement designs from which users can download climate files in hardware configuration definition (HCD) format from the Long-Term Pavement

Performance (LTPP) infopave website at <https://infopave.fhwa.dot.gov/Tools/MEPDGInputsFromMERRA>.

- Availability of Level 1 inputs for entering tensile strength data, adding the capability for predicting changes in tensile strength over different temperature ranges.
- Recalibration and revision of flexible and flexible rehabilitation, including semi-rigid pavement coefficients in performance prediction models.
- Increase of design period to up to 100 years.
- Various other software issues and bugs that were resolved.

Version 2.5.2 – Released on August 30, 2018

- Flexible pavement rehabilitation default level was changed to Level 2.
- Climate user interface (UI) changes were updated in the Help manual.
- User-defined values for water table depth can be exchanged with default values for trial design options.
- Additional coefficient changes for performance prediction models.
- Several minor bugs that were resolved.

Version 2.5.3 – Released on October 16, 2018

- Various default databases fixes that were made.
- Several minor bugs that were resolved.

Version 2.5.4 – Released on April 8, 2019

- Update of the climate UI using Google maps for finding map locations. Additional changes to climate UI included properly storing project location and elevation, zoom in/out features for maps, and added project location and climate-data selection distinctions to maps.
- Several minor bugs that were resolved.

Version 2.5.5 – Released on July 1, 2019

- Analysis subsystem completely reworked and can run independently of the file system.
- Climate UI updated to use Google maps API.
- Various other software issues and bugs that were resolved.

EVALUATION OF NASA'S MERRA CLIMATE DATA FOR IOWA PAVEMENT SYSTEMS

Background

The PMED model takes traffic loading, climate, material properties, and complete pavement structure into account to predict individual pavement performance (i.e., distress or smoothness).

Hourly climate data are one of the primary inputs in the PMED software. The climate effects are generally observed through predicted pavement performance.

Asphalt concrete (AC) layer properties are directly impacted by extremities in temperatures (low and high). AC design primarily considers the climatic factors through asphalt binder selection.

Pavement foundation systems are mostly unbound materials, and their properties are sensitive to moisture content (Cetin et al. 2019, Satvati et al. 2019). Moreover, high moisture content can result in frost action and be otherwise detrimental to pavement life (Breakah et al. 2011, Hossain et al. 2018, Gopisetti 2017).

Pavement temperature can also result in rutting, with significant damage occurring at high temperatures (Notani et al. 2020), while very low pavement temperatures lead to the occurrence of thermal cracks.

Surface shortwave radiation (SSR) and longwave radiation are two factors that have a direct impact on pavement temperature. SSR is more related to daytime pavement temperature modeling, and longwave radiation is associated with the percent cloudiness at night. The climate models in the PMED software do not have SSR and longwave radiation as direct inputs, but instead estimates these indirectly as percent sunshine measurements.

This study evaluates the direct effects of SSR available through MERRA on PMED pavement performance predictions. However, evaluation of longwave radiation is not performed in this study due to the unavailability of data in the hourly format required by the PMED software. Additionally, longwave radiation values are assumed in this study to have a negligible effect on pavement performance based on findings from a previous study (Gopisetti et al. 2019).

Over the years, extensive efforts to investigate and develop better climate data sources and climate inputs have been made by researchers across the country (Cetin et al. 2015, Durham et al. 2019, Schwartz et al 2015). Breakah et al. (2011) investigated the effects of the accuracy of the ground-based weather station (GBWS) climate data on pavement distresses modeled through the MEPDG (v1.0). They further analyzed and compared the climate files available in the MEPDG and those based on the historical information for Iowa counties through a source called the Iowa Environmental Mesonet (IEM).

Heitzman (2007) presented an approach that builds a virtual climate database by using the available broad historical trends that can better project historical cycles than any 10- to 20-year historical climate record. This method is an excellent replacement for conventional techniques such as interpolation or the repetition of climate databases after every short period.

Schwartz et al. (2015) performed comparisons of MERRA climate data with the GBWS climate data to evaluate the impacts of using climate files from various sources on pavement performance predictions using the MEPDG. Additional analyses, such as statistical analyses comparing MERRA against operating weather stations (OWS) and evaluation of the correctness of MEPDG SSR measurements, were also performed. Their study concludes that MERRA is a superior climate data source compared to the conventional ground-based sources.

Cetin et al. (2015) compared flexible and rigid pavement performance predictions using three climate data sources (which included the AASHTO-based weather station database, GBWS, and MERRA-1) for South Dakota. Their results showed that the use of MERRA climate data has various advantages such as better spatial coverage; climate data availability for more extended periods without temporal gaps; and high-quality, low-error data.

Gopiseti et al. (2019) performed four-way comparisons for AC and jointed plain concrete pavements (JPCP) for Georgia using the GBWS, NARR, MERRA-1, and MERRA-2 data. They additionally developed an SSR regression model to produce a synthetic percent sunshine that eliminated the discrepancies observed in the comparisons.

The uniqueness of this research study is presenting the four-way comparisons of Gopiseti et al. (2019) applied to the flexible, rigid, and composite pavement systems in Iowa. (Iowa currently has more than 50% AC-over-JPCP composite pavements. It was also necessary to evaluate the impact of climate on major distresses such as IRI, total transverse cracking, and thermal cracking that are observed mainly in the states where extreme low temperatures are recorded during winters.

Objective

The primary objective of this research study is to evaluate MERRA estimates as a significant climate data source in PMED to improve pavement designs across Iowa. Predicted pavement performance generated by PMED through MERRA is compared with that based on climate data from ground-based weather stations and other previously available sources such as NARR.

This chapter further presents discrepancies in climate estimates across different climate data sources and recommends the direct input of climate data from MERRA as an alternative for the most reliable and accurate pavement performance predictions.

Climate Data Sources

The PMED software requires five primary climate inputs to make runs. These inputs include hourly precipitation, hourly relative humidity, hourly wind speed, hourly air temperature, and hourly percent sunshine. This study uses four climate data sources that provide all these inputs. These climate data sources include GBWS; NARR; MERRA-1; and MERRA-2, which is the official source of climate inputs in the recent versions of the PMED software.

Ground-Based/Airport-Based Weather Stations (GBWS)

Ground-/airport-based weather stations were used in the MEPDG and PMED since the release of its first version of the software in 2004 until July 2016. The GBWS files were derived from two data sources provided by the National Climate Data Center, the Unedited Local Climatological Data (ULCD) and the Quality-Controlled Local Climatological Data (Gopiseti et al. 2019).

The significant limitations with the GBWS files are incomplete data and limited data availability. The previous versions of the MEPDG and PMED included GBWS climate data from more than 1,083 locations across the United States. Iowa had only 15 of these stations to inform its pavement designs. These PMED weather stations of Iowa considered in this study for comparison to other climate data sources are shown in Table 1.

Table 1. Ground-based weather stations in Iowa

Station ID	City	Latitude	Longitude
94989	Ames	41.992	-93.622
14931	Burlington	40.783	-91.125
14990	Cedar Rapids	41.884	-91.709
94982	Davenport	41.614	-90.591
14933	Des Moines	41.538	-93.666
94908	Dubuque	42.398	-90.704
94971	Estherville	43.408	-94.746
14937	Iowa City	41.633	-91.543
94991	Lamoni	40.633	-93.902
94988	Marshalltown	42.113	-92.918
14940	Mason City	43.158	-93.331
14950	Ottumwa	41.107	-92.448
14943	Sioux Falls	42.391	-96.379
14972	Spencer	43.164	-95.202
94910	Waterloo	42.554	-92.401

North American Regional Reanalysis (NARR)

The climate data from NARR have been incorporated into the PMED software since 2016, replacing the GBWS. The NARR was developed using the NCEP to model observational data to produce a long-term overview of weather in North America. The model is initialized by using real-world temperature, winds, precipitation, and moisture conditions from surface observations (Brink et al. 2017). The NARR data are available for a 32×32 km grid across North America. Three-hour, daily, and monthly values from NARR are available starting from 1979. Since the PMED software requires hourly data, one-hour estimates were obtained by linear interpolation between NARR's three-hour values, the need for which procedure is one of the major limitations in using the NARR climate data (Gopiseti et al. 2019). Climate files from NARR can be generated for any latitude or longitude across North America.

The Modern-Era Retrospective Analysis for Research and Application (MERRA)

The MERRA climate data from NASA are another reanalysis tool tested in this study. The MERRA climate data were added into the PMED software in July 2018, replacing NARR. Surface weather history and high-quality atmospheric data are obtained through MERRA in the hourly format as required by PMED. The MERRA data are available from 1979 and are updated every 6 hours. The MERRA data are analyzed and validated regularly to ensure consistency and continuity as the estimates are recorded in near real-time. Furthermore, MERRA is capable of providing all the climate inputs required by PMED. The fourth climate data source, MERRA-2, is also considered in this study. MERRA-2 has a better horizontal resolution, improved data assimilation, and better precipitation modeling compared to MERRA-1 (Schwartz et al. 2015).

Measurement Product Collocation

The collocation of the MERRA and GBWS data was required before synchronizing the recorded sequences in time.

The first step of the collocation process was performed using the GBWS location information, which means all the computed distance measurements considering the GBWS station as located at the center of the search area (Cetin et al. 2018). The next step was performed by computing horizontal distance for the MERRA grid locations for the climate files in Iowa. This completed process guarantees that at least one MERRA grid cell would match with all the GBWS climate files considered.

The separation distances between the GBWS and MERRA climate station locations range between 3.1 miles and 31 miles (5 and 50 km).

Results

The inputs required for pavement design for use in PMED were determined based on typical values utilized for Iowa's primary road design practices. Base cases were then developed in

PMED, and only the climate files from different sources were changed by keeping the same base cases for all the performed runs. Table 2 lists the summary of PMED pavement design inputs, and Table 3 summarizes the layer thicknesses of investigated Iowa composite pavements.

Table 2. Overview of PMED design inputs and layer properties

Input Parameter	Input Value
Design life	20 years
Reliability	50% for all distresses
AADTT category	Principal arterials – Interstate and defense routes
Number of lanes in design direction	2 for low traffic/3 for medium and high traffic
Truck direction factor	50
Truck lane factor	75 for low traffic/55 for medium traffic/50 for high
Default growth rate	0
First layer material type	AC
Second layer material type	PCC
Base type	Granular base
Subgrade material type	Soil

Table 3. Layer thicknesses of Iowa pavements investigated

Pavement Type	Composite (AC over JPCP)
AADTT	7,500
New surface layer	3 inches (7.62 cm) of AC
Existing surface layer	10 inches (25.4 cm) of JPCP
Base layer	6 inches (15.24 cm) of granular materials

Comparison of Flexible Pavement Predictions

Comparisons of flexible pavement distresses predicted by PMED using GBWS climate files vs. NARR vs. MERRA-1 vs. MERRA-2 are shown in Figure 1 through Figure 6.

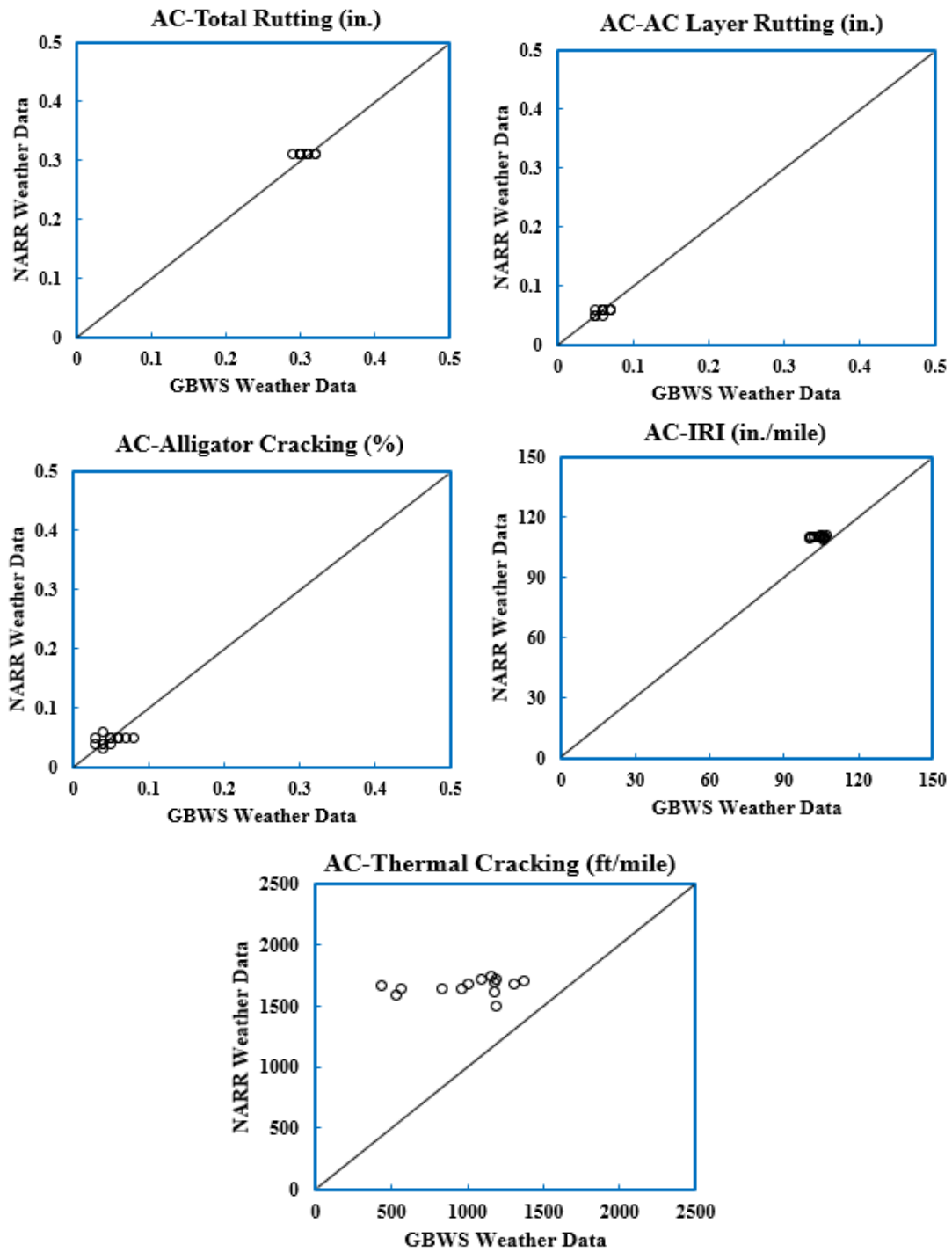


Figure 1. Comparison of flexible/asphalt concrete predictions using GBWS vs. NARR weather data

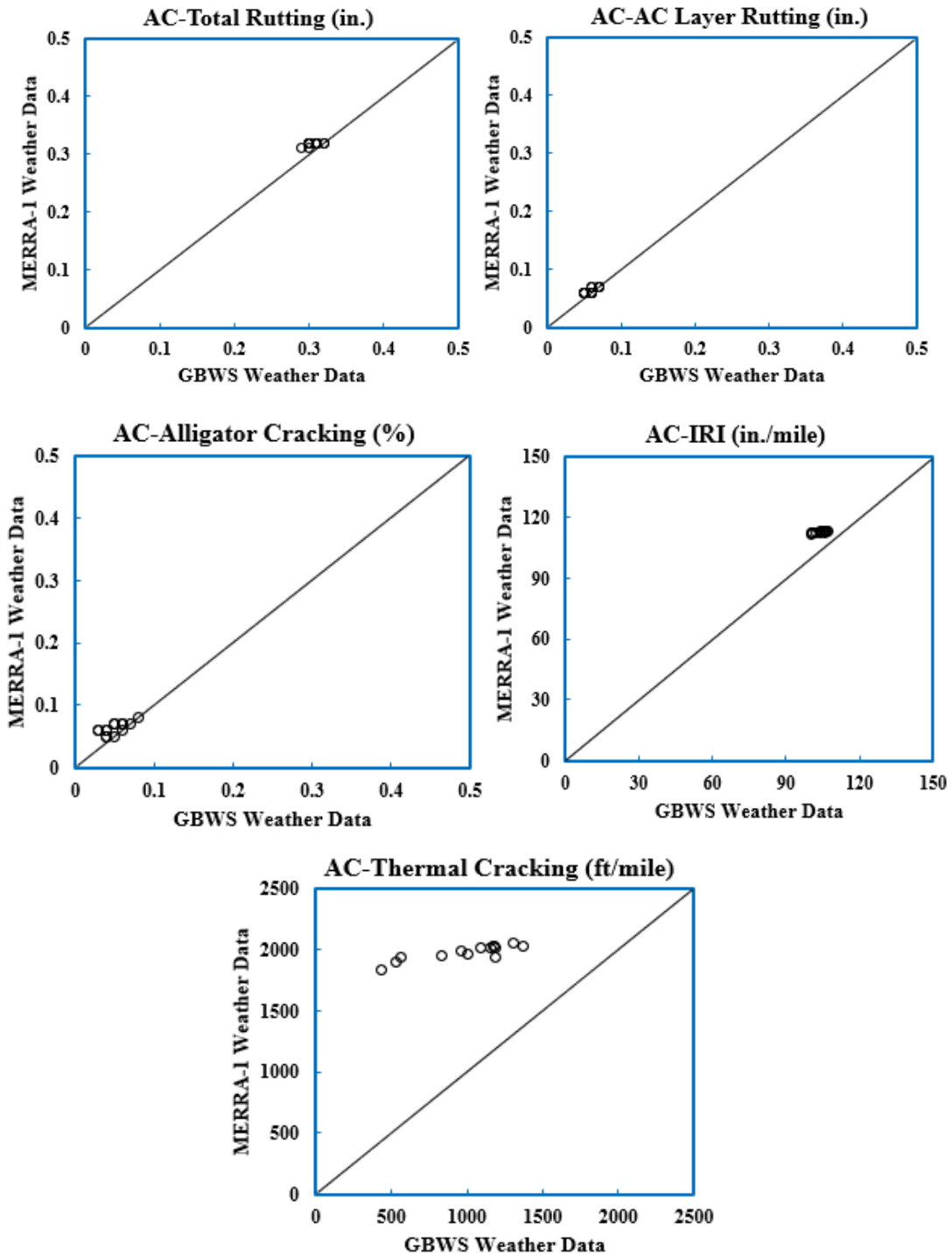


Figure 2. Comparison of flexible/asphalt concrete predictions using GBWS vs. MERRA-1 weather data

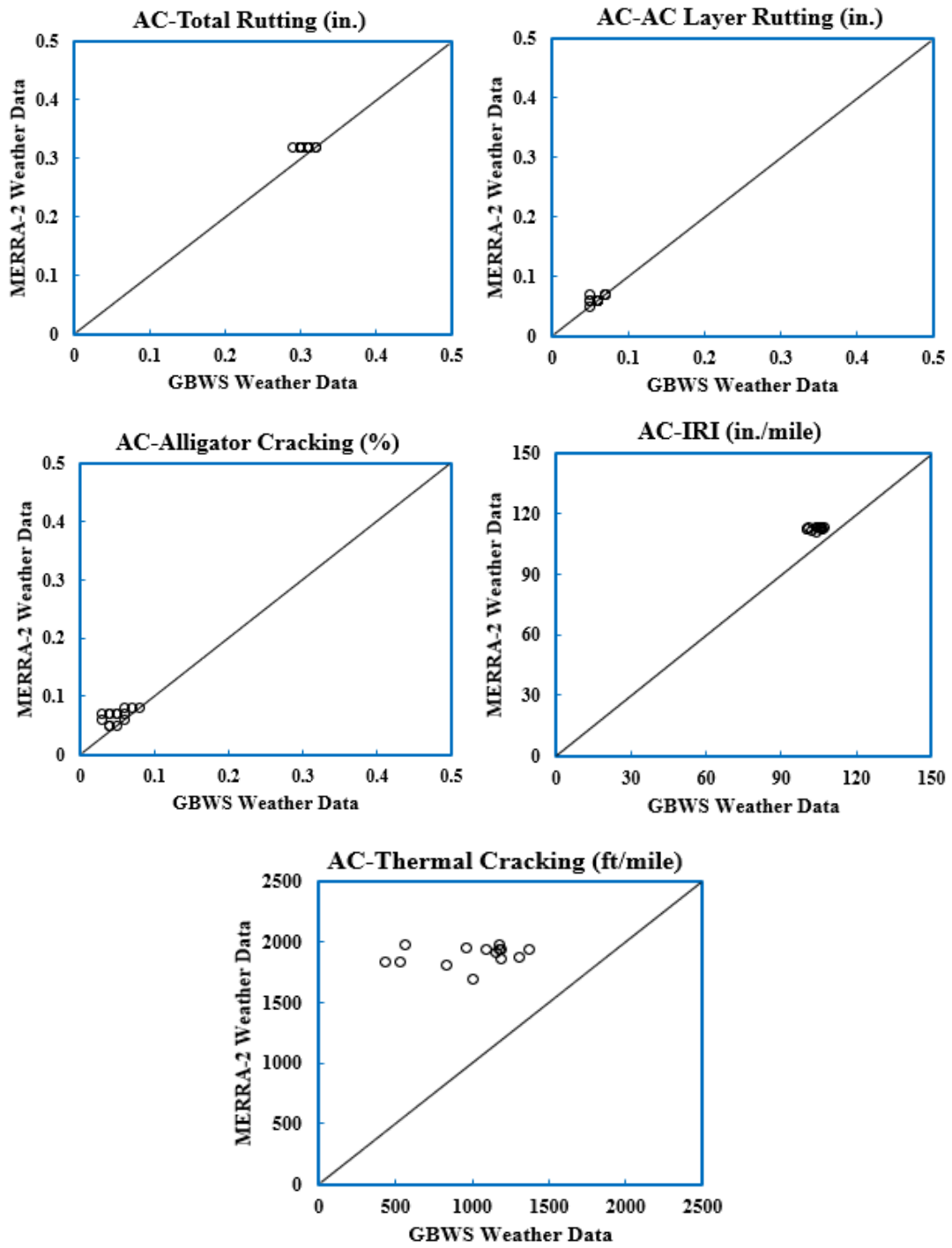


Figure 3. Comparison of flexible/asphalt concrete predictions using GBWS vs. MERRA-2 weather data

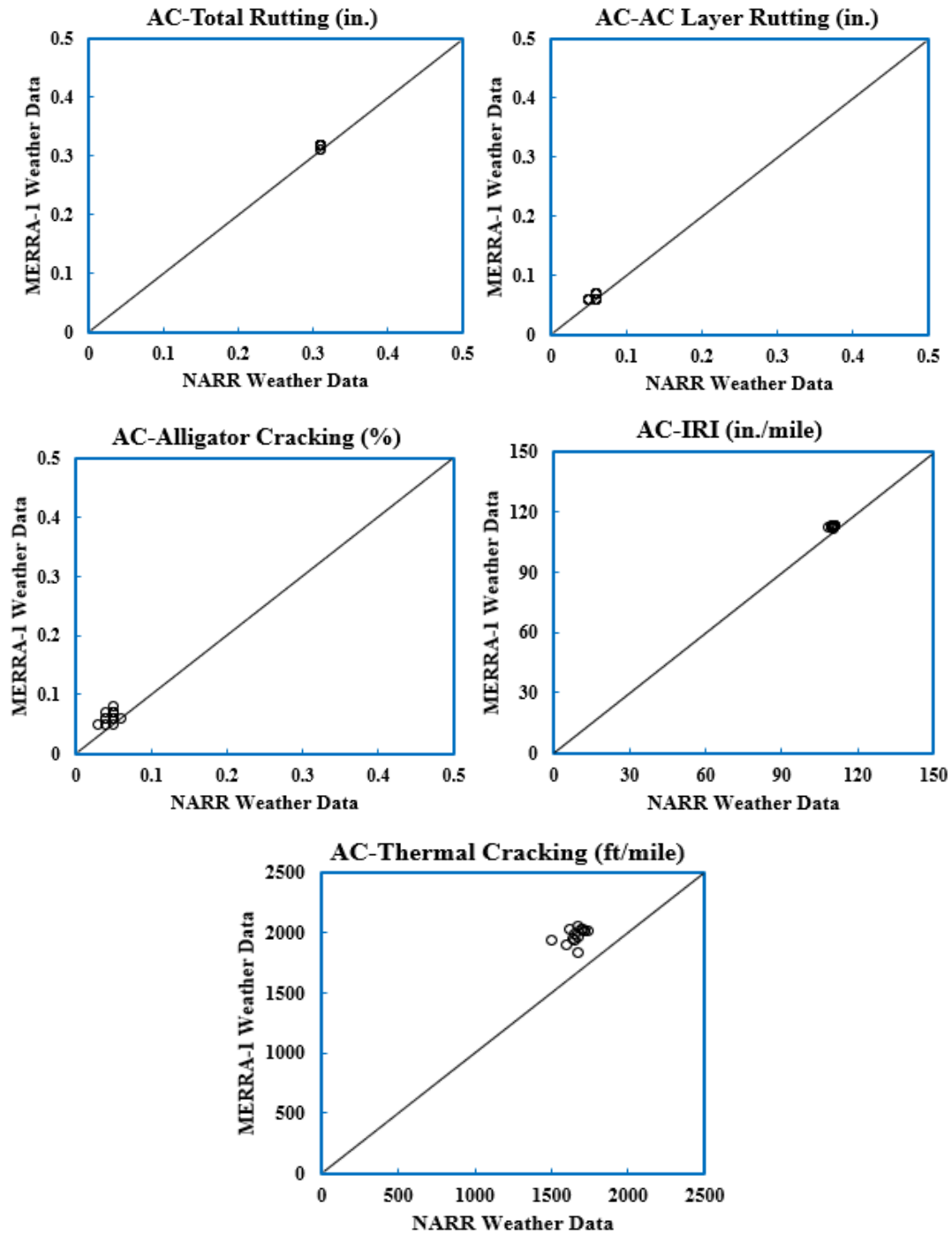


Figure 4. Comparison of flexible/asphalt concrete predictions using NARR vs. MERRA-1 weather data

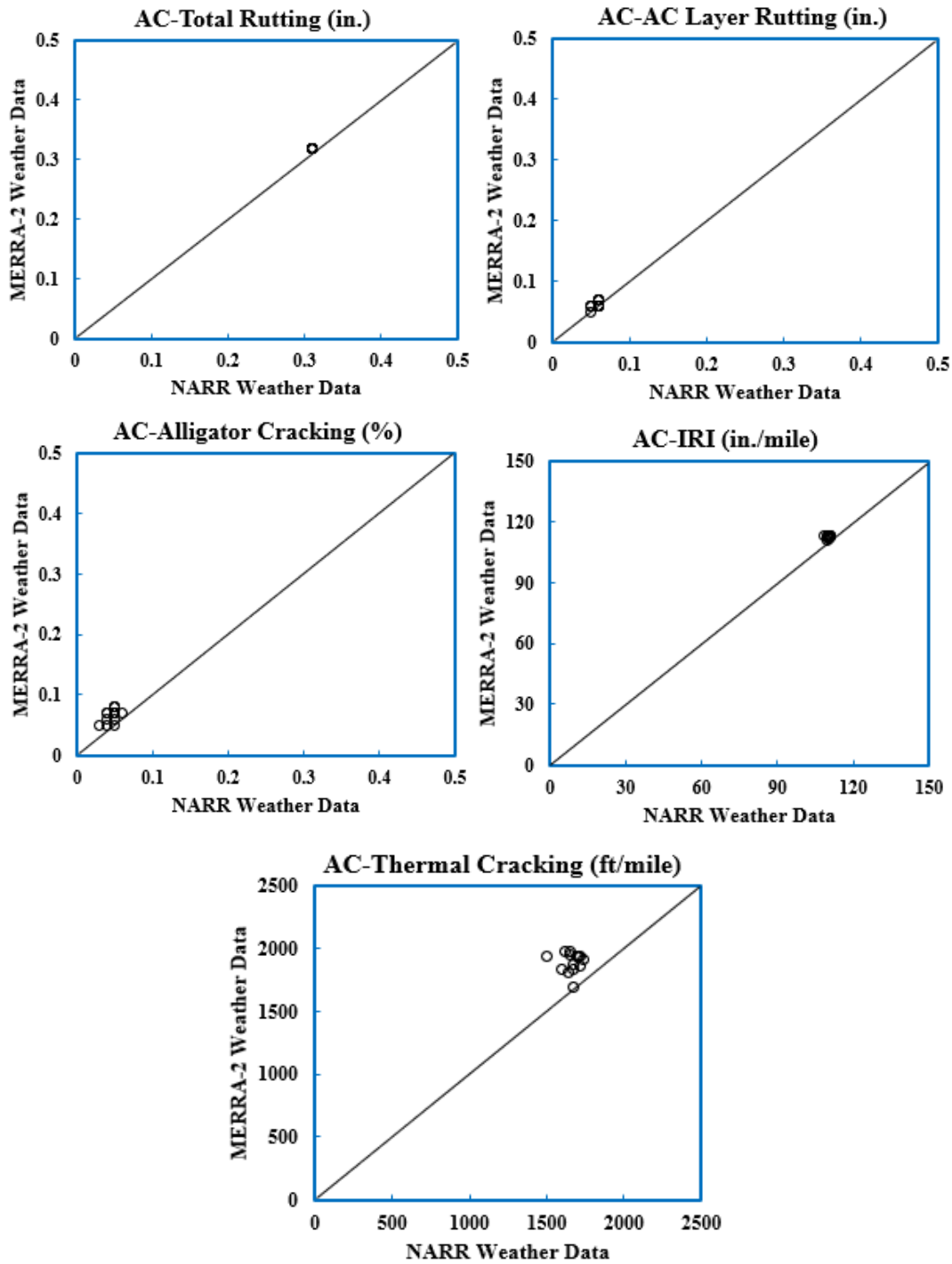


Figure 5. Comparison of flexible/asphalt concrete predictions using NARR vs. MERRA-2 weather data

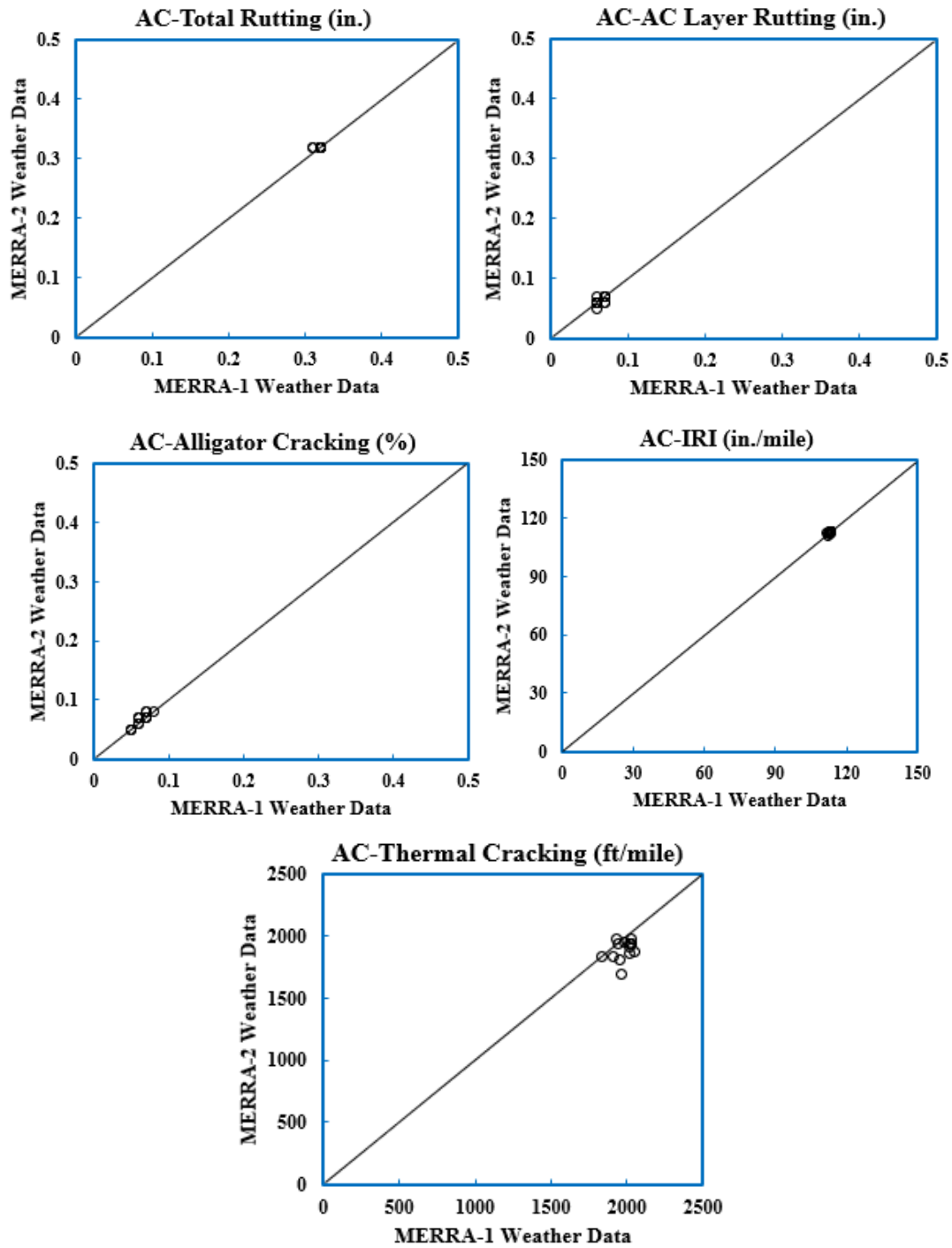


Figure 6. Comparison of flexible/asphalt concrete predictions using MERRA-1 vs. MERRA-2 weather data

In most cases, the predicted distress showed good agreement among climate data sources except with the thermal cracking distress. The NARR, MERRA-1, and MERRA-2 sources resulted in significantly higher thermal cracking when compared to the GBWS data. It was surprising to see minor differences in thermal cracking predicted using MERRA-1 vs. MERRA-2, as their climate

data are from the same source. Nevertheless, the NARR, MERRA-1, and MERRA-2 results are consistent with the previous studies that showed thermal cracking occurs at very low temperatures.

In consideration of Iowa being located in a Wet-Freeze climate zone, thermal cracking is one of its most sensitive pavement distresses to climate inputs.

Comparison of JPCP Predictions

Comparisons of JPCP distresses predicted by PMED using GBWS climate files vs. NARR vs. MERRA-1 vs. MERRA-2 are shown in Figure 7 through Figure 12.

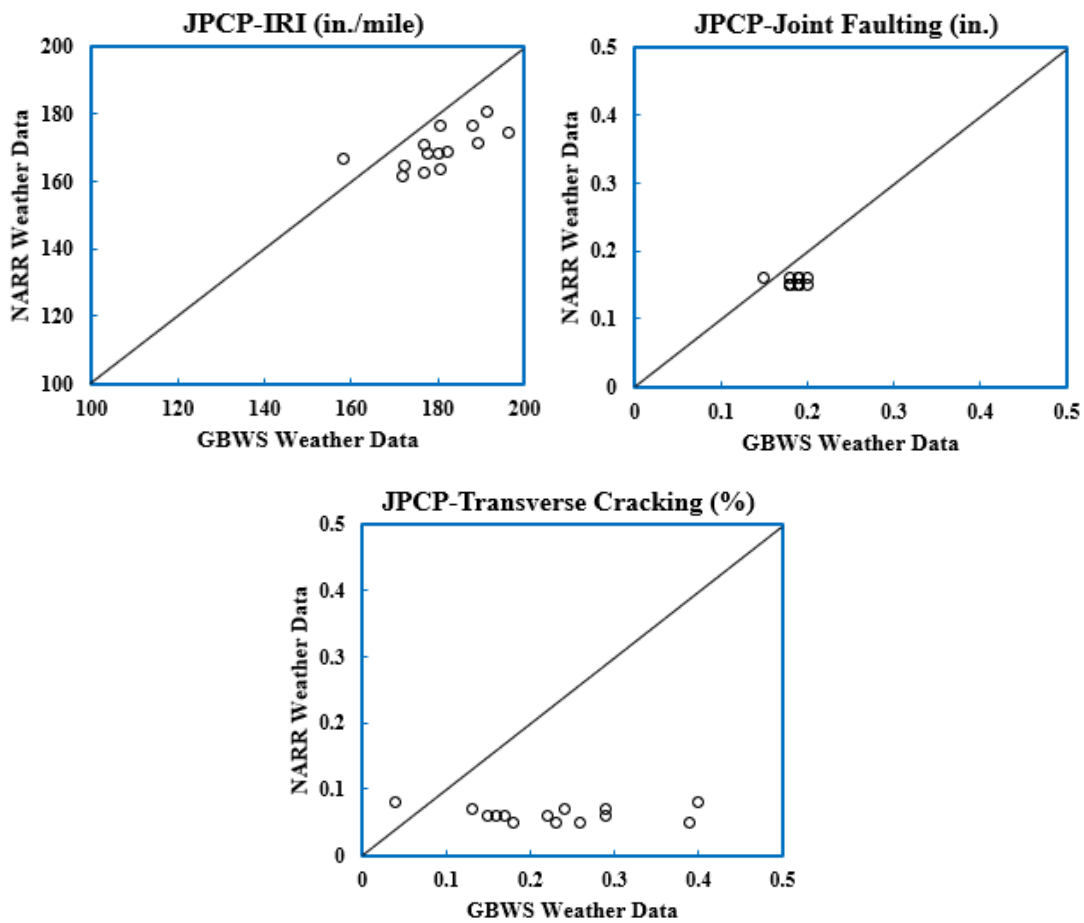


Figure 7. Comparison of rigid/JPCP predictions using GBWS vs. NARR weather data

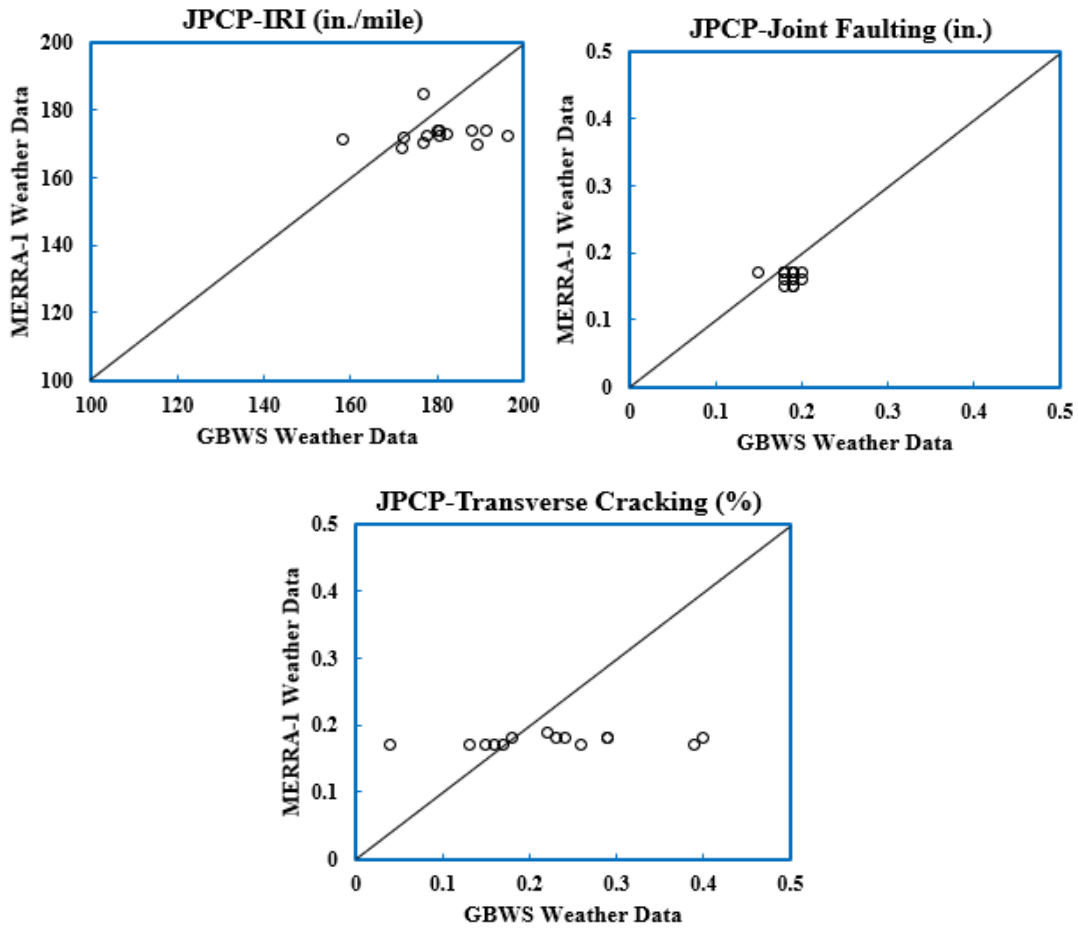


Figure 8. Comparison of rigid/JPCP predictions using GBWS vs. MERRA-1 weather data

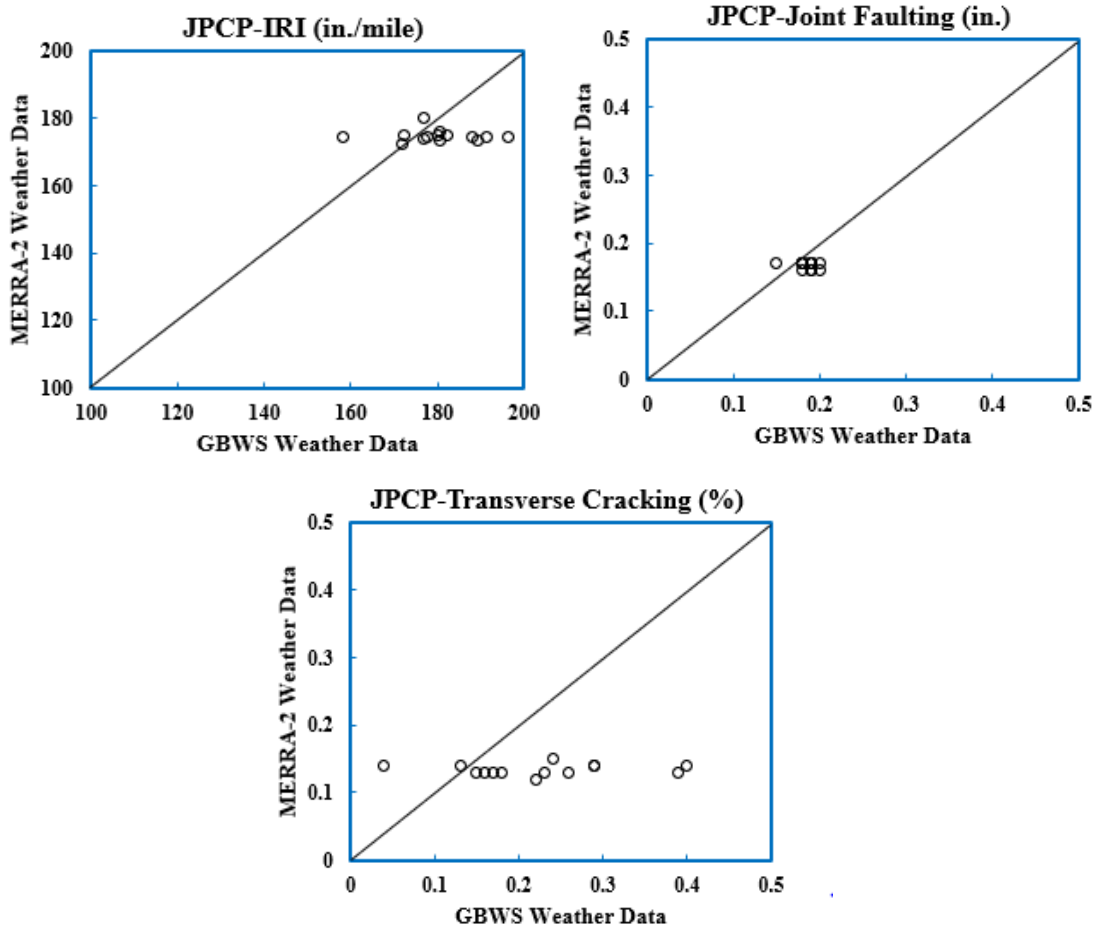


Figure 9. Comparison of rigid/JPCP predictions using GBWS vs. MERRA-2 weather data

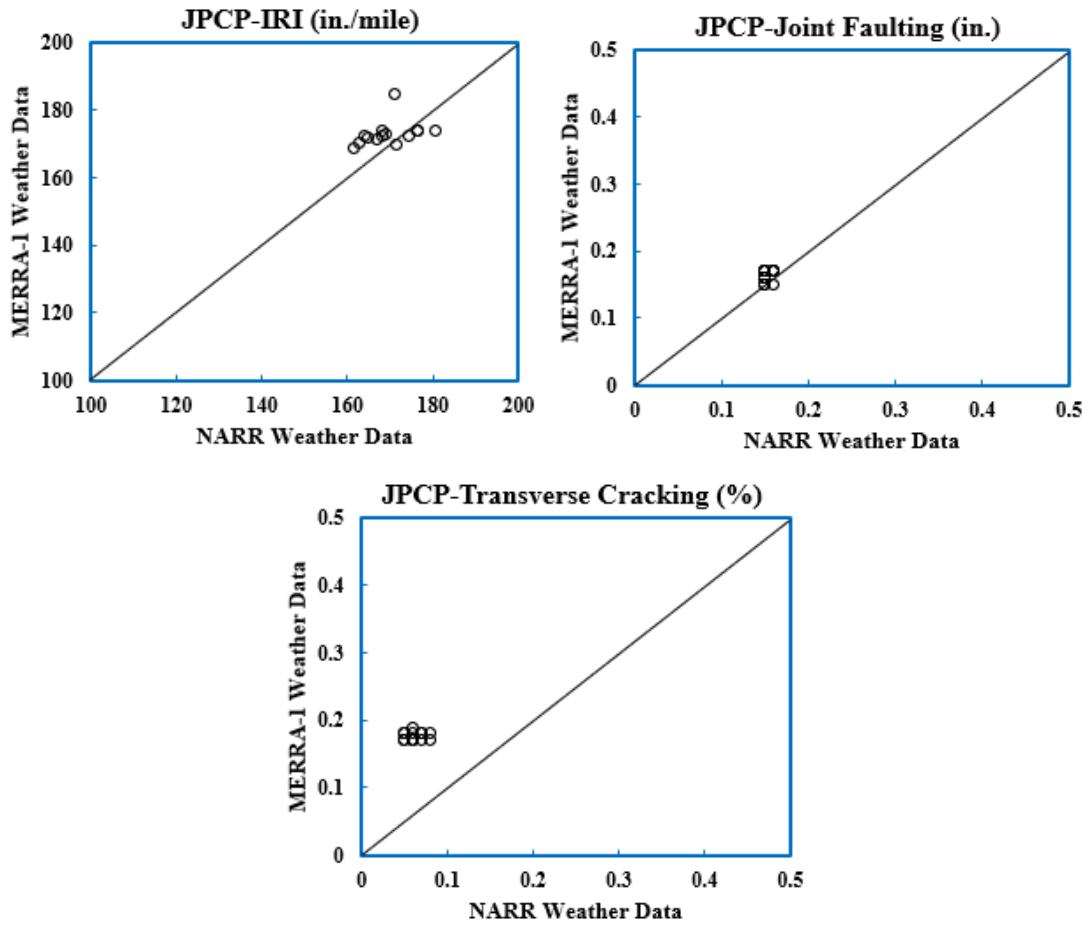


Figure 10. Comparison of rigid/JPCP predictions using NARR vs. MERRA-1 weather data

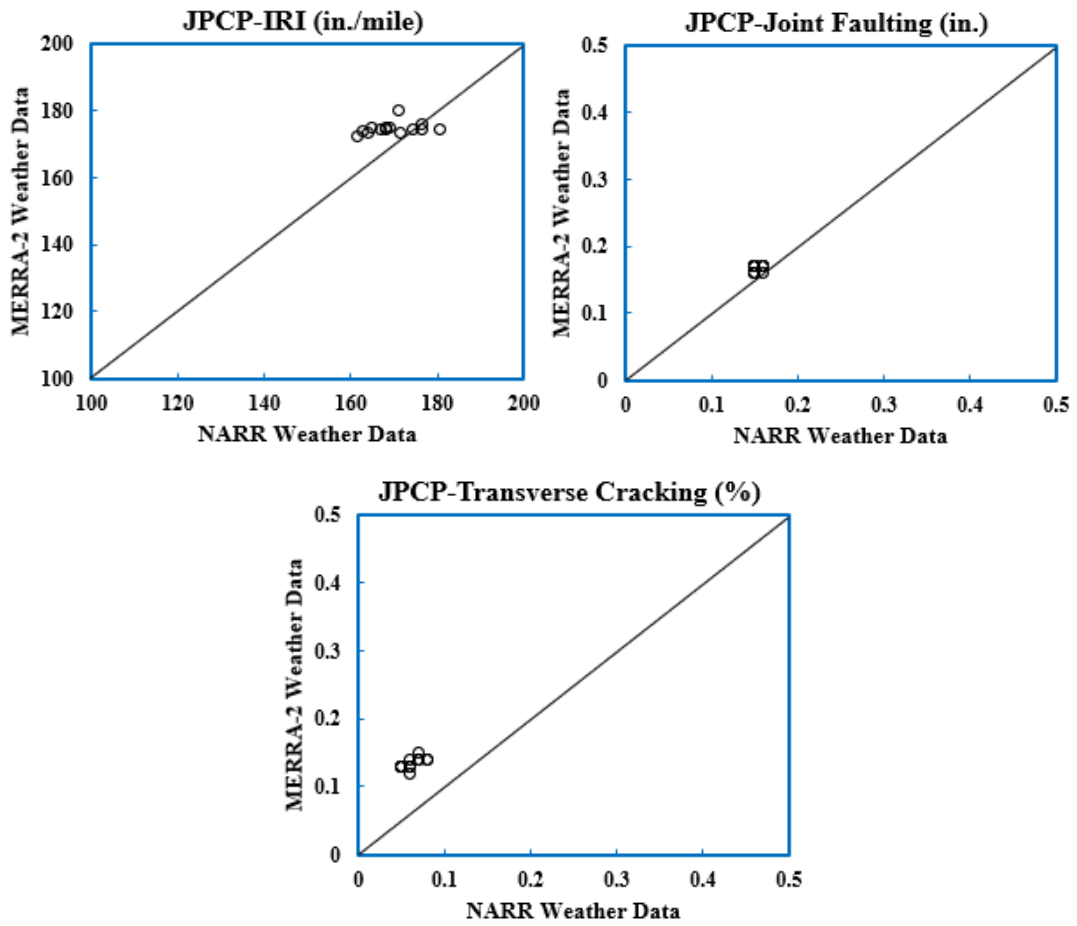


Figure 11. Comparison of rigid/JPCP predictions using NARR vs. MERRA-2 weather data

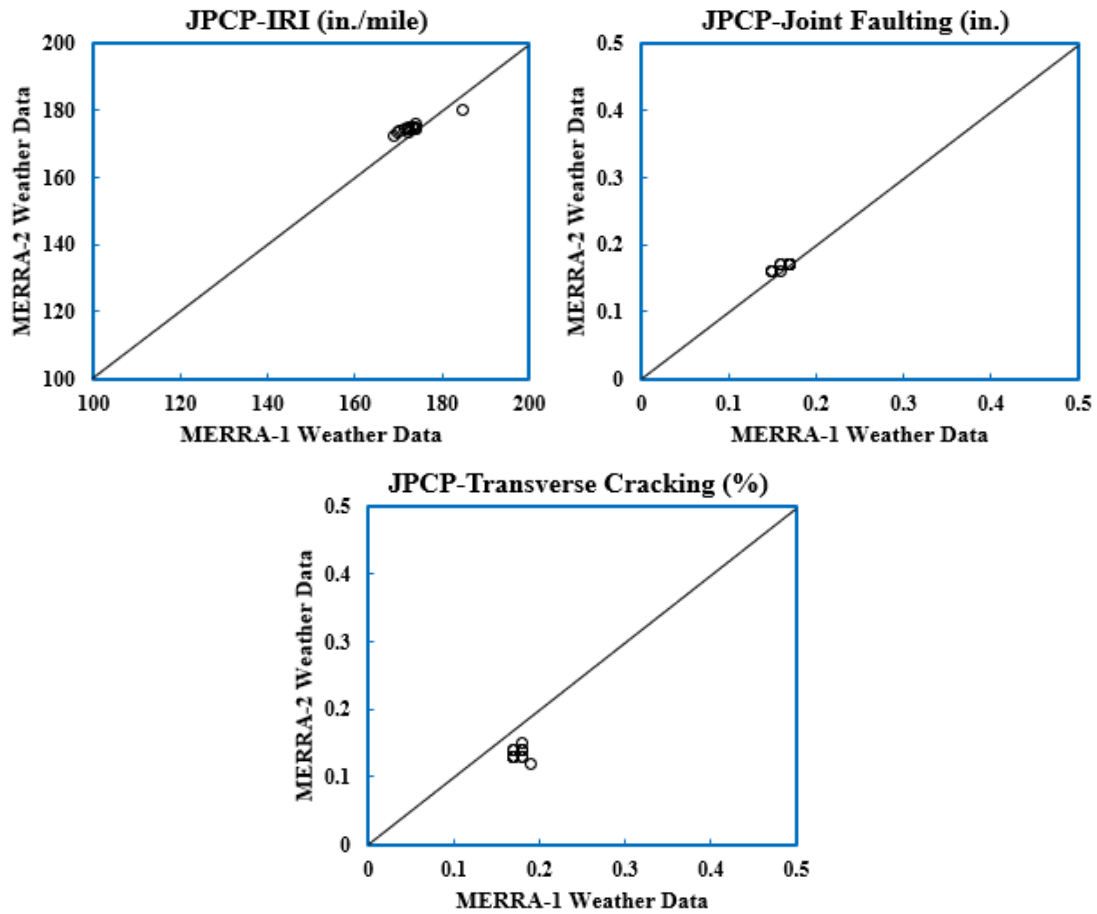


Figure 12. Comparison of rigid/JPCP predictions using MERRA-1 vs. MERRA-2 weather data

For the JPCP predictions, disagreement was observed among the climate sources in the cases of IRI and transverse cracking. It was expected for IRI as the prediction of IRI in JPCPs has been found the most sensitive to slight climate data changes compared to other distresses (Cetin et al. 2015). In the case of transverse cracking, PMED reported the prediction within 0 to 0.5% precision, which indicates the climate influence in transverse cracking is negligible.

Comparison of Composite Pavement Predictions

Figure 13 through Figure 18 show the comparison of AC-over-JPCP pavement distresses predicted by PMED using GBWS vs. NARR vs. MERRA-1 vs. MERRA-2 data.

With Iowa’s composite pavements, for IRI, AC layer rutting, alligator cracking, and JPCP transverse cracks, very good agreement was observed among the different climate data sources with very few exceptions. However, for total transverse cracking and thermal cracking, the GBWS predictions were significantly lower compared to predictions using NARR, MERRA-1, and MERRA-2.

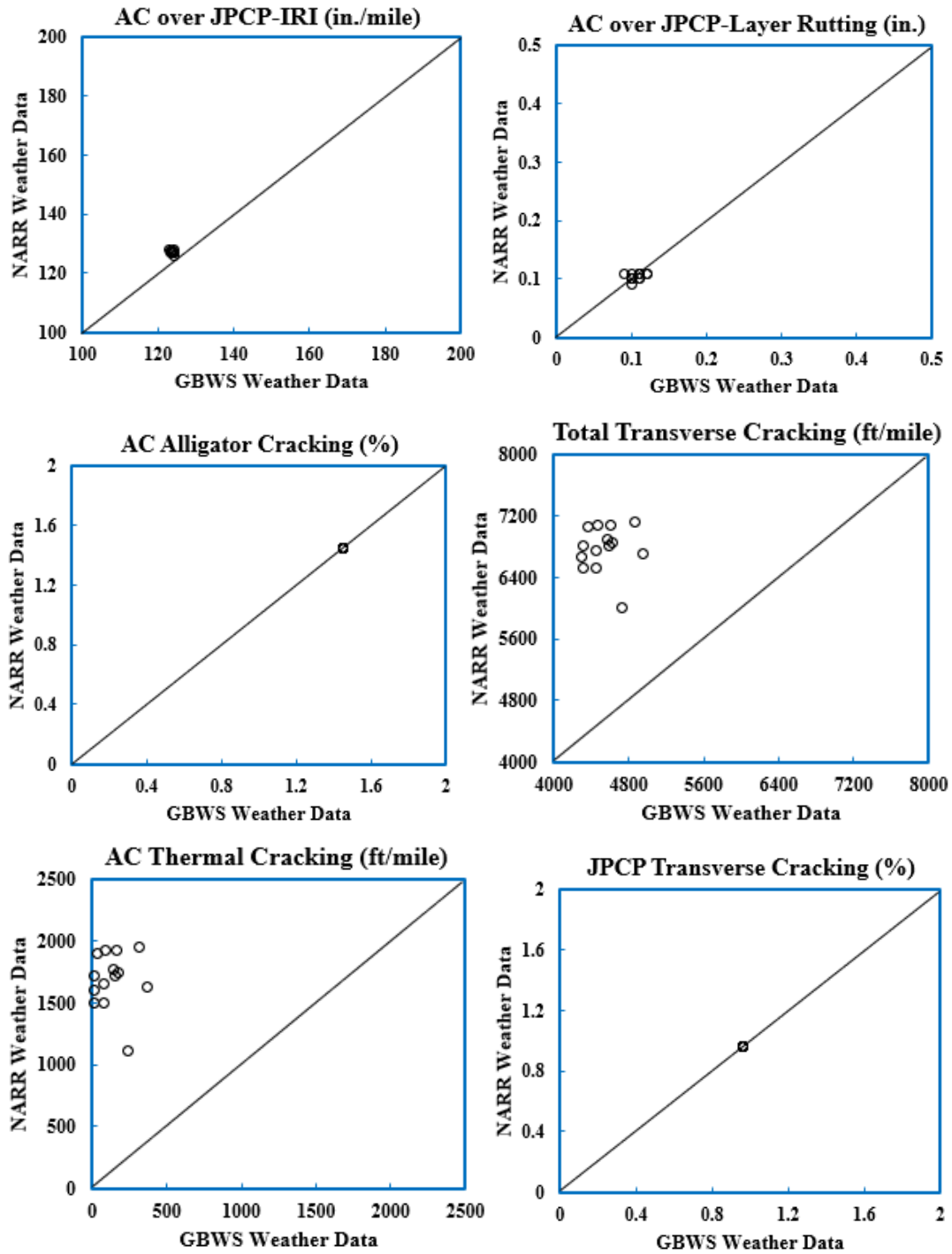


Figure 13. Comparison of AC-over-JPCP predictions using GBWS vs. NARR weather data

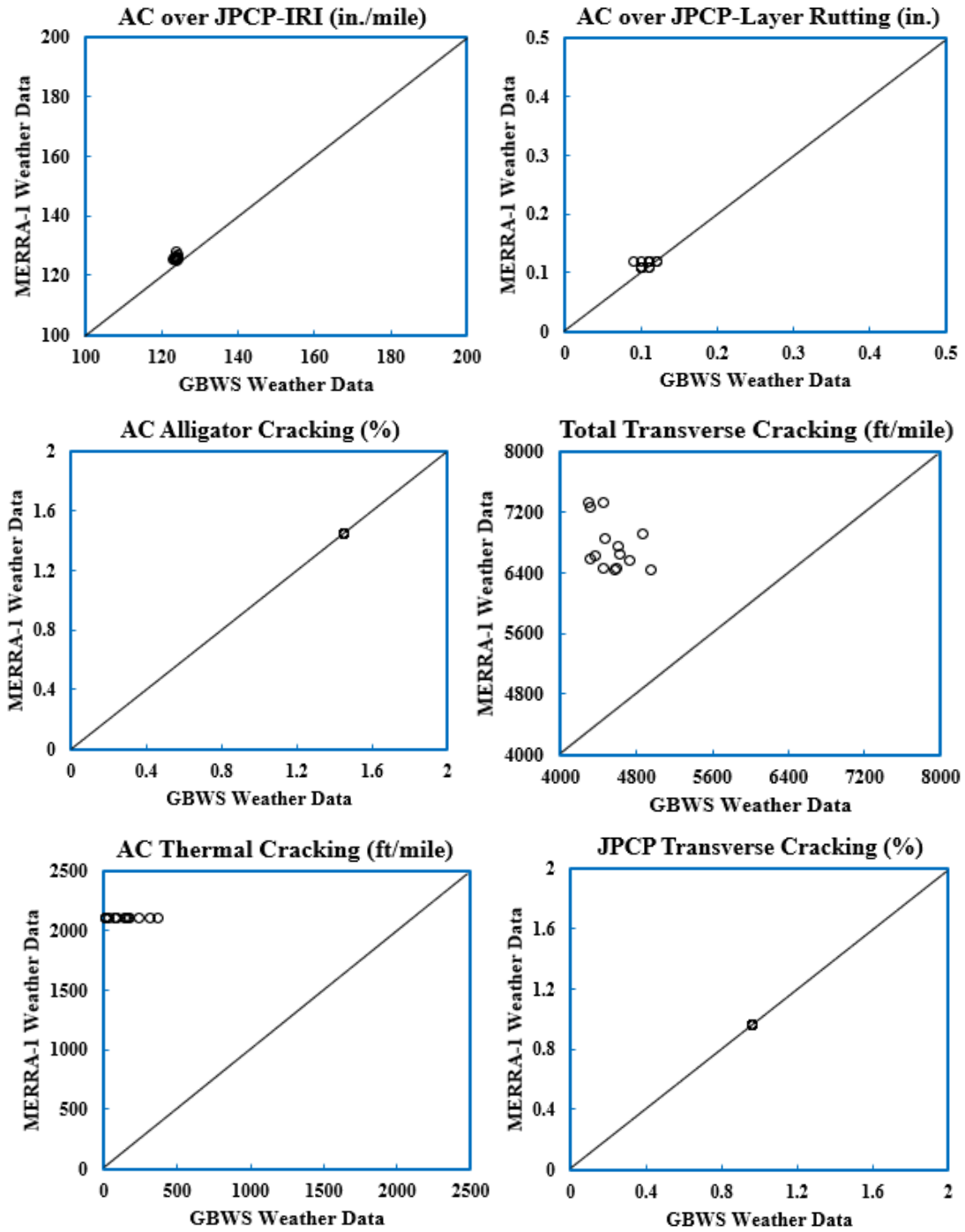


Figure 14. Comparison of AC-over-JPCP predictions using GBWS vs. MERRA-1 weather data

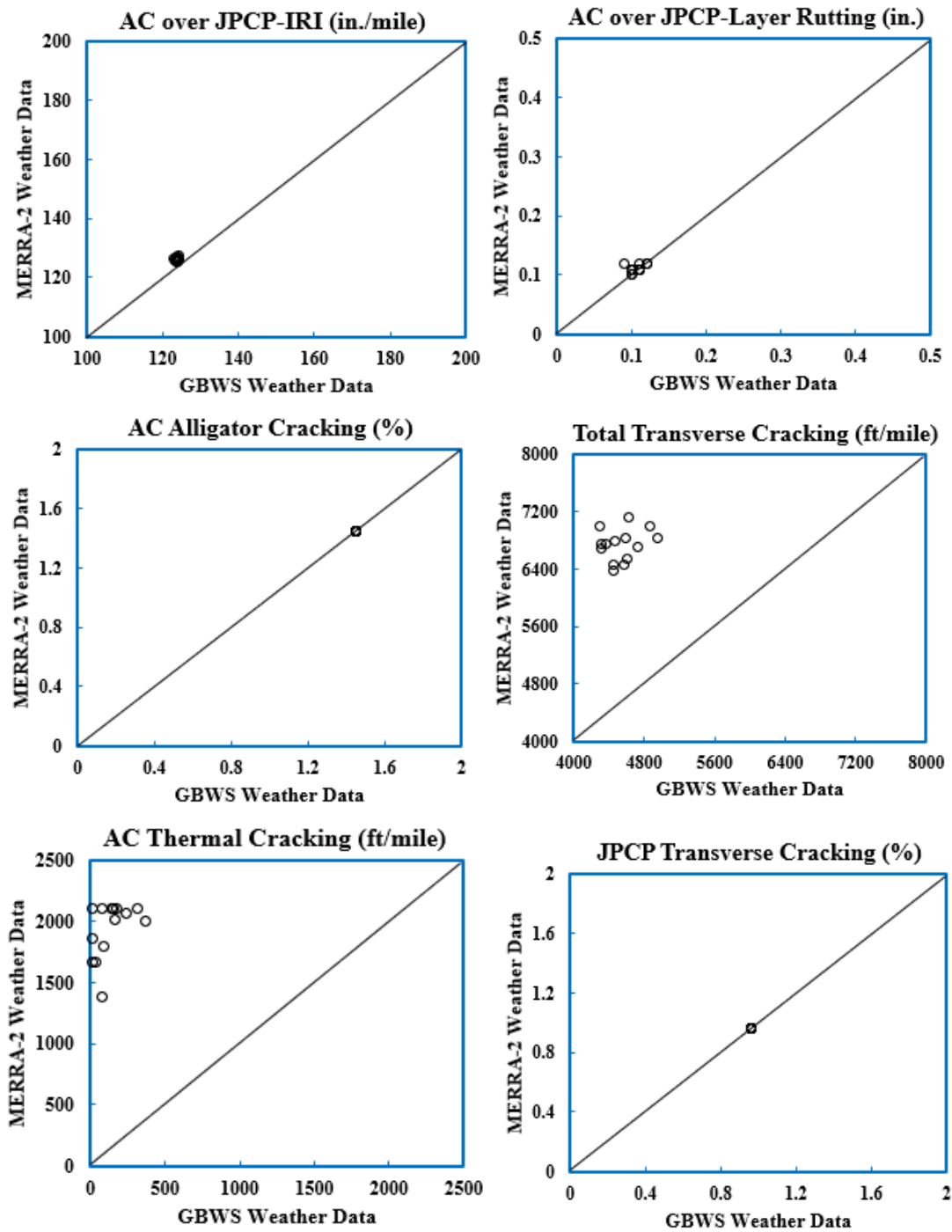


Figure 15. Comparison of AC-over-JPCP predictions using GBWS vs. MERRA-2 weather data

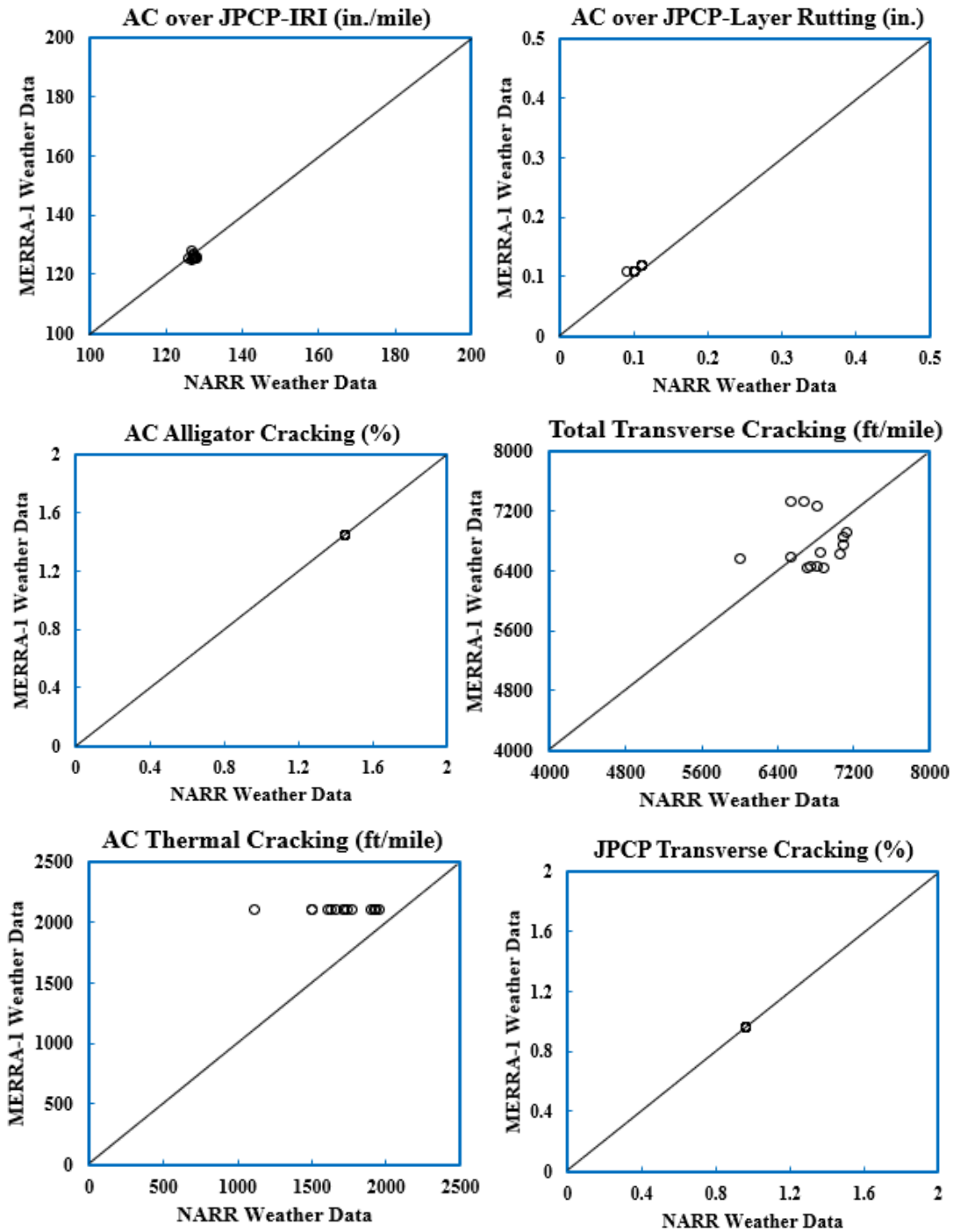


Figure 16. Comparison of AC-over-JPCP predictions using NARR vs. MERRA-1 weather data

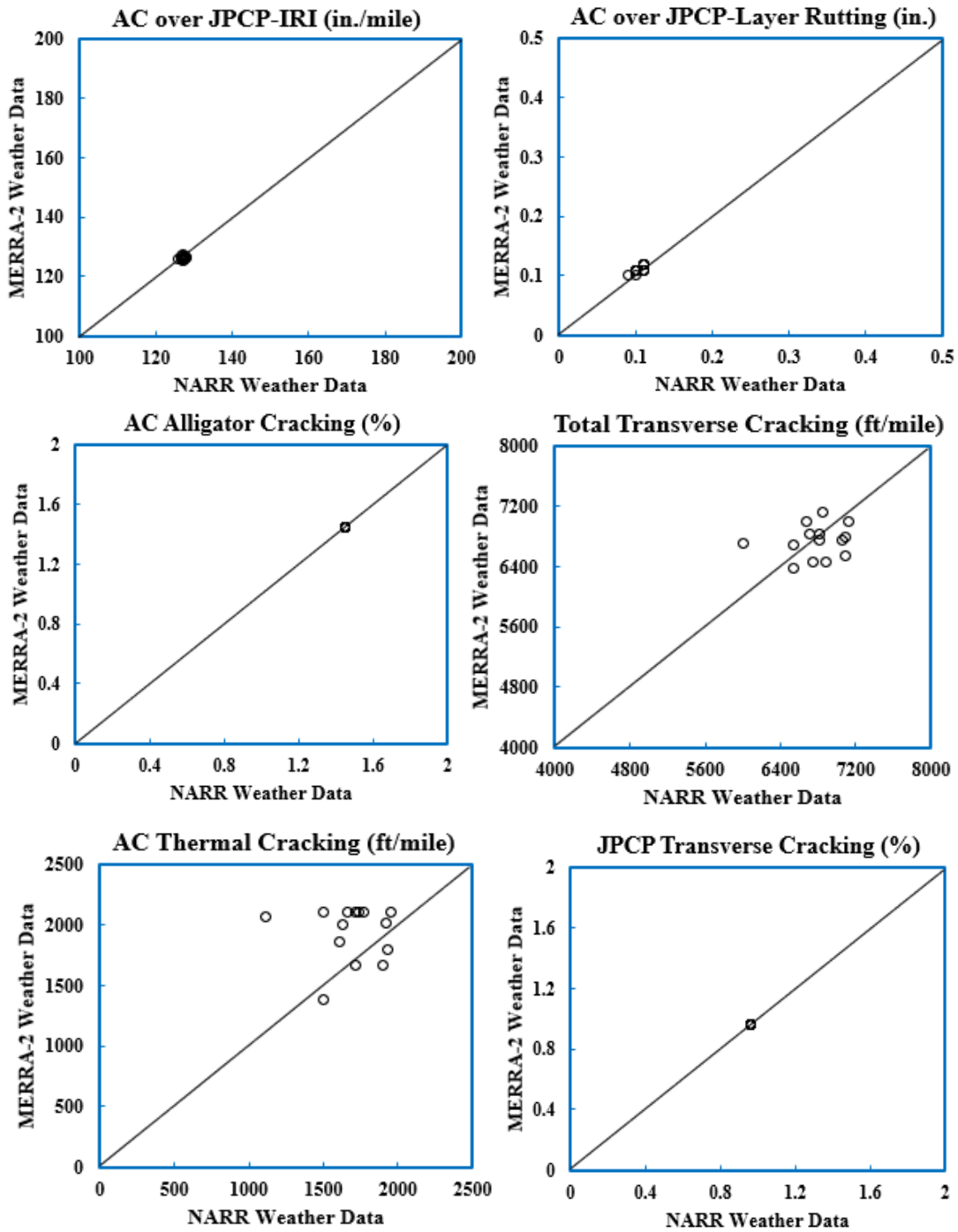


Figure 17. Comparison of AC-over-JPCP predictions using NARR vs. MERRA-2 weather data

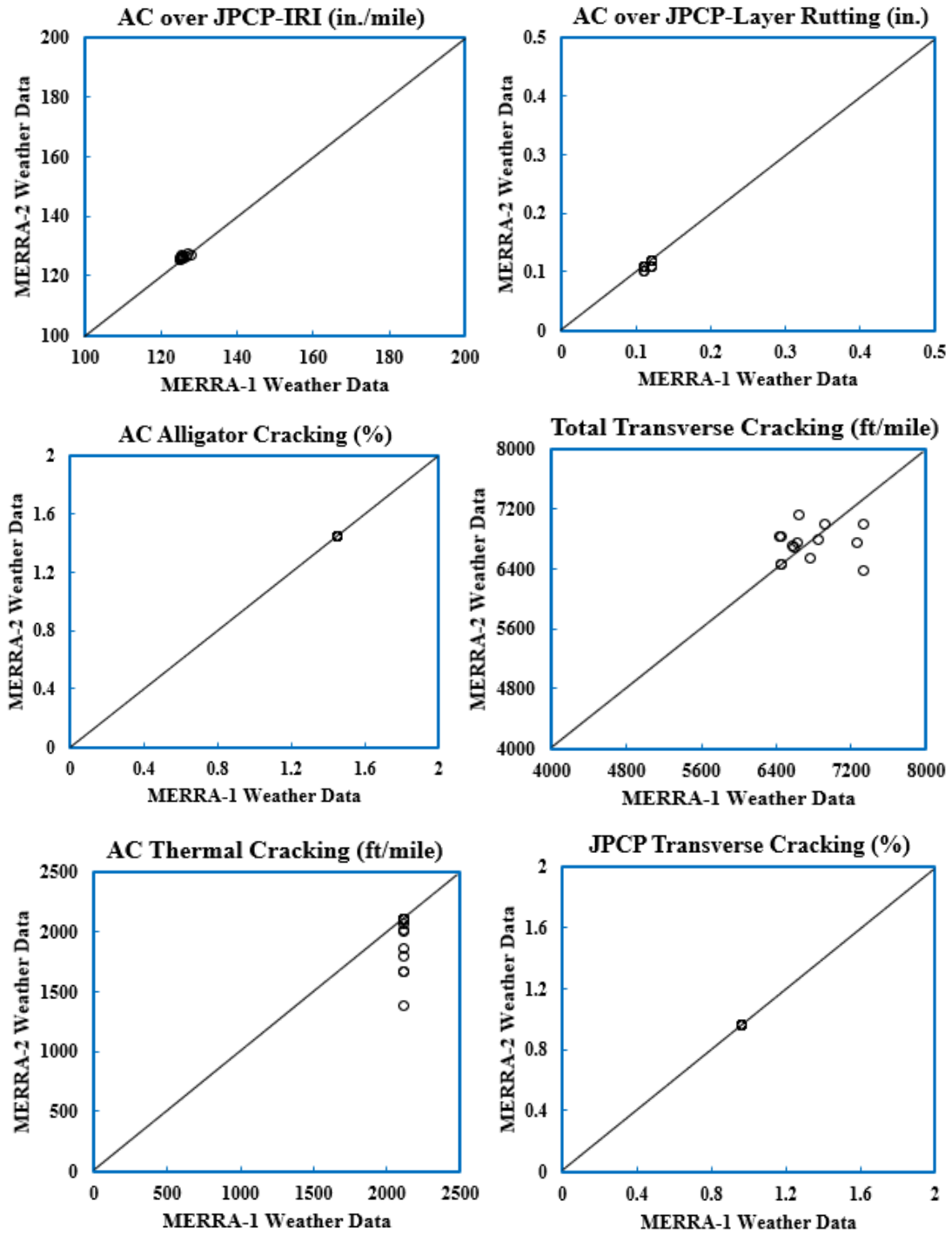


Figure 18. Comparison of AC-over-JPCP predictions using MERRA-1 vs. MERRA-2 weather data

Reason for Differences and Use of the Shortwave Radiation Regression Model

The four-way comparisons for GBWS, NARR, MERRA-1, and MERRA-2 climate data on AC, JPCP, and AC-over-JPCP pavements in Iowa show the significance of climate inputs to pavement performance predictions. The poor agreement in some cases indicates the existence of differences in the tested data sources' climate files.

Thus, the diurnal variation was analyzed for each of the four sources of climate input for all the tested locations for randomly selected days. This resulted in good agreement for all the climate inputs except for percent sunshine, which is one of the sensitive climate inputs for PMED's pavement distress predictions (Schwartz and Li 2010, Schwartz et al. 2011). Figure 19 shows the diurnal variation in percent sunshine at one of the Iowa locations for a 3-day period.

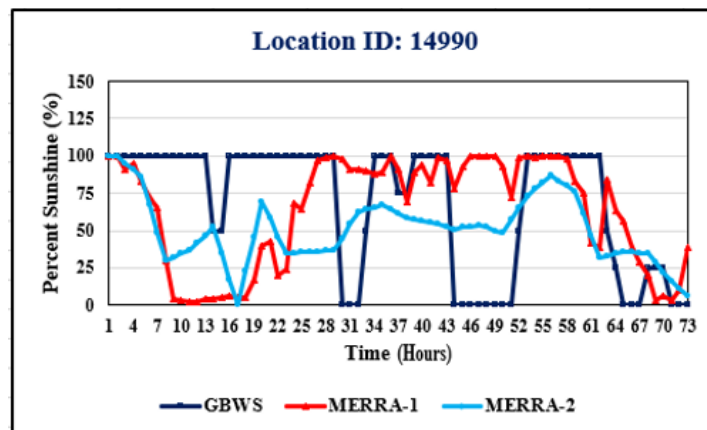


Figure 19. Diurnal variation in percent sunshine based on GBWS, MERRA-1, and MERRA-2 data

The agreement regarding diurnal variation in percent sunshine is obviously very poor across all these climate data sources. It was surprising to observe poor agreement for the same location even between the MERRA-1 and MERRA-2 percent sunshine data .

The PMED climate model has been using percent sunshine data since the release of its first version. The PMED percent sunshine inputs compute daytime SSR and both daytime and nighttime longwave radiation. The software's primary function requires the time of the day and relative percent cloud cover for the evaluation of percent sunshine. (Zero percent cloudiness represents one hundred percent sunshine, while one hundred percent cloudiness represents zero percent sunshine.)

The existence of differences in percent sunshine across the various climate data sources is due to a variety of reasons. The collected percent sunshine measurements from the GBWS are indirectly estimated from the cloudiness percentage using a laser ceilometer and generally cover a limited altitude range. Moreover, the percent cloudiness in the GBWS data is categorized in quartiles as 0%, 25%, 50%, 75%, or 100% (Gopiseti et al. 2019). This does not provide a direct estimate of either shortwave or longwave radiation.

To overcome such issues and improve the accuracy of PMED performance predictions, the shortwave radiation regression model was used in this study to derive a “synthetic” percent sunshine by using SSR estimates from MERRA-1 and MERRA-2. Equation 1 shows the regression model used in PMED to estimate the SSR (Gopiseti et al. 2019, Schwartz et al. 2015).

$$Q_i = R^* \left[A + B \frac{Sc}{100} \right] \quad (1)$$

where:

Q_i = incoming shortwave radiation received at ground level

R^* = shortwave radiation incident on a horizontal surface at the top of the atmosphere

A, B = empirical constants that account for diffuse scattering and adsorption by the atmosphere ($A= 0.202$ and $B=0.539$)

Sc = average percent sunshine

The average value of percent cloudiness at night is computed as $100 - Sc$ (Schwartz et al. 2015). The synthetic percent sunshine estimates generated through this approach were used to replace PMED’s built-in percent sunshine values. Through the use of synthetic percent sunshine, the MERRA-1 and MERRA-2 comparisons improved, and all the resulting pavement performance predictions were very close to the lines of equality, as shown in Figure 20, Figure 21, and Figure 22 for flexible, rigid, and AC over JPCP, respectively.

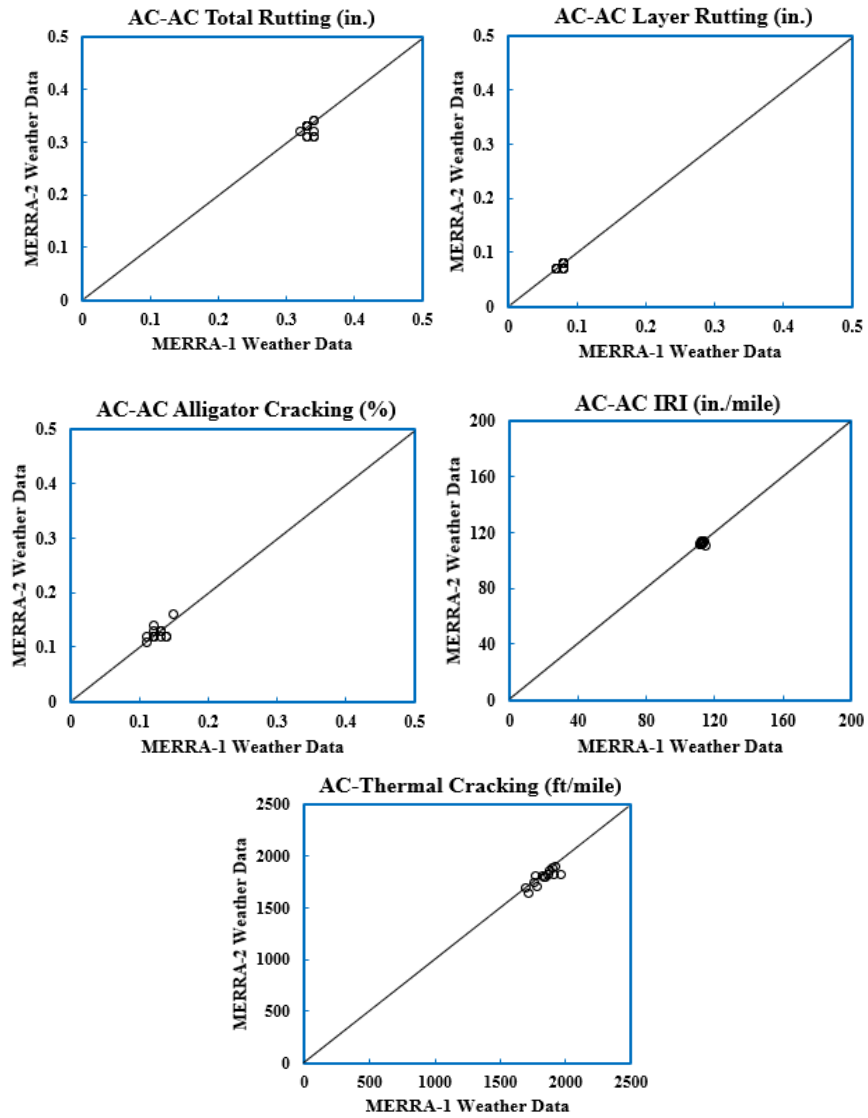


Figure 20. Comparison of flexible/asphalt concrete predictions for MERRA-1 vs. MERRA-2 using a back-calculated percent sunshine

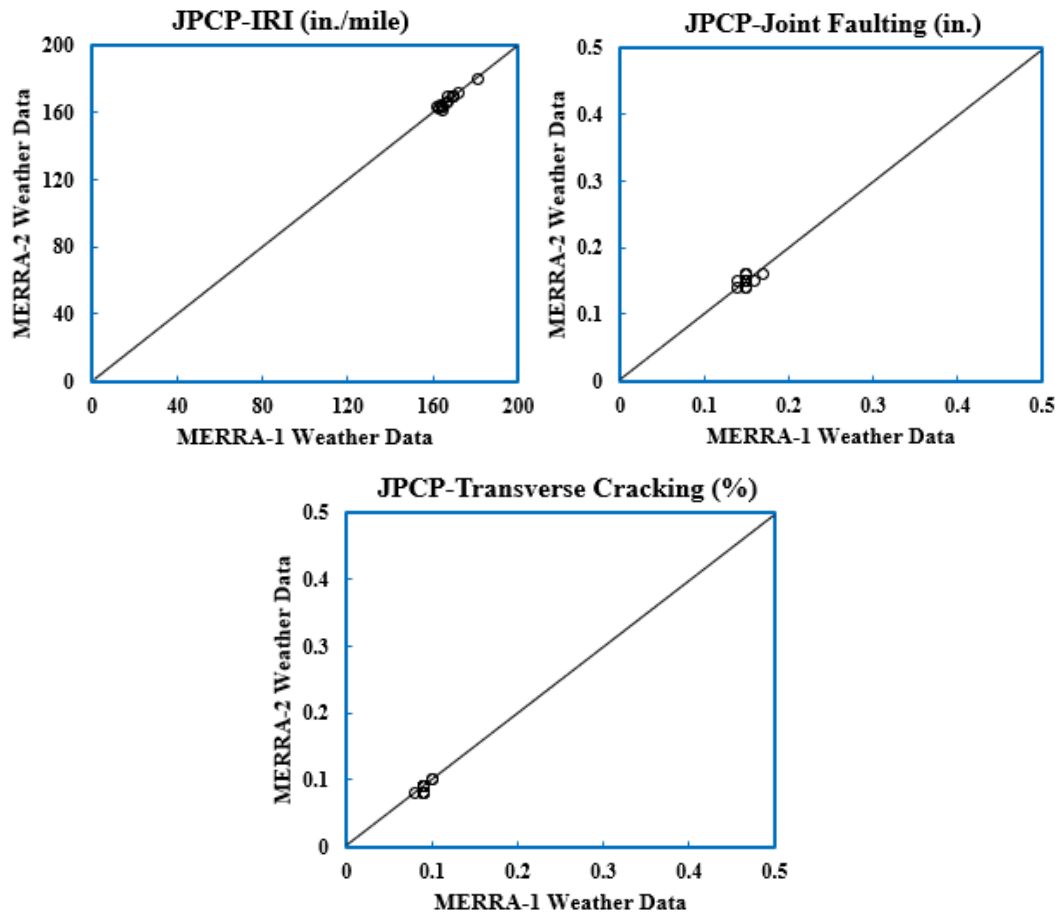


Figure 21. Comparison of rigid/JPCP predictions for MERRA-1 vs. MERRA-2 using a back-calculated percent sunshine

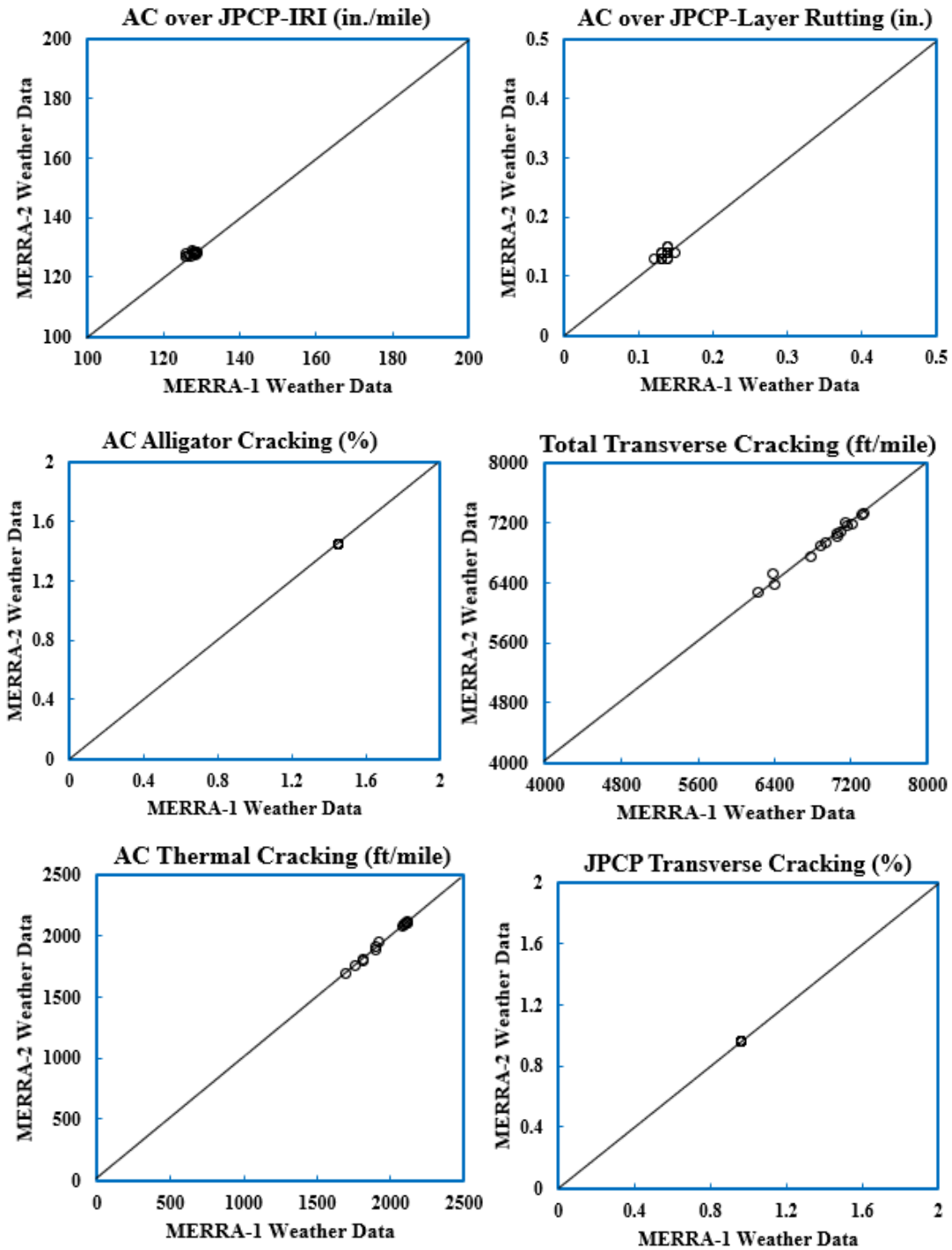


Figure 22. Comparison of AC-over-JPCP predictions for MERRA-1 vs. MERRA-2 using a back-calculated percent sunshine

Summary of Key Findings

The primary objective of this research study was to evaluate the climate data produced from various data sources as relates to their use in the PMED software. Its findings are summarized below.

- Four-way comparisons of the PMED pavement performance predictions across the different climate data sources for Iowa showed disagreements in distresses, which are very sensitive to climate inputs.
- To use the MERRA-1 and MERRA-2 SSR values, a synthetic percent sunshine was back-calculated, since PMED accepts percent sunshine as one of its inputs only in the hourly format. This back-calculated synthetic percent sunshine was then used to replace the actual percent sunshine values embedded in the software. Comparison of predicted distresses using the synthetic percent sunshine found that the back-calculated values eliminated almost all the discrepancies among the distresses predicted across climate data sources.

Recommendations

Based on these findings, it is recommended the percent sunshine model currently being used in the PMED software be reevaluated. The authors further recommend incorporating SSR into PMED as a direct independent input, since SSR can be directly accessed through MERRA in PMED's required hourly format from 1979 to the present. The use of SSR as a direct independent input would help SHAs to improve their pavement designs and could increase the service life of their pavements.

EVALUATION OF PMED'S NEW REFLECTIVE CRACKING MODEL

Background

Of the many updates to the PMED software, one of the major additions is inclusion of a mechanistic-based reflective cracking model developed under National Cooperative Highway Research Program (NCHRP) Project 1-41 titled Models for Predicting Reflection Cracking of Hot-Mix Asphalt Overlays (Lytton et al. 2010).

Prior to development of any implementation plan involving new models, it is very important to perform sensitivity analysis to determine the sensitivity indices of MEPDG and PMED design inputs and material properties; such indices can vary from state to state depending on local conditions, especially those related to climate, that can have huge impacts on pavement designs (Hossain et al. 2018, Cetin et al. 2015, Gopiseti 2017, Hossain et al. 2017, Gopiseti et al. 2018).

Researchers across the country have over the years reported several sensitivity studies using the MEPDG and PMED software. Kim et al. (2005) conducted a study to evaluate the relative sensitivity of MEPDG input parameters with respect to asphalt cement concrete (ACC) properties, traffic, and climate inputs based on field data from two existing Iowa flexible pavement systems. The sensitivities of the MEPDG performance predictions (longitudinal cracking, alligator cracking, thermal cracking, rutting, fatigue cracking, and smoothness) were studied by either varying a single input parameter or by varying two input parameters at a time. The results showed that binder PG grade, volumetric properties, climate, AADTT, and type of base were the most sensitive inputs to pavement performance measures. Alligator cracking was observed to be the least critical distress, especially with the relatively thicker pavement structures considered in this study. The complete findings of this study provided pavement designers with a better understanding of the design parameters that most affect certain types of pavement distress.

Guclu et al. (2009) conducted sensitivity studies on jointed plain concrete pavement (JPCP) and continuously-reinforced concrete pavement (CRCP) in Iowa using the MEPDG software (v0.7, v0.9, and v1.0), with results from different versions of the software indicating that distresses predicted through MEPDG v0.9 and v1.0 are more sensitive to inputs than those predicted by v0.7. This confirms that updates made in the MEPDG distress models have had a significant impact both on pavement performance prediction and on the need for new sensitivity analysis after the release of every new version of the software.

Schwartz et al. (2011) performed a comprehensive study to determine the sensitivity of pavement performance predicted by the MEPDG with respect to design input values. Extensive one-variable-at-a-time (OAT) sensitivity analyses and comprehensive global sensitivity analyses (GSA) were performed for five pavement types under three traffic levels and five climate conditions, using design inputs that included traffic volume, layer thicknesses, material properties, groundwater depth, geometric parameters, etc. Detailed findings for each specific pavement type and distress type were reported.

Ceylan et al. (2013a) performed a quantitative and qualitative sensitivity analysis for two types of JPCP base cases: (1) new construction on a granular base (i.e., a new JPCP case) and (2) new construction/reconstruction on both stabilized foundations and rehabilitated underlying asphalt/concrete layers. To evaluate their sensitivity with respect to predicted distresses in the MEPDG software, three traffic levels in five climate zones served as base cases, with findings that revealed that sensitivities of the design inputs with respect to the portland cement concrete (PCC) surface layer were most important for JPCP types and related distresses. That study also suggests that, in using the MEPDG software in JPCP design, particular caution is required in selecting PCC slab design features and PCC material properties.

Ceylan et al. (2014) further used comprehensive local sensitivity analyses (LSA) and global sensitivity analyses (GSA) methodologies to evaluate CRCP performance predictions using the MEPDG software under various climate and traffic conditions. Two response surface modeling (RSM) approaches, multivariate linear regressions (MVLN), and artificial neural networks (ANNs or NNs), were developed to model the GSA results for the evaluation of MEPDG CRCP input sensitivities across the entire problem domain. The results from that study suggest the use of ANN-based RSMs can produce robust and accurate representations of the complex relationships between MEPDG input variables and pavement distress outputs and can also capture the variations in sensitivities across the problem domain.

Brink et al. (2013) performed detailed preliminary OAT sensitivity analysis to evaluate the impact of various design inputs on pavement performance predictions by the MEPDG software for various pavement rehabilitation options. Full factorials were further designed to determine two-way interactions and statistically significant main effects. The most important variables impacting the MEPDG software's predicted performance for JPCP rehabilitation pavement designs were identified through the OAT analysis.

Cetin et al. (2018) conducted and reported comprehensive sensitivity analysis results for rural asphalt concrete (AC) and JPCP sections representing a variety of climate zones and traffic levels across South Dakota (i.e., located in Rapid City, Sioux Falls, Pierre, and Mobridge).

Although numerous sensitivity analysis results have been reported over the years, none have reported the sensitivity to MEPDG and PMED design inputs and material properties with respect to reflective cracking distress. Earlier versions of the MEPDG and PMED included an empirically-based reflective cracking model, making it challenging to perform sensitivity studies. However, since a mechanistically-based reflective cracking model has been incorporated into the latest versions of the software, this study focuses on performing a comprehensive sensitivity analysis potentially useful for state highway agencies (SHAs) and departments of transportation (DOTs) in modifying their pavement designs, especially in states where reflective cracking has been of major concern.

Objective

The objective of this study was to identify the set of PMED design inputs and material properties most sensitive with respect to reflective cracking distress at six selected locations in different climate zones across the United States. The specific objectives are as follows:

- Determining the set of most important input variables and suitable ranges for these variables
- Evaluating all design inputs based on their associated levels of sensitivity

AC-over-JPCP sections were considered for this study and analysis was performed using the PMED software (v2.5.2). Since PMED requires a broad set of inputs for pavement designs, and it is often time-consuming to evaluate each input required by the software, 25 inputs assumed to have a major impact based on the results from previous studies were shortlisted, and then initial runs were performed using the PMED software (Schwartz et al. 2011).

PMED's New Reflective Cracking Model—Overview and Literature Review

One of the primary distress types observed in AC overlays is reflective cracking, which mainly occurs because of existing cracks or joints in the overlaid pavement surface layer growing through the overlay (Tsai et al. 2010). This growth is induced by bending or shearing actions resulting from traffic loads or temperature changes and is influenced by traffic volume, daily and seasonal temperature factors, pavement structure and condition, hot-mixed asphalt (HMA) mixture properties, and the degree of load transfer at joints and cracks.

The penetration of moisture and water through reflective cracks can result in premature failure of the aggregate base and subgrade, so such penetration must be prevented. Under NCHRP Project 1-41, mechanistic-based models for predicting reflective cracking in AC overlays were developed along with associated computational software for use in mechanistic-empirical procedures for overlay design and analysis. The approach employed to forecast reflective cracking combines finite-element modeling and fracture mechanics, reflecting a mechanistic philosophy based on Paris' law for modeling crack propagation (Lytton et al. 2010).

Tsai et al. (2010) presented a development process and computed results of a reflective cracking design method for predicting the reflective cracking of HMA overlays over AC or JPCP. The study's results were calibrated to observed reflective cracking distress in more than 400 pavement test sections in most of the states of the United States. The study's mechanistic model was programmed to predict the reflective cracking life expectancy of a specified HMA overlay related to bending and shearing traffic stresses and thermal stresses. The study results revealed that the relationship between the mechanistically-computed service life of an asphalt overlay and the appearance, extent, and severity of observed reflective cracking in the field depends on the characteristics of the pavement structure, the overlay structure, and the traffic and climatic conditions at the project location.

Yunhe et al. (2011) performed a comprehensive survey and an in-depth analysis of the main factors influencing reflective cracking and further described the effects of these factors on reflective cracking in relation to a semi-rigid base to seek methods for effective prevention of this type of distress at its early stage of formation.

PMED requires many computations by finite-element models to simulate crack propagation and support reflective cracking prediction throughout a pavement's design life. To improve the computational speed and efficiency of PMED, ANNs have been further tested for use in developing surrogate models. Ceylan et al. (2011) adopted an ANN methodology to model the stress intensity factor (SIF) because cracks grow upward through an HMA overlay as a result of both load and thermal effects whether with or without reinforcing interlayers. Nearly 100,000 runs of a finite-element program were used to develop ANN-based surrogate models to calculate SIFs at the tips of reflective cracks for a wide variety of crack lengths and pavement structures, and the coefficient of determination (R^2) of all the developed ANN models except for one was higher than 0.99.

Titus-Glover et al. (2016) adapted NCHRP 1-41 reflective cracking models for the design of new semi-rigid pavements using the PMED software. Their significant adaptations to the NCHRP models included (1) replacement of the NCHRP Project 1-41 AC fracture properties (A and n) and tensile strength computational models with PMED-equivalent models to ensure compatibility between the new reflection-cracking models and existing AC transverse "thermal" crack initiation and propagation models, (2) replacement of the NCHRP Project 1-41 default climate variables with real-time simulations of temperature profiles in the AC layer using the integrated climatic model in PMED, (3) replacement of ANN models for estimating SIF at the crack tip to ensure that the new ANN models covered the typical ranges of PMED inputs, and (4) modification of the NCHRP 1-41 approach for modeling crack propagation through the AC surface layer to make it compatible with the PMED philosophy.

Methodology

One-At-A-Time (OAT) Sensitivity Analysis

The OAT sensitivity analysis approach was used in this study, and values obtained were normalized by comparing changes in pavement performance with changes in inputs. The normalized sensitivity index (NSI) allows easy comparison with respect to the magnitude of the effect of input on pavement performance predicted by the PMED software. A large positive NSI value indicates that increasing the input will significantly increase the output value, and a negative NSI value indicates that increasing the input will decrease the output value. In contrast, an NSI value of zero represents no change in the predicted distress due to differences over the range of an input variable.

The NSI equation used in this study is shown below as Equation 2 (Schwartz et al. 2011).

$$NSI_{jk}^{DL} = \frac{(\Delta Y_j / DL_j)}{(\Delta X_k / X_k)} \quad (2)$$

where ΔY_j is the change in predicted distress j corresponding to a change in design input, ΔX_k is the change in design input k about the baseline, DL_j is the design limit of the distress j , and X_k is the baseline value of design input k . For example, consider the design limit (DL) of reflective cracking to be 2,000 ft/mile (378.78 m/km) and the NSI of reflective cracking to the JPCP layer thickness evaluated as -1.57, implying that an assumed 30% increase in JPCP layer thickness would decrease reflective cracking by $\Delta Y = (-1.57)(30\%)(2,000 \text{ ft/mile}) = -942 \text{ ft/mile}$ (-178.41 m/km).

In this study, based on results from previous sensitivity studies, 25 design inputs were shortlisted from the complete set of input variables required by PMED software (Schwartz et al. 2011), and initial trial runs were performed for these base cases. For analysis, the value of only one input variable at a time was varied in the PMED software to determine whether it significantly impacted the predicted distress value.

The outcome of this OAT analysis was the categorization of sensitivity levels for the six locations from different climate zones across the United States shown in Table 4.

Table 4. Overview of locations across the United States considered for sensitivity analysis

MERRA Cell ID	Location	Climate Zone	Latitude	Longitude
145867	Des Moines, Iowa	Cold-Wet	41.586	-93.624
130911	Orlando, Florida	Hot-Wet	28.538	-81.379
136622	Phoenix, Arizona	Hot-Dry	33.448	-112.074
148208	Portland, Maine	Cold-Wet	43.601	-70.474
153932	International Falls, Minnesota	Cold-Dry	48.602	-93.404
137188	Los Angeles, California	Temperate	34.052	-118.243

NSI Ranking

The absolute maximum NSI is the largest determined NSI value (in an absolute value sense) for the design input in any tested base case. The ranges for maximum absolute NSI values were categorized as very sensitive (greater than 1), sensitive (between 0.1 and 1), and insensitive (less than 0.1).

Test Matrix and Input Ranges

To perform sensitivity analysis, an initial test matrix with variable design input parameters was formed. Three base cases representing varying traffic levels (low, medium, and high) related to layer thicknesses were initially considered, as shown in Table 5.

Table 5. Base cases with varying traffic levels

Traffic level	Low Traffic Case			Medium Traffic Case			High Traffic Case		
	Base	Lower	Upper	Base	Lower	Upper	Base	Lower	Upper
AADTT	1,000	500	5,000	7,500	5,000	10,000	25,000	20,000	30,000
AC Thick., in.	2	1.5	3	3	2	4	6	4	8
JPCP Layer Thick., in.	8	4	12	10	5	14	12	6	16
Base Thick., in.	4	2	6	6	3	9	8	5	12

For example, a pavement section with a higher traffic level would generally require a thicker pavement layer. Table 6 gives a summary of the complete major design inputs shortlisted for the PMED software analyses.

Table 6. Overview of PMED design inputs and layer properties

Input Parameter	Input Value
Design life	20 years
Reliability	50% for all distresses
AADTT category	Principal arterials—Interstates and defense routes
Number of lanes in design direction	2 for low traffic/3 for medium and high traffic
Truck direction factor	50
Truck lane factor	75 for low traffic/55 for medium traffic/50 for high traffic
First layer material type	Asphalt concrete
Second layer material type	Portland cement concrete
Base type	Granular base
Subgrade material type	Soil

Back-Calculation of Reflective Cracking Distress

Even though the PMED software now incorporates a reflective cracking model into its designs, it does not directly report reflective cracking distress as one of its pavement performance prediction factors in its output file but instead merges it with thermal cracking distress and reports the result as total transverse cracking, as shown in Figure 23.

Performance Criteria	Limit	Reliability	Report Visibility
Initial IRI (in/mile)	63		<input checked="" type="checkbox"/>
Terminal IRI (in/mile)	172	90	<input checked="" type="checkbox"/>
AC top-down fatigue cracking (ft/mile)	2000	90	<input checked="" type="checkbox"/>
AC bottom-up fatigue cracking (% lane area)	25	90	<input checked="" type="checkbox"/>
AC thermal cracking (ft/mile)	1000	50	<input checked="" type="checkbox"/>
Permanent deformation - AC only (in)	0.25	90	<input checked="" type="checkbox"/>
AC total transverse cracking: thermal + reflective (ft/mile)	2500	90	<input checked="" type="checkbox"/>
JPCP transverse cracking (percent slabs)	15	90	<input checked="" type="checkbox"/>

Figure 23. PMED output information for AC over JPCP (PMED v2.5.2 screenshot)

The total transverse cracking output in the PMED software is defined as Total transverse cracking (ft/mile) = total reflective cracking (ft/mile) + total thermal cracking (ft/mile). It also reports Total thermal cracking (ft/mile) as a separate output, as shown in Figure 23. Therefore, to evaluate the sensitivity of total reflective cracking (ft/mile) specifically, simple back-calculation was performed by subtracting the total thermal cracking value from the total transverse cracking value over the same design period.

Summary of OAT Sensitivity Analysis Approach

Table 7 depicts the complete test matrix considered for the OAT sensitivity analysis.

Table 7. Test matrix for OAT sensitivity analysis

Input Parameter	Base Case	Lower Case	Upper Case
AC Layer Input Parameters			
AC Surface Shortwave Absorption	0.85	0.80	0.98
Delta in AC Sigmoidal Curve	2.834	× 0.99	× 1.01
Alpha in AC Sigmoidal Curve	3.904	× 0.998	× 1.01
Effective Binder Content in AC, %	10.14	× 0.9	× 1.1
Air Voids in AC, %	6.54	× 0.9	× 1.1
Tensile Strength at -10°C, psi	500	100	2,000
Aggregate Coefficient of Contraction in AC, in./in./°F	5×10^{-6}	2×10^{-6}	7×10^{-6}
JPCP Layer Input Parameters			
Design Lane Width, ft	12	10	14
Joint Spacing, ft	15	10	20
Dowel Diameter, in.	1.2	1.0	1.5
Tied PCC Load Transfer Equivalent (LTE), %	50	25	75
PCC Unit Weight, pcf	150	140	160
PCC Poisson's Ratio	0.15	0.10	0.20
PCC Coefficient of Thermal Expansion (CTE), in./in./°F × 10 ⁻⁶	5.5	5.0	6.0
PCC Thermal Conductivity, BTU/hr/ft/°F	1.3	0.5	2.0
PCC Modulus of Rupture at 28 days, psi	690	× 0.8	× 1.2
Slabs Distressed or Replaced after Restoration(%) / before Restoration(%)	20/20	0/0	40/40
Ratio of Slabs Distressed or Replaced after Restoration (%) / before Restoration (%)	1 (= 20/20)	0 (= 0/20)	0.5 (= 10/20)
Transverse Joint LTE, %	50	25	75
Granular Base Layer Input Parameters			
Base Resilient Modulus, psi	25,000	15,000	40,000
Subgrade Layer Input Parameters			
Subgrade Resilient Modulus, psi	10,000	5,000	20,000

OAT sensitivity analysis as described in Table 7 was investigated for the following three base cases:

- Case 1—PMED’s short-term reflection cracking performance prediction based on NSI ($NSI_{\text{year at 4000 ft/mile}}$): age at the year when the reflective cracking prediction reaches 4,000 ft/mile (757.71 m/km)
- Case 2—PMED’s long-term reflection cracking performance prediction based on $NSI_{20 \text{ years}}$: 20-year design life
- Case 3 - summary of sensitive PMED inputs from overall sensitivity analyses

An extensive set of analyses were performed by executing more than 2,000 PMED runs, and the results were then used to calculate NSI values for each design input from all the selected locations.

Based on the results from initial runs on the base cases, it was observed that reflective cracking distress occurs at a very early stage of a pavement’s design life after the construction of the overlay, and the final prediction remains the same for the rest of the service life. These initial results are consistent with national survey responses received from SHAs in a study conducted by Bennert (2010). In Bennert’s study, survey responses based on field observations were received from twenty-six SHAs having PCC pavement with hot-mix asphalt overlays, and twenty-two of them (85%) reported that reflective cracking was observed within the first four years after the HMA overlay was placed, while seven (27%) reported observing reflective cracking within the first two years.

Therefore, to improve our OAT sensitivity analysis evaluation, the average value of predicted reflective cracking—namely, 4,000 ft/mile (757.71 m/km)—was taken as a threshold, based on results from multiple trial runs and assuming that maximum reflective cracking is the same as the total transverse joint length of the underlying pavement. For example, if an underlying JPCP has a joint spacing of 20 feet (6.09 m), the maximum reflective cracking occurring on a lane of AC layer overlay could be [Total number of joints per mile for a 20-foot joint spacing (i.e., 264) × design lane width (12 feet [3.65 m]) = 3,168 ft/mile (600.11 m/km)]. Since the design lane width is assumed to vary from state to state, the final threshold was set to 4,000 ft/mile (757.71 m/km) for our OAT sensitivity analyses, as shown in case 1 below. Case 2 refers to the prediction of reflective cracking at the end of a pavement’s design life, which was considered to be 20 years for all the Iowa sections considered for our analyses. Figure 24 overviews the Case 1 and Case 2 scenarios.

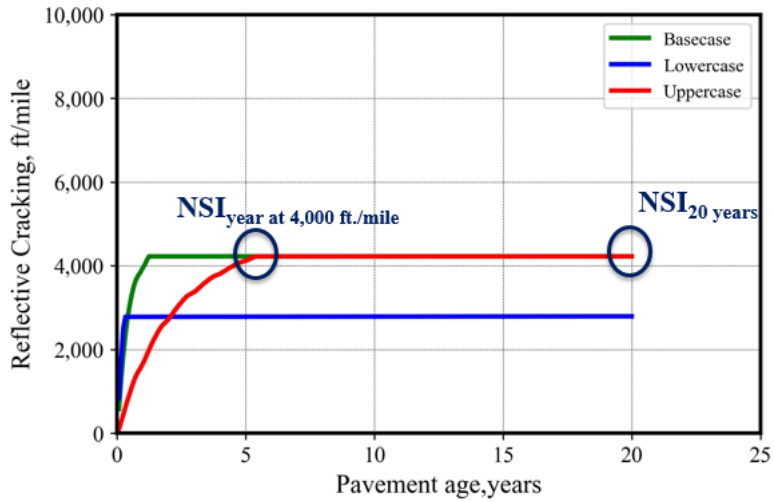


Figure 24. Overview of two scenarios for reflective cracking considered for sensitivity analysis

Case 3 described below summarizes a list of both the most sensitive and moderately sensitive inputs from the overall sensitivity analyses performed for Case 1 and Case 2.

Results

Case 1 – Short-Term Reflective Cracking Performance Prediction

Table 8 shows the summary of NSI values for predicted reflective cracking distress with respect to PMED inputs for low traffic levels.

Table 8. Sensitivity of design inputs by maximum absolute NSI: PMED inputs to reflective cracking (NSI at 4,000 ft/mile) for LOW traffic cases

Location	Des Moines	Orlando	Phoenix	Portland	International Falls	Los Angeles
Design Input						
AADTT	0.01	0.11	0.10	0.11	1.37	0.09
AC Surface Shortwave Absorption	0.05	0.04	0.04	0.05	0.45	0.04
Base Resilient Modulus	0.00	0.00	0.00	0.00	0.00	0.00
Base Thickness	0.00	0.00	0.00	0.00	0.10	0.00
Aggregate Coefficient of Contraction in AC	0.00	0.00	0.00	0.00	0.00	0.00
PCC CTE	0.00	0.00	0.00	0.01	0.61	0.00
Design Lane Width	0.00	0.00	0.00	0.00	0.00	0.00
Dowel Diameter	0.00	0.00	0.00	0.00	0.00	0.00
Alpha in AC Sigmoidal Curve	3.10	3.85	3.08	2.88	2.09	2.85
Delta in AC Sigmoidal Curve	0.14	1.15	0.93	0.89	0.65	0.88
Effective Binder Content in AC	0.15	0.09	0.07	0.09	0.53	0.06
Air Voids in AC	0.03	0.10	0.08	0.07	0.66	0.07
Tensile Strength at -10°C (14°F)	0.44	0.44	0.44	0.44	0.44	0.44
AC Thickness	0.76	1.45	1.48	0.45	0.86	1.47
Joint Spacing	1.24	1.21	1.29	1.20	1.99	1.30
JPCP Layer Thickness	0.31	0.39	0.46	0.45	0.64	0.51
PCC Unit Weight	0.04	0.02	0.03	0.04	1.07	0.02
PCC Modulus of Rupture at 28 Days	0.00	0.00	0.00	0.00	0.02	0.00
PCC Poisson's Ratio	0.00	0.00	0.00	0.00	0.00	0.00
Slabs Distressed/Replaced after Restoration & before Restoration	0.00	0.00	0.00	0.00	0.00	0.00
Ratio of Slabs Distressed or Replaced after Restoration (%) / before Restoration (%)	0.28	0.27	0.27	0.27	0.18	0.26
Subgrade Resilient Modulus	0.00	0.00	0.00	0.00	0.00	0.00
PCC Thermal Conductivity	0.01	0.01	0.02	0.02	0.18	0.01
Tied PCC LTE	0.00	0.00	0.00	0.00	0.00	0.00
Transverse LTE	1.37	1.40	1.41	1.38	1.16	1.42

Yellow – Very Sensitive (NSI >1), Green – Sensitive (NSI between 0.1 to 1), White – Insensitive (NSI < 0.1)

It can be seen that, while in most cases, sensitivity levels with respect to individual design inputs remained the same even for changing climate zones, most of the inputs were either very sensitive or sensitive to reflective cracking in International Falls, Minnesota, a climate zone that experiences extreme cooling cycles. This could be because of extremely cold winter temperatures and extensive snow accumulation in states like Minnesota that can result in excessive infiltration of moisture through cracks, leading to premature failure of pavement overlays. These sensitive analysis results are also consistent with the predicted reflective cracking distress results presented by Tsai et al. (2010) based on calibration models and coefficients generated from field-observed data.

In Tsai et al.'s study (2010), three different levels were considered for severity of reflective cracking for AC overlays over a jointed reinforced concrete pavement in a wet-freeze climate zone (Beaver, Pennsylvania) with low, medium, and high distresses appearing early (i.e., approximately 1,000 days after overlay construction). In contrast, the reflective cracking extent and severity of an HMA overlay over a cracked AC pavement in a dry – no freeze climate zone

(San Bernardino, California) exhibited all three levels of severity only after five years, clearly showing the level of impact of climate on reflective cracking.

Findings from Bennert (2010) also show that critical reflective cracking conditions in composite/PCC pavements occur when the air/pavement temperatures are already cold, and the climate is undergoing a cooling cycle. This suggests an already-brittle HMA layer that must be able to withstand further tensile straining caused by both contraction occurring at the PCC joint/crack and material contraction.

Overall, the most sensitive PMED inputs with respect to reflective cracking at all locations were Joint Spacing, Transverse LTE, and Alpha in an AC Sigmoidal Curve.

Reflective-crack initiation and propagation are mainly influenced by the existing pavement structure and conditions, HMA mixture properties, and degree of load transfer at joints and cracks (Tsai et al. 2010). Engineering experience and previous similar sensitivity analyses using the MEPDG/PMED software have also shown that a tendency toward increased cracking is highly influenced by an increase in joint spacing (Schwartz et al. 2011). Also, transverse joint LTE, generally indexed with the shearing mechanism at cracks, is usually not a crack initiator but rather an accelerator, i.e., once a crack has been initiated from tensile stress/strain, a change in LTE will accelerate the propagation of the reflective crack toward the pavement surface. With respect to alpha in the AC sigmoidal curve, it is essential to note that typical ranges of this parameter are very narrow, and the high sensitivity of cracking distresses with respect to alpha in an AC sigmoidal curve suggests a level of care in Level 1 characterization is required for important projects (Schwartz et al. 2011), though that is beyond the scope of this study. A similar observation would apply to the case of delta in an AC sigmoidal curve.

The moderately sensitive PMED inputs were AADTT, Delta in the AC Sigmoidal Curve, AC Thickness, JPCP Layer Thickness, Tensile Strength, and Ratio of Slabs distressed before and after restoration. Traffic data are one of the major inputs considered when developing a reflective cracking model. Since the annual number of axle loads for each vehicle class and axle type are therefore used to analyze traffic load effects for reflective cracking, AADTT is one of the most sensitive parameters for the prediction of reflective cracking.

Various sensitivity studies conducted over the years have reported that layer thicknesses are one of the most sensitive inputs for the prediction of pavement distresses by the MEPDG/PMED software (Schwartz et al. 2011, Cetin et al. 2015, Kim et al. 2005). The results of the current study show a similarly high sensitivity to layer thicknesses in reflective cracking predictions, consistent with previous studies that considered other types of cracking predictions. The choice of inputs such as AC layer thickness and JPCP layer thickness varies from agency to agency, so it is recommended that optimized design thickness values be specified very precisely. It is also recommended that, for PMED inputs such as layer thickness that exhibit sensitivity in most cases, project-specific design sensitivity studies be performed along with field validations.

With respect to tensile strength, previous findings have shown that, according to the cohesive crack model (CCM) analogy, crack length can be divided into two separate regions: a traction-

free length and a cohesive part. Within the cohesive part, crack openings that resist traction exist and there is still stress transfer between faces, the crack opening having been dealt with through the introduction of closure stresses (Tsai et al. 2010). The CCM postulates that the cohesive part of a crack begins to form at the point when and where the maximum principal stress reaches the tensile strength of the material and that the crack propagation is perpendicular to the maximum stress direction. This postulation represents a crack-initiation criterion that is the primary reason accounting for tensile strength being one of the PMED software's sensitive inputs (Tsai et al. 2010).

Additionally, the main reason for the initiation of reflective cracking distress is the presence of untreated cracks in the underlying pavement section, so the ratio of slabs distressed before and after restoration is assumed to impact the prediction of reflective cracking distress significantly, an assumption that is supported by the findings of the current study.

OAT sensitivity analysis found all the other PMED inputs were either relatively insensitive or had a negligible impact on reflective cracking. Table 9 and Table 10 give a summary of NSI values for predicted reflective cracking distress with respect to PMED inputs for medium and high traffic levels, respectively.

Table 9. Sensitivity of design inputs by maximum absolute NSI: PMED inputs to reflective cracking (NSI at 4,000 ft/mile) for MEDIUM traffic cases

Location	Des Moines	Orlando	Phoenix	Portland	International Falls	Los Angeles
Design Input						
AADTT	0.10	0.12	0.12	0.10	0.57	0.11
AC Surface Shortwave Absorption	0.04	0.07	0.07	0.15	1.43	0.08
Base Resilient Modulus	0.00	0.00	0.00	0.00	0.00	0.00
Base Thickness	0.00	0.00	0.00	0.00	0.07	0.00
Aggregate Coefficient of Contraction in AC	0.00	0.00	0.00	0.00	0.00	0.00
PCC CTE	0.00	0.00	0.00	0.00	1.78	0.00
Design Lane Width	0.00	0.00	0.00	0.00	0.00	0.00
Dowel Diameter	0.00	0.00	0.00	0.00	0.00	0.00
Alpha in AC Sigmoidal Curve	0.33	4.56	3.62	0.47	6.40	3.59
Delta in AC Sigmoidal Curve	0.14	1.38	1.80	1.00	2.06	1.11
Effective Binder Content in AC	0.04	0.07	0.05	0.04	0.90	0.05
Air Voids in AC	0.08	0.13	0.10	0.09	1.68	0.10
Tensile Strength at -10°C (14°F)	0.44	0.44	0.44	0.44	0.44	0.44
AC Thickness	2.29	2.30	2.23	2.27	2.27	2.24
Joint Spacing	1.37	1.26	1.21	1.28	1.56	1.23
JPCP Layer Thickness	0.18	0.25	0.31	0.24	0.54	0.31
PCC Unit Weight	0.01	0.02	0.03	0.02	2.75	0.02
PCC Modulus of Rupture at 28 Days	0.00	0.00	0.00	0.00	0.00	0.00
PCC Poisson's Ratio	0.00	0.00	0.00	0.00	0.00	0.00
Slabs Distressed/Replaced after Restoration & before Restoration	0.00	0.00	0.00	0.00	0.00	0.00
Ratio of Slabs Distressed or Replaced after Restoration (%) / before Restoration (%)	0.27	0.27	0.27	0.27	0.27	0.28
Subgrade Resilient Modulus	0.00	0.00	0.00	0.00	0.00	0.00
PCC Thermal Conductivity	0.04	0.02	0.01	0.00	0.44	0.01
Tied PCC LTE	0.00	0.00	0.00	0.00	0.00	0.00
Transverse LTE	1.33	1.40	1.38	1.34	1.10	1.39

Yellow – Very Sensitive (NSI >1), Green – Sensitive (NSI between 0.1 to 1), White – Insensitive (NSI < 0.1)

Table 10. Sensitivity of design inputs by maximum absolute NSI: PMED inputs to reflective cracking (NSI at 4,000 ft/mile) for HIGH traffic cases

Location	Des Moines	Orlando	Phoenix	Portland	International Falls	Los Angeles
Design Input						
AADTT	0.21	0.12	0.13	0.12	0.12	0.12
AC Surface Shortwave Absorption	0.05	0.11	0.09	0.14	0.10	0.11
Base Resilient Modulus	0.00	0.00	0.00	0.00	0.00	0.00
Base Thickness	0.00	0.00	0.00	0.00	0.00	0.00
Aggregate Coefficient of Contraction in AC	0.00	0.00	0.00	0.00	0.00	0.00
PCC CTE	0.00	0.00	0.00	0.00	0.02	0.00
Design Lane Width	0.00	0.00	0.00	0.00	0.00	0.00
Dowel Diameter	0.00	0.00	0.00	0.00	0.00	0.00
Alpha in AC Sigmoidal Curve	0.33	4.19	3.33	0.52	3.13	3.43
Delta in AC Sigmoidal Curve	0.68	1.28	1.01	0.87	0.93	1.03
Effective Binder Content in AC	0.04	0.01	0.03	0.04	0.01	0.03
Air Voids in AC	0.11	0.14	0.12	0.11	0.09	0.12
Tensile Strength at -10°C (14°F)	0.44	0.44	0.42	0.44	0.44	0.44
AC Thickness	2.14	2.10	2.12	2.14	2.24	2.12
Joint Spacing	1.18	1.20	1.20	1.19	1.21	1.20
JPCP Layer Thickness	0.26	0.18	0.21	0.26	0.26	0.19
PCC Unit Weight	0.00	0.08	0.01	0.01	0.04	0.01
PCC Modulus of Rupture at 28 Days	0.00	0.00	0.00	0.00	0.00	0.00
PCC Poisson's Ratio	0.00	0.00	0.00	0.00	0.00	0.00
Slabs Distressed/Replaced after Restoration & before Restoration	0.00	0.00	0.00	0.00	0.00	0.00
Ratio of Slabs Distressed or Replaced after Restoration (%) / before Restoration (%)	0.27	0.26	0.26	0.26	0.26	0.27
Subgrade Resilient Modulus	0.00	0.00	0.00	0.00	0.00	0.00
PCC Thermal Conductivity	0.02	0.00	0.00	0.00	0.20	0.00
Tied PCC LTE	0.00	0.00	0.00	0.00	0.00	0.00
Transverse LTE	1.49	1.40	1.48	1.49	1.49	1.48

Yellow – Very Sensitive (NSI >1), Green – Sensitive (NSI between 0.1 to 1), White – Insensitive (NSI < 0.1)

Similar to the low traffic findings (see previous Table 8), reflective cracking distress for the medium and high traffic cases was found to be sensitive to most of the PMED inputs tested for the International Falls location in Minnesota. In addition, based on the summary of NSI predictions from the medium and high traffic cases, Joint Spacing, AC Thickness, Transverse LTE, and Alpha and Delta in the AC Sigmoidal Curve were the most sensitive PMED inputs, while AADTT, AC Surface Shortwave Absorption, Air Voids in AC, Tensile Strength, JPCP Layer Thickness, and Ratio of Slabs Distressed before and after Restoration were moderately-sensitive PMED inputs. All remaining inputs fell into the least sensitive category.

Case 2 – Long-Term Reflective Cracking Performance Prediction

Based on preliminary results, in all cases reflective cracking occurs very early during pavement service life because of untreated cracks in the underlying pavement, an example of which was shown in the previous Figure 24. This is the major reason for considering both the short-term and long-term cases for OAT analysis.

Table 11, Table 12, and Table 13 present summaries of NSI values for predicted reflective cracking distress to PMED inputs for low, medium, and high traffic levels, respectively, and for a 20-year service life.

Table 11. Sensitivity of design inputs by maximum absolute NSI: PMED inputs to reflective cracking (NSI at 20 years) for LOW traffic cases

Location	Des Moines	Orlando	Phoenix	Portland	International Falls	Los Angeles
Design Input						
AADTT	0.00	0.00	0.02	0.02	1.37	0.01
AC Surface Shortwave Absorption	0.00	0.00	0.02	0.02	0.45	0.01
Base Resilient Modulus	0.00	0.00	0.00	0.00	0.00	0.00
Base Thickness	0.00	0.00	0.00	0.00	0.10	0.00
Aggregate Coefficient of Contraction in AC	0.00	0.00	0.00	0.00	0.00	0.00
PCC CTE	0.01	0.00	0.00	0.00	0.61	0.00
Design Lane Width	0.01	0.01	0.04	0.05	0.00	0.02
Dowel Diameter	0.00	0.00	0.00	0.00	0.00	0.00
Alpha in AC Sigmoidal Curve	0.00	0.03	0.03	0.00	2.09	0.06
Delta in AC Sigmoidal Curve	0.00	0.02	0.00	0.02	0.65	0.02
Effective Binder Content in AC	0.00	0.00	0.00	0.00	0.53	0.00
Air Voids in AC	0.00	0.00	0.00	0.00	0.66	0.00
Tensile Strength at -10°C (14°F)	0.09	0.11	0.11	0.11	0.40	0.09
AC Thickness	0.76	0.66	0.27	0.45	0.86	0.71
Joint Spacing	1.80	1.88	1.85	1.83	0.99	1.85
JPCP Layer Thickness	1.33	1.30	1.34	1.34	0.85	1.33
PCC Unit Weight	0.00	0.00	0.01	0.00	1.07	0.00
PCC Modulus of Rupture at 28 Days	0.01	0.04	0.02	0.01	0.02	0.07
PCC Poisson's Ratio	0.00	0.00	0.00	0.00	0.00	0.00
Slabs Distressed/Replaced after Restoration & before Restoration	0.00	0.00	0.00	0.00	0.00	0.00
Ratio of Slabs Distressed or Replaced after Restoration (%) / before Restoration (%)	0.33	0.33	0.33	0.33	0.18	0.33
Subgrade Resilient Modulus	0.00	0.00	0.00	0.00	0.00	0.00
PCC Thermal Conductivity	0.00	0.00	0.01	0.01	0.18	0.00
Tied PCC LTE	0.00	0.00	0.01	0.01	0.00	0.00
Transverse LTE	0.08	0.00	0.00	0.05	1.16	0.00

Yellow – Very Sensitive (NSI >1), Green – Sensitive (NSI between 0.1 to 1), White – Insensitive (NSI < 0.1)

Table 12. Sensitivity of design inputs by maximum absolute NSI: PMED inputs to reflective cracking (NSI at 20 years) for MEDIUM traffic cases

Location	Des Moines	Orlando	Phoenix	Portland	International Falls	Los Angeles
Design Input						
AADTT	0.00	0.00	0.00	0.00	0.57	0.00
AC Surface Shortwave Absorption	0.00	0.00	0.00	0.00	1.43	0.00
Base Resilient Modulus	0.00	0.00	0.00	0.00	0.00	0.00
Base Thickness	0.00	0.00	0.00	0.00	0.07	0.00
Aggregate Coefficient of Contraction in AC	0.00	0.00	0.00	0.00	0.00	0.00
PCC CTE	0.00	0.00	0.00	0.00	1.78	0.00
Design Lane Width	0.00	0.00	0.00	0.00	0.00	0.00
Dowel Diameter	0.00	0.00	0.00	0.00	0.00	0.00
Alpha in AC Sigmoidal Curve	0.00	0.00	0.00	0.00	6.40	0.00
Delta in AC Sigmoidal Curve	0.00	0.00	0.00	0.00	2.06	0.00
Effective Binder Content in AC	0.00	0.00	0.00	0.00	0.90	0.00
Air Voids in AC	0.00	0.00	0.00	0.00	1.68	0.00
Tensile Strength at -10°C (14°F)	0.08	0.10	0.09	0.09	0.11	0.07
AC Thickness	0.00	0.00	0.00	0.08	0.00	0.00
Joint Spacing	1.90	1.90	1.90	1.89	1.56	1.90
JPCP Layer Thickness	1.25	1.27	1.42	1.42	1.79	1.42
PCC Unit Weight	0.00	0.00	0.00	0.00	2.75	0.00
PCC Modulus of Rupture at 28 Days	0.00	0.00	0.00	0.00	0.00	0.00
PCC Poisson's Ratio	0.00	0.00	0.00	0.00	0.00	0.00
Slabs Distressed/Replaced after Restoration & before Restoration	0.00	0.00	0.00	0.00	0.00	0.00
Ratio of Slabs Distressed or Replaced after Restoration (%) / before Restoration (%)	0.33	0.33	0.33	0.33	0.27	0.33
Subgrade Resilient Modulus	0.00	0.00	0.00	0.00	0.00	0.00
PCC Thermal Conductivity	0.01	0.01	0.00	0.00	0.44	0.00
Tied PCC LTE	0.00	0.00	0.00	0.00	0.00	0.00
Transverse LTE	0.00	0.00	0.00	0.00	1.10	0.00

Yellow – Very Sensitive (NSI >1), Green – Sensitive (NSI between 0.1 to 1), White – Insensitive (NSI < 0.1)

Table 13. Sensitivity of design inputs by maximum absolute NSI: PMED inputs to reflective cracking (NSI at 20 years) for HIGH traffic cases

Location	Des Moines	Orlando	Phoenix	Portland	International Falls	Los Angeles
Design Input						
AADTT	0.00	0.00	0.00	0.00	0.00	0.00
AC Surface Shortwave Absorption	0.00	0.00	0.00	0.00	0.00	0.00
Base Resilient Modulus	0.00	0.00	0.00	0.00	0.00	0.00
Base Thickness	0.00	0.00	0.00	0.00	0.00	0.00
Aggregate Coefficient of Contraction in AC	0.00	0.00	0.00	0.00	0.00	0.00
PCC CTE	0.00	0.00	0.00	0.00	0.00	0.00
Design Lane Width	0.00	0.00	0.00	0.00	0.00	0.00
Dowel Diameter	0.00	0.00	0.00	0.00	0.00	0.00
Alpha in AC Sigmoidal Curve	0.00	0.00	0.00	0.00	0.00	0.00
Delta in AC Sigmoidal Curve	0.00	0.00	0.00	0.02	0.00	0.00
Effective Binder Content in AC	0.00	0.00	0.00	0.00	0.00	0.00
Air Voids in AC	0.00	0.00	0.00	0.00	0.00	0.00
Tensile Strength at -10°C (14°F)	0.36	0.37	0.37	0.37	0.37	0.36
AC Thickness	0.37	0.49	0.49	0.45	0.27	0.38
Joint Spacing	1.90	1.90	1.90	1.89	1.89	1.90
JPCP Layer Thickness	0.00	0.00	0.00	0.00	0.00	0.00
PCC Unit Weight	0.00	0.00	0.00	0.00	0.00	0.00
PCC Modulus of Rupture at 28 Days	0.00	0.00	0.00	0.00	0.00	0.00
PCC Poisson's Ratio	0.00	0.00	0.00	0.00	0.00	0.00
Slabs Distressed/Replaced after Restoration & before Restoration	0.00	0.00	0.00	0.00	0.00	0.00
Ratio of Slabs Distressed or Replaced after Restoration (%)/before Restoration (%)	0.33	0.33	0.33	0.33	0.33	0.33
Subgrade Resilient Modulus	0.00	0.00	0.00	0.00	0.00	0.00
PCC Thermal Conductivity	0.03	0.00	0.00	0.00	0.00	0.00
Tied PCC LTE	0.00	0.00	0.00	0.00	0.00	0.00
Transverse LTE	0.56	0.80	0.74	0.65	0.47	0.63

Yellow – Very Sensitive (NSI >1), Green – Sensitive (NSI between 0.1 to 1), White – Insensitive (NSI < 0.1)

These results compared to the short-term results in Case 1 show that very few PMED inputs in the long-term are either most sensitive or moderately sensitive with respect to reflective cracking distress. For the long-term case, Joint Spacing and JPCP Thickness were found to be the most sensitive inputs, while AC Thickness, Tensile Strength, Ratio of Slabs Distressed before and after Restoration, and Transverse LTE were found to be moderately sensitive inputs.

Since the PMED inputs either most sensitive or moderately sensitive with respect to both short-term and long-term reflective cracking performance are similar, the importance of these inputs (explained earlier for the short-term Case 1) was validated for both the short-term and long-term prediction of reflective cracking. The remaining inputs have essentially no impact on PMED's short-term or long-term prediction of reflective cracking.

Case 3 – Overall Summary of Sensitive Inputs from All Sensitivity Analyses

Based on the overall findings from the sensitivity analyses performed for both the short-term and long-term scenarios, the PMED software's most sensitive inputs overall with respect to reflective cracking distress were Joint Spacing, JPCP Layer Thickness, Transverse LTE, and Alpha and Delta in the AC Sigmoidal Curve. The PMED software's moderately sensitive inputs overall with respect to reflective cracking distress were AADTT, AC Surface Shortwave Absorption, Effective Binder Content, Air Voids in AC, Tensile Strength, AC Thickness, Ratio of Slabs Distressed before and after Restoration, Transverse LTE, and PCC Thermal Conductivity.

While the other inputs were found to be the least sensitive or to have negligible impact on the prediction of reflective cracking distress using the PMED software, for the sensitivity analyses performed for the location International Falls, Minnesota, a cold-dry climate zone, it was observed that the majority of the PMED inputs were either most sensitive or moderately sensitive with respect to predicting reflective cracking distress, as shown in Table 8 through Table 13. This is not the case for any of the other considered climate stations.

The very sensitive ($NSI > 1$) PMED inputs for the International Falls location based on the complete sensitivity analyses performed for all short-term and long-term cases, were AADTT, Alpha in AC Sigmoidal Curve, Delta in AC Sigmoidal Curve, PCC Unit Weight, Transverse LTE, AC Surface Shortwave Absorption, PCC Coefficient of Thermal Expansion (CTE), Air Voids in AC, AC Thickness, JPCP Layer Thickness, Joint Spacing, and PCC Unit Weight. In other words, for the International Falls cold-dry climate station only, twelve out of twenty-five (48%) of the total number of considered inputs were very sensitive ($NSI > 1$) with respect to reflective cracking predictions by the PMED software, and the majority of the other inputs were moderately sensitive (NSI between 0.1 and 1). This clearly shows the impact of climate location on PMED prediction of pavement distress.

Summary of Key Findings

This study analyzed the sensitivity of AC-over-JPCP reflective cracking distress with respect to the most important PMED design inputs and material properties. Typical base cases considered were chosen in light of current practices for pavement designs in the United States. To conduct a comprehensive sensitivity analysis across the country, six locations from different climatic zones were selected. NSI values were utilized to quantitatively evaluate different PMED inputs' sensitivity with respect to reflective cracking.

Case 1 reflects NSI values based on short-term reflective cracking prediction (i.e., the year at which reflective cracking reaches 4,000 ft/mile (757.71 m/km), and Case 2 reflects NSI values based on the long-term reflective cracking prediction of a 20-year design service life. Based on the analyses from both the short- and long-term scenarios at various traffic levels, the overall findings from this study can be summarized as follows:

- Joint Spacing, JPCP Layer Thickness, Transverse LTE, and Alpha and Delta in the AC

Sigmoidal Curve were the most sensitive PMED inputs with respect to reflective cracking distress.

- AADTT, AC Surface Shortwave Absorption, Effective Binder Content, Air Voids in AC, Tensile Strength, AC Thickness, Ratio of Slabs Distressed before and after Restoration, and PCC Thermal Conductivity were moderately sensitive PMED inputs with respect to reflective cracking distress.
- The remaining design inputs considered had either very little or no impact on reflective cracking based on the evaluated absolute NSI values.
- Another interesting observation is that most of the PMED inputs did have a significant impact on reflective cracking at the International Falls, Minnesota, location. Since these analyses were performed while keeping all the base-case values the same and just changing the climate station location in the PMED software, this shows the impact of climate on the predicted distress.

These results provide a reference for pavement designers who use the PMED software for design, enabling them to modify the most sensitive and moderately sensitive inputs in cases of design failure and thereby potentially save a great deal of time.

Recommendations

Among the inputs that were most sensitive, there are not many alternatives for pavement design engineers to modify inputs related to the underlying JPCP (e.g., joint spacing and JPCP layer thickness). In terms of practical implications, however, extreme attention must be paid while collecting the data with respect to the existing JPCP, and based on the information obtained, the pavement design engineer must test and decide the optimum AC thickness that needs to be overlaid.

In addition, since very high sensitivity was found for Transverse LTE and Alpha and Delta in the AC Sigmoidal Curve, it is very important to note that the typical ranges used in the PMED software for these inputs are very narrow and it is therefore suggested pavement design engineers perform a careful Level 1 characterization to obtain these values for important projects.

This study selected only six major locations across different climate zones in the United States, and it is recommended in the future to perform similar studies at more locations (specifically, site-specific locations before construction) and to use location-specific design input values in agencies' current practice. Agencies should also consider performing field validations by comparing the results produced in the field to such predicted sensitivity analyses. Based on the results of this study, it would also be helpful to suitably vary the material properties and design inputs to match conditions in agencies' particular states.

LOCAL CALIBRATION FOR IOWA PAVEMENT SYSTEMS

Background

The performance prediction models in the PMED software have been globally and nationally calibrated based on NCHRP 1-37A, but to achieve complete implementation of target results, performing local calibration of PMED models by assessing local conditions is recommended. The local calibration concept in MEPDG procedures implies the use of a mathematical process to minimize the bias and standard error between field-observed pavement distresses and PMED-predicted pavement performance (AASHTO 2010).

After the release of the MEPDG in 2004, SHAs began using the software, and numerous state-level studies have been conducted over the years to recalibrate the included performance models. Muthadi and Kim (2008) selected a total of 53 flexible pavement sections from the LTPP database and the North Carolina DOT (NCDOT) databases to recalibrate permanent deformation and bottom-up cracking models contained in the MEPDG software. Microsoft Excel Solver was used for this optimization process, and the study recommended further updating of the revised models at frequent intervals in future calibration efforts both by updating the database and the total number of sections.

Hoegh et al. (2010) performed a comprehensive local calibration for an MEPDG rutting model using time-history rutting data for pavement sections studied at the Minnesota DOT (MnDOT) full-scale pavement research facility (MnROAD), and detailed comparison of predicted total rutting, layer rutting, and measured rutting was provided. This study showed that the use of a locally calibrated model greatly improved PMED predictions for Minnesota conditions.

El-Badawy et al. (2012) addressed the influence of the binder input characterization level on the prediction model's dynamic modulus accuracy for Idaho conditions, and local calibration was performed for Idaho HMA mixes to further enhance the overall model performance.

Various other states and researchers have performed local calibration studies over the years (Haider et al. 2015, Guo 2013, Darter et al. 2014, Kaya et al. 2016, Ma et al. 2015, Haider et al. 2016, Waseem and Yuan 2013, Brink 2015, Bhattacharya et al. 2015, Sun et al. 2015). Jannat (2012) proposed a hierarchical network for developing a database containing the measured input parameters required for local calibration processes. This study demonstrated the significance of having a reliable database and further listed limitations and addressed potential outcomes of using a database containing serious issues.

Some recent studies have highlighted the use of updated models and enhanced optimization methods for local calibration (Gong et al. 2017, Haider et al. 2017, Esfandiarpour and Shalaby 2017, Yuan and Nemtsov 2018). Because much pavement deterioration occurs because of existing cracks in an underlying pavement system, a reflective cracking model has also been recently added to the PMED software (Titus-Glover et al. 2016, Tsai et al. 2010, Lytton et al. 2010, Gopiseti et al. 2020a, Gopiseti et al. 2020b).

The Iowa DOT has conducted a comprehensive local calibration effort by performing multiple studies in this area over the years, and specific information about a total of 130 pavement sites representing flexible, rigid, and composite pavements throughout Iowa is now available. Significant findings, methodologies, and recommendations have been provided for SHAs through these efforts (Ceylan et al. 2013b, Kim et al. 2014, Ceylan et al. 2015).

Ceylan et al. (2015) performed multiple local calibration studies using MEPDG v1.1, DARWinME, PMED v2.1.24, and PMED v2.2 and observed differences in predictions resulting from using these different versions. Haider et al. (2020) verified performance predictions for rigid pavements in Michigan using PMED v2.2 and v2.3, and their findings exhibited significant changes across versions in transverse cracking and IRI prediction. Additional findings from the Haider et al. study are significant decreases in slab thicknesses using the same local calibration coefficients obtained from their studies previously performed using PMED v2.0. The results from all these studies emphasize the urgent need for recalibration with the latest PMED version (v2.5.5) to enhance SHA confidence in PMED pavement designs.

The main objectives of this study are as follows: (1) summarize all the updates made to the PMED software in recent versions, (2) perform local calibration for Iowa using PMED v2.5.5 for asphalt concrete (flexible) pavements, jointed plain concrete (rigid) pavements (JPCP), and AC over JPCP, (3) test and present the findings from the use of multiple advanced optimization approaches in the local calibration process that will be useful for SHAs and researchers in developing robust local calibration models, and (4) determine the best set of revised local calibration coefficients for Iowa.

Enhancements in AASHTOWare Pavement ME Design

The major enhancement impacting local calibration results in the PMED software is the integration of Modern-Era Retrospective Analysis for Research and Applications v2.0 (MERRA-2) climate data for the design of flexible pavements and flexible overlays and North American Regional Reanalysis (NARR) climate data for the design of rigid pavements. The previously used Ground-Based Weather Stations (GBWS) climate data are no longer an available default. Multiple studies have compared PMED's pavement-performance predictions using different climate sources and found significant differences (Schwartz et al. 2015, Brink et al. 2017, Cetin et al. 2018, Durham et al. 2019, Gopiseti et al. 2019).

Applied Research Associates, Inc. (ARA) (2015) addendum #FY2015.2 reported new global model coefficients for rigid pavements embedded in PMED v2.2 and later determined based on NCHRP 20-07 Task 327. Major changes were also made to PMED calibration coefficient values for transverse cracking and mean joint-faulting models. ARA (2018a) addendum #FY2018.4 reported modifications made to PMED's global model coefficients derived from the recalibration efforts performed in 2018 for flexible pavements. Specifically, changes in global calibration coefficients were reported for fatigue cracking, transverse/thermal cracking (all input levels), AC rut depth, unbound-layer rut depth and bottom-up alligator cracking.

ARA (2018b) addendum #FY2018.5 provided guidelines for modifying local calibration coefficients with PMED v2.5 and subsequent versions released since 2018. Comprehensive guidelines on how to identify thickness-dependent coefficients and processes for entering modified coefficients were also reported. The major finding was that PMED's K calibration coefficient used for thermal cracking distress is dependent on mean annual air temperature (MAAT), and a complete set of steps for using a locally calibrated K instead was presented. (Several other bugs affecting the process of calculating distresses have also been reported and fixed.) All these documents can be accessed at <https://me-design.com/MEDesign/Documents.html>.

With all these significant changes, since SHAs using PMED v2.5 and later should no longer use the local calibration coefficients determined for use with previous PMED versions, recalibration using the latest PMED version (v2.5.5) is recommended. The recalibration process will additionally include more years of historical distress data measurement to help in developing robust local calibration models that provide better accuracy.

Methodology

Local calibration based on AASHTO guidelines (AASHTO 2010) involves a step-by-step process. This process includes the selection of typical pavement sites reflecting all geographical areas across a particular state, identification of sources of input data, characterization of the desired level at which data should be obtained, development of a comprehensive database that records measured data along with typical material properties and design inputs based on state-specific conditions, PMED runs using the default national calibration coefficients, and evaluation of bias to help with decisions as to whether local calibration is, in fact, necessary. The calibration coefficients for specific distresses must be identified and revised using optimization techniques and validation should be performed using new coefficients to check for model robustness.

Site Selection and Pavement Distress Database

The measured distress data required for local calibration were collected and developed through a PMIS, an automated system used by SHAs (including Iowa's) for storing, retrieving, and reporting pavement condition status. In this study, PMIS data available up through 2017 were used.

To perform local calibration, since the measured data should be organized with minimal differences and discrepancies, the following issues required identification and resolution:

- The units reported by the PMIS system for some of the distresses were different from those predicted by the PMED software, so to permit meaningful comparisons of the results, all such distresses were identified and units converted to achieve consistency (Ceylan et al. 2015).

- As previously mentioned, a new reflective cracking model has been added to the PMED software even though SHAs have not yet begun to collect reflective cracking distress as an independent type of distress. Reflective cracking can, however, be back-calculated using the transverse cracking data available through PMIS under the following two assumptions (Bennert 2010):
 - Assuming that the underlying JPCP does not have severe untreated cracks, the maximum reflective cracking occurring in an AC layer is the same as the total transverse joint length of the underlying JPCP.
 - All transverse cracking occurring within five years of service life is assumed to be reflective cracking.
- The PMED software also does not report reflective cracking as one of its direct output distresses, but rather total reflective cracking is added to total thermal cracking and reported as total transverse cracking (Total transverse cracking [feet/mile] = total reflective cracking [feet/mile] + total thermal cracking [feet/mile]) with total thermal cracking also reported separately as an independent distress. Therefore, to perform local calibration for reflective cracking in this study, only a simple back-calculation was required, namely subtracting total thermal cracking values from the total transverse cracking values available from PMED's Excel output reports.
- Occasional irregularities were observed in the measured distresses, such as their decrease with time without any recorded maintenance. To maintain measurement consistency, the data were therefore modified such that the distress curves increased over design life.

A total of 35 flexible, 35 JPCP, and 60 AC-over-JPCP sections previously used for Iowa local calibration studies were selected for this study from the Iowa PMIS.

Optimization Methods

The optimization process relies on both the transfer functions and the individual components of the transfer-function model. Since PMED is commercial software, all its component transfer-function values are not directly available to its users, and this represents one of the significant challenges to satisfactorily performing the local calibration process.

To properly evaluate the PMED model predictions outside the software using the transfer functions, all transfer-function components need to be directly available in the set of output/intermediate files the software generates for every pavement design run, because this permits application of nonlinear optimization techniques to the calibration of the PMED distress models. In cases where all such transfer-function components are unavailable, we are led to trial-and-error procedures that involve performing repeated runs with changing calibration coefficients until the desired results are produced.

Ceylan et al. (2013b) developed a linear optimization approach based on sensitivity analysis for calibration coefficients to minimize the total number of required trial-and-error-based PMED runs. The optimization methods tested in this study are discussed in detail below.

Linear Optimization Technique

This method can be used when all transfer-function components of a model are not known. A sensitivity-analysis matrix generated by changing calibration coefficients is developed to minimize the total number of the trial-and-error-based runs. This involves evaluating the best combination of coefficients that provides the least mean squared error (MSE) between the measured and PMED-predicted distress values. Ceylan et al. (2013b) provides the detailed methodology and steps involved in using this approach, whose major limitation is that it is a very time-consuming process with a very large computational burden.

Nonlinear Optimization Techniques

Microsoft Excel Solver

Solver is a powerful analysis tool, available in the Windows version of Microsoft Excel, that is widely used to fit experimental data to nonlinear functions. Its easy-to-use procedure and its operational mode make it quite easy to understand the principle of least-squares curve fitting. Three sub-option tools that depend on the linear or nonlinear nature of the equation are available in Solver.

The generalized reduced gradient (GRG) method is used for nonlinear equations, the simplex method (Simplex linear programming [LP]) is used for linear equations, and the evolutionary method can be used for both linear and nonlinear equations. The GRG method considers the slope or the gradient of the objective function as the input or the decision values and determines that the desired solution is reached when the partial derivatives are zero. The algorithm within a GRG is highly dependent on the initial conditions and may not be global optimum conditions in cases where Solver stops the optimization process close to the initial conditions. However, GRG is the best approach in terms of speed compared to the simplex and evolutionary methods.

Because of its robust nature, GRG has been used in this study to determine the best possible combination of calibration coefficients in transfer-function models.

LINGO

LINGO v18.0 is a commercial optimization tool designed to solve linear, nonlinear, quadratic, semi-definite, stochastic, and integer models more easily, faster, and more efficiently. This user-friendly tool, comprised of a wide range of commands, provides a guide through a systematic usage of its functions based on the nature of the equation under study. LINGO is available in two versions: a generic, text-based version that runs under the UNIX and LINUX operating systems and a Windows-based version.

The major advantage of the LINGO software is its ability to produce global solutions to a problem. It uses “branch and bound methodology” as an algorithm design paradigm for solving optimization problems. This algorithm finds the optimal solutions especially in discrete and combinatorial optimization. Its optimization process consists of a systematic enumeration of all candidate solutions where large subsets of its candidates are dropped from consideration by the use of upper and lower estimated bounds.

LINGO can also be used to verify and compare results with other traditional and metaheuristic optimization methods. Additionally, LINGO is more powerful commercial software than many with the capability to generate results in a very short time, making it a unique optimization tool.

SciPy Optimize

SciPy is an open-source library for the Python programming language that includes algorithms for optimization, algebraic equations, integration, differential equations, and interpolation. It is one of the most recognized optimization tools across the world and a top choice for many mathematicians and hard-core engineers for performing complex numerical computations (Blanco-Silva 2013).

SciPy can be used to deal with extremely large amounts of data and is a perfect solution for coordinating optimization processes in a smooth and reliable way. To perform ordinary least squares fitting using SciPy, measured and predicted data can be formulated as an optimization problem in the form of vectors and matrices, thereby allowing for efficient computations that produce the best fit and the best combination of calibration coefficients.

SciPy’s ‘minimize’ function provides a unified interface to find the local minima of nonlinear optimization problems. The underlying methods such as dogleg, trust-ncg, trust-exact and trust-krylov build a local model of the objective function based on first and second derivative information and further iteration is performed until the local minima of the objective function is reached.

The other benefits of the SciPy tool include automated graphing and plotting using Python library packages such as Hippo Draw, MayaVi, Biggles, Chaco, and Python Imaging Library (PIL). The Python programming language can be accessed from the official Python website (www.python.org/download) and can be installed on all major platforms such as Windows, UNIX, LINUX, and Mac OS X. Very recent statistics show that there have been more than 13,096,468 downloads of SciPy and the official SciPy website (<http://www.scipy.org/>) has been cited over 3,000 times, reflecting the prominent use of this tool to solve complex problems (Virtanen et al. 2020).

Since no previous pavement studies have considered the SciPy tool for the optimization of local calibration coefficients in the PMED software, the comprehensive results from this study’s use of SciPy will be a valuable reference for pavement engineers and researchers across the country.

Resampling Techniques

Resampling techniques randomly draw a subsample from a given selected sample and evaluate the statistics from this subsample. This process can be repeated multiple times until a collection of statistical values is produced that can provide evidence sufficient to provide confidence in the precision of the test statistic.

Bootstrapping

Bootstrapping is an approach used for estimating confidence intervals, variances, and other statistical parameters of a population from a sample (Haider et al. 2017). One goal of inferential statistics is to determine the value/characteristics of a specific sample taken from a population. It is virtually impossible to measure this value directly, so statistical sampling is used in cases where such a sample is taken from a population, and a conclusion is drawn using the resulting statistics such as mean, standard deviation, confidence intervals, and standard errors. If we consider any different sample from the same population, the statistics might therefore be slightly different. Bootstrapping is a resampling technique with replacement that assumes that all subsamples from a selected sample have an equal probability of being selected, perhaps multiple times, so a subsample selected could have a duplicate.

The concept of bootstrapping helps in understanding the properties and trends of measured and predicted distresses used for local calibration through its capability for replacing and duplicating subsamples; the differences between the measured and predicted datasets are minimized as much as possible and represented in terms of the least statistical differences (e.g., mean, standard deviation) that correspond to the best combination of calibration coefficients.

Jackknifing

Jackknifing is a resampling method for refining and confirming the calibration coefficients of a regression model whose validation statistics are developed independently of the data used for calibration. Multiple jackknifing is used to assess the sensitivity of validation goodness-of-fit statistics (Haider et al. 2016).

Unlike bootstrapping, jackknifing uses a sample from a total set of observations (N) and sequentially deletes one observation in the dataset followed by recomputing the desired statistic using the remaining $N - 1$ observations, with the error then computed as the difference between the measured and predicted values. As a second round of computation, a second observation is removed while replacing the first observation and the process is continued until N observations have been evaluated and the errors for each observation have been produced. The observations corresponding to the greatest errors are then minimized in the calibration process to produce a new set of calibration coefficients.

The major difference between bootstrapping and jackknifing techniques is that while bootstrapping is a computationally intensive process, the jackknifing method can be performed even by hand if the measured and predicted datasets are available and organized in spreadsheets.

Genetic Algorithm (GA) Techniques

GAs can solve constrained and unconstrained optimization problems based on processes related to biological evolution (Brink 2015). An initial solution set is randomly selected from the population and the fitness value for each member of the population is evaluated. Each member within the population is then randomly selected to represent a parent function and used to determine the children of the next generation.

In terms of biological analogy, the encoding is very similar to that of chromosomes, in which specific genes describe various characteristics of an individual. An expected solution for the optimization can be the set that describes common features in each parent function, and the process is repeated until some desired termination criterion is met.

Three main rules at each step in the process are used to create the next generation from the current population: Selection Rules for selecting the individuals called parents that contribute to the population of the next generation, Crossover Rules for combining two parents to form children for the next generation, and Mutation Rules for applying random changes to individual parents to form children.

GA tools have proven to be robust for various parameter settings and particular problems even in cases with an extremely great number of outliers. The MATLAB function *ga* was used in this study to perform GA-based optimization. Based on the availability of the components of PMED transfer functions, Table 14 presents a summary of PMED distresses and the respective optimization approaches tested in each case.

Table 14. Summary of optimization methods utilized for local calibration

Pavement Type	PMED Distress	Optimization Method
Flexible/AC over JPCP	Rutting Load-related cracking (longitudinal and alligator) Thermal cracking IRI Reflective cracking	Linear optimization Linear optimization Linear optimization Nonlinear optimization, Resampling and Genetic Algorithms Nonlinear optimization, Resampling and Genetic Algorithms
Rigid	Faulting Transverse cracking IRI	Nonlinear optimization, Resampling and Genetic Algorithms Linear optimization Nonlinear optimization, Resampling and Genetic Algorithms

Accuracy Evaluation Criteria

A major step in the local calibration process is evaluating the accuracy of the national calibration of pavement performance predictions performed using default (global) calibration coefficients to make a decision as to whether or not to perform local calibration at all. Statistical metrics such as

the mean bias, standard error estimate (SEE), coefficient of determination (R^2), and mean absolute percentage error (MAPE) were evaluated in this study to measure the accuracy of both the national and local calibration results. Higher accuracy is represented by a lower mean bias, a lower SEE, a lower MAPE, a higher R^2 , and a higher R^2 at the line of equality (LOE).

Local Calibration Results

PMED runs were initially performed using the global calibration coefficients, and the software's predictions were compared to PMIS-measured distresses. The appropriate optimization approaches were chosen based on the severity of distresses, accuracy of comparisons, and the availability of transfer-function components.

Prior to this study, two research studies on performing local calibration have been sponsored by the Iowa DOT (Ceylan et al. 2013b, Ceylan et al. 2015), and performance prediction models and their respective transfer functions and usage in the PMED software have been explained in detail in these studies as well as in numerous other SHA research studies performed across the country since the release of the PMED software. Additional information on PMED performance prediction models is also provided in the *MEPDG Manual of Practice* available through the HELP tool in the PMED software (AASHTO 2015).

Since the form of PMED performance prediction models has not changed and updates have been reported only for the calibration coefficients used in the latest version, recommendations on how to modify the local calibration coefficients depending on overprediction and underprediction for each distress are presented here.

Flexible/AC Pavements

Rutting, top-down (longitudinal) fatigue cracking, bottom-up (alligator) fatigue cracking, thermal/transverse cracking, and IRI are the flexible pavement distresses predicted by the PMED software. Table 15 shows PMED's global calibration coefficients for flexible pavements.

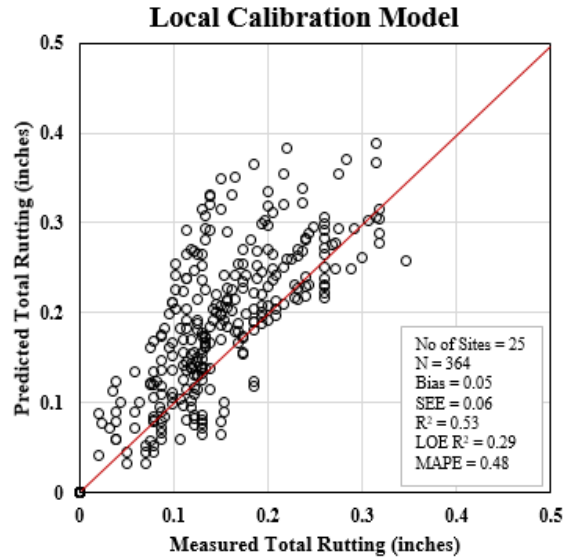
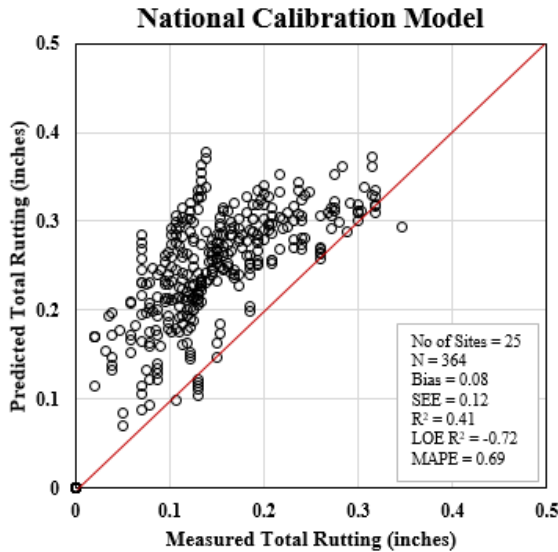
Table 15. Summary of global PMED coefficients for flexible pavements

Distress	Factors	Global Coefficients
HMA Rut	B1	0.4
	B2	0.52
	B3	1.36
GB Rut	B1_Granular	1
SG Rut	B1_Fine grain	1
Fatigue for ACrack and Lcrack	B1	0.001032
	B2	1.38
	B3	0.88
Lcrack	C1_Top	7
	C2_Top	3.5
	C4_Top	1,000
ACrack	C1_Bottom	1.31
	C2_Bottom	3.966
	C3_Bottom	6,000
Tcrack	K3_Level	$((3 \times \text{Pow}(10,-7)) \times \text{Pow}(\text{MAAT},4.0319)) \times 1 + 0$
IRI	C1	40
	C2	0.4
	C3	0.008
	C4	0.015

Rutting is one of the most common distress types observed in flexible pavement systems. The PMED software predicts total rutting (HMA Rut), a combination of AC layer rutting; granular-base rutting (GB Rut); and subgrade rutting (SG Rut). Rutting is internally calculated in PMED as the summation of rut depths at each layer.

The transfer-function components of PMED’s rutting models were extensively searched within the PMED output/intermediate files and since none were found to be available, a linear optimization approach was employed to perform local calibration. The comparison of national and local calibration results in Figure 25 shows a slight improvement with the use of locally calibrated models with an R^2 estimate above 53%. The overall findings can therefore be recommended for use in Iowa’s flexible pavement design practices.

Calibration Set



Validation Set

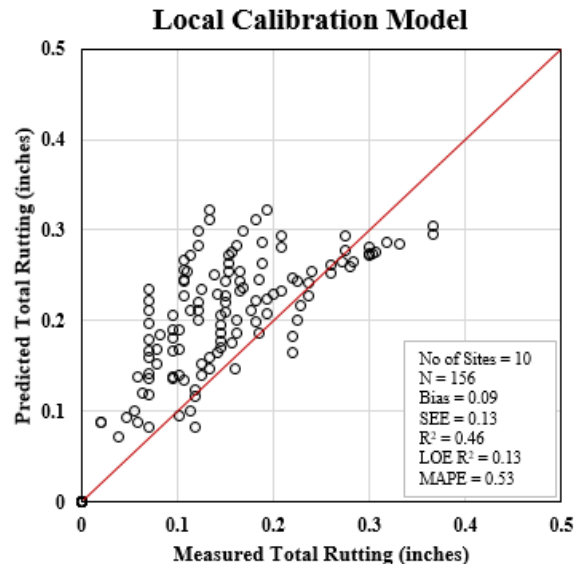
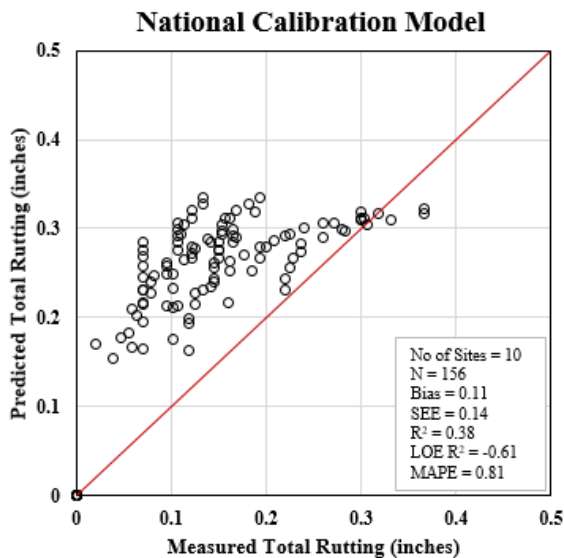
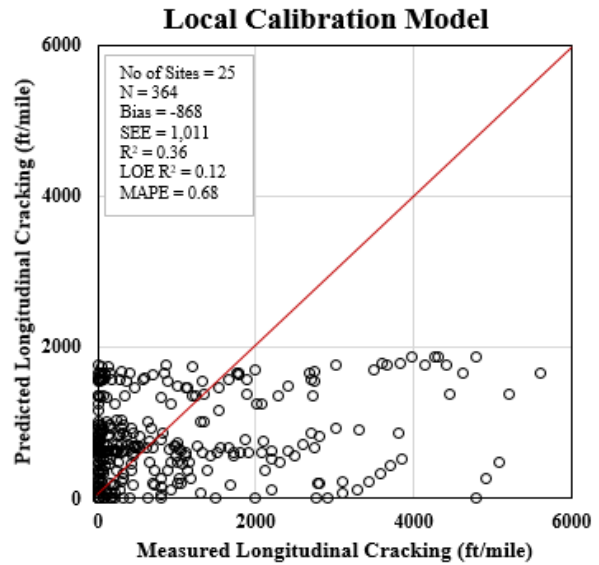
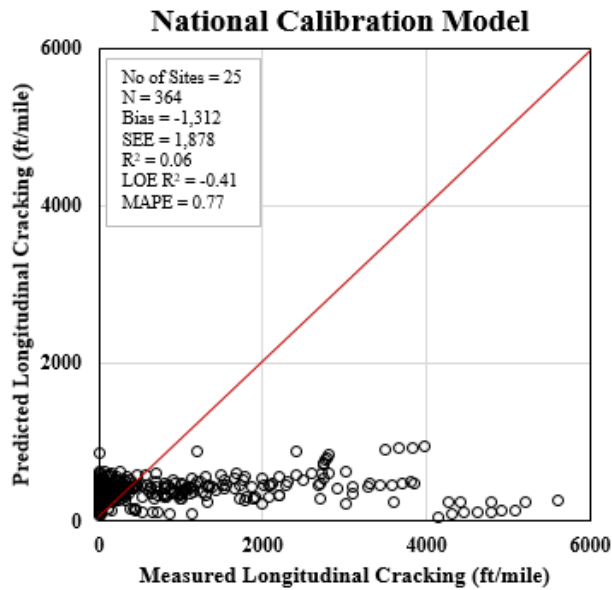


Figure 25. Comparisons between measured and predicted total rutting distress

Calibration experience from this study would recommend either increasing the B1, B2, and B3 values shown in Table 15 to increase the overall magnitude of rutting or decreasing these values to minimize the overall magnitude of their associated PMED performance predictions.

Figure 26 and Figure 27 present the global and local PMED calibration results of top-down and bottom-up cracking, respectively.

Calibration Set



Validation Set

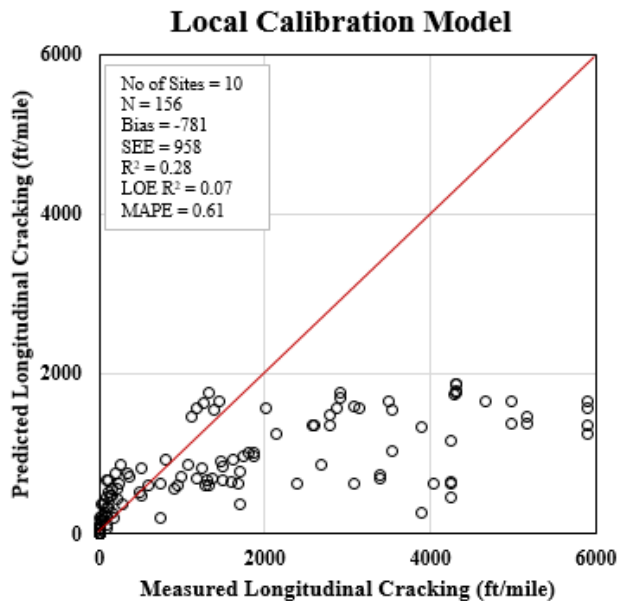
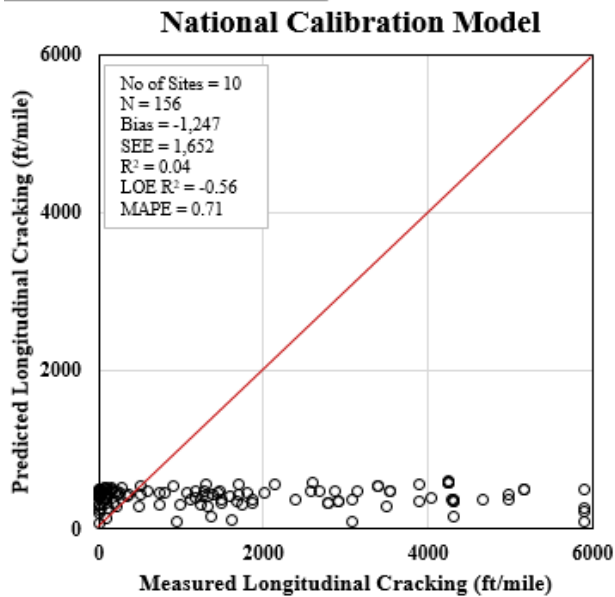
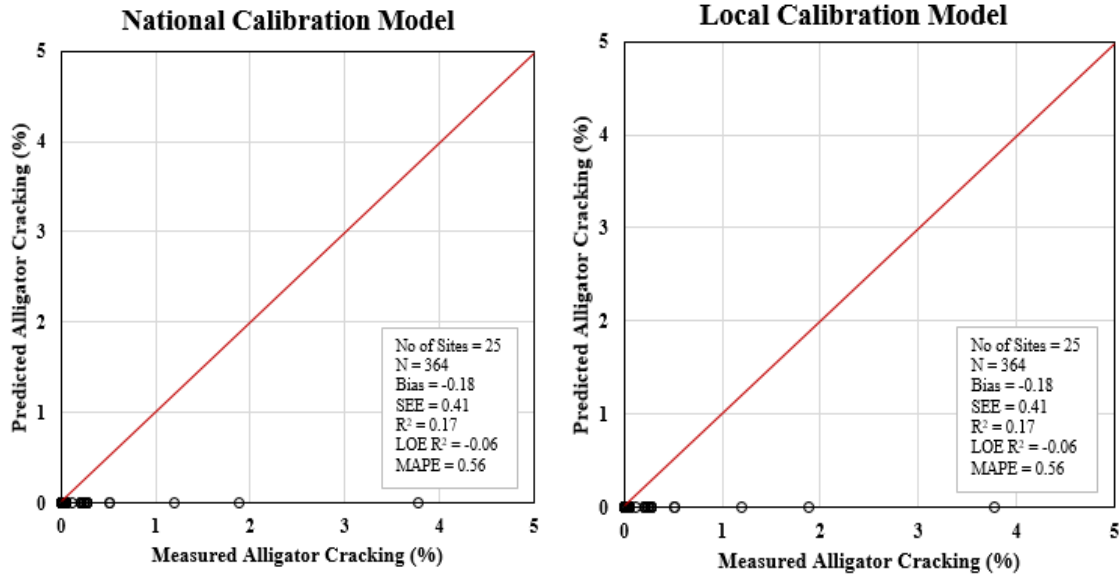


Figure 26. Comparisons between measured and predicted top-down (longitudinal) cracking distress

Calibration Set



Validation Set

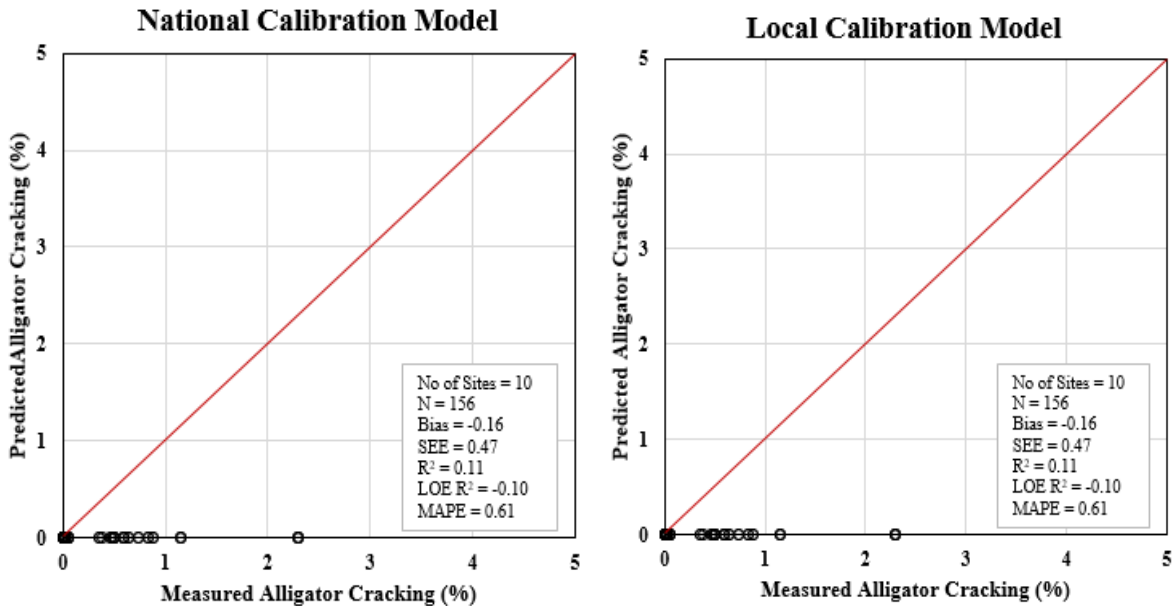


Figure 27. Comparisons between measured and predicted bottom-up (alligator) cracking distress

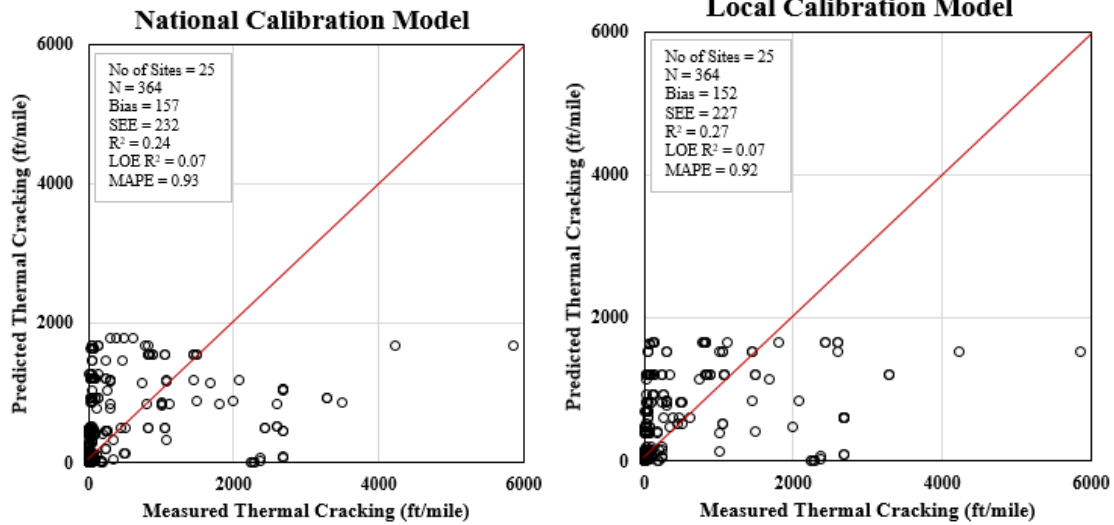
Top-down (longitudinal) and bottom-up (alligator) cracking distresses are categorized as load-related cracking, and local calibration coefficients for each must be modified based on PMED's fatigue model and bottom-up or top-down transfer functions. Linear optimization was used to recalibrate the PMED transfer functions based on sensitivity analyses performed to determine a suitable local calibration approach.

Since fatigue model calibration is considered the biggest challenge in the local calibration process because Level 1 laboratory-determined data are needed to produce the best results (Ceylan et al. 2015), this study instead recommends the use of the default global calibration values in the PMED fatigue model. For bottom-up cracking specifically, PMED predictions are near zero for every case, reflecting the inability of the software to capture the field behavior of flexible pavement and recommending the use of global rather than local calibration coefficients. For top-down cracking, the overall accuracy was slightly improved by the use of local calibration coefficients. The use of local calibration coefficients is therefore recommended for top-down cracking distress only.

Better data availability for fatigue models using Level 1 characterization will improve the overall accuracy of top-down cracking observations because fatigue and top-down cracking models are directly related to each other.

Figure 28 presents the global and local calibration results for thermal cracking distress.

Calibration Set



Validation Set

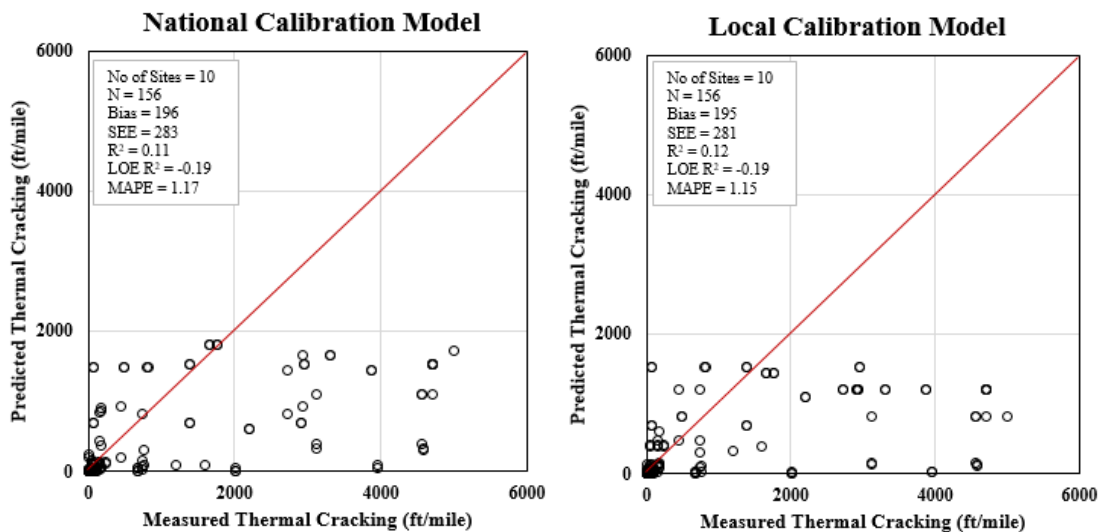


Figure 28. Comparisons between measured and predicted thermal cracking distress

The thermal cracking coefficient value K has been completely modified in the PMED v2.5 series, and the coefficient now considers a MAAT value from the climate database to evaluate the thermal cracking magnitude.

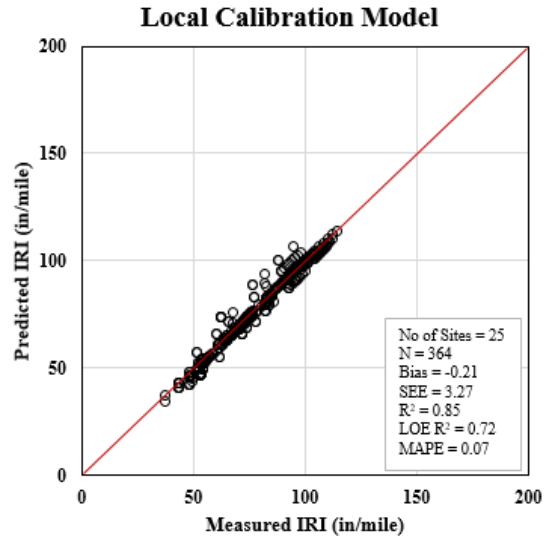
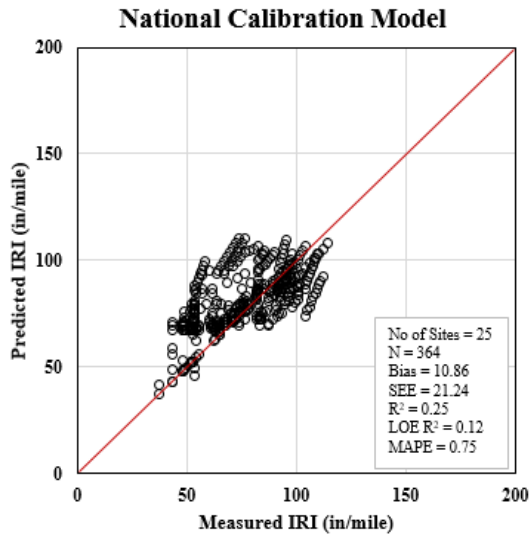
After careful inspection of the PMED thermal cracking transfer function, it was found that not all of the transfer function's model components were available, so linear optimization was performed through trial-and-error PMED runs, and a slight improvement in mean bias was observed using a locally calibrated model. The increase in the coefficient K value will increase

the prediction of overall thermal cracking while decreasing K will decrease thermal cracking prediction.

All the distresses described above are used in PMED to predict the smoothness (IRI) of flexible pavements. When performing local calibration, IRI must always be the last distress considered, because the recommended (global/local) calibration coefficients based on the evaluation of other distresses must be used for the local calibration of IRI.

In the case of IRI, the components required to solve the transfer function outside the software are available from the intermediate files. All the optimization approaches were tested for IRI, and Figure 29 shows the best results, which were produced using the SciPy optimization tool.

Calibration Set



Validation Set

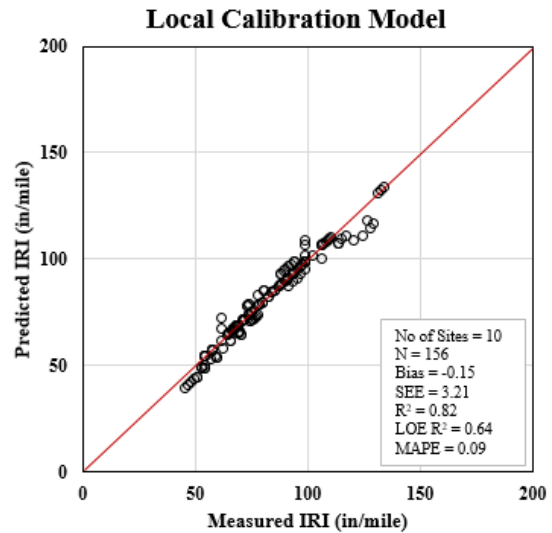
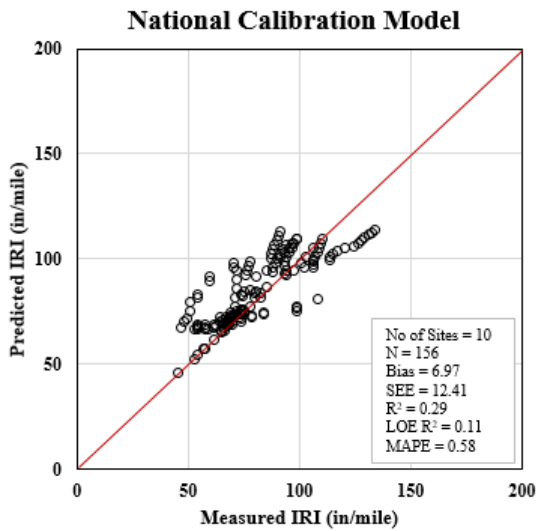


Figure 29. Comparisons between measured and predicted IRI distress

Table 16 presents a complete comparison of results using different optimization methods for calibration and validation analysis.

Table 16. Summary of local calibration results for flexible pavement IRI model using different optimization methods for (a) calibration sites and (b) validation sites

Method	Number of Sites	Mean Bias	SEE	R ²	LOE R ²	MAPE
National Calibration	25	10.86	21.24	0.25	0.12	0.75
Excel Solver	25	0.29	5.32	0.78	0.55	0.10
LINGO	25	0.79	6.12	0.65	0.52	0.21
Bootstrapping	25	-1.07	7.96	0.61	0.47	0.17
Jackknifing	25	-1.84	8.52	0.71	0.59	0.15
Genetic Algorithms	25	1.24	8.01	0.77	0.60	0.10
SciPy Optimize	25	-0.21	3.27	0.85	0.72	0.07

(a)

Method	Number of Sites	Mean Bias	SEE	R ²	LOE R ²	MAPE
National Calibration	10	6.97	12.41	0.29	0.11	0.58
Excel Solver	10	0.71	7.05	0.75	0.52	0.12
LINGO	10	0.45	6.32	0.71	0.55	0.16
Bootstrapping	10	0.39	6.86	0.73	0.56	0.10
Jackknifing	10	0.32	6.41	0.69	0.53	0.15
Genetic Algorithms	10	0.80	6.79	0.79	0.62	0.11
SciPy Optimize	10	-0.15	3.21	0.82	0.64	0.09

(b)

While none of the tools produced the exact same results, the higher R² values observed for each case recommend the use of their respective tools, assuming their availability at a given agency.

C1, C2, C3, and C4 are the IRI calibration factors shown in Table 15. For each of these coefficients, increasing its value will increase the IRI predictions and vice versa. However, the optimization tools will automatically adjust the C1, C2, C3, and C4 values based on the underprediction and overprediction of the global models.

Rigid Pavements (New JPCP)

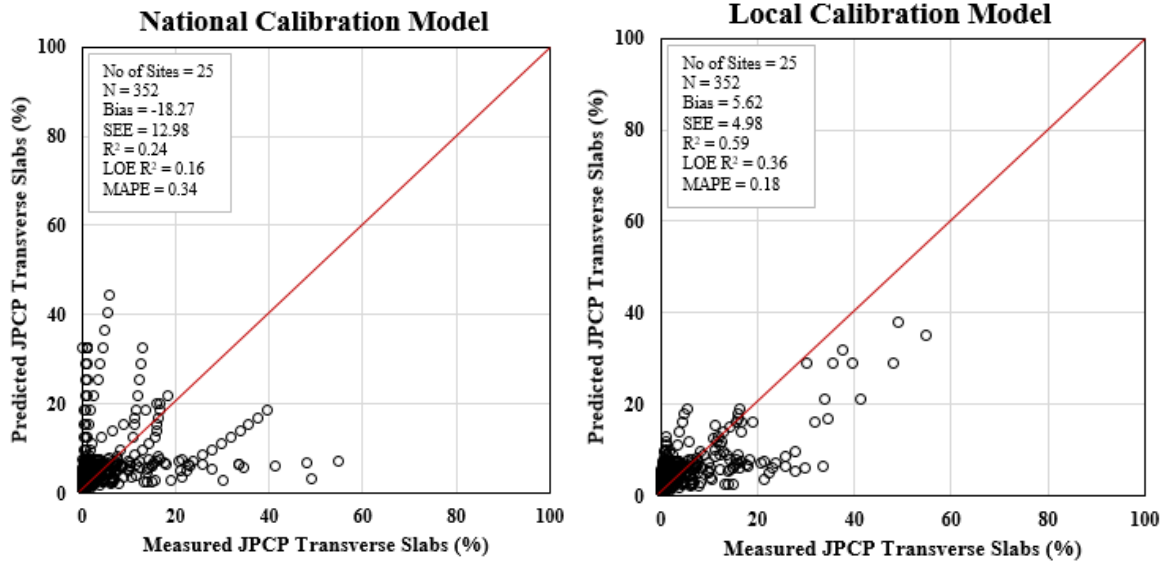
For rigid pavements, the PMED distresses are mean joint faulting, transverse cracking, and IRI. Table 17 shows the global calibration coefficients for rigid pavements in PMED v2.5.5.

Table 17. Summary of global PMED coefficients for rigid pavements

Distress	Factors	Global Coefficients
Faulting	C1	0.595
	C2	1.636
	C3	0.0021848
	C4	0.00444
	C5	250
	C6	0.47
	C7	7.3
	C8	400
Cracking	C1 (fatigue)	2
	C2 (fatigue)	1.22
	C4 (crack)	0.52
	C5 (crack)	-2.17
IRI	C1	0.8203
	C2	0.4417
	C3	1.4929
	C4	25.24

Figure 30 presents transverse cracking results (% of slabs cracked) using globally and locally calibrated models. PMED's transverse cracking transfer functions and fatigue-damage models were used to calculate Figure 30's predictions of transverse cracking.

Calibration Set



Validation Set

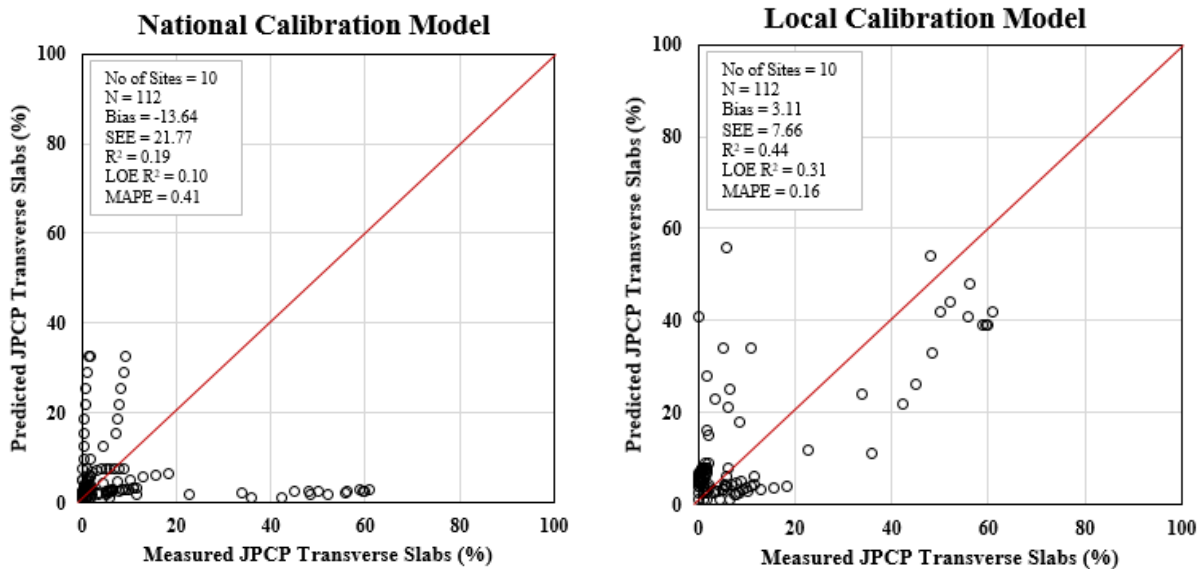


Figure 30. Comparisons between measured and predicted JPCP transverse cracking distress

In rigid pavements, since cracks can be initiated either from bottom or top but not from both directions, the total transverse cracking is the summation of bottom-up and top-down cracking.

In this case, the components of the transfer-function model were not available from the intermediate files and the use of a linear optimization approach improved the R^2 value from 0.24

for the global model to 0.59 for the locally calibrated model, recommending the use of local calibration coefficients. C1, C2, C4, and C5 are the coefficients for the transverse cracking models. The C4 and C5 coefficients should be optimized first, and if this results in a poor fit, the C1 and C2 coefficients should be adjusted to improve the bias.

In the case of mean joint faulting, as shown in Figure 31, all components were directly available from the intermediate files.

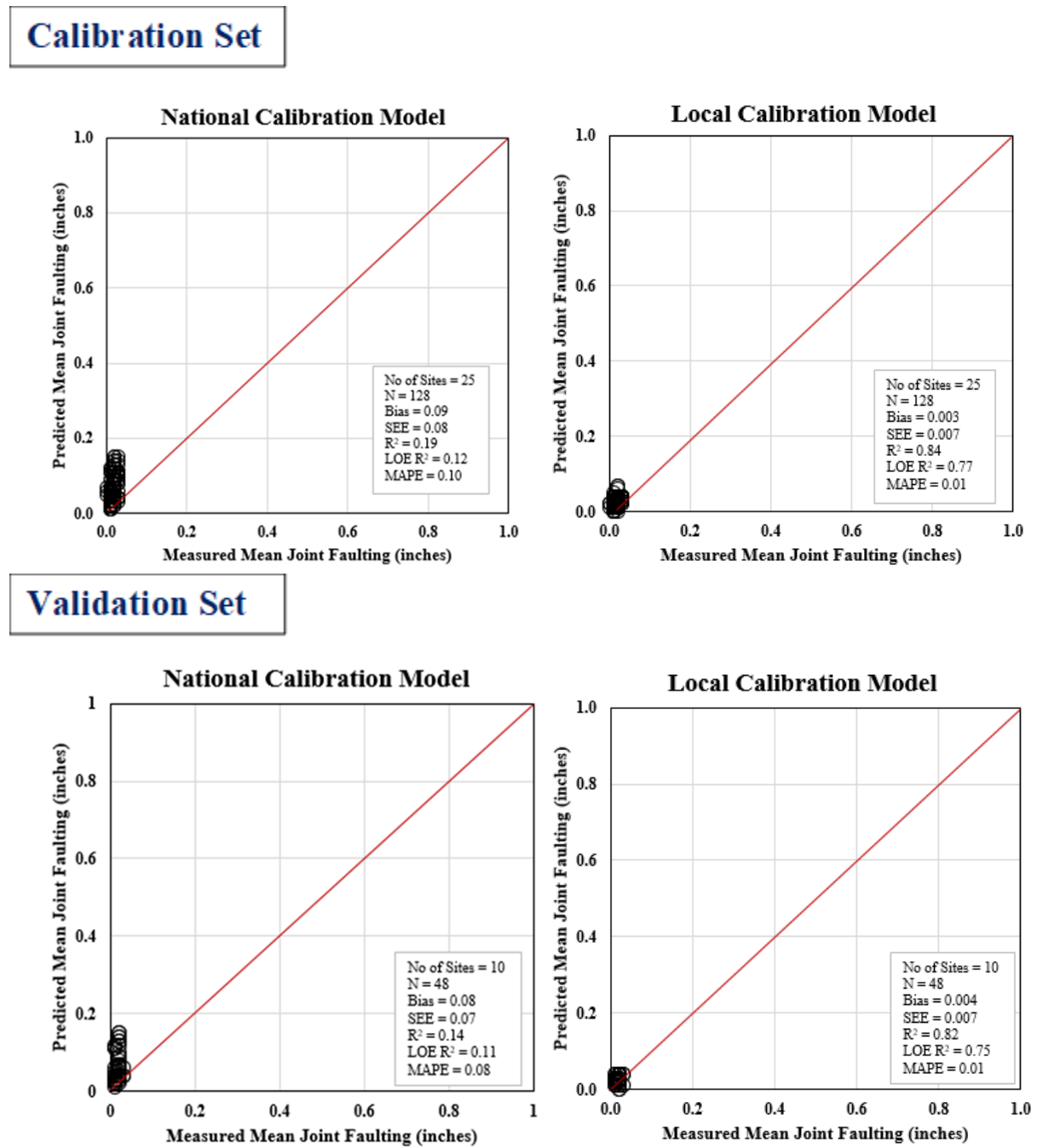
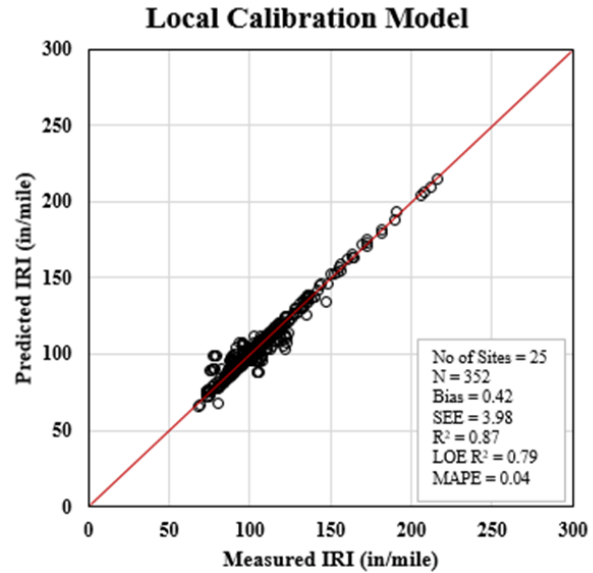
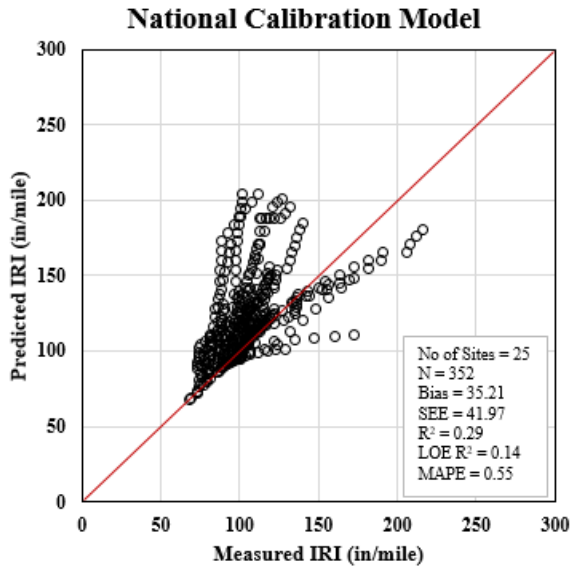


Figure 31. Comparisons between measured and predicted mean joint faulting distress

In the previous local calibration studies sponsored by the Iowa DOT, the maximum faulting data were used for local calibration because Iowa's PMIS did not report mean joint faulting data until 2015. However, in this study, the 5-year mean joint faulting data available for 2015–2019 were used, and the values reported for these years were very low (close to zero). Multiple optimization approaches capable of solving models with limited data were therefore used, and SciPy provided the best fit, with an R^2 value of 0.84 for a locally calibrated model.

Similarly to the IRI evaluation for flexible pavements, all optimization methods were tested for rigid pavements as well, with locally calibrated transverse cracking and mean joint-faulting models used for IRI evaluation. Figure 32 shows comparisons of (SciPy-optimized) global and local IRI models, with the R^2 value of the model improved from 0.29 to 0.87 and an observed mean bias of almost zero for the local models.

Calibration Set



Validation Set

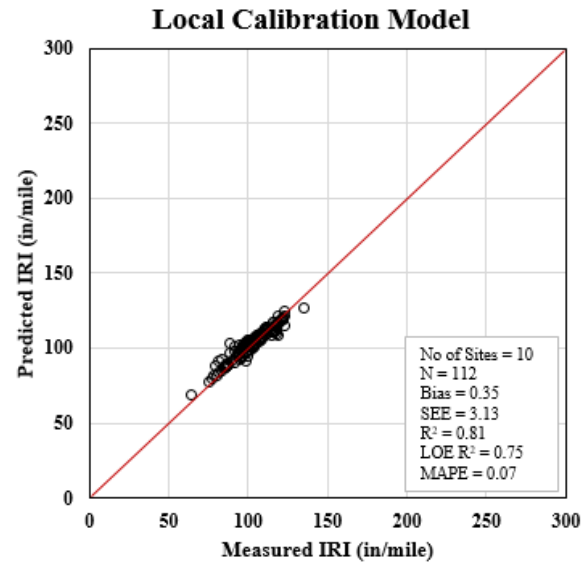
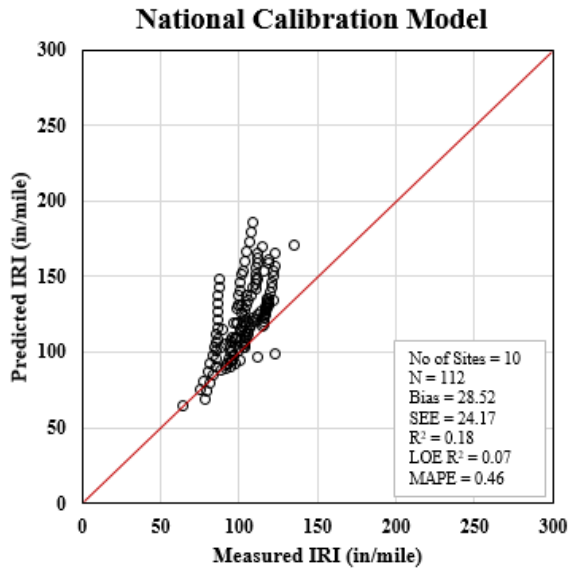


Figure 32. Comparisons between measured and predicted IRI distress

Table 18 shows a comparison of results using different optimization methods for IRI modeling, with findings very similar to those observed for flexible pavements.

Table 18. Summary of local calibration results for rigid pavement IRI model using different optimization methods for (a) calibration sites and (b) validation sites

Method	Number of Sites	Mean Bias	SEE	R ²	LOE R ²	MAPE
National Calibration	25	35.21	41.97	0.29	0.14	0.55
Excel Solver	25	0.54	6.32	0.82	0.73	0.07
LINGO	25	1.67	9.15	0.73	0.65	0.22
Bootstrapping	25	3.11	9.87	0.62	0.48	0.23
Jackknifing	25	3.39	11.54	0.58	0.45	0.25
Genetic Algorithms	25	1.37	6.96	0.78	0.67	0.12
SciPy Optimize	25	0.42	3.98	0.87	0.79	0.04

(a)

Method	Number of Sites	Mean Bias	SEE	R ²	LOE R ²	MAPE
National Calibration	10	28.52	24.17	0.18	0.07	0.46
Excel Solver	10	0.78	5.12	0.76	0.63	0.10
LINGO	10	1.56	7.17	0.68	0.52	0.21
Bootstrapping	10	2.07	8.12	0.70	0.55	0.18
Jackknifing	10	2.92	9.69	0.65	0.50	0.23
Genetic Algorithms	10	1.88	6.05	0.73	0.63	0.12
SciPy Optimize	10	0.35	3.13	0.81	0.75	0.07

(b)

Overall, both the flexible and rigid pavement results indicate that SciPy Optimize is a robust tool capable of providing consistent results for analyzing local-calibration models.

AC over JPCP

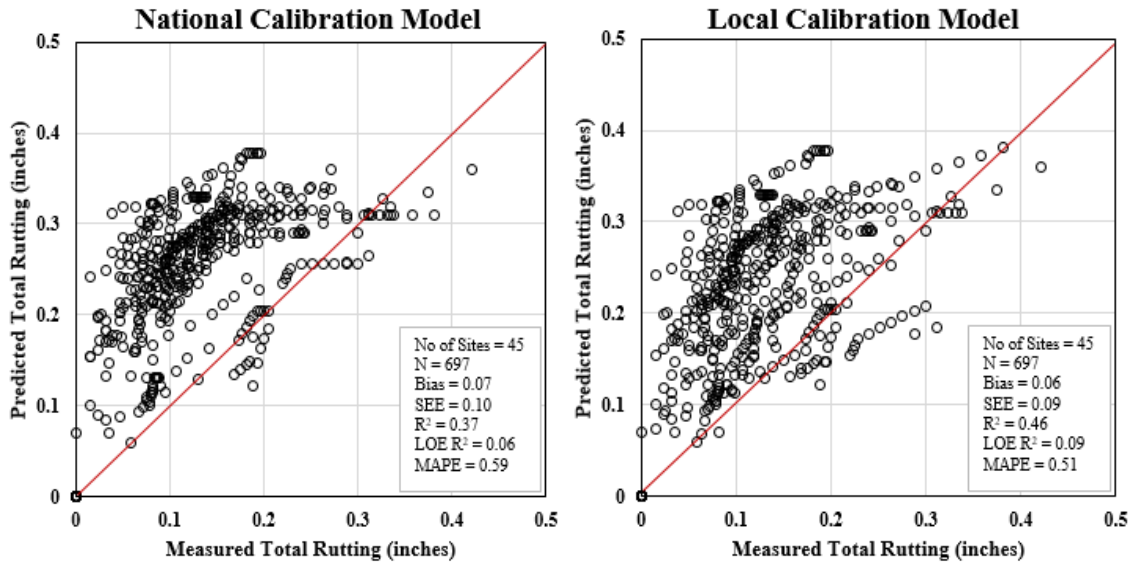
The distresses predicted by the PMED software for AC over JPCP include IRI, top-down fatigue cracking (longitudinal cracking), bottom-up fatigue cracking (alligator cracking), thermal cracking, total rutting, and total transverse cracking (thermal + reflective). Table 19 shows the complete list of (default) national calibration coefficients for designing AC over JPCP in PMED v2.5.5.

Table 19. Summary of default PMED coefficients for AC over JPCP

Distress	Factors	National
HMA Rut	B1	0.4
	B2	0.52
	B3	1.36
GB Rut	B1_Granular	1
SG Rut	B1_Fine grain	1
Fatigue for ACrack and Lcrack	B1	0.001032
	B2	1.38
	B3	0.88
Lcrack	C1_Top	7
	C2_Top	3.5
	C4_Top	1,000
ACrack	C1_Bottom	1.31
	C2_Bottom	3.966
	C3_Bottom	6,000
Tcrack	K3_Level	$((3 \times \text{Pow}(10,-7)) \times \text{Pow}(\text{MAAT},4.0319)) \times 1 + 0$
Reflective Transverse Cracking	C1	0.1
	C2	0.52
	C3	3.1
	C4	79.5
	C5	-2.71
IRI	C1	40.8
	C2	0.575
	C3	0.0014
	C4	0.00825

Using data from the national and local calibration models, Figure 33 compares the measured and predicted values for total rutting distress.

Calibration Set



Validation Set

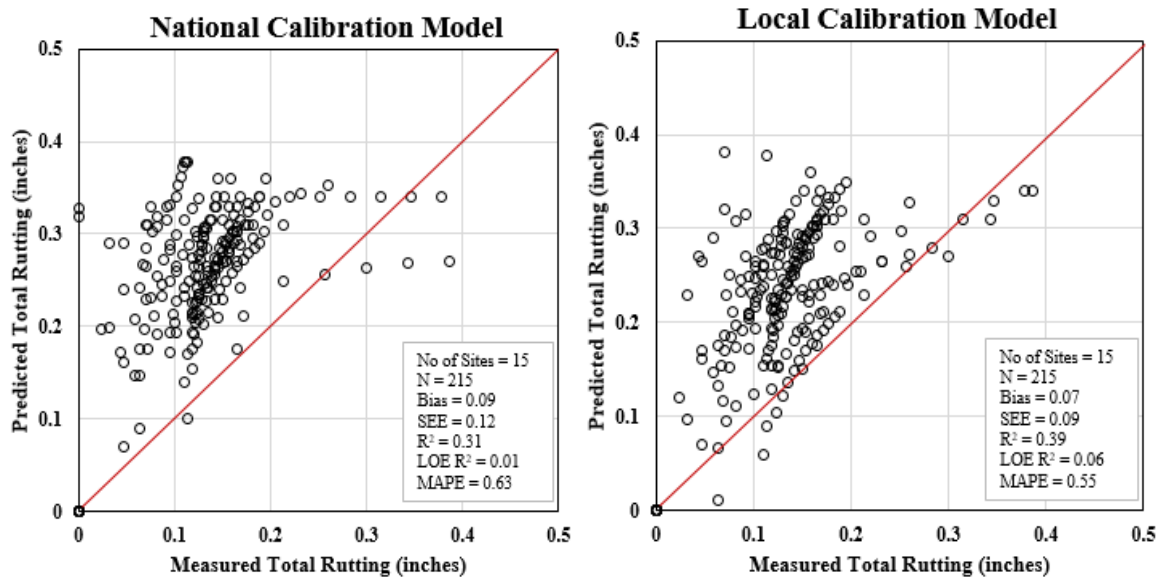


Figure 33. Comparisons between measured and predicted total rutting distress

Total rutting in the PMED software is the combination of AC-layer rutting, granular-base rutting, and subgrade rutting, whose respective coefficients are shown in the previous Table 19.

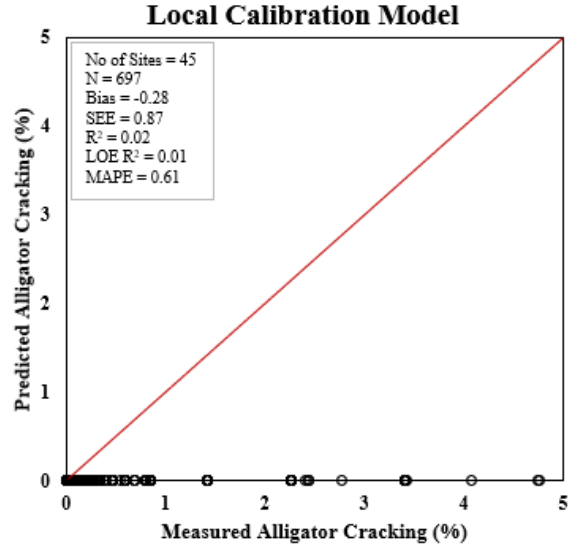
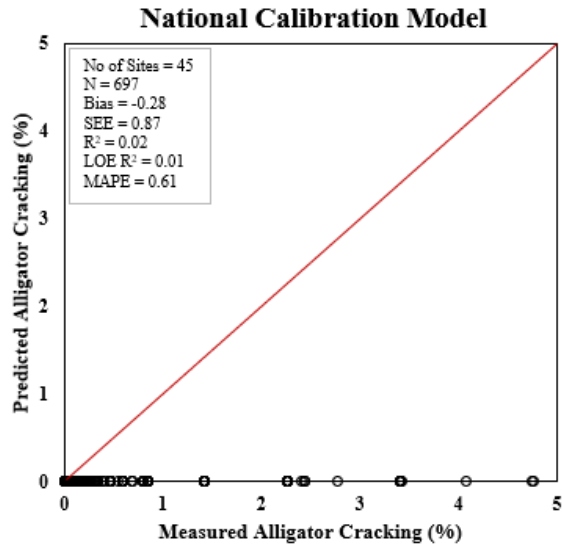
For AC over JPCP, the use of an existing JPCP layer that creates a strong foundation can result in very minimal base and subgrade rutting, with most rutting occurring in the AC layer. This means that the default B1_granular and B1_fine grain coefficients need not be revised for local calibration.

When none of the components of the rutting transfer-function model were available through the PMED output files, sensitivity analysis was the only optimization approach available. The sensitivity analysis results slightly improved the accuracy of the comparisons, and the overall sensitivity analysis results are acceptable for design practice under Iowa conditions.

Based on these calibration experiences, PMED's overall rutting prediction increases with increased values for the B1, B2, and B3 coefficients. As regards the national calibration coefficients, PMED predictions were observed to be underpredicting when compared to measured values, so in this study these coefficients were systematically decreased to improve the mean bias.

Figure 34 and Figure 35 compare alligator cracking (bottom-up) and longitudinal cracking (top-down), respectively.

Calibration Set



Validation Set

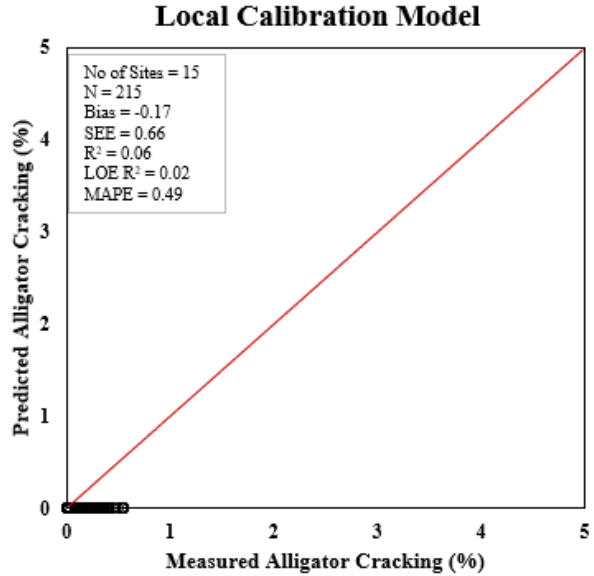
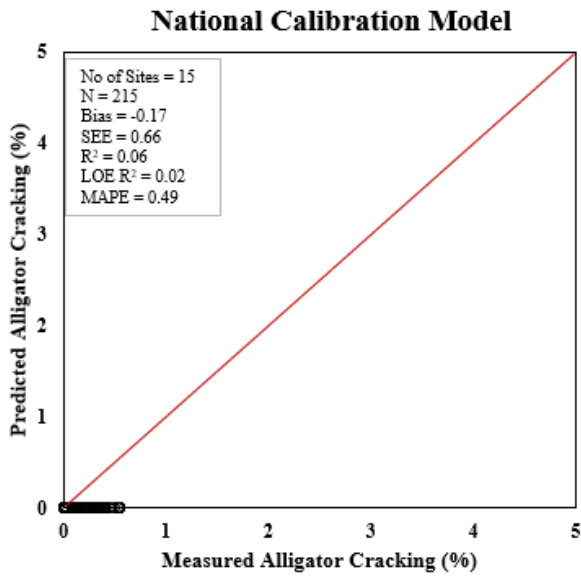
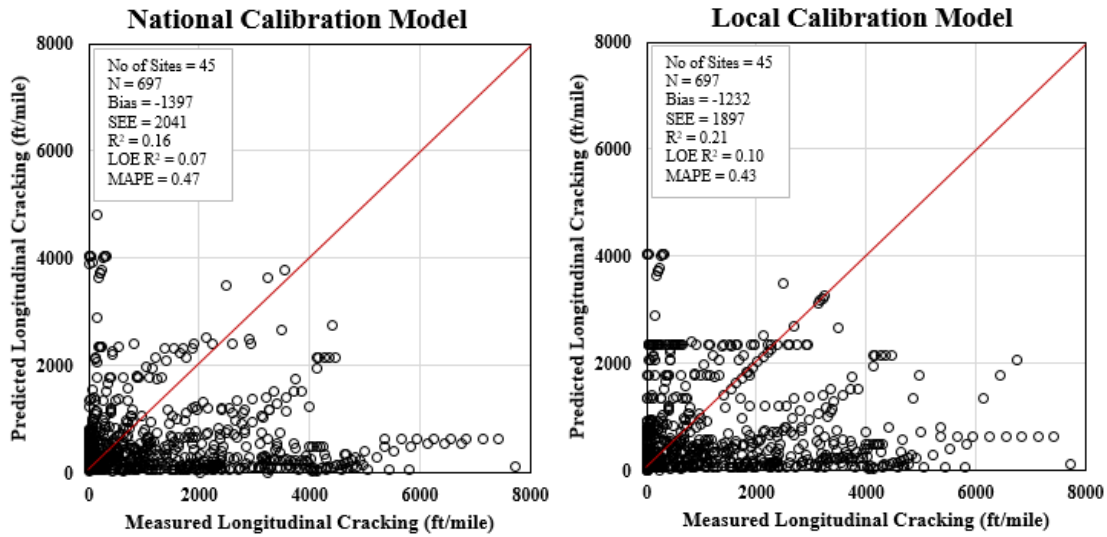


Figure 34. Comparisons between measured and predicted alligator cracking distress

Calibration Set



Validation Set

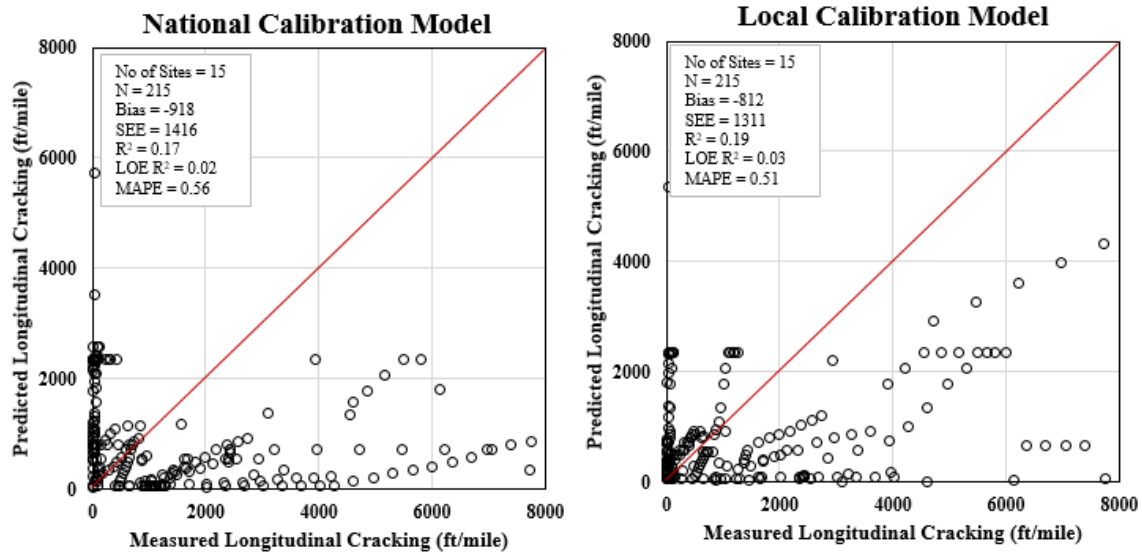


Figure 35. Comparisons between measured and predicted longitudinal cracking distress

For both alligator and longitudinal cracking, their set of coefficients should be revised based on two models—a fatigue model and a top-down or bottom-up transfer function.

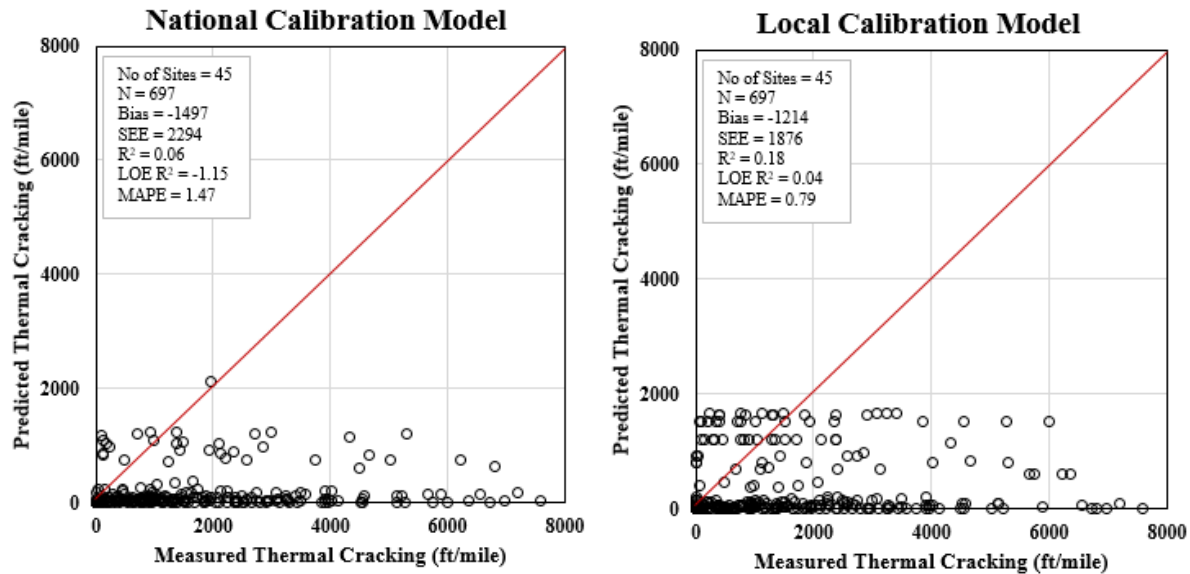
Sensitivity analysis was performed to help determine the order in which local calibration should be performed, and nonlinear optimization techniques were used to recalibrate the top-down and bottom-up transfer functions. Note that fatigue model calibration has always been a challenge for local calibration studies because it requires Level 1 values/laboratory testing to yield accurate results (Ceylan et al. 2015). As a result, PMED’s default national calibration coefficients were used for the current study’s fatigue model.

For alligator cracking, the comparisons show that most of the PMED-predicted values are very low (almost zero), so it can be concluded that the model is unable to adequately simulate the field behavior of AC over JPCPs. Performing local calibration is therefore not a solution in this case. For longitudinal cracking, a general improvement in accuracy was observed in the local calibration comparisons, but it was not significant.

In future local calibration studies, the use of laboratory values for the fatigue model could improve the accuracy of the PMED predictions. Based on this study, it is recommended PMED's default alligator cracking coefficients be used, while for longitudinal cracking, adjustments in C1 and C2 are suggested. Increasing C1 and C2 will decrease overall longitudinal cracking predictions and vice versa.

Similar to the rutting case, not all components of the thermal cracking transfer-function model were available in the PMED output files, so a sensitivity-analysis-based trial-and-error method was used to revise these calibration coefficients. Based on the Level 3 coefficient of the thermal cracking transfer-function model, the national calibration results in Figure 36 show that the PMED software underpredicts its estimates and, based on the sensitivity analysis' trial-and-error runs, it was observed that increasing the coefficient $k_{\text{level 3}}$ increases overall thermal cracking predictions. This process was continued until the accuracy had improved, with the mean bias reduced from -283.52 m/km to -229.92 m/km for the calibration sites and from -305.68 m/km to -249.24 for the validation sites.

Calibration Set



Validation Set

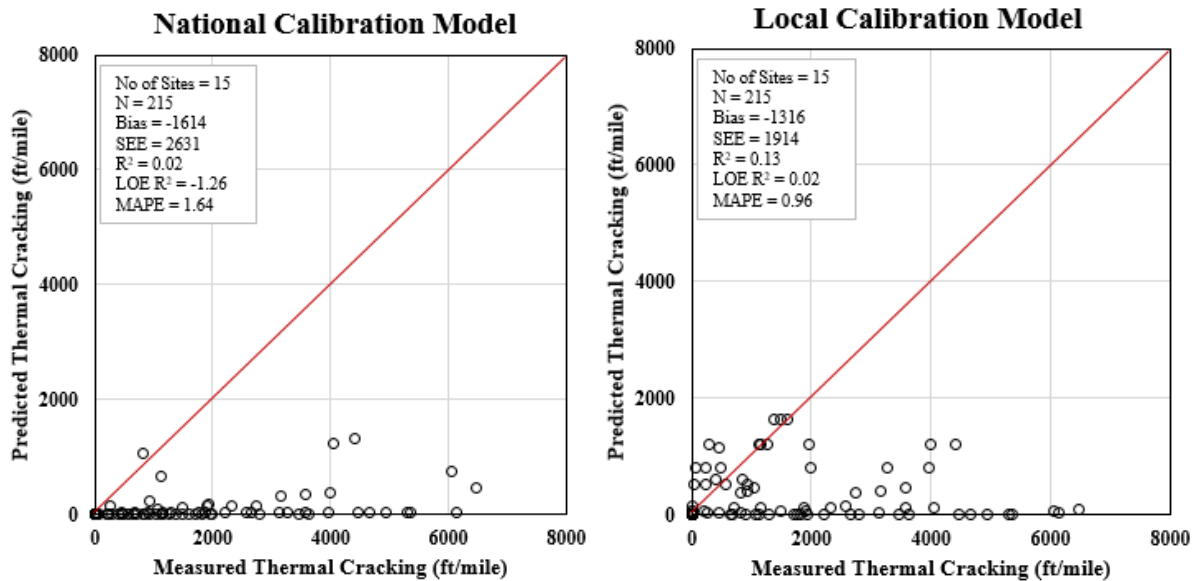


Figure 36. Comparisons between measured and predicted thermal cracking distress

With respect to reflective cracking distress, measured data were not directly available through Iowa's PMIS so, as mentioned previously, two assumptions were made in preparing a database using the available total transverse cracking data. Assumption 1 is the total transverse joint length criterion that assumes the maximum possible reflective cracking occurrence is the same as the total transverse joint length of the underlying JPCP layer, while assumption 2 is that the first five years of transverse cracking are reflective cracking and the rest are thermal cracking.

Unlike for other distresses, all components of this transfer function were directly available through the PMED software's output files and intermediate files, so all the optimization approaches were tested for reflective cracking distress and, as shown in Figure 37 and Figure 38, the SciPy optimization tool provided the best results with a much-improved accuracy.

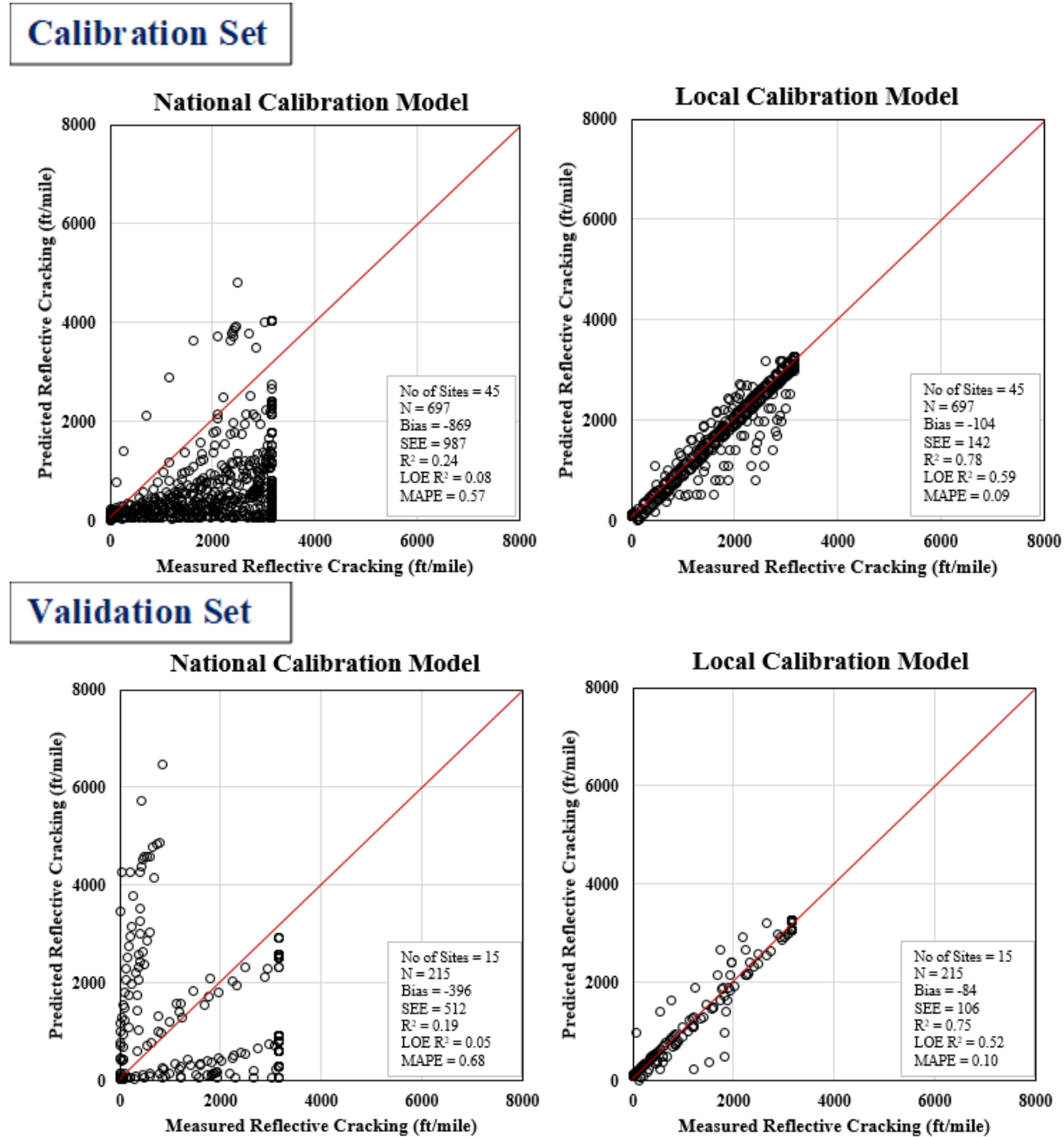
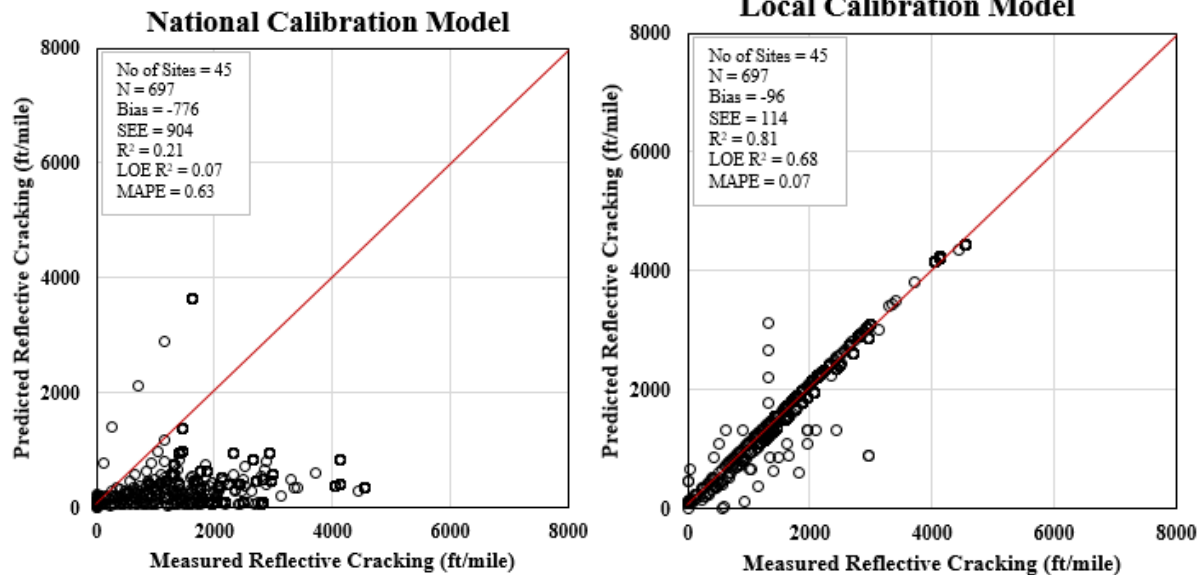


Figure 37. Comparisons between measured and predicted reflective cracking distress for Assumption 1: Total transverse length criterion (SciPy optimization)

Calibration Set



Validation Set

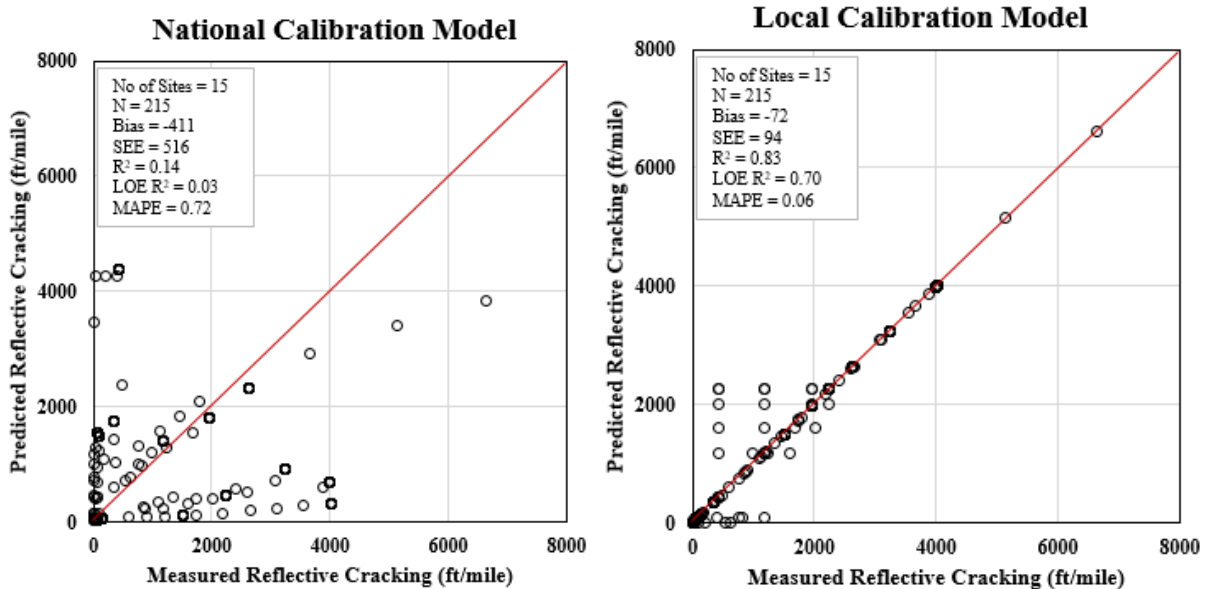


Figure 38. Comparisons between measured and predicted reflective cracking distress for Assumption 2: Five-year service life criterion (SciPy optimization)

The R^2 value for the total transverse length criterion increased from 0.24 to 0.78 for the calibration sites, and similar results were observed with respect to the 5-year criterion, with R^2 increasing from 0.21 to 0.81.

The calibration factors C4 and C5 are the translation and slope factors, respectively, that affect the overall existing cracking and cracks' load transfer efficiency. It was observed that increasing C4 decreases reflective cracking predictions.

The IRI describes a combination of all surface-related distress leading to the prediction of smoothness. Since calibration of the transfer-function model for IRI requires data on the total area of fatigue cracking (which is a combination of alligator and longitudinal cracking), reflective cracking, and rut depth, so that all local calibration models evaluated for these other distresses are incorporated into the IRI model, IRI must always be the last distress used to perform local calibration.

In this study, however, since there were two sets of local calibration models for reflective cracking distress, IRI was calibrated for both assumptions, as shown in Table 20 and Table 21, respectively. The availability of each transfer-function component required was carefully checked in the PMED output files and the location of each of the required values was identified and extracted. All the optimization methods described previously were tested to identify the best locally calibrated model. Table 20 shows the complete results for the local calibration and validation of IRI for the total-transverse-joint-length criterion.

Table 20. Summary of local calibration results for PMED's AC-over-JPCP IRI model using different optimization methods based on the total transverse joint length criterion for (a) calibration sites and (b) validation sites

Method	Number of Sites	Mean Bias	SEE	R ²	LOE R ²	MAPE
National Calibration	45	-27.59	36.47	0.35	0.22	0.47
Excel Solver	45	0.69	4.12	0.78	0.66	0.08
LINGO Optimization Tool	45	1.21	7.98	0.71	0.59	0.18
Bootstrapping	45	3.12	11.89	0.58	0.43	0.27
Jackknifing	45	5.62	14.61	0.52	0.40	0.28
Genetic Algorithms	45	1.02	5.83	0.80	0.70	0.08
SciPy Optimize	45	0.61	3.48	0.83	0.71	0.05

(a)

Method	Number of Sites	Mean Bias	SEE	R ²	LOE R ²	MAPE
National Calibration	15	-21.62	32.11	0.31	0.26	0.41
Excel Solver	15	0.81	4.82	0.74	0.61	0.09
LINGO Optimization Tool	15	1.47	9.88	0.70	0.54	0.20
Bootstrapping	15	3.99	12.32	0.56	0.41	0.29
Jackknifing	15	5.98	15.62	0.50	0.41	0.26
Genetic Algorithms	15	1.17	5.97	0.78	0.69	0.09
SciPy Optimize	15	0.73	4.71	0.81	0.70	0.04

(b)

Similarly, Table 21 shows the complete results of the local calibration and validation of IRI for the 5-year cracking assumption.

Table 21. Summary of local calibration results for PMED’s AC-over-JPCP IRI model using different optimization methods based on the five-year service life criterion for (a) calibration sites and (b) validation sites

Method	Number of Sites	Mean Bias	SEE	R ²	LOE R ²	MAPE
National Calibration	45	-27.59	36.47	0.35	0.22	0.47
Excel Solver	45	0.68	4.11	0.78	0.67	0.07
LINGO Optimization Tool	45	1.08	7.11	0.73	0.60	0.16
Bootstrapping	45	3.02	10.97	0.60	0.49	0.22
Jackknifing	45	5.21	13.03	0.57	0.42	0.25
Genetic Algorithms	45	0.97	5.12	0.81	0.73	0.07
SciPy Optimize	45	0.49	3.11	0.86	0.74	0.04

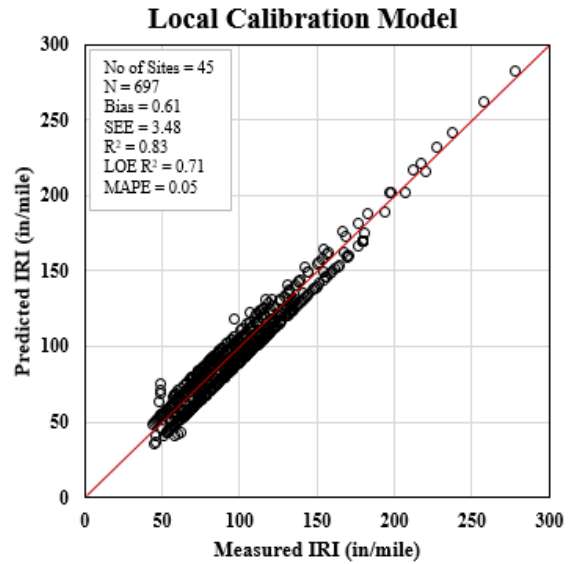
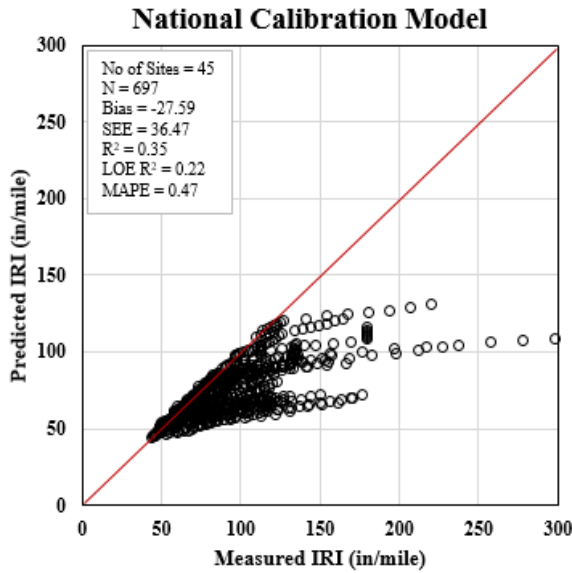
(a)

Method	Number of Sites	Mean Bias	SEE	R ²	LOE R ²	MAPE
National Calibration	15	-21.62	32.11	0.31	0.26	0.41
Excel Solver	15	0.75	4.93	0.76	0.65	0.06
LINGO Optimization Tool	15	1.01	8.37	0.71	0.57	0.18
Bootstrapping	15	3.99	10.86	0.59	0.48	0.20
Jackknifing	15	5.33	14.11	0.55	0.40	0.27
Genetic Algorithms	15	1.01	5.63	0.77	0.68	0.10
SciPy Optimize	15	0.58	3.02	0.82	0.71	0.05

(b)

The SciPy optimization tool provided the best results. Its comparisons of measured and predicted data are shown further in Figure 39 and Figure 40.

Calibration Set



Validation Set

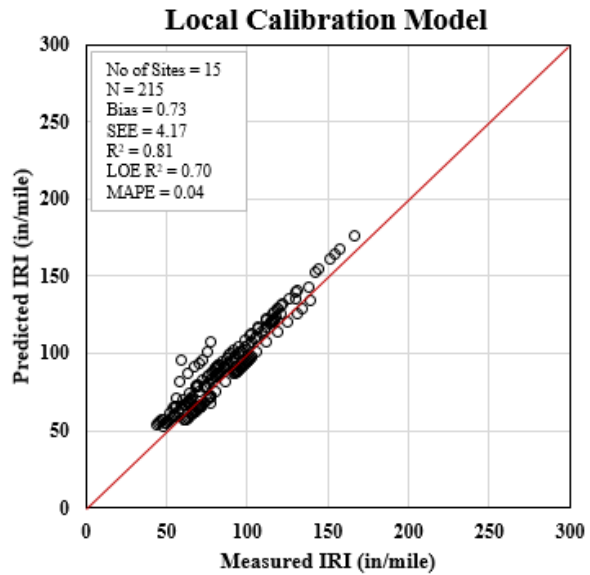
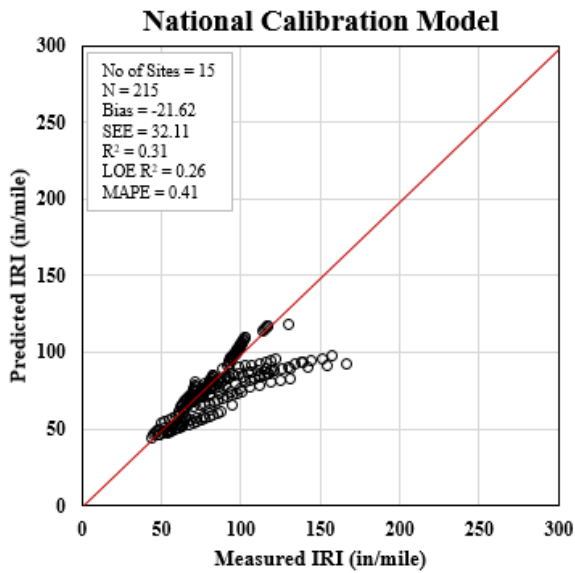
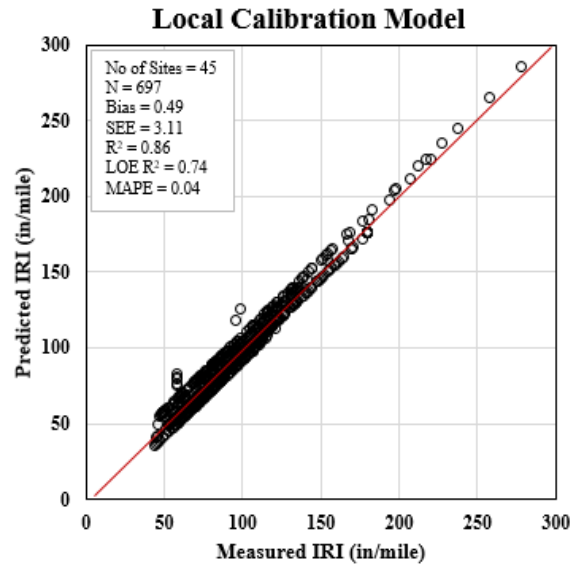
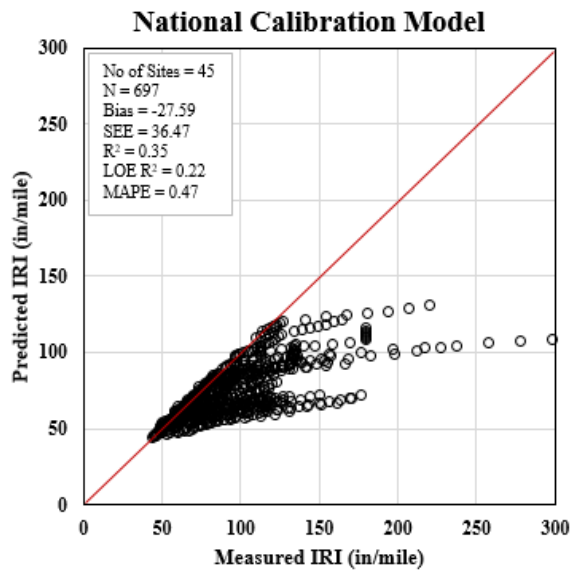


Figure 39. Comparisons between measured and predicted IRI distress based on the total transverse joint length criterion

Calibration Set



Validation Set

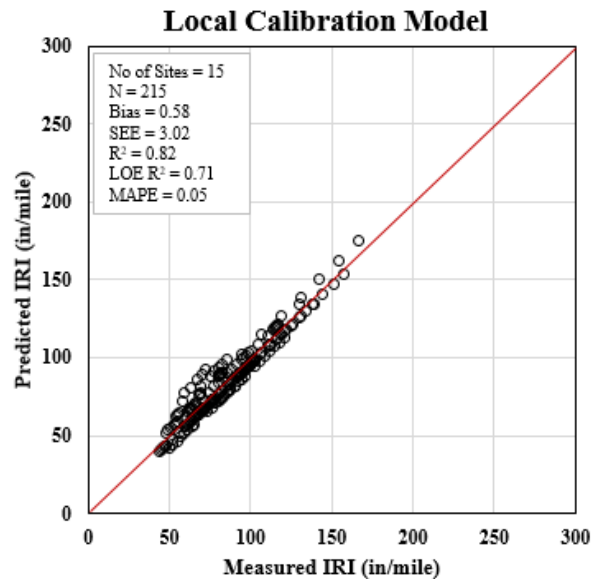
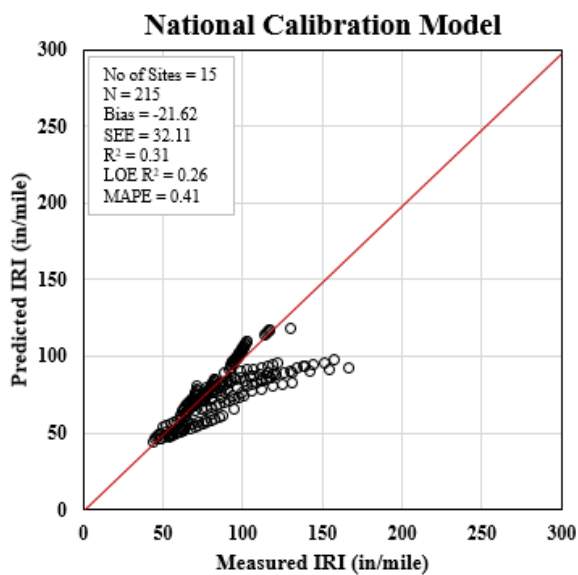


Figure 40. Comparisons between measured and predicted IRI distress based on the five-year service life criterion

It was also observed that genetic algorithms provided much better results than PMED's default nationally calibrated coefficients, suggesting a possibly useful alternative optimization tool available through MATLAB for engineers who do not want to use programming-based tools.

The calibration factors in PMED's IRI transfer-function model are C1, C2, C3, and C4, and based on the results of this study's PMED runs, decreasing all four coefficients will decrease

overall IRI predictions and vice versa. It must also be noted, however, that decreasing C1 will decrease the impact of rutting on IRI, decreasing C2 will decrease the impact of total fatigue cracking, decreasing C3 will decrease the impact of transverse cracking, and decreasing C4 will decrease the impact of site factors on IRI. Clearly, therefore, the local calibration results of these other distresses must be carefully evaluated first to make appropriate adjustments in locally calibrating PMED's IRI model. Such evaluation can also help in minimizing the effect of the significant differences sometimes observed between national and local calibration findings for these other distresses.

Summary of Key Findings

- Distress-oriented data collection and database preparation are the most important initial steps in a local calibration process. Measured distress data and the availability of a number of years of historical data are crucial in estimating the best fit.
- Performance prediction models/transfer functions must be well understood, and access to each component or variable in these models must be carefully studied and recorded.
- The optimization tools used to minimize mean bias and standard error are the final and most important part of the calibration process. This study has shown that the use of different approaches can produce variation in results that impacts the final local calibration coefficient values.
- Units for distresses collected from sources such as PMIS must be checked for compatibility and it must be ensured that differences between PMED and PMIS units are properly handled by applying appropriate conversion factors.
- The overall mean bias and coefficient of determination (R^2) using local calibration coefficients were significantly improved, especially with respect to distresses for which all their components/parameters were directly available from the PMED output files. Use of the SciPy tool for optimization produced the best results, although SciPy does require some basic knowledge of programming and coding that is available through various sources. (The genetic algorithm tool in MATLAB could be a better alternative for engineers who do not want to use programming-based tools.)
- The use of sensitivity analysis for distress situations for which not all the required components of PMED transfer functions were available also resulted in improvement in local calibration compared to the national calibration, but since the improvement was not very significant, SHAs may vary in their decision as to whether they should use local coefficients or stick with PMED's default national coefficients.
- Minimizing overestimation and underestimation of distresses is crucial to success in local calibration studies, and the experience gained in this study provides comprehensive guidance on how to change local calibration coefficients based on comparisons of measured and

predicted data. These guidelines can be implemented by any state that uses the PMED software.

- The local calibration coefficients recommended for the Iowa DOT to use in design practice as alternatives to their nationally calibrated counterparts are summarized in Table 22 for Iowa’s flexible pavements, Table 23 for Iowa’s rigid pavements, and Table 24 for Iowa’s AC over JPCP. (Note that the recommended local calibration coefficients in red in Table 22 through Table 24 show that these numbers are different from their counterparts in the nationally calibrated models.)

Table 22. Summary of PMED v2.5.5’s national vs. recommended local calibration coefficients for Iowa’s flexible pavements

Distress	Factors	Global	R ²	Local	R ²
HMA Rut	B1	0.4	0.41	0.4	0.53
	B2	0.52		0.55	
	B3	1.36		1.30	
GB Rut	B1_Granular	1		1	
SG Rut	B1_Fine Grain	1		1	
Fatigue for Acrack and Lcrack	B1	0.001032	N/A	0.001032	N/A
	B2	1.38		1.38	
	B3	0.88		0.88	
Lcrack	C1_Top	7	0.06	4.26	0.36
	C2_Top	3.5		1.93	
	C4_Top	1000		1000	
Acrack	C1_Bottom	1.31	0.17	1.31	0.17
	C2_Bottom	3.966		3.966	
	C3_Bottom	6,000		6,000	
Tcrack	K3_Level	$((3 \times \text{Pow}(10,-7)) \times \text{Pow}(\text{MAAT},4.0319)) \times 1 + 0$	0.24	$((0.5 \times \text{Pow}(10,-7)) \times \text{Pow}(\text{MAAT},4.0319)) \times 1 + 0$	0.27
IRI	C1	40	0.25	49.61	0.85
	C2	0.4		0.411	
	C3	0.008		0.007	
	C4	0.015		0.004	

Table 23. Summary of PMED v2.5.5's national vs. recommended local calibration coefficients for Iowa's rigid pavements

Distress	Factors	Global	R²	Local	R²
Faulting	C1	0.595	0.19	0.126	0.84
	C2	1.636		0.796	
	C3	0.0021848		0.0032	
	C4	0.00444		0.0012	
	C5	250		1721.63	
	C6	0.47		0.21	
	C7	7.3		4.6	
	C8	400		352	
Cracking	C1 (Fatigue)	2	0.24	2.3	0.59
	C2 (Fatigue)	1.22		1.35	
	C4 (Crack)	0.52		2.61	
	C5 (Crack)	-2.17		-1.48	
IRI	C1	0.8203	0.29	0.5328	0.87
	C2	0.4417		0.4719	
	C3	1.4929		0.2362	
	C4	25.24		21.21	

Table 24. Summary of PMED v2.5.5's national vs. recommended local calibration coefficients for Iowa's AC over JPCP

Distress	Factors	National	R ²	Local	R ²
HMA Rut	B1	0.4	0.37	0.4	0.46
	B2	0.52		0.48	
	B3	1.36		1.26	
GB Rut	B1_Granular	1		1	
SG Rut	B1_Fine grain	1		1	
Fatigue for Acrack and Lcrack	B1	0.001032	N/A	0.001032	N/A
	B2	1.38		1.38	
	B3	0.88		0.88	
Lcrack	C1_Top	7	0.16	3.89	0.21
	C2_Top	3.5		1.67	
	C4_Top	1000		1000	
Acrack	C1_Bottom	1.31	0.02	1.31	0.02
	C2_Bottom	3.966		3.966	
	C3_Bottom	6000		6000	
Terack	K3_Level	$((3 \times \text{Pow}(10,-7)) \times \text{Pow}(\text{MAAT},4.0319)) \times 1 + 0$	0.06	$((3.3 \times \text{Pow}(10,-7)) \times \text{Pow}(\text{MAAT},4.0319)) \times 1 + 0$	0.18
Approach 1 Reflective Transverse Cracking (Total Transverse Crack Length)	C1	0.1	0.24	0.1	0.78
	C2	0.52		0.52	
	C3	3.1		3.1	
	C4	79.5		81.67	
	C5	-2.71		-4.94	
Approach 2 Reflective Transverse Cracking (5-Year)	C1	0.1	0.21	0.1	0.81
	C2	0.52		0.52	
	C3	3.1		3.1	
	C4	79.5		82.53	
	C5	-2.71		-4.68	
Approach 1 IRI (Total Transverse Crack Length)	C1	40.8	0.35	47.91	0.83
	C2	0.575		0.473	
	C3	0.0014		0.0091	
	C4	0.00825		0.00554	
Approach 2 IRI (5-Year)	C1	40.8	0.35	48.63	0.86
	C2	0.575		0.494	
	C3	0.0014		0.0083	
	C4	0.00825		0.00563	

Additional validation with respect to independent Iowa pavement sections of the local calibration coefficients shown in Table 22 for Iowa's flexible pavements, in Table 23 for Iowa's rigid pavements, and in Table 24 for Iowa's AC over JPCP is shown in Appendix E.

EVALUATION OF THE PAVEMENT ME DESIGN CONCRETE OVERLAY DESIGN TOOL

Background

The United States road network is comprised of over 2 million miles of paved roads, and because of the enormous construction costs required to build new pavements, SHAs are shifting their focus to maintenance and rehabilitation techniques (Adams and Vandenbossche 2013).

One of the most popular rehabilitation methods that has been in use for a long time is the use of bonded concrete overlay on asphalt (BCOA) pavements. While the methods developed by the Portland Cement Association (Wu 1998) and the Colorado DOT (CDOT) (Tarr et al. 1998, Sheehan et al. 2004) for the BCOA procedure are widely used by SHAs, these methods have been validated with very limited field data because of several limitations. To address these limitations, the University of Pittsburgh developed a new procedure, Bonded Concrete Overlay of Asphalt Mechanistic-Empirical (BCOA-ME) design under the FHWA Pooled Fund Study TPF-5(165) (FHWA, n.d.), with comprehensive validations and enhancements to stress-prediction models and climate-consideration models (Adams and Vandenbossche 2013, Li et al. 2013, Vandenbossche and Sachs 2013, Vandenbossche et al. 2017). Access to the BCOA-ME tool is directly available through <https://www.engineering.pitt.edu/Vandenbossche/BCOA-ME/>.

A portion of the BCOA-ME procedure was integrated into the AASHTOWare Pavement ME Design (PMED) software v2.3 and renamed as Short-Jointed Plain Concrete Pavement over Asphalt Concrete (SJPCP/AC) (ARA 2017, Bhattacharya et al. 2017). During this process, the majority of the framework, key concepts, and inputs from the BCOA-ME procedure were integrated, with certain changes in assumptions made to ensure compatibility with PMED computational procedures. The major differences in assumptions were for the fatigue models used to predict failure, estimate asphalt stiffness, treat various environmental conditions, address traffic loading, and enable structural fiber design. Also, BCOAs of less than 6 inches in full-lane-width slabs were not included in the PMED software because other existing concrete overlay models with higher thickness options had already been included in the software. Bottom-up longitudinal fatigue cracking is therefore the only distress type included and predicted by the SJPCP/AC model in PMED, as other distresses such as faulting and IRI were not developed in the BCOA-ME procedure.

While Alland et al. 2018 evaluated the BCOA-ME and SJPCP/AC procedures, compared their differences in distress predictions, and presented their relative strengths and limitations, the impact of design inputs and material properties on predicted distresses that is required for design consideration by SHAs was not evaluated in their study. The goal of this study is therefore to perform further evaluation of the SJPCP/AC model in PMED by testing the individual inputs needed for SHA analyses. The results from this study will therefore serve as a useful reference for SHAs considering implementing the PMED SJPCP/AC procedure in their design practices.

Objective

The focus of this study was to perform comprehensive sensitivity analyses to evaluate the SJPCP/AC model added into the PMED software and to identify and rank the design inputs and material properties based on their observed levels of sensitivity. To compare the results over a broader range, four different PMED software cases were considered:

- 40-year design life and 50% reliability
- 20-year design life and 50% and reliability
- 40-year design life and 90% reliability
- 20-year design life and 90% and reliability

In all four cases, five locations from different climate zones were considered: Des Moines, Iowa (cold-wet); Orlando, Florida (hot-wet); Phoenix, Arizona (hot-dry); International Falls, Minnesota (cold-dry); and Los Angeles, California (temperate). Fifteen PMED inputs assumed to have a major impact on longitudinal fatigue cracking were considered. The overall methodology was similar to that of the NCHRP 01-47 research study, Sensitivity Evaluation of MEPDG Performance Prediction (Schwartz et al. 2011). The findings from this study continue from the tasks accomplished in the NCHRP 01-47 study and should provide valuable insights to SHAs.

Longitudinal Fatigue Cracking—Overview

The output distress included for the structural design of SJPCP/AC in PMED is bottom-up longitudinal fatigue cracking calculated in terms of the percentage of the total number of slabs. Figure 41 shows a PMED screenshot of the SJPCP/AC model and its corresponding predicted distress criteria.

Project1:Project*

General Information

Design type: Overlay

Pavement type: SJPCP over AC

Design life (years):

Existing construction:

Pavement construction:

Traffic opening:

Special traffic load

Performance Criteria	Limit	Reliability	Report Visibility
Initial IRI (in/mile)	N/A		<input checked="" type="checkbox"/>
SJPCP longitudinal cracking (percent slabs)	15	50	<input checked="" type="checkbox"/>

Figure 41. PMED v2.5.5 screenshot of performance criteria for SJPCP over AC

The underlying theory behind the inclusion of longitudinal fatigue cracking as the only SJPCP/AC output distress is based on the idea that when truck axles are closer to the transverse joint in the area of the wheel path, usually between the longitudinal joints, critical tensile-bending stress at the bottom of the slab under the wheel load occurs (ARA 2017). Because the top of the slab is usually warmer than the bottom of the slab, stress increases occur whenever the positive temperature gradient is higher through the slab thickness, and repetitive heavy axle loadings under such conditions result in fatigue damage along the bottom of the transverse joint of the slab. The damage eventually propagates to the surface along the length of the slab, leading to the formation of longitudinal fatigue cracks.

PMED Climate Data – North American Regional Reanalysis (NARR)

NARR climate data are used to provide the default climate inputs for designing a SJPCP/AC model in the PMED software. As mentioned earlier, the NARR data replace the previously used climate data derived from Ground-Based Weather Stations (GBWS) based mainly at airfield stations across the country.

Over the years, numerous limitations of the GBWS data have been reported by PMED users, including missing data, data availability for only a limited number of years, and low spatial coverage, impacting overall state design practices and leading to early design failures. NARR, providing high-quality atmospheric weather data addressing all these limitations, is available for a 32 x 32 km grid covering every location across the country (Brink et al. 2017, Gopiseti et al. 2019, Gopiseti et al. 2020a). NARR data, developed by the NCEP, are provided in hourly, daily, and monthly formats for the period from 1979 through the present. Using almost 40 years of continuous data from NARR rather than the 5–10 years of data from GBWS will significantly improve the accuracy of PMED predictions (Durham et al. 2019).

The only NARR limitation is that, during its implementation in PMED, files were created for only the existing 1,083 GBWS climate stations, with merely minor revisions and additions. However, since several quality control checks have been performed, the NARR data do not require any further quality assurance or data smoothing.

Methodology

OAT Sensitivity Analyses

OAT sensitivity analyses were used in this study as this is the most common methodology used for models such as PMED that include diverse sets of input parameters (Schwartz et al. 2011, Ceylan et al. 2013b, Ceylan et al. 2014). Even though the OAT sensitivity analysis process carries a huge computational burden, results from previous studies have proven it to be reliable and it is widely accepted by SHAs considering the modification of design practices (Guclu et al. 2009, Gopiseti et al. 2020a).

The normalized sensitivity index (NSI) for this study’s OAT sensitivity analysis was evaluated by varying the magnitude of an input parameter for PMED distress prediction. A higher NSI represents a significant increase in the PMED-predicted distress with an increase in input, and a lower NSI represents a decrease in the PMED-predicted distress with an increase in input. An NSI value of zero represents no impact on the predicted distress with either an increase or decrease in the input. The greater the magnitude of the NSI either positively or negatively represents greater sensitivity. The equation for NSI evaluation is given in Equation 3 (Schwartz et al. 2011).

$$NSI_{jk}^{DL} = \frac{(\Delta Y_j / DL_j)}{(\Delta X_k / X_k)} \quad (3)$$

where ΔY_j is the change in predicted distress j corresponding to a change of design input, ΔX_k is the change in design input k about the baseline, DL_j is the design limit of distress j , and X_k is the baseline value of design input k . The final outcome of this study’s OAT sensitivity analyses is categorization of the sensitivity levels for each design input considered.

NSI Ranking

For all tested cases, the maximum NSI (absolute value) for each considered design input was evaluated, with the results categorized as follows:

- Hypersensitive – NSI greater than 5
- Very Sensitive – NSI between 1 and 5
- Sensitive – NSI between 0.1 and 1
- Not Sensitive – NSI less than 0.1

Sensitivity Analysis Matrix – Ranges of Design Inputs

Fifteen PMED design inputs assumed to have significant impact on predicted longitudinal fatigue cracking were considered for analysis. Table 25 shows the list of inputs and ranges considered using the OAT methodology.

Table 25. Input ranges for sensitivity analyses

Design Input	Base Case	Lower Case (Alternative Case 1)	Upper Case (Alternative Case 2)
SJPCP Thickness, in.	6	4	8
AC Thickness, in.	6	4	8
Base Thickness, in.	6	3	9
AADTT	4,000	2,000	6,000
AC Layer Input Parameters			
Effective Binder Content in AC, %	10.14	× 0.9	× 1.1
Air Voids in AC, %	6.54	× 0.9	× 1.1
AC Poisson's Ratio	0.35	0.30	0.40
SJPCP Layer Input Parameters			
Joint Spacing in Terms of Slab Size (i.e., Panel Size), sq. ft	6 x 6	5 x 5	7 x 7
PCC Unit Weight, pcf	150	140	160
PCC Poisson's Ratio	0.15	0.10	0.20
PCC Coefficient of Thermal Expansion (CTE), in/in/°F × 10 ⁻⁶	5.5	5.0	6.0
PCC Modulus of Rupture at 28 Days, psi	690	× 0.8	× 1.2
PCC Thermal Conductivity, BTU/hr-ft-°F	1.25	1	1.50
PCC Surface Shortwave Absorptivity	0.85	0.80	0.98
Transverse Joint LTE, %	50	25	75

The PMED-allowable thickness range for SJPCP overlay designs was between 3 inches and 8 inches), the allowable range for AC thickness was between 3 inches and 10 inches, and for joint spacing in terms of slab size (i.e., panel size), the allowable range was between 5 ft x 5 ft and 8 ft x 8 ft. Based on these limitations, the final ranges for these inputs were determined and analyzed. Over 1,000 PMED runs were executed to test all these design inputs for each location, and by varying design life and reliability criteria, to analyze the findings over a broader scale.

Results

Cases 1 and 2 – 50% Reliability – 20- and 40-Year Design Life

Table 26 contains a summary of NSI results for Case 1 (40-year design life with 50% reliability) and Table 27 contains a summary of results for Case 2 (20-year design life with 50% reliability).

Table 26. NSI summary: 40-year design life and 50% reliability

Location	Des Moines	Orlando	Phoenix	International Falls	Los Angeles
Design Input					
AC Thickness	12.88	0.83	0.03	16.65	6.80
AADTT	0.05	0.00	0.00	2.23	0.01
AC Poisson's Ratio	0.00	0.00	0.00	0.00	0.00
Air Voids in AC	0.01	0.00	0.00	0.59	0.00
Base Thickness	0.56	0.02	0.00	9.04	0.16
Effective Binder Content in AC	0.01	0.00	0.00	0.63	0.00
Joint Spacing	0.01	0.00	0.00	1.10	0.00
PCC Unit Weight	0.00	0.00	0.00	0.00	0.00
PCC Poisson's Ratio	0.00	0.00	0.00	0.00	0.00
PCC Coefficient of Thermal Expansion	0.00	0.00	0.00	0.03	0.00
PCC Modulus of Rupture at 28 Days	0.92	0.02	0.00	13.83	0.31
PCC Thermal Conductivity	0.00	0.00	0.00	0.03	0.00
PCC Surface Shortwave Absorptivity	0.00	0.00	0.00	0.42	0.00
SJPCP Thickness	0.45	0.01	0.00	8.18	0.13
Transverse Joint LTE	0.40	0.01	0.00	10.04	0.11

Light red – Hypersensitive (NSI > 5), Yellow – Very Sensitive (NSI between 1 and 5), Green – Sensitive (NSI between 0.1 and 1), White – Insensitive (NSI < 0.1)

Table 27. NSI summary: 20-year design life and 50% reliability

Location	Des Moines	Orlando	Phoenix	International Falls	Los Angeles
Design Input					
AC Thickness	9.54	2.41	0.13	9.99	8.06
AADTT	0.13	0.00	0.00	2.93	0.03
AC Poisson's Ratio	0.00	0.00	0.00	0.00	0.00
Air Voids in AC	0.02	0.00	0.00	1.03	0.00
Base Thickness	0.81	0.05	0.01	5.61	0.38
Effective Binder Content in AC	0.02	0.00	0.00	1.13	0.00
Joint Spacing	0.02	0.00	0.00	1.45	0.01
PCC Unit Weight	0.00	0.00	0.00	0.01	0.00
PCC Poisson's Ratio	0.01	0.00	0.00	0.01	0.00
PCC Coefficient of Thermal Expansion	0.00	0.00	0.00	0.05	0.00
PCC Modulus of Rupture at 28 Days	1.78	0.06	0.00	6.44	0.70
PCC Thermal Conductivity	0.00	0.00	0.00	0.06	0.00
PCC Surface Shortwave Absorptivity	0.02	0.00	0.00	0.75	0.00
SJPCP Thickness	2.45	0.11	0.00	13.50	0.78
Transverse Joint LTE	0.89	0.03	0.00	5.84	0.27

Light red – hypersensitive (NSI > 5), Yellow – Very Sensitive (NSI between 1 and 5), Green – Sensitive (NSI between 0.1 and 1), White – Insensitive (NSI < 0.1)

Reliability (R) in PMED is defined as the probability that the predicted distress will remain less than the critical level over the design period (AASHTO 2010). For example, a reliability of 80% for longitudinal fatigue cracking represents the probability (for 8 out of 10 projects) that the predicted distress will not exceed the distress criteria over the design life. More important projects such as sections with higher recorded traffic volumes will require higher reliability values as inputs. Case 1 and Case 2 results are based on 50% reliability, representing less important projects.

The major observation from both cases is that most inputs except for a few were hypersensitive, very sensitive, or sensitive for the location International Falls, Minnesota, a cold-dry climate zone where extreme freezing cycles occur throughout a typical year. Overlay failures usually occur due to extremely low temperatures and enormous accumulations of snow that result in moisture infiltration through cracks. These results are consistent with previous studies on

sensitivity results for AC overlays using PMED (Gopiseti et al. 2020a) and sensitivity results using the BCOA-ME tool (Li et al. 2013). The hypersensitive inputs include the various layer thicknesses, PCC Modulus of Rupture (MOR), and Transverse Joint LTE. These inputs were also found to be very sensitive in BCOA-ME, American Concrete Pavement Association (ACPA), and CDOT procedures, and this is mainly because their sensitivity is derived from the model base and the way the effects of these inputs are incorporated considering the extremities of climate.

During the development of the BCOA-ME procedure, sensitivity analyses were performed for six design inputs (traffic, PCC MOR, AC layer thickness, PCC CTE, AC elastic modulus, and subgrade k-value) at four locations representing different climate zones (Minneapolis, Minnesota; Seattle, Washington; Phoenix, Arizona; and Miami, Florida). For all inputs, higher sensitivities were observed for Minneapolis, in the same climate zone as the International Falls location considered in this study.

AC layer thickness was observed to be one of the most sensitive inputs for all locations, while SJPCP thickness and base thickness were observed to be sensitive for some locations. This is consistent with engineering intuition and engineering experience when considering the nature of the behavior of asphalt, concrete, and soil type in the base and sub-base with respect to extremities of climate cycles (i.e., higher and lower temperatures). Multiple studies have found these inputs to be sensitive (Schwartz et al. 2011, Kim et al. 2005, Tarefder et al. 2014, Tarefder and Sumee 2011, Cetin et al. 2018). Since thickness values vary across state-to-state design practices, it is recommended that field validation with previously measured data be performed before finalizing designs.

Other inputs that have a slight impact at certain locations are AADTT, Transverse Joint LTE, and PCC MOR. For AADTT, the annual values of axle loads for different vehicle classes and axle types are usually considered in design practices, making AADTT one of the sensitive inputs that therefore requires careful consideration. Transverse Joint LTE is usually indexed to a shearing mechanism at cracks, and a significant change in the LTE value accelerates crack propagation from the bottom to the top of the slab, making it one of the most sensitive inputs. PCC MOR is usually observed to be sensitive for designs with shorter slabs. The sensitivity results of PCC MOR in this study are consistent with those from BCOA-ME evaluation (Li et al. 2013).

Joint spacing and CTE are two important inputs that are carefully considered by SHAs when designing concrete overlays. As mentioned in the introduction, only a portion of BCOA-ME procedures were added to the Pavement ME Design software, renamed as SJPCP (ARA 2017). The terminology SJPCP represents designs with “short” joint spacing/panel size/slab size, and therefore only limited options for joint spacing (5, 6, 7, and 8 ft) are allowed for use as inputs in the PMED software. However, the BCOA-ME procedure developed by the University of Pittsburgh allows analyses of low and very high joint spacings not included in the PMED software. Bhattacharya et al. (2017) studied the impact of joint spacing on SJPCP and found that joint spacings between 5 to 8 sq. ft are reliable for achieving better performance and reasonable

construction costs. Because of the limited range of joint-spacing options in PMED, the sensitivity results from this study came out as Insensitive.

The CTE value and its sensitivity depends on the joint spacing considered for the design. Li et al. (2013), the developers of the BCOA-ME model, found the CTE to be sensitive for designs with joint spacings (in terms of slab size) of 4 sq. ft or lower. As joint spacing increases, the CTE sensitivity decreases. It was observed in the Li et al. (2013) study that the CTE was “insensitive” for designs with joint spacings of 5 sq. ft, the minimum input value in PMED, and higher, so it is not surprising that the CTE sensitivity from this study came out as Insensitive.

Cases 3 and 4 – 90% Reliability – 20- and 40-Year Design Life

Table 28 gives a summary of NSI results for Case 3 (40-year design life with 90% reliability), and Table 29 gives the summary results for Case 4 (20-year design life with 90% reliability).

Table 28. NSI summary: 40-year design life and 90% reliability

Location	Des Moines	Orlando	Phoenix	International Falls	Los Angeles
Design Input					
AC Thickness	9.86	0.00	0.00	16.27	2.29
AADTT	0.00	0.00	0.00	0.00	0.00
AC Poisson's Ratio	0.00	0.00	0.00	0.00	0.00
Air Voids in AC	0.00	0.00	0.00	0.00	0.00
Base Thickness	0.00	0.00	0.00	5.10	0.00
Effective Binder Content in AC	0.00	0.00	0.00	0.00	0.00
Joint Spacing	0.00	0.00	0.00	0.00	0.00
PCC Unit Weight	0.00	0.00	0.00	0.00	0.00
PCC Poisson's Ratio	0.00	0.00	0.00	0.00	0.00
PCC Coefficient of Thermal Expansion	0.00	0.00	0.00	0.00	0.00
PCC Modulus of Rupture at 28 Days	0.00	0.00	0.00	11.15	0.00
PCC Thermal Conductivity	0.00	0.00	0.00	0.00	0.00
PCC Surface Shortwave Absorptivity	0.00	0.00	0.00	0.00	0.00
SJPCP Thickness	0.00	0.00	0.00	4.09	0.00
Transverse Joint LTE	0.00	0.00	0.00	2.53	0.00

Light red – Hypersensitive (NSI > 5), Yellow – Very Sensitive (NSI between 1 and 5), Green – Sensitive (NSI between 0.1 and 1), White – Insensitive (NSI < 0.1)

Table 29. NSI summary: 20-year design life and 90% reliability

Location	Des Moines	Orlando	Phoenix	International Falls	Los Angeles
Design Input					
AC Thickness	14.33	0.00	0.00	16.45	10.61
AADTT	0.00	0.00	0.00	4.75	0.00
AC Poisson's Ratio	0.00	0.00	0.00	0.00	0.00
Air Voids in AC	0.00	0.00	0.00	0.00	0.00
Base Thickness	0.00	0.00	0.00	12.36	0.00
Effective Binder Content in AC	0.00	0.00	0.00	0.11	0.00
Joint Spacing	0.00	0.00	0.00	2.75	0.00
PCC Unit Weight	0.00	0.00	0.00	0.00	0.00
PCC Poisson's Ratio	0.00	0.00	0.00	0.00	0.00
PCC Coefficient of Thermal Expansion	0.00	0.00	0.00	0.00	0.00
PCC Modulus of Rupture at 28 Days	0.00	0.00	0.00	14.79	0.00
PCC Thermal Conductivity	0.00	0.00	0.00	0.00	0.00
PCC Surface Shortwave Absorptivity	0.00	0.00	0.00	0.00	0.00
SJPCP Thickness	0.00	0.00	0.00	11.81	0.00
Transverse Joint LTE	0.00	0.00	0.00	13.06	0.00

Light red – Hypersensitive (NSI > 5), Yellow – Very Sensitive (NSI between 1 and 5), Green – Sensitive (NSI between 0.1 and 1), White – Insensitive (NSI < 0.1)

Similar to the summary of results in Table 26 and Table 27, the majority of the inputs are seen to be sensitive at the International Falls, Minnesota, location, and AC thickness is sensitive for some of the locations. The other distresses had no impact on the predicted distresses.

However, it is important to note that sensitivity analyses do not consider distress criteria or limits in their evaluation. For example, the PMED default design limit shown in Figure 41 for longitudinal fatigue cracking is 15%. As the reliability requirement increases for important projects, predicted distresses for a given design life also increase. If AADTT is considered for a sensitivity study (base case – 4,000 trucks, lower case – 2,000 trucks, and higher case – 6,000 trucks), in all cases, the predicted distress could be 100% (much higher than the 15% limit), and the sensitivity values will be zero, thereby misleading designers. It is therefore recommended that sensitivity analyses using 50% reliability for all pavement types always be used in

performing such studies. The recommended default reliability in PMED for longitudinal fatigue cracking is also 50%, as shown in Figure 41.

Summary of Key Findings

Sensitivity of PMED input parameters to longitudinal fatigue cracking distress of the new SJPCP/AC model was analyzed, with 15 design inputs and five locations representing different US climatic zones considered. Four cases with varying design life and reliability were considered. Based on the summary of results from all cases, the major conclusions are as follows:

- In all cases, most input parameters were sensitive to longitudinal fatigue cracking at the International Falls, Minnesota, location, where extreme cold weather and moisture infiltration through cracks result in premature failure of the overlay.
- Layer thicknesses were sensitive input parameters in all cases and careful consideration should be given to performing field surveys to collect information on the existing AC layer and base layer thicknesses, and the appropriate SJPCP layer should be optimized.
- Based on the summary of results, AADTT, Transverse Joint LTE, and PCC MOR were moderately sensitive inputs.
- Joint spacing and CTE were observed as “insensitive” due to the limited range of input options in the PMED software.
- All other inputs had either very minimal or no impact on predicted longitudinal fatigue cracking.
- It can also be concluded that sensitivity analyses studies should be performed using a mean reliability of 50%, because the use of higher reliabilities for sensitivity analyses could result in misleading conclusions for design practices.

Recommendations

Five locations from different climate zones were considered in this study, and since it could be observed that climate conditions can play a major role in design considerations, performing site-specific evaluation for every project before finalizing the design inputs is recommended. Also, although the SJPCP/AC model in PMED currently predicts longitudinal fatigue cracking as its output distress, other important distresses such as faulting, transverse cracking, and IRI should be studied and incorporated into future versions of the software to support broader analyses that would help SHAs in better decision-making.

DATA-DRIVEN DETERMINATION OF OPTIMAL PAVEMENT THICKNESS BASED ON AASHTOWARE-PAVEMENT-ME-DESIGN-RECOMMENDED DISTRESS CRITERIA AND RELIABILITY LEVELS

Background

PMED design and analysis involves an iterative process comprised of three steps: (1) create a trial design, (2) predict distresses for the trial design by performing PMED runs, and (3) review the predicted distresses against the distress criteria considered for the trial design, then modify the trial design to produce an acceptable design satisfying the distress criteria (AASHTO 2015). The overall PMED process remains the same for all users, though the distress criteria/performance limits and reliability levels considered for a trial design can vary depending on local conditions (e.g., climate, traffic) and to meet specific needs.

The PMED software provides default values for these distress criteria inputs determined based on global and national calibration performed for selected representative sections across the country. Table 30 depicts an example of the home screen of the PMED software for the distress criteria and reliability input section for flexible pavement design.

Table 30. Distress criteria and reliability level as displayed on the home screen of the PMED software

Performance Criteria	Limit	Reliability
Initial IRI (in./mile)	63	—
Terminal IRI (in./mile)	172	90
AC top-down fatigue cracking (% lane area)	25	90
AC bottom-up fatigue cracking (% lane area)	25	90
AC thermal cracking (ft/mile)	1,000	90
Permanent deformation - total pavement (in.)	0.75	90
Permanent deformation - AC only (in.)	0.25	90

The PMED distress criteria are used to reflect the magnitude of pavement distresses in terms of the maximum acceptable damage based on allocated construction costs for a given design period. These limits also can vary due to various other factors such as climate, traffic, material properties, and design inputs considered for the design procedure.

The reliability (R) considered for each distress in the trial design is the probability that the predicted distress will not exceed the established design limit during the design period considered ($R = P [\text{Distress over Design Period} < \text{Critical Distress Level}]$) (AASHTO 2015). A balance between the design criteria and reliability is necessary to achieve thinner pavement thickness (i.e., lower construction costs) that can still result in low predicted distress.

Tran et al. (2017) evaluated the sensitivity of pavement design thickness in relation to distress criteria and reliability level for four roadway classifications (Interstate, Principal Arterial, Minor Arterial and Major Collectors) based on CDOT's design procedures. However, their analysis was performed only for flexible pavements and the findings related to the sensitivity of only two types of pavement distresses: bottom-up fatigue cracking and permanent deformation to pavement thickness.

The objective in our study presented previously in this report was to present comprehensive analysis of the sensitivity at two different reliability levels for both flexible and rigid pavement types with respect to all PMED distresses. Additionally, in the current study, to seek an understanding of actual state practices related to distress criteria and reliability levels, a survey was sent out to PMED users across the United States and Canada and its results are summarized and presented as follows.

Survey Results

A survey questionnaire was developed and sent to all SHAs in the United States and Canada as well as to various other PMED users, including pavement engineers from private agencies, consultants, pavement associations, and academia. A total of 26 responses (22 from US SHAs, 1 from a Canadian SHA, 2 from private agencies, and 1 from a pavement association) were received. The complete list of respondent organizations is shown in Table 31, which shows only the respondents that responded to this survey *and* were actively using the software as of March 2020.

Table 31. Survey respondent organizations

Classification	Respondent
United States – SHAs	Alabama DOT
	Alaska DOT
	Arizona DOT
	California DOT
	Colorado DOT
	Florida DOT
	Iowa DOT
	Indiana DOT
	Louisiana DOT
	Maine DOT
	Maryland DOT
	Michigan DOT
	Minnesota DOT
	Mississippi DOT
	Missouri DOT
	Nebraska DOT
	North Carolina DOT
	Oklahoma DOT
Pennsylvania DOT	
South Carolina DOT	
South Dakota DOT	
Utah DOT	
Canada – SHA	Alberta Transportation
Private Agencies/Consultants	Consulting firm in Illinois
	Consulting firm in Colorado
Pavement Association	Southeast Cement Promotion Association

All 26 respondents (100%) reported using the PMED software for designing new flexible pavements, and 23 of 26 respondents (88%) reported the use of the software for rigid-pavement designs.

As shown in Figure 42, 10 respondents (38%) reported the use of the PMED software's default/nationally calibrated values, while 16 respondents (62%) reported the use of agency-specific values used to replace the PMED default values for their own design procedures.

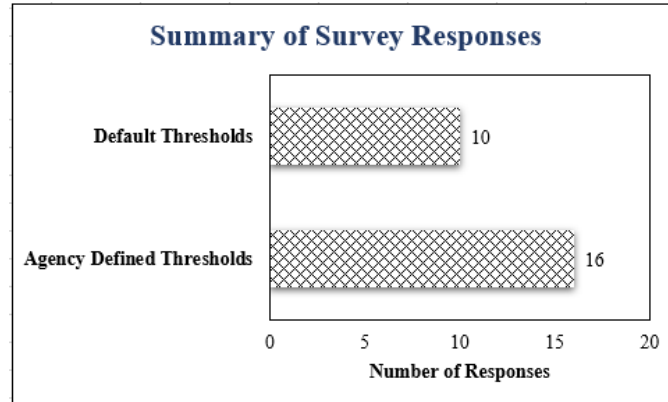


Figure 42. Summary of the number of agencies using PMED default vs. agency-specific values

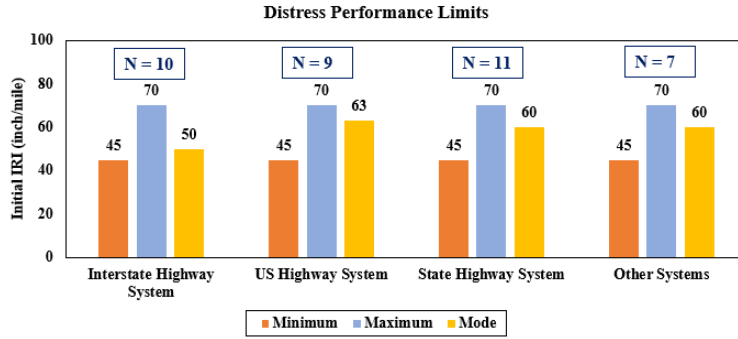
In other words, Figure 42 clearly shows that the PMED design criteria and/or reliability values vary from agency to agency.

Summary of Practices – Distress Criteria and Reliability Levels in PMED

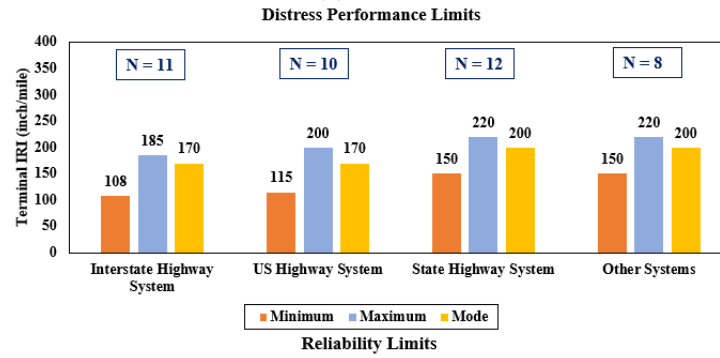
Survey respondents were asked to provide agency-specific distress criteria and reliability levels from their own state practices for four different pavement/road classifications – the Interstate highway system, US highway system, state highway system, and Others. These classifications are based on various factors such as truck traffic, traffic growth rate, number of lanes in the design direction, and speed limit. The Interstate highway system represents the highest traffic level, the US and state highway systems represent medium to low traffic levels, and the Others represent a very low traffic level with lower speed limits.

Figure 43 and Figure 44 show a summary of responses for agency-recommended distress criteria and reliability levels for flexible and rigid pavement distresses, respectively. While this summary is based on the 16 responses that mentioned the use of agency-specific values, according to the survey results, agencies/PMED users evaluate only specific distresses for a pavement type during the design process instead of all distresses predicted by the software.

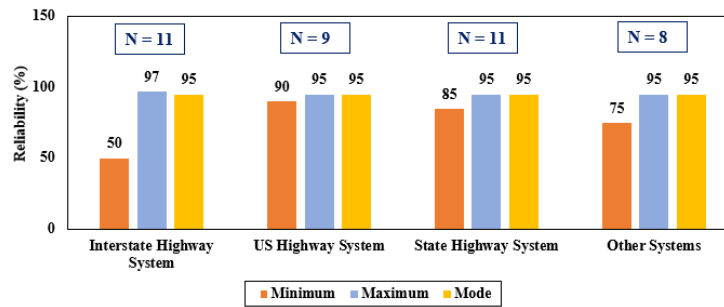
This decision is due to two reasons: (1) the specific distress evaluated was the most commonly observed in their state and distresses not evaluated were not observed in their state (e.g., rutting is generally observed in states with very hot temperatures and thermal cracking—i.e., low-temperature cracking—is observed in states with freezing temperatures) or (2) users may have already used other procedures such as AASHTO 1993 or earlier methods to evaluate specific distresses. Hence, for each distress shown in Figure 43 and Figure 44, the number of responses is shown as N. Based on the responses received, the minimum, maximum, and mode (i.e., the most-frequently repeated response) for each distress are evaluated and presented.



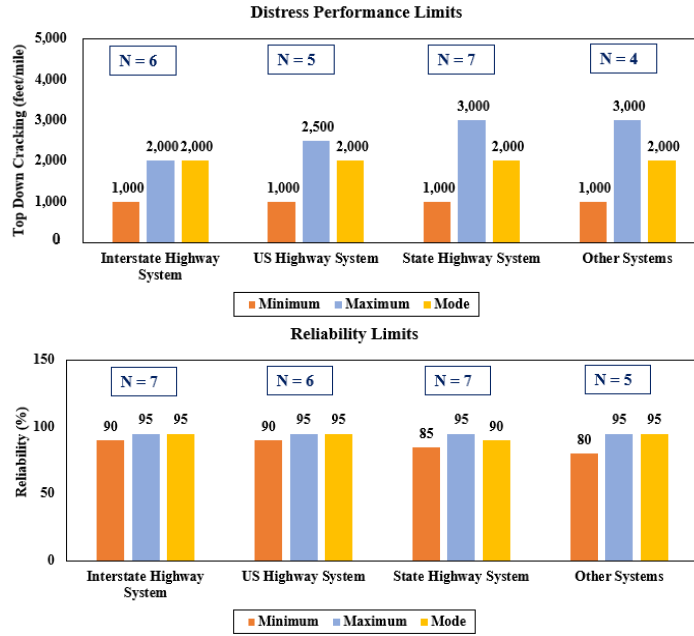
(a) Initial IRI



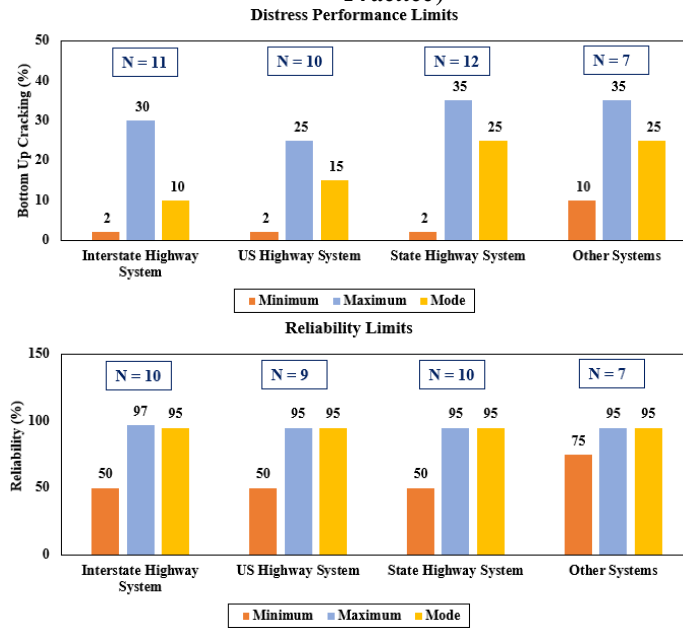
Reliability Limits



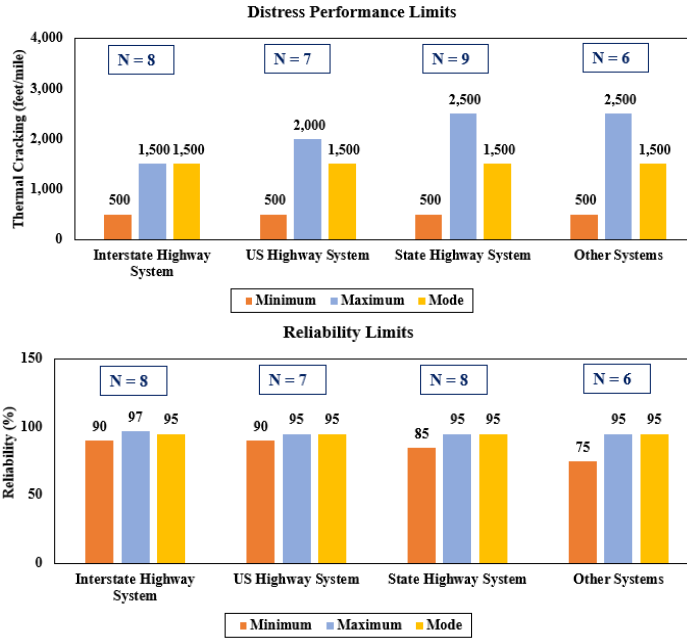
(b) Terminal IRI (*Manual of Practice* distress criteria—Interstate: 160 inches/mile; US, State, and Others: 200 inches/mile)



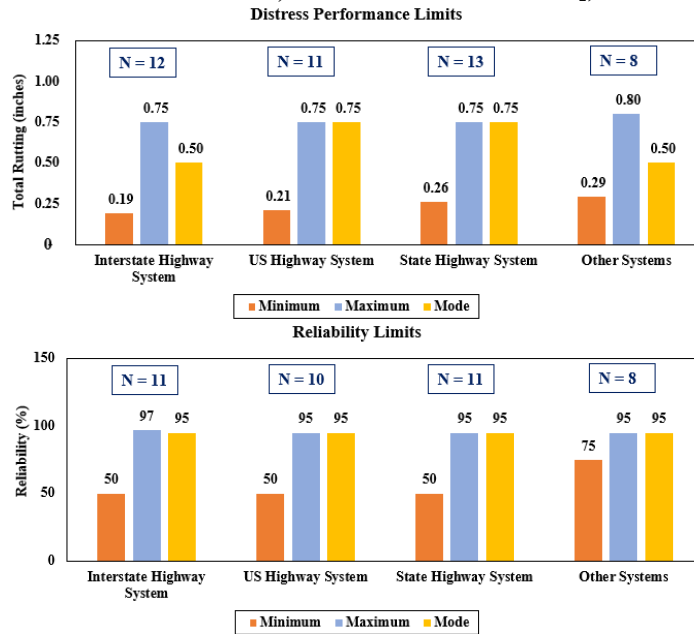
(c) Top-down/longitudinal cracking (no recommended distress criteria provided in the *Manual of Practice*)



(d) Bottom-up/alligator cracking (*Manual of Practice* distress criteria—Interstate: 10%, US: 20%, State: 35%, Others: 35%)

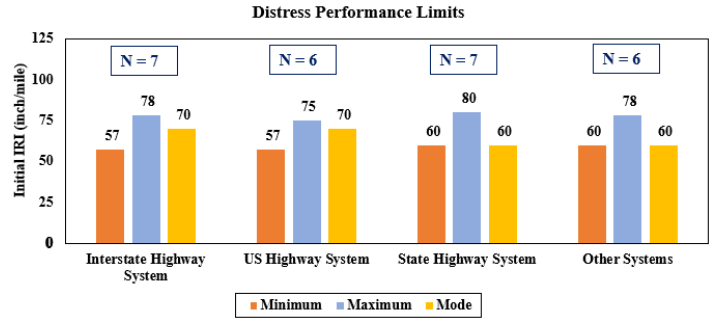


(e) Thermal/transverse cracking (*Manual of Practice* distress criteria—Interstate: 500 feet/mile; US, State, and Others: 700 feet/mile)

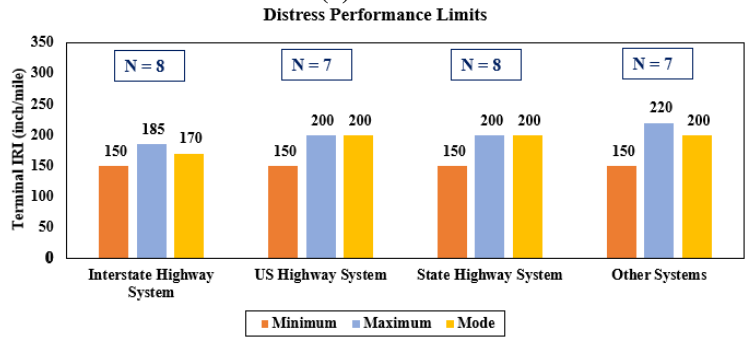


(f) Total rutting (*Manual of Practice* distress criteria—Interstate: 0.40 inches, US: 0.50 inches, State: 0.50 inches, Others: 0.65 inches)

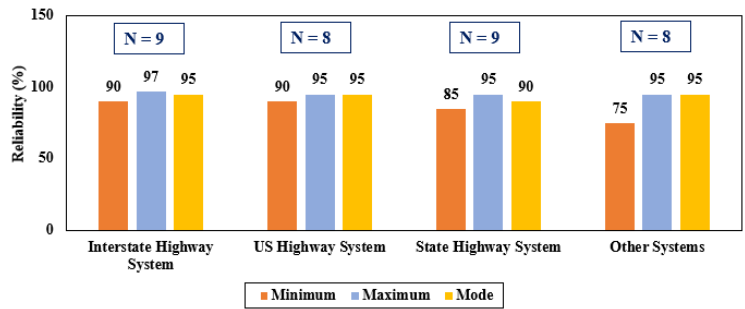
Figure 43. Summary of survey results for flexible pavement distresses: Agency-recommended design criteria and reliability levels



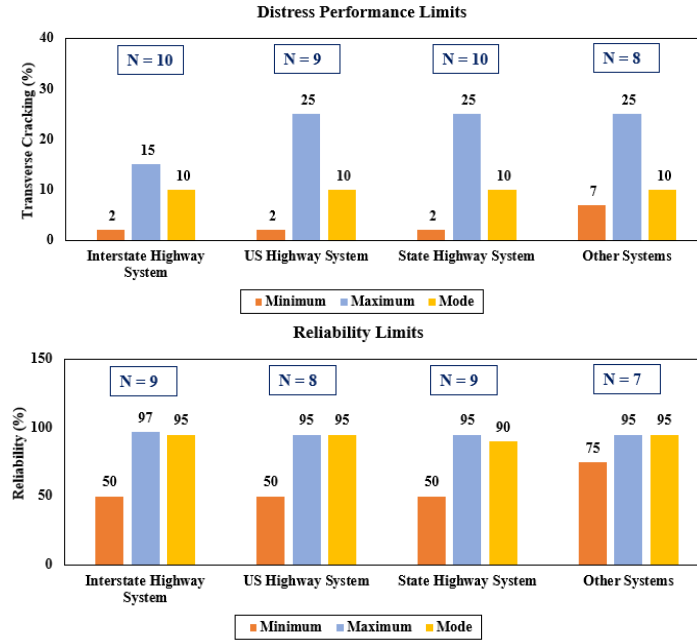
(a) Initial IRI



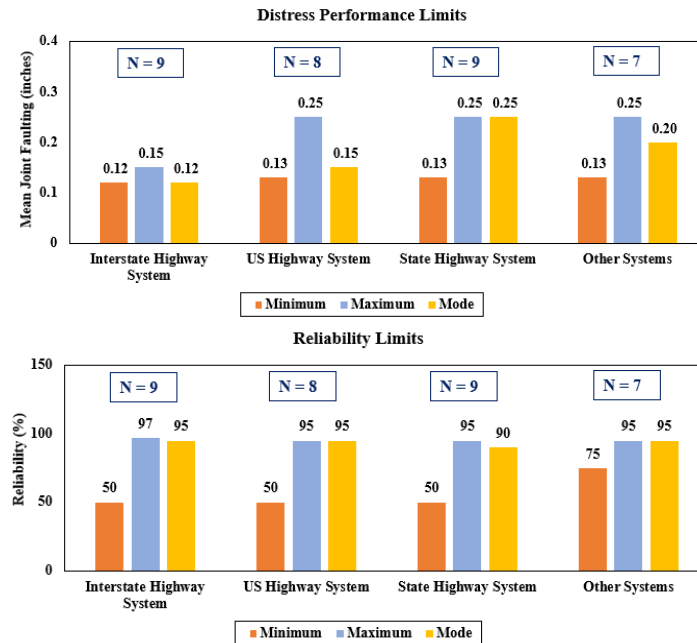
Reliability Limits



(b) Terminal IRI (*Manual of Practice* distress criteria—Interstate: 160 inches/mile; US, State and Others: 200 inches/mile)



(c) JPCP transverse cracking (*Manual of Practice* distress criteria—Interstate: 10%, US: 15%, State: 20%, Others: 20%)



(d) Mean joint faulting (*Manual of Practice* distress criteria—Interstate: 0.15 inches, US: 0.20 inches, State: 0.25 inches, Others: 0.25 inches)

Figure 44. Summary of survey results for rigid pavement distresses: Agency-recommended design criteria and reliability levels

For all distresses, in Figure 43 and Figure 44, the metrics clearly reflect significant variability in distress performance limits and reliability levels, with recommended values drastically differing

from agency to agency. For example, Figure 43(b) shows that the minimum, maximum and mode values for terminal IRI in flexible pavements that are part of the Interstate system are 108 inches/mile, 185 inches/mile, and 170 inches/mile, respectively. However, the limits increase to 115 inches/mile, 200 inches/mile, and 170 inches/mile for the US highway system, and 150 inches/mile, 220 inches/mile and 200 inches/mile for the state highway and other systems.

This shows a significant increase over a pavement’s design life in the terminal IRI limits associated with the decrease in traffic for different pavement systems. The summary of survey results in Figure 43 and Figure 44 will provide an understanding to agencies across the country in the process of determining their agency-specific limits of what nondefault values/limits other agencies have specified for each distress relative to that of the national calibration models recommended in the *PMED Manual of Practice*.

Thickness Determination Based on Achieved Reliability

The survey results shown in Figure 43 and Figure 44 and the recommendations provided in the *Manual of Practice* for distress criteria/performance limits were compared, and it was determined that the maximum recommended nationally calibrated default limits for each distress in PMED were the same or only slightly different than the reported agency-specific limits in most cases.

PMED distress prediction models are nationally calibrated, and performing local calibration depending on the local conditions is strongly recommended. The Iowa DOT implemented the PMED software soon after its release and has sponsored multiple research studies to perform local calibration (Ceylan et al. 2013b, Ceylan et al. 2015). The current research study has performed local calibration using the version of the software PMED v2.5.5 because of numerous changes made to the distress models in the software over the last few years. Based on the findings from this report’s various studies, a set of local calibration coefficients has been determined and used in this task to enhance the capability of the software to predict distresses based on Iowa conditions. Additional analyses have also been performed using the PMED-recommended limits provided in the *Manual of Practice* (and shown in Figure 43 and Figure 44) to determine the recommended minimum thicknesses for implementing the design of flexible and rigid pavements for Iowa.

Table 32 shows the recommended reliability levels to be used for different road classifications based on the *Manual of Practice* (AASHTO 2015).

Table 32. Recommended level of reliability for different road classifications

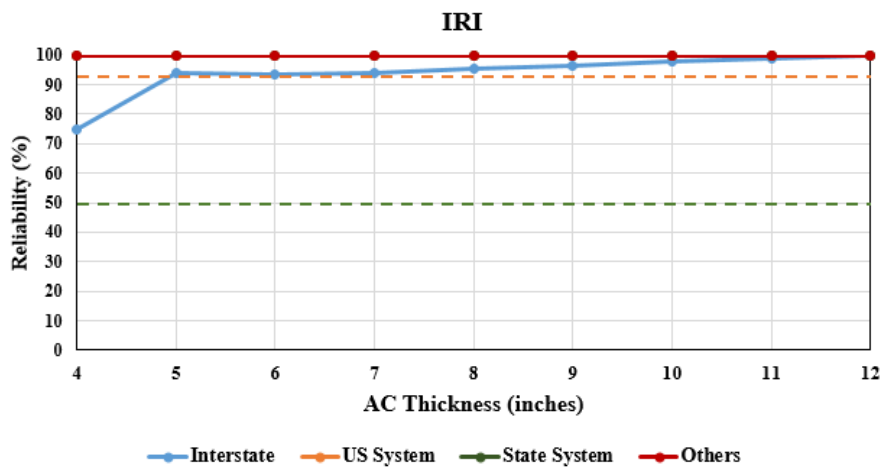
Road Classification	Level of Reliability
Interstate highway system	95%
US highway system	85%–90%
State highway system	75%–80%
Others	70%–75%

Source: Adapted from AASHTO 2015

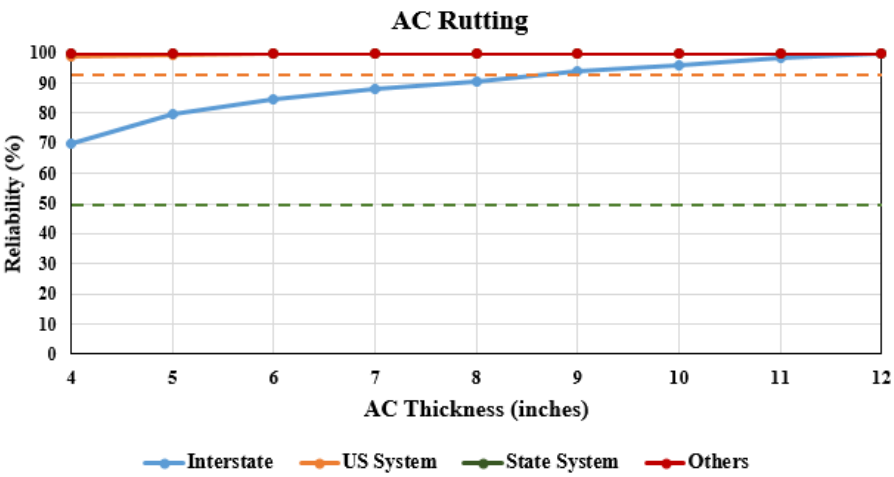
These various distress criteria and reliability recommendations were taken into consideration when determining the recommended minimum thicknesses resulting from using this study's latest recommended local calibration coefficients (see Table 22 for Iowa's flexible pavements, Table 23 for Iowa's rigid pavements, and Table 24 for Iowa's AC over JPCP).

Flexible Pavements

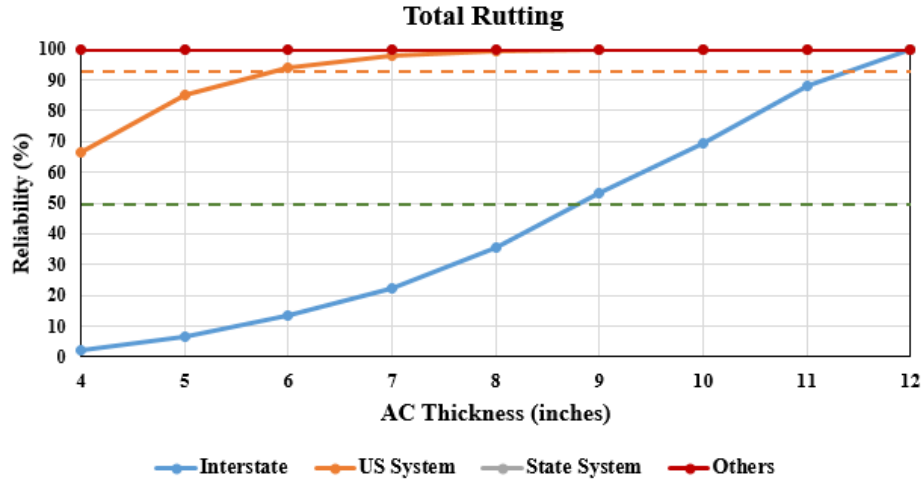
Flexible pavement distresses predicted by the PMED software include IRI, rutting, top-down (longitudinal) cracking, bottom-up (alligator) cracking, and thermal/transverse cracking. Figure 45(a – e) shows the levels of reliability for flexible pavement distresses that can be achieved using PMED for AC thicknesses varying between 4 and 12 inches.



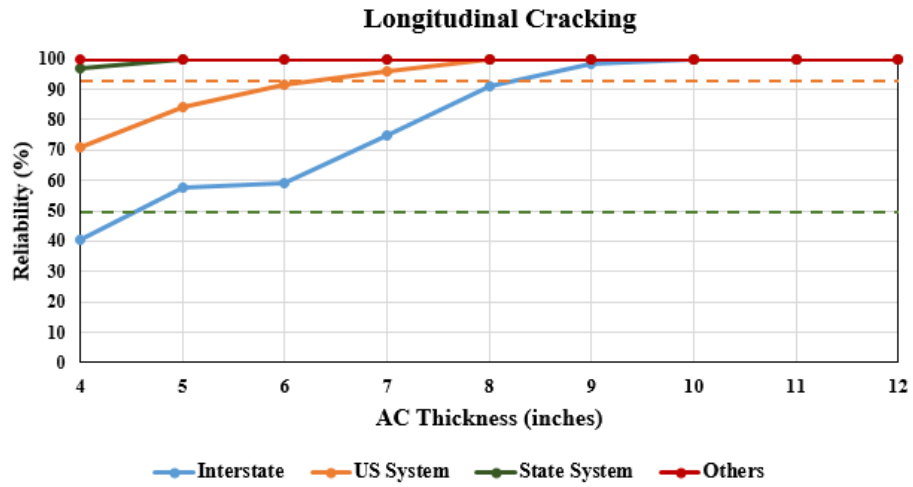
(a)



(b)



(c)



(d)

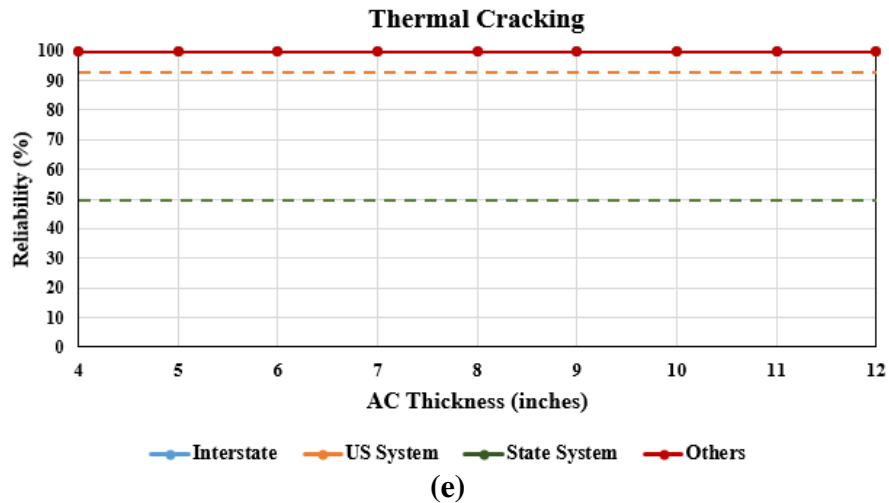


Figure 45. Reliability level versus AC thickness for flexible pavement distresses: (a) IRI, (b) AC layer rutting, (c) total rutting, (d) longitudinal (top-down) cracking, and (e) thermal/transverse cracking (Note that the various colors of solid lines represent various road classifications that in some cases showed exactly the same results and therefore stack on top of one another. Also, the orange line marks 92% reliability and the green line 50% reliability.)

Note that the Figure 45 simulations utilized a 20-year design life, PG 64-28 grade asphalt binder, this study’s latest recommended local calibration coefficients (see the previous Table 22 for Iowa’s flexible pavements), and the other PMED inputs listed in Appendix H.

For IRI, as shown in Figure 45(a), in Interstate design, when the reliability was between 80% and 90%, a 1-inch increase in AC thickness improved the reliability level by approximately 10%. When the reliability level was around 90%, a 1-inch increase in AC thickness increased the reliability level by usually only less than 5%. When the reliability was above 95%, a 1-inch increase in AC thickness had a very minimal impact on design reliability levels. These findings suggest that the reliability for Interstates can be set at 95% with a recommended minimum AC thickness of 9 inches if IRI is a major distress observed in a given agency’s pavement systems. For US, state, and other pavement systems with medium-to-low traffic, the AC thickness design remained the same if the reliability selected was anywhere between 70% and 95%, recommending the use of a minimum AC thickness of 4 inches.

Figure 45(b and c) shows the achieved reliability for AC layer rutting and total rutting distresses respectively. In Interstate design, a 1-inch increase in AC thickness increased reliability by about 10% for AC layer rutting and 1.5-inch increase in AC thickness increased reliability by about 10% for total rutting. This recommends the use of a reliability set at 95% with a recommended minimum AC thickness of 12 inches for Interstate highway systems. For US, state and other systems, the AC thickness had minimal impact on recommended reliability levels, suggesting the use of a lower minimum AC thickness than that recommended for Interstate highway systems.

Figure 45(d) shows the reliability levels achieved for top-down cracking, and it was determined that a 95% reliability level was achieved for all the selected pavement systems with the use of 9 inches of minimum AC thickness for Interstates and a lower thickness for other pavement systems.

Figure 45(e) shows the findings for thermal cracking and that AC thickness has no impact on reliability levels for all the investigated pavement systems.

The overall findings suggest the use of the recommended minimum thickness and reliability levels derived for IRI and total rutting distress as shown in Figure 45(a) and (c) will also achieve the target reliability for the other AC distresses. The recommended minimum AC thickness from these overall findings for Iowa-specific conditions to meet the recommended reliabilities in Table 32 is 12 inches for Interstates, 6 inches for the US highway system, and more than 4 inches for the state highway system and other systems.

Rigid Pavements

Rigid pavement distresses predicted by the PMED software are IRI, mean joint faulting, and transverse cracking (percent of slabs). Note that the following simulations utilized a 20-year design life, 20 feet of joint spacing, this study's latest recommended local calibration coefficients for Iowa (see the previous Table 23 for Iowa's rigid pavements), and the other PMED inputs listed in Appendix H.

Figure 46 (a–c) shows the level of reliability for rigid pavement distresses that can be achieved using PMED for PCC thicknesses varying between 4 and 12 inches.

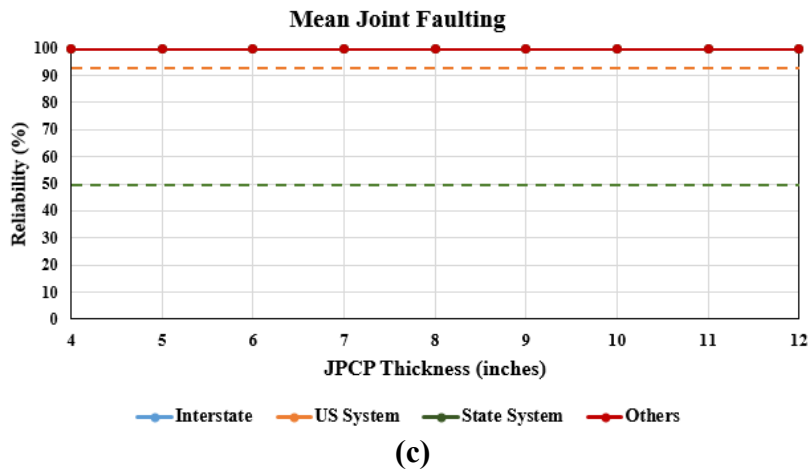
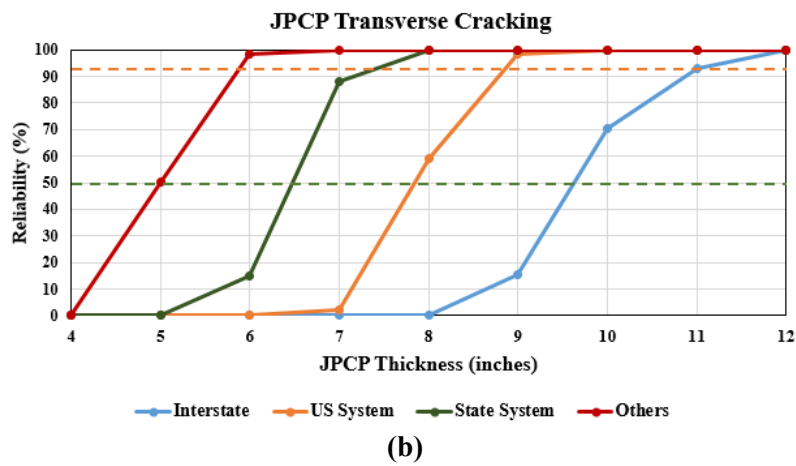
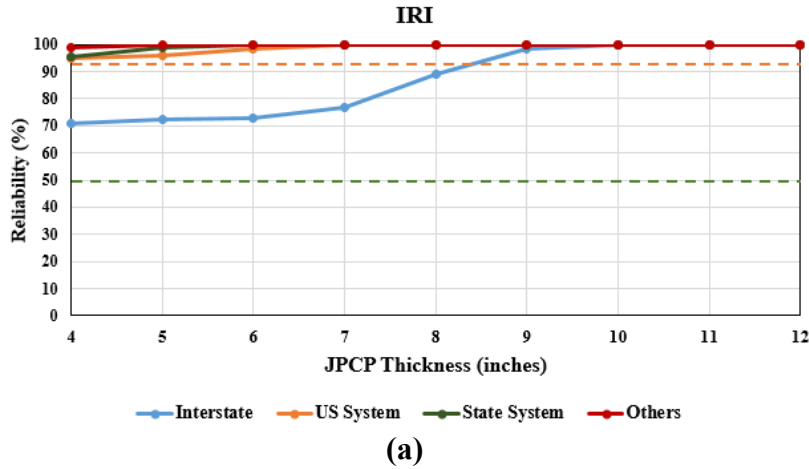


Figure 46. Reliability level versus JPCP thickness for the rigid pavement distresses (a) IRI, (b) transverse cracking, and (c) mean joint faulting (Note that the various colors of solid lines represent various road classifications that in some cases showed exactly the same results and therefore stack on top of one another. Also, the orange line marks 92% reliability and the green line 50% reliability.)

In all the cases, the recommended reliability was achieved for Other pavement systems, suggesting the use of lower PCC thickness for these pavements.

Figure 46(a) shows the reliability levels achieved for IRI. One of the major observations from this study's measured IRI collected from the Iowa Pavement Management Information System (PMIS) was that Iowa's IRI values recorded have been consistently low. As this study's new local calibration coefficients for Iowa were used in the current analysis, the PMED software was able to produce higher reliability levels even with lower PCC thickness.

Figure 46(b) shows the reliability levels achieved for JPCP transverse cracking distress. This figure shows that thickness has a significant impact on reliability levels for this distress. For Interstate design, when the reliability was set between 80% and 90%, a 0.5 inch increase in PCC thickness increased the reliability level by 10%. When the reliability was above 95%, a 0.5 inch increase in PCC thickness had a very minimal impact on design reliability levels, suggesting the use of 95% reliability with about a 12-inch minimum PCC thickness. For the US highway system, the design PCC thickness was not affected much when the reliability level selected was between 85% and 90%, suggesting the use of about a 9-inch minimum PCC thickness. For the state highway system, the design PCC thickness was not affected much when the reliability level selected was between 75% to 80%, suggesting the use of about a 7-inch minimum PCC thickness to address transverse cracking distress.

Figure 46(c) shows the findings for mean joint faulting and that JPCP thickness has no impact on mean joint faulting reliability levels for all pavement systems.

Effects of Joint Spacing for Rigid Pavements

In addition to questions related to PMED distress criteria and reliability levels, additional questions were included in the study survey to seek an understanding of agency practices related to specific design inputs and material properties. The overall survey results suggested that agencies' PMED joint spacing input for rigid pavement design varied between 15 and 20 feet, a significant spread.

Multiple studies have previously reported joint spacing to be one of the most sensitive inputs to predict pavement distresses (Ceylan et al. 2013b, Schwartz et al. 2011). Therefore, additional analyses were performed in this study to determine the impact of joint spacing on recommended pavement thickness and PMED-achieved reliability for rigid pavements. Three values for joint spacing (i.e., 15, 17, and 20 feet) were considered. The previous Figure 46 shows neither the state highway system nor the other systems exhibit significant differences in achieved reliability and recommended thicknesses for the various rigid pavement distresses, so only the Interstate and US highway pavement systems were considered for these analyses.

Figure 47, Figure 48, and Figure 49 show pavement thickness vs. achieved reliability for various joint spacings across all the rigid pavement distress types.

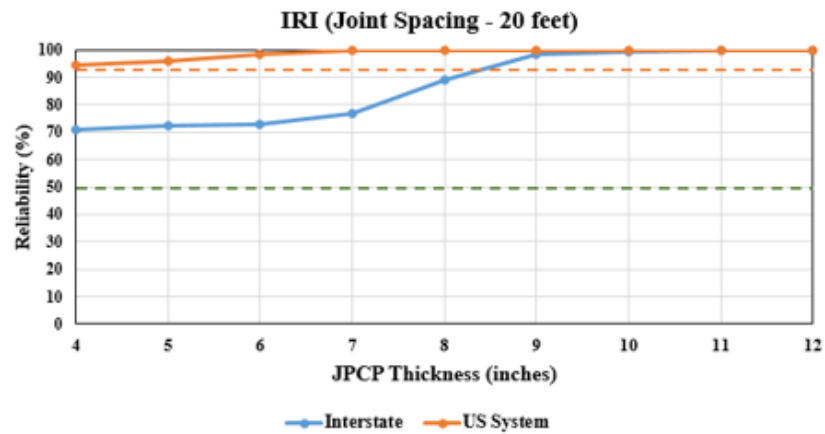
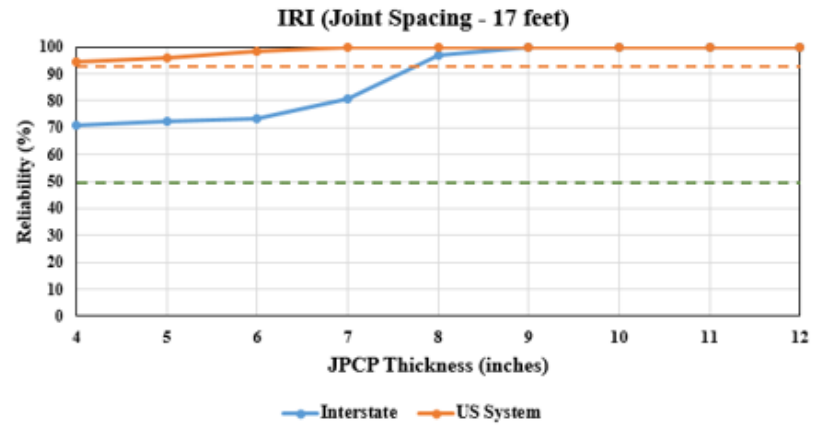
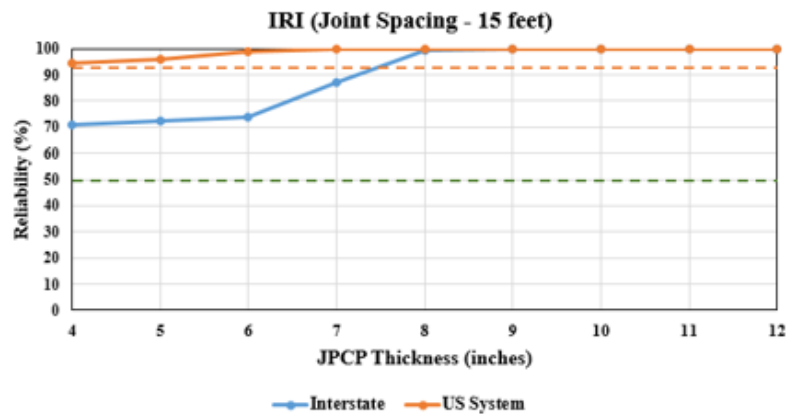


Figure 47. Effect of joint spacing on reliability and thickness for PMED-predicted IRI (Note that the orange line marks 92% reliability and the green line 50% reliability.)

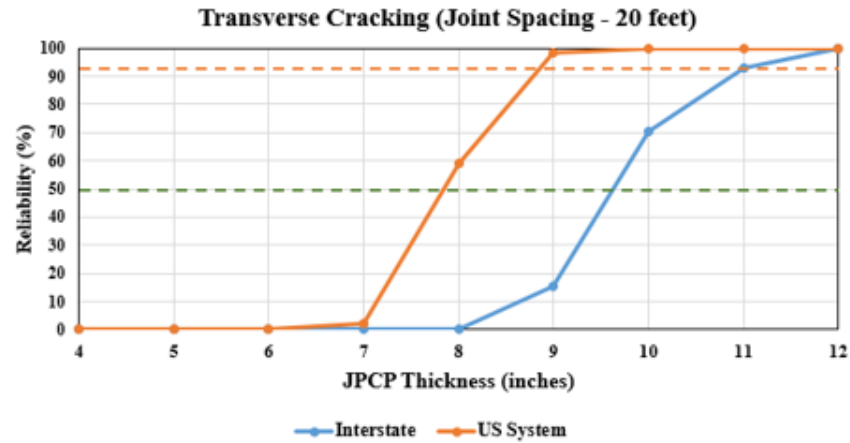
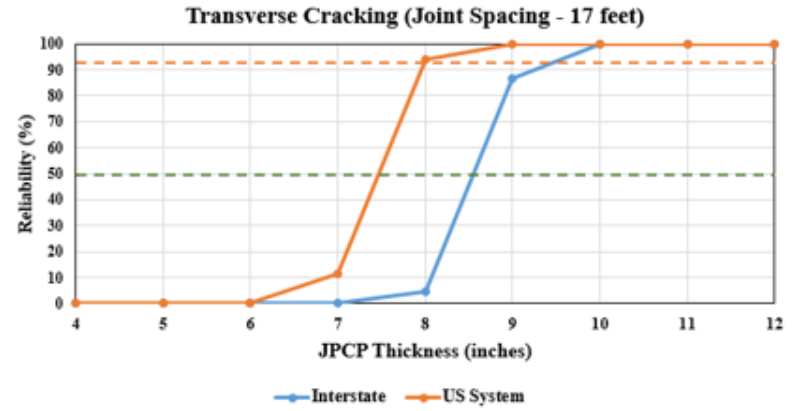
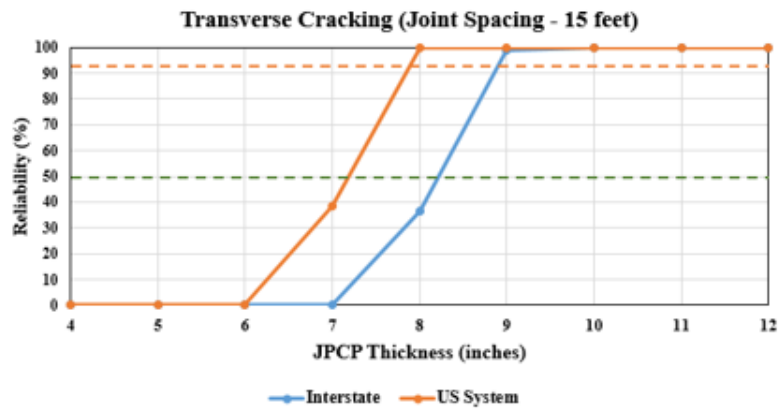


Figure 48. Effect of joint spacing on reliability and thickness for PMED-predicted transverse cracking (Note that the orange line marks 92% reliability and the green line 50% reliability.)

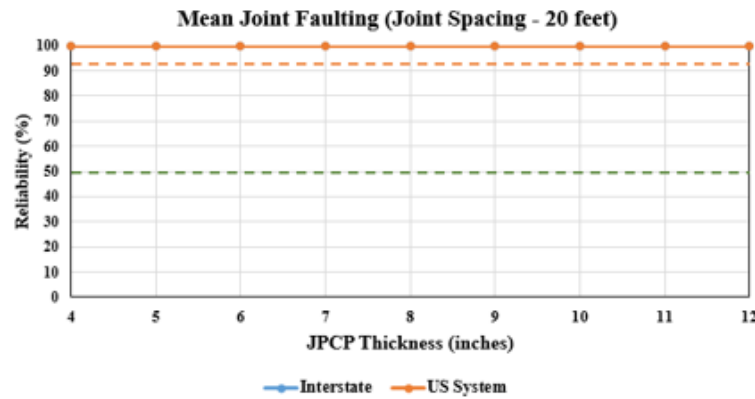
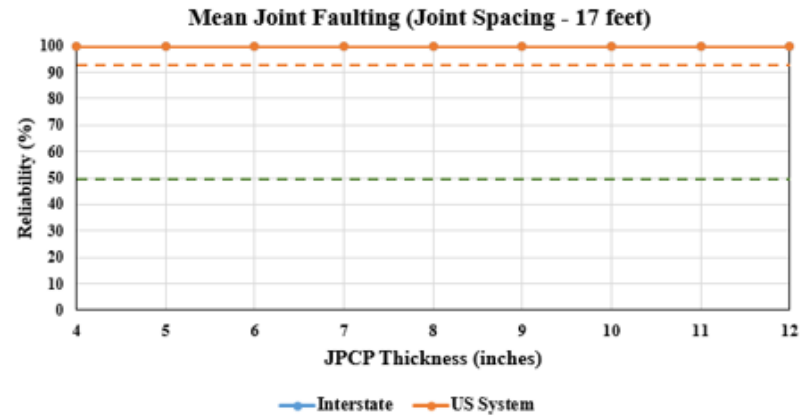
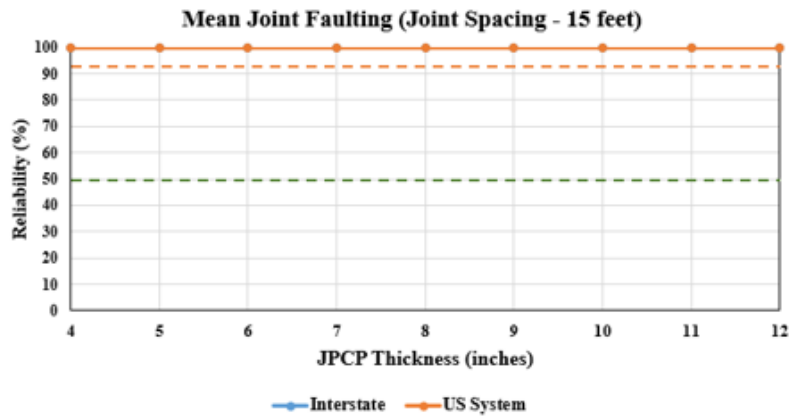


Figure 49. Effect of joint spacing on reliability and thickness for PMED-predicted mean joint faulting (Note that the solid lines represent various road classifications that in some cases showed exactly the same results and therefore stack on top of one another. Also, the orange line marks 92% reliability and the green line 50% reliability.)

A major observation for all the JPCP distresses (except mean joint faulting) was that decreasing the joint spacing increased the PMED-achieved reliability (i.e., achieved higher reliability levels), suggesting the use of lower joint spacing to decrease the recommended minimum PCC thicknesses required for meeting the distress criteria at a given recommended reliability level. For instance, for Interstate highway systems, an approximately 10.5-inch PCC thickness was required if a 17-foot joint spacing was used, while an approximately 11-inch PCC thickness was required if a 20-foot joint spacing was used to meet distress criteria and recommended reliability (i.e., 95% of reliability level).

Summary of Key Findings

This study addresses the importance of the distress criteria and reliability levels used in the PMED software based on the 26 responses to our study survey received from SHAs and pavement engineers. Additional analyses were also conducted per Iowa DOT design procedures to determine optimal layer thicknesses. The major findings from this study's flexible pavement analyses can be summarized as follows:

- For the Interstate highway system, in most cases, a reliability level of 95% was achieved for a 12-inch minimum AC thicknesses.
- For US and state highway systems representing medium- to low- traffic conditions, in most cases, the recommended reliability level (see the previous Table 32) was achieved for a 6-inch and 4-inch minimum AC thickness, respectively.
- In all cases, a 100% reliability was achieved for other pavement systems (i.e., very-low-traffic and low-speed-limit systems) and for design purposes, a minimum thickness of 4 inches for these pavement systems could be considered.

The major findings from this study's rigid pavement analysis can be summarized as follows:

- For the Interstate highway system, the recommended reliability of 95% to address transverse cracking distress—which is the governing distress type for determining minimum PCC thickness in the use of 20-foot joint spacing—was achieved for 12-inch minimum JPCP thicknesses.
- For the US highway system, the recommended reliability (see the previous Table 32) to address transverse cracking distress was achieved for about 9-inch minimum JPCP thicknesses.
- For the state highway system, the recommended reliability (see the previous Table 32) to address transverse cracking distress was achieved for about 7-inch minimum JPCP thicknesses.

- 100% reliability was achieved for all the distress types with other pavement systems, suggesting the use of lower PCC thicknesses for these pavement systems could be considered.
- A major observation for all the distresses from this study's joint spacing analysis was that decreasing the joint spacing increased the achieved reliability (i.e., achieved higher reliability levels), suggesting the use of lower joint spacing to decrease the minimum PCC thicknesses required for meeting the distress criteria at a given recommended reliability level.

The overall results from this study should be useful for all users of the PMED software in helping them understand how PMED practices vary from state to state before they finalize their own pavement designs.

The approach presented in this study to determine pavement layer thicknesses can also be utilized by PMED software users in evaluating and validating their final or previous designs. The distress criteria/limits in this analysis are from the PMED *Manual of Practice*. Hence, the approach presented in this study can be used as a reference to demonstrate how the minimum thicknesses and reliability levels for a specific pavement type would be determined by the PMED software for given distress criteria/limits.

However, the minimum thicknesses identified in this particular study are not necessarily recommended for the Iowa DOT's implementation and practice unless the Iowa DOT selects the same distress criteria/limits and reliability levels as the PMED *Manual of Practice*.

CONCLUSIONS AND RECOMMENDATIONS

Conclusions

This study provides a comprehensive evaluation of major tools recently incorporated into the PMED software. A summary of conclusions from the accomplished tasks is as follows.

Evaluation of Climate Data Sources in the PMED Software

- Four different climate data sources that can be used in the PMED software were evaluated for the design of flexible, rigid, and composite pavement systems. Four-way comparisons of these climate data sources' impact on predicted pavement distresses were presented.
- The MERRA-2 climate data resulted in higher predicted distress as compared to that predicted with the other PMED climate data sources for flexible and rigid pavements.
- In the composite pavement analysis, very good agreement was observed for IRI, AC layer rutting, alligator cracking, and JPCP transverse cracks. However, for total transverse cracking and thermal cracking, GBWS predictions were significantly lower compared to predictions using NARR, MERRA-1, and MERRA-2.
- The diurnal variation in percent sunshine from the four climate data sources showed substantial and nonsystematic differences, and additional sensitivity analysis on climate inputs showed a significant impact for percent sunshine on pavement performance. The agreement between the MERRA-1 and the MERRA-2 percent sunshine data was particularly poor, which is concerning as both the datasets were produced by NASA and use similar methods to collect their climate data estimates.
- Surface shortwave radiation (SSR) data are directly available in the PMED-required hourly format from the MERRA database, and comparisons of the MERRA-1 and MERRA-2 SSR predictions against ground-based observations of downwelling shortwave radiation collected by the U.S. Climate Reference Network were quite good, suggesting the use of SSR as an alternative to percent sunshine.
- In order to use the MERRA-1 and MERRA-2 SSR values to drive the environmental calculations, it was necessary to back-calculate a synthetic percent sunshine to meet PMED requirements. The empirical relationship between SSR and percent sunshine was used to back-calculate synthetic percent sunshine values consistent with the MERRA-1 and MERRA-2 SSR values. These back-calculated synthetic percent sunshine values were then used to replace the percent sunshine values in the climate data files provided with PMED. Comparisons of predicted pavement performance using MERRA-1 vs. MERRA-2 climate data and their respective synthetic percent sunshine histories showed dramatically improved

agreement for both AC pavements and JPCP with the resulting predictions clustered tightly along their respective lines of equality.

Sensitivity Analysis for PMED's New Reflective Cracking Model

- The sensitivity of AC-over-JPCP reflective cracking distress with respect to the most important PMED design inputs and material properties was presented. Case 1 reflects NSI values based on short-term reflective cracking prediction (i.e., the year at which reflective cracking reaches 4,000 ft/mile [757.71 m/km]), and Case 2 reflects NSI values based on the long-term reflective cracking prediction of a 20-year design service life. An additional case providing an overall summary of Case 1 and Case 2 findings was further reported.
- Joint Spacing, JPCP Layer Thickness, Transverse LTE, and Alpha and Delta in the AC Sigmoidal Curve were the most sensitive PMED inputs with respect to reflective cracking distress. Specifically, the PMED software shows that a tendency toward increased cracking is highly influenced by an increase in joint spacing. Transverse (joint) LTE, generally indexed with the shearing mechanism at cracks, is usually not a crack initiator but rather an accelerator (i.e., once a crack has been initiated from tensile stress/strain, a change in LTE will accelerate the propagation of the reflective crack toward the pavement surface). With respect to Alpha and Delta in the AC Sigmoidal Curve, it is essential to note that typical ranges for these parameter are very narrow, and the high sensitivity to cracking distresses with respect to Alpha and Delta in an AC Sigmoidal Curve suggests a level of care is required in Level 1 characterization for important projects.
- AADTT, AC Surface Shortwave Absorption, Effective Binder Content, Air Voids in AC, Tensile Strength, AC Thickness, Ratio of Slabs Distressed before and after Restoration, and PCC Thermal Conductivity were moderately sensitive PMED inputs with respect to reflective cracking distress.
- The remaining design inputs considered had either very little or no impact on reflective cracking based on the evaluated NSI absolute values.
- Another interesting observation is that most of the PMED inputs had a significant impact on reflective cracking at the International Falls, Minnesota, location. This study's analyses were performed keeping all the base-case values the same while changing just the climate station location in the PMED software. This study thus shows the impact of climate on PMED-predicted distress. This could be because of extremely cold winter temperatures and extensive snow accumulation in states like Minnesota that can result in excessive infiltration of moisture through cracks that then leads to premature failure of pavement overlays.

Sensitivity Analysis for PMED's New SJPCP/AC Model

- Sensitivity analysis of PMED input parameters to longitudinal fatigue cracking distress for the software's new SJPCP/AC model was performed, considering fifteen design inputs and

five locations representing different US climatic zones. A summary of the NSI ranking for four cases varying in design life and reliability was presented.

- In all cases, most input parameters were sensitive to longitudinal fatigue cracking at the International Falls, Minnesota, location, where extreme cold weather and moisture infiltration through cracks result in premature failure of overlays.
- Layer thicknesses were sensitive input parameters in all cases and careful consideration should be given to performing field surveys to collect information on the existing AC layer and base layer thicknesses, so the appropriate SJPCP layer can be optimized.
- AADTT, Transverse (joint) LTE, and PCC Modulus of Rupture were moderately sensitive inputs.
- Joint spacing and the CTE were observed to be “insensitive” due to their limited range of input options in the PMED software.
- All other inputs had either very minimal or no impact on predicted longitudinal fatigue cracking
- Sensitivity analysis studies should be performed using a mean reliability of 50%, because the use of higher reliabilities for sensitivity analyses can result in misleading conclusions for design practices.

Local Calibration of Flexible, Rigid, and Composite Pavements

- Local calibration of flexible, rigid, and composite pavements using PMED v2.5.5 was performed, and the complete methodology and calibration process for individual distresses were presented.
- Methods such as sensitivity analysis, nonlinear optimization techniques (i.e., Solver, LINGO, and SciPy), resampling techniques (i.e., bootstrapping and jackknifing), and genetic algorithms were used to optimize local calibration coefficients.
- The overall mean bias and coefficient of determination (R^2) using local calibration coefficients were significantly improved, especially with respect to distresses for which all their components/parameters were directly available from the PMED output files. Use of the SciPy tool for optimization produced the best results, although SciPy does require some basic knowledge of programming and coding that is available through various sources. (The genetic algorithm tool in MATLAB could be a better alternative for engineers who do not want to use programming-based tools.)

- The use of sensitivity analysis for distress situations for which not all the required components of PMED transfer functions were available also resulted in improvement in local calibration compared to the national calibration, but since the improvement was not very significant, SHAs may vary in their decision as to whether they should use local coefficients or stick with PMED's default national coefficients.
- A new set of local calibration coefficients based on state-of-Iowa conditions was developed and is recommended for Iowa pavement design practice. This is the first study presenting local calibration of PMED's new reflective cracking model after this model's addition to the PMED software.
- Distress-oriented data collection and database preparation are the most important initial steps in a local calibration process. Measured distress data and the availability of a number of years of historical data are crucial in estimating the best fit.
- Minimizing overestimation and underestimation of distresses is crucial to success in local calibration studies, and the experience gained in this study provides comprehensive guidance on how to change local calibration coefficients based on comparisons of measured and predicted data. These guidelines can be implemented by any state that uses the PMED software.
- Units for distresses collected from sources such as PMIS must be checked for compatibility with PMED, and it was ensured in this study that differences between PMED and PMIS units were properly handled by applying appropriate conversion factors.

Determination of Optimal Pavement Thickness Based on Distress Criteria and Reliability Levels

- A national survey on latest practices in regard to PMED distress criteria and reliability levels was sent out to pavement engineers and researchers across the United States and Canada, and a summary of the survey results based on 26 responses was presented.
- For use in the design of Iowa pavement systems, optimal layer thicknesses for flexible and rigid pavements were determined based on survey responses and AASHTO guidelines. The resulting recommended thicknesses vary significantly for different pavement systems and traffic levels.
- The impact of joint spacing on optimal pavement thickness was additionally presented, and based on the overall findings, a 15-foot joint spacing provides the best pavement design life.
- The approach presented in this study to determine optimal layer thicknesses can also be used in evaluating and validating SHAs' final or previous designs. (It should be noted the selection of reliability level can have a significant effect in calculating optimal thicknesses.)

Recommendations

Pavement engineering is a very broad area within civil engineering, and the PMED software addresses almost all of its components. While this software has advanced over the years, with multiple updates and tools being added over time, it is still in the process of development, and multiple researchers and agencies continue to work together to develop more models with the aim of making the PMED software a complete pavement engineering package combined into one.

Based on the findings and experiences of this study, the following recommendations are provided:

- The MERRA-2 data are recommended for use in Iowa pavement design practice.
- The sensitivity-analysis results presented in this study must be carefully reviewed to eliminate issues frequently observed regarding reflective cracking and distresses associated with BCOA pavement types.
- The local calibration coefficients recommended for the Iowa DOT to use in design practice as alternatives to PMED's default nationally calibrated counterparts are summarized in Table 22 for Iowa's flexible pavements, Table 23 for Iowa's rigid pavements, and Table 24 for Iowa's AC over JPCP. (Note that the recommended local calibration coefficients in red in Table 22 through Table 24 show that these numbers are different from their counterparts in the nationally calibrated default PMED models.)
- The locally calibrated rutting, longitudinal (top-down) cracking, thermal cracking, and IRI prediction models identified in this study are recommended for use with Iowa's AC pavements as alternatives to the equivalent nationally calibrated PMED models.
- The locally calibrated JPCP performance models (addressing faulting, transverse cracking, and IRI) identified in this study are recommended for use with Iowa's JPCPs as alternatives to the equivalent nationally calibrated PMED models.
- The locally calibrated rutting, longitudinal (top-down) cracking, thermal cracking, reflective cracking, and IRI prediction models identified in this study are recommended for use with Iowa's AC over JPCPs as alternatives to the equivalent nationally calibrated PMED models.

Future research recommendations related to the use of the PMED software for Iowa pavement systems are presented as follows:

- Based on this study's findings and limitations with respect to the climate models in the current PMED software, it is recommended that shortwave and longwave radiation models be evaluated and included as direct climate inputs in future versions of the software.

- The current PMED SJPCP/AC model predicts only longitudinal fatigue cracking as its output distress type, while other commonly observed distress types such as IRI and transverse cracking have not been added. If these were to be added, comparisons of PMED predictions with field-observed distresses should be performed before local implementation.
- Local calibration is a very complex and time-consuming process, but AASHTO recommends that all users should perform this process to account for local conditions when implementing the tool in their practices. To ease the local calibration process, a calibrator tool was recently released that could save significant amounts of time in future calibration studies, and a comprehensive evaluation and comparison of local calibration methods using this calibrator tool versus previously used local calibration methods could be performed in future research.

REFERENCES

- AASHTO. 1993. *AASHTO® Guide for Design of Pavement Structures*. American Association of State Highway and Transportation Officials, Washington, DC.
- . 2010. *Guide for the Local Calibration of the Mechanistic-Empirical Pavement Design Guide*. American Association of State Highway and Transportation Officials, Washington, DC.
- . 2015. *Mechanistic-Empirical Pavement Design Guide – A Manual of Practice*. Second edition. American Association of State Highway and Transportation Officials, Washington, DC.
- Adams, T. and J. M. Vandenbossche 2013. *Bonded Concrete Overlay of Asphalt Pavements Mechanistic-Empirical Design Guide (BCOA-ME): Assessing the Need for Preoverlay Repairs When Construction BCOA*. University of Pittsburgh, PA.
- Alland, K., J. M. Vandenbossche., J. W. DeSantis., M. B. Snyder., and L. Khazanovich. 2018. Comparing the Bonded Concrete Overlays of Asphalt-Mechanistic Empirical Design Procedure and the Short Jointed Plain Concrete Pavement Module in the Pavement Mechanistic Empirical Design Procedure. *Transportation Research Record: Journal of the Transportation Research Board*, Vol. 2672, No. 40, pp. 242–253.
- ARA, Inc. 2004. *Guide for Mechanistic-Empirical Design of New and Rehabilitated Pavement Structures*. National Cooperative Highway Research Program 1-37 A, Washington, DC.
- . 2015. *New PCC Calibration Coefficients from NCHRP 20-07, Task 327: Enhancements to the Mechanistic-Empirical Pavement Design Guide – A Manual of Practice*. Applied Research Associates, Inc., Champaign, IL.
- . Revised 2017. *Integrating the Bonded Concrete Overlay of Asphalt (BCOA-ME) Design Procedure into the AASHTOWare Pavement ME Software*. Applied Research Associates, Inc., Champaign, IL.
- . 2018a. *Enhancements to the Mechanistic-Empirical Pavement Design Guide – A Manual of Practice: Using Local Calibration Coefficients with Pavement ME Design Version 2.5*. Applied Research Associates, Inc., Champaign, IL.
- . 2018b. *Enhancements to the Mechanistic-Empirical Pavement Design Guide – A Manual of Practice: Revised Model/Global Calibration Coefficients from Recalibration*. Applied Research Associates, Inc., Champaign, IL.
- Bennert, T. 2010. *Flexible Overlays for Rigid Pavements*. New Jersey Department of Transportation, Trenton, NJ.
- Bhattacharya, B. B., H. L. Von Quintus., and M. I. Darter. 2015. *Implementation and Local Calibration of the MEPDG Transfer Functions in Wyoming*. Wyoming Department of Transportation, Cheyenne, WY.
- Bhattacharya, B. B., A. Gotlif., and M. I. Darter. 2017. Implementation of the Thin Bonded Concrete Overlay of Existing Asphalt Pavement Design Procedure in the AASHTOWare Pavement ME Design Software. *Transportation Research Record: Journal of the Transportation Research Board*, No. 2641, pp. 12–20.
- Blanco-Silva, F. J. 2013. *Learning SciPy for Numerical and Scientific Computing*. Packt Publishing.
- Breakah, T. M., R. C. Williams., D. E. Herzmann, and E. S. Takle. 2011. Effects of Using Accurate Climatic Conditions for Mechanistic-Empirical Pavement Design. *Journal of Transportation Engineering*, Vol. 137, No. 1, pp. 84–90.

- Brink, W. C. 2015. Use of Statistical Resampling Techniques for the Local Calibration of the Pavement Performance Prediction Models. PhD dissertation. Michigan State University, East Lansing, MI.
- Brink, W. C., I. Harsini., S. W. Haider., N. Buch., K. Chatti., G. Y. Baladi., and E. Kutay. 2013. Sensitivity of Input Variables for Flexible Pavement Rehabilitation Strategies in the MEPDG. *Airfield and Highway Pavement Conference 2013: Sustainable and Efficient Pavements*, Volume 1, pp. 539–550.
- Brink, W., H. Von Quintus., and L. F. Osborne, Jr. 2017. Updates to Hourly Climate Data for Use in AASHTOWare Pavement Mechanistic–Empirical Design. *Transportation Research Record: Journal of the Transportation Research Board*, No. 2640, pp. 11–20.
- Cetin, B., C. W. Schwartz., B. A. Forman., L. Roberts., and M. M. Gribb. 2015. *Climate and Groundwater Data to Support Mechanistic-Empirical Design in South Dakota*. South Dakota Department of Transportation, Pierre, SD.
- Cetin, B., B. A. Forman., C. W. Schwartz., and B. Ruppelt. 2018. Performance of Different Climate Data Sources in Mechanistic–Empirical Pavement Distress Analyses. *Journal of Transportation Engineering, Part B: Pavements*, Vol. 144, No. 1, pp. 1–18.
- Cetin, B., S. Satvati, S., J. C. Ashlock., and C. Jahren. 2019. *Performance-Based Evaluation of Cost-Effective Aggregate Options for Granular Roadways*. Institute for Transportation, Iowa State University, Ames, IA. <https://intrans.iastate.edu/app/uploads/2019/12/cost-effective-aggregate-options-for-granular-roadways-eval-w-cvr.pdf>.
- Ceylan, H., K. Gopalakrishnan., and R. L. Lytton. 2011. Neural Networks Modeling of Stress Growth in Asphalt Overlays Due to Load and Thermal Effects during Reflection Cracking. *Journal of Materials in Civil Engineering*, Vol. 23, No. 3, pp. 221–229.
- Ceylan, H., S. Kim., K. Gopalakrishnan., C. W. Schwartz., and R. Li. 2013a. Sensitivity Quantification of Jointed Plain Concrete Pavement Mechanistic–Empirical Performance Predictions. *Construction and Building Materials*, Vol. 43, pp. 545–556.
- Ceylan, H., S. Kim., K. Gopalakrishnan., and D. Ma. 2013b. *Iowa Calibration of MEPDG Performance Prediction Models*. Institute for Transportation, Iowa State University, Ames, IA. https://intrans.iastate.edu/app/uploads/2018/03/MEPDG_Iowa_calibration_w_cvr1.pdf.
- Ceylan, H., S. Kim., K. Gopalakrishnan., C. W. Schwartz., and R. Li. 2014. Sensitivity Analysis Frameworks for Mechanistic–Empirical Pavement Design of Continuously Reinforced Concrete Pavements. *Construction and Building Materials*, Vol. 73, pp. 498–508.
- Ceylan, H., S. Kim., O. Kaya., and K. Gopalakrishnan. 2015. *Investigation of AASHTOWare Pavement ME Design/Darwin-ME Performance Prediction Models for Iowa Pavement Analysis and Design*. Program for Sustainable Pavement Engineering and Research (ProSPER), Institute for Transportation, Iowa State University, Ames, IA. https://intrans.iastate.edu/app/uploads/2018/03/AASHTOWare_performance_prediction_models_w_cvr.pdf.
- Darter, M. I., L. Titus-Glover., H. Von Quintus., B. B. Bhattacharya., and M. Jagannath. 2014. *Calibration and Implementation of the AASHTO Mechanistic–Empirical Pavement Design Guide in Arizona*. Arizona Department of Transportation Research Center, Phoenix, AZ.
- Li, Z., N. Dufalla, and J. M. Vandenbossche. 2013. *Bonded Concrete Overlay of Asphalt Pavements Mechanistic–Empirical Design Guide (BCOA-ME): User’s Guide*. University of Pittsburgh, PA. [Microsoft Word - BCOA ME User's Guide \(pitt.edu\)](https://www.pitt.edu/~bcme/BCOA_ME_User's_Guide.pdf).

- Durham, S. A., B. Cetin., C. W. Schwartz., B. A. Forman., and L. S. P. Gopiseti. 2019. *Improvement of Climate Data for Use in MEPDG Calibration and Other Pavement Analysis*. Georgia Department of Transportation, Forest Park, GA.
- El-Badawy, S., F. Bayomy., and A. Awed. 2012. Performance of MEPDG Dynamic Modulus Predictive Models for Asphalt Concrete Mixtures: Local Calibration for Idaho. *Journal of Materials in Civil Engineering*, Vol. 24, No. 11, pp. 1412–1421.
- Esfandiarpour, S. and A. Shalaby. 2017. Local Calibration of Creep Compliance Models of Asphalt Concrete. *Construction and Building Materials*, Vol. 132, pp. 313–322.
- FHWA. n.d. Transportation Pooled Fund study TPF-5(165): Development of Design Guide for Thin and Ultrathin Concrete Overlays of Existing Asphalt Pavements. <https://www.pooledfund.org/details/study/389>.
- Gong, H., B. Huang., X. Shu., and S. Udeh. 2017. Local Calibration of the Fatigue Cracking Models in the Mechanistic-Empirical Pavement Design Guide for Tennessee. *Road Materials and Pavement Design*, Vol. 18, pp. 130–138.
- Gopiseti, L. S. P. 2017. International Roughness Index Prediction of Flexible and Rigid Pavements using Climate and Traffic Data. MS thesis. Bradley University, Peoria, IL.
- Gopiseti, L. S. P., M. I. Hossain., M. S. Miah., and K. Schattler. 2018. Artificial Neural Network Models for Predicting Pavement Roughness of Flexible and Rigid Pavements. Transportation Research Board 97th Annual Meeting, January 7–11, Washington, DC.
- Gopiseti, L. S. P., B. Cetin., B. A. Forman., S. Durham., C. W. Schwartz., and H. Ceylan. 2019. Evaluation of Four Different Climate Sources on Pavement Mechanistic-Empirical Design and Impact of Surface Shortwave Radiation. *International Journal of Pavement Engineering*.
- Gopiseti, L. S. P., H. Ceylan., S. Kim., and B. Cetin. 2020a. Sensitivity Index Comparison of Pavement Mechanistic-Empirical Design Input Variables to Reflective Cracking Model for Different Climatic Zones. *Road Materials and Pavement Design*.
- Gopiseti, L. S. P., H. Ceylan., B. Cetin., S. Kim., and O. Kaya. 2020b. Sensitivity Analysis of New Reflective Cracking Model in Pavement Mechanistic-Empirical Design. Geo-Congress 2020, February 25–28, Minneapolis, MN.
- Guclu, A., H. Ceylan., K. Gopalakrishnan., and S. Kim. 2009. Sensitivity Analysis of Rigid Pavement Systems Using the Mechanistic-Empirical Design Guide Software. *Journal of Transportation Engineering*, Vol. 135, No. 8, pp. 555–562.
- Guo, X. 2013. Local Calibration of the MEPDG Using Test Track Data. MS thesis. Auburn University, AL.
- Haider, S. W., W. C. Brink., and N. Buch., and K. Chatti. 2015. Process and Data Needs for Local Calibration of Performance Models in the AASHTOWARE Pavement ME Software. *Transportation Research Record: Journal of the Transportation Research Board*, No. 2523, pp. 80–93.
- Haider, S. W., W. C. Brink., and N. Buch. 2016. Local Calibration of Flexible Pavement Performance Models in Michigan. *Canadian Journal of Civil Engineering*, Vol. 43, No. 11, pp. 986–997.
- Haider, S. W., G. Musunuru., M. E. Kutay, M. A. Lanotte, and N. Buch. 2017. *Recalibration of Mechanistic-Empirical Rigid Pavement Performance Models and Evaluation of Flexible Pavement Thermal Cracking Model*. Michigan Department of Transportation, Lansing, MI.

- Haider, S. W., G. Musunuru., N. Buch., and W. C. Brink. 2020. Local Recalibration of JPCP Performance Models and Pavement-ME Implementation Challenges in Michigan. *Journal of Transportation Engineering, Part B: Pavements*, Vol. 146, No. 1, pp. 1–12.
- Heitzman M. 2007. Evaluation of Iowa Climate Data for the Mechanistic-Empirical Pavement Design Guide. Proceedings of the 2007 Mid-Continent Transportation Research Symposium, August 16–17, Institute for Transportation, Iowa State University, Ames, IA.
- Hoegh, K., L. Khazanovich., and M. Jensen. 2010. Local Calibration of Mechanistic-Empirical Pavement Design Guide Rutting Model: Minnesota Road Research Project Test Sections. *Transportation Research Record: Journal of the Transportation Research Board*, No. 2180, pp. 130–141.
- Hossain, M. I., L. S. P. Gopiseti., and M. S. Miah. 2017. Prediction of International Roughness Index of Flexible Pavements from Climate and Traffic Data Using Artificial Neural Network Modeling. *Airfield and Highway Pavements 2017: Design, Construction, Evaluation, and Management of Pavements – Proceedings of the International Conference on Highway Pavements and Airfield Technology 2017*.
- Hossain, M. I., L. S. P. Gopiseti., and M. S. Miah. 2018. International Roughness Index Prediction of Flexible Pavements using Neural Networks. *Journal of Transportation Engineering, Part B: Pavements*, Vol. 145, No. 1.
- Jannat, G. E. 2012. Database Development for Ontario’s Local Calibration of Mechanistic-Empirical Pavement Design Guide (MEPDG) Distress Models. MASc thesis. Ryerson University, Toronto, Ontario.
- Kaya, O., H. Ceylan., S. Kim., and K. Gopalakrishnan. 2016. Alternative Approaches to the Local Calibration of AASHTOWare Pavement ME Design Jointed Plain Concrete Pavement (JPCP) Smoothness Models. Geotechnical and Structural Engineering Congress 2016, Geotechnical and Structural Engineering Congress 2016, February 14–17, Phoenix, AZ.
- Kim, S., H. Ceylan., and M. Heitzman. 2005. Sensitivity Study of Design Input Parameters for Two Flexible Pavement Systems Using the Mechanistic-Empirical Pavement Design Guide. Proceedings of the 2005 Mid-Continent Transportation Research Symposium, August 18–19, Center for Transportation Research and Education, Iowa State University, Ames, IA.
- Kim, S., H. Ceylan., D. Ma., and K. Gopalakrishnan. 2014. Calibration of Pavement ME Design and Mechanistic-Empirical Pavement Design Guide Performance Prediction Models for Iowa Pavement Systems. *Journal of Transportation Engineering*, Vol. 140, No. 10.
- Lytton, R. L., F. L. Tsai., S.-I. Lee, R. Luo, S. Hu, and F. Zhou. 2010. *NCHRP Report 669: Models for Predicting Reflection Cracking of Hot-Mix Asphalt Overlays*. National Cooperative Highway Research Program, Washington, DC.
- Ma, H., D. Wang., C. Zhou., and D. Feng. 2015. Calibration on MEPDG Low Temperature Cracking Model and Recommendation on Asphalt Pavement Structures in Seasonal Frozen Region of China. *Advances in Materials Science and Engineering, Advances in Building Technologies and Construction Materials.*, Vol. 2015, Article ID: 830426, 11 pages.
- Muthadi, N. R. and Y. R. Kim. 2008. Local Calibration of Mechanistic-Empirical Pavement Design Guide for Flexible Pavement Design. *Transportation Research Record: Journal of the Transportation Research Board*, No. 2087, pp. 131–141.

- Notani, M. A., A. Arabzadeh., S. Satvati., M. T. Tabesh., N. G. Hashjin., S. Estakhri., and M. Alizadeh. 2020 Investigating the High Temperatures Performance and Activation Energy of Carbon Black-Modified Asphalt Binder. *Springer Nature Applied Sciences*, Vol. 2, No. 303.
- Satvati, S., J. C. Ashlock., A. Nahvi., C. T. Jahren., B. Cetin., and H. Ceylan. 2019. A Novel Performance-Based Economic Analysis Approach: Case Study of Iowa Low-Volume Roads. 12th International Conference on Low-Volume Roads. Research Circular EC248, pp. 207–234.
- Schwartz, C. W. and R. Li. 2010. *Sensitivity of Predicted Flexible Pavement Performance to Unbound Material Hydraulic Properties*. GeoFlorida 2010: Advances in Analysis, Modeling & Design, February 20–24, Orlando, FL, pp. 2022–2031.
- Schwartz, C. W., R. Li., S. Kim., H. Ceylan., and K. Gopalakrishnan. 2011. *Sensitivity Evaluation of MEPDG Performance Prediction*. Interim report for the National Cooperative Highway Research Program, Iowa State University, Ames, IA.
- Schwartz, C. W., G. E. Elkins., R. Li., B. A. Visintine., B. Forman., G. R. Rada., and J. L. Groeger. 2015. *Evaluation of LTPP Climatic Data for Use in Mechanistic-Empirical Pavement Design Guide Calibration and Other Pavement Analysis*. Federal Highway Administration, Turner-Fairbank Highway Research Center, McLean, VA.
- Sheehan, M. J., S. M. Tarr., and S. Tayabji. 2004. *Instrumentation and Field Testing of Thin Whitetopping Pavement in Colorado and Revision of the Existing Colorado Thin Whitetopping Procedure*. Colorado Department of Transportation, Denver, CO.
- Sun, X., J. Han., R. L. Parsons., A. Misra., and J. K. Thakur. 2015. *Calibrating the Mechanistic-Empirical Pavement Design Guide for Kansas*. Kansas Department of Transportation, Topeka, KS.
- Tarefder, R. and N. Sumee. 2011. Evaluating Sensitivity of Pavement Performance to Mix Design Variable in MEPDG. *ASCE Geotechnical Special Publication*, pp. 49–56.
- Tarefder, R., N. Sumee., and C. Storlie. 2014. Study of MEPDG Sensitivity Using Nonparametric Regression Procedures. *Journal of Computing in Civil Engineering*, Vol. 28, No. 1, pp. 134–144.
- Tarr, S. M., M. J. Sheehan., and P. A. Okamoto. 1998. *Guidelines for the Thickness Design of Bonded Whitetopping Pavement in the State of Colorado*. Colorado Department of Transportation, Denver, CO.
- Titus-Glover, L., B. B. Bhattacharya, D. Raghunathan., J. Mallela., and R. L. Lytton. 2016. Adaptation of NCHRP Project 1-41 Reflection Cracking Models for Semi Rigid Pavement Design in AASHTOWare Pavement ME Design. *Transportation Research Record: Journal of the Transportation Research Board*, No. 2590, pp. 122–131.
- Tran, N., M. M. Robbins., C. Rodezno., and D. H. Timm. 2017. *Pavement ME Design - Impact of Local Calibration, Foundation Support, and Design and Reliability Thresholds*. National Center for Asphalt Technology, Auburn University, AL.
- Tsai, F. L., R. L. Lytton., and S. Lee. 2010. Prediction of Reflection Cracking in Hot-Mix Asphalt Overlays. *Transportation Research Record: Journal of the Transportation Research Board*, No. 2155, pp. 43–54.
- Vandenbossche, J. M. and S. Sachs. 2013. *Rehabilitation Strategies for Bonded Concrete Overlays of Asphalt Pavements*. University of Pittsburg, PA.

- Vandenbossche, J. M., N. Dufalla., and Z. Li. 2017. Bonded Concrete Overlay of Asphalt Mechanical-Empirical Design Procedure. *International Journal of Pavement Engineering*, Vol. 18, No. 11, pp. 1004–1015.
- Virtanen, P., R. Gommers., and T. E. Oliphant. 2020. SciPy 1.0: Fundamental Algorithms for Scientific Computing in Python. *Nature Methods*, Vol. 17, pp. 261–272.
- Waseem, A. and X. X. Yuan. 2013. Longitudinal local calibration of MEPDG permanent deformation models for reconstructed flexible pavements using PMS data. *International Journal of Pavement Research and Technology*, Vol. 6, No. 4, pp. 304–312.
- Wu, C. L. 1998. *Development of Ultra-Thin Whitetopping Design Procedure*. Portland Cement Association, Skokie, IL.
- Yuan, X. X. and I. Nemtsov. 2018. Local Calibration of the MEPDG Distress and Performance Models for Ontario’s Flexible Roads: Overview, Impacts, and Reflection. *Transportation Research Record: Journal of the Transportation Research Board*, Vol. 2672, No. 40, pp. 207–216.
- Yunhe, C., W. Zhang., Y. Jun., and Y. Yiwen. 2011. Survey and Analysis for Reflective Cracking of Asphalt Pavement with Semi-Rigid Base. GeoHunan International Conference 2011: Emerging Technologies for Material, Design, Rehabilitation, and Inspection of Roadway Pavements, June 9–11, Hunan, China.

APPENDIX A: MERRA-1 CLIMATE DATA INPUT CHARTS FOR ALL IOWA LOCATIONS

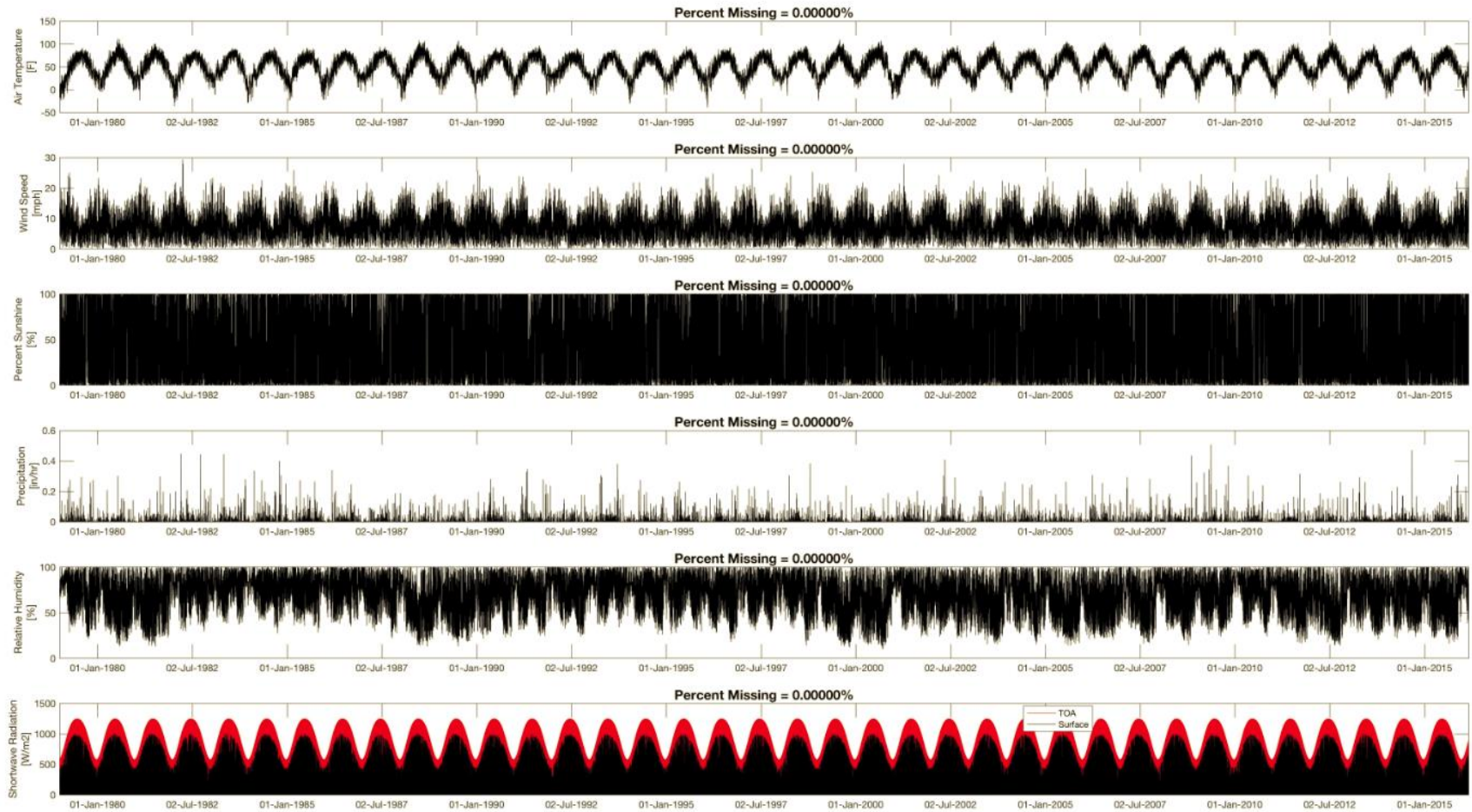


Figure A.1. Climate Location ID: 146443 (Ames Municipal Airport)

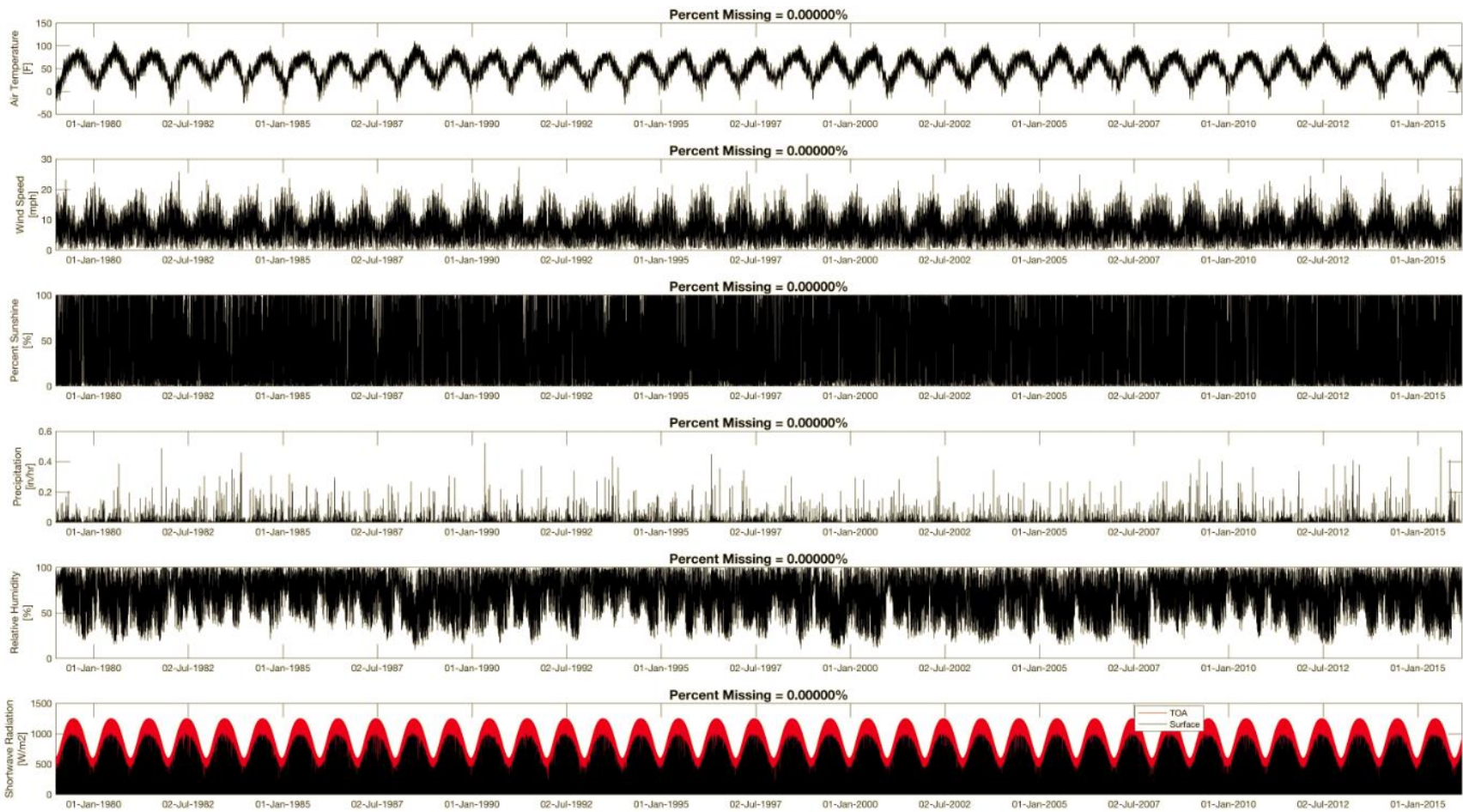


Figure A.2. Climate Location ID: 145295 (Iowa Regional Airport, Burlington)

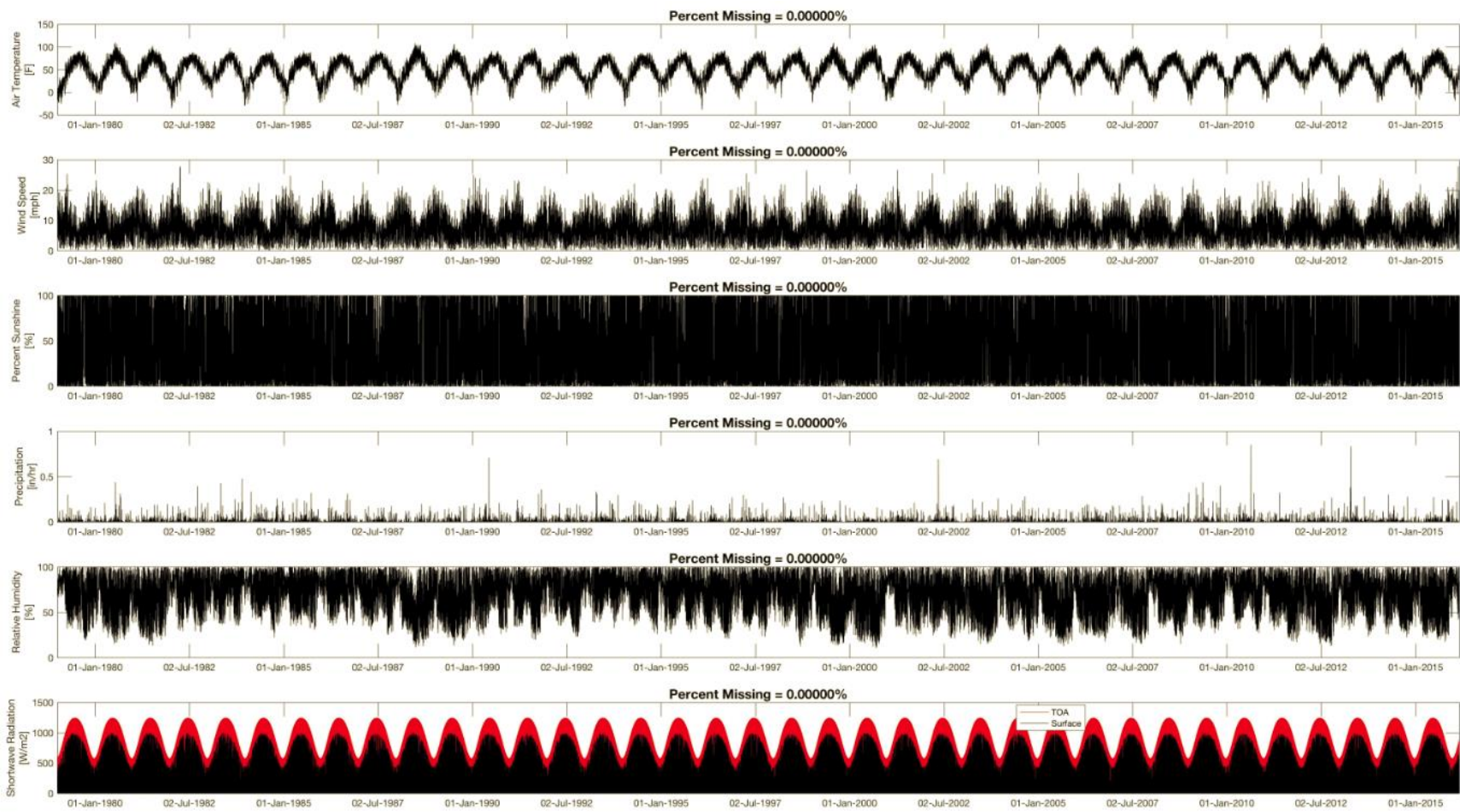


Figure A.3. Climate Location ID: 146446 (Eastern Iowa Airport, Cedar Rapids)

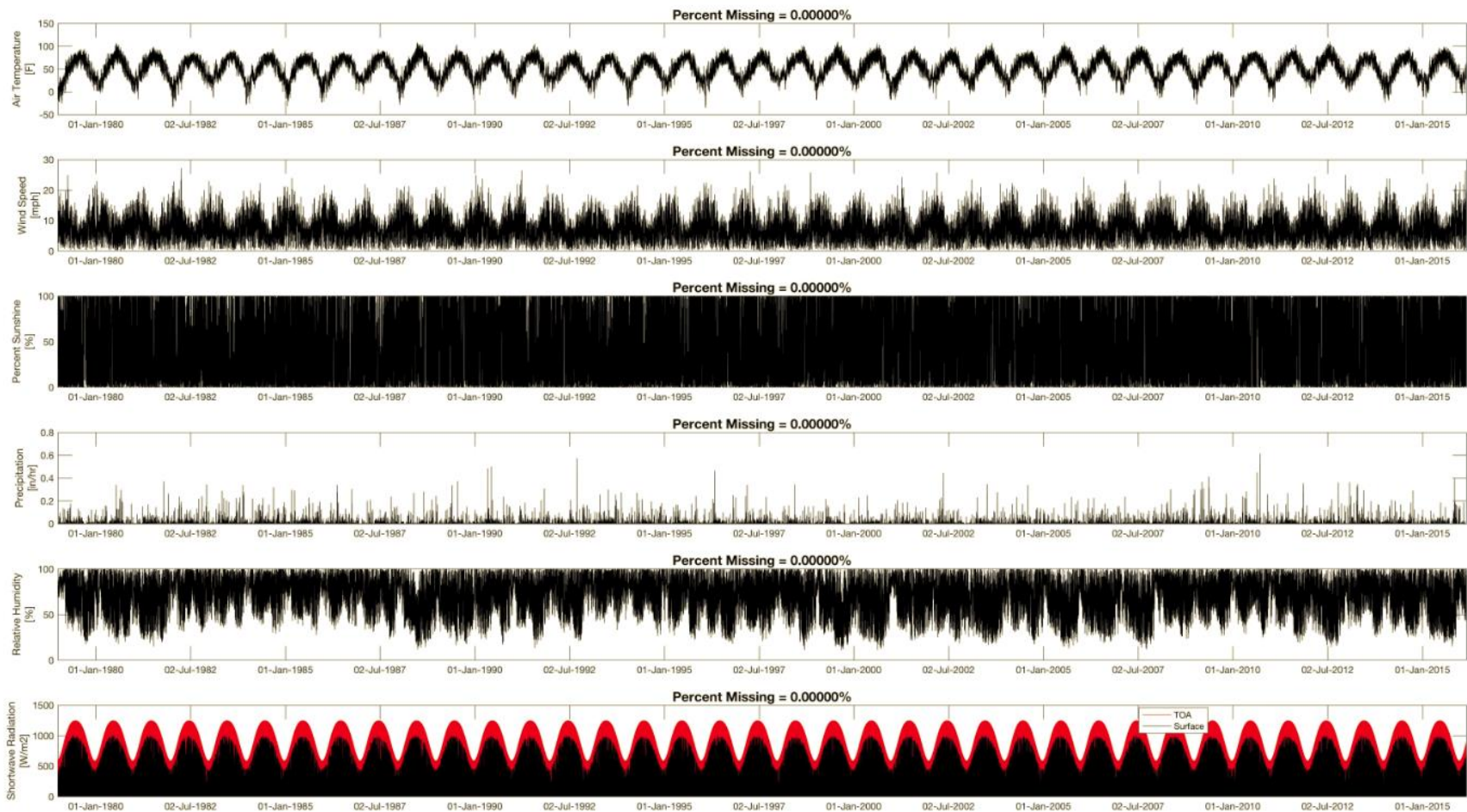


Figure A.4. Climate Location ID: 145872 (Davenport Municipal Airport)

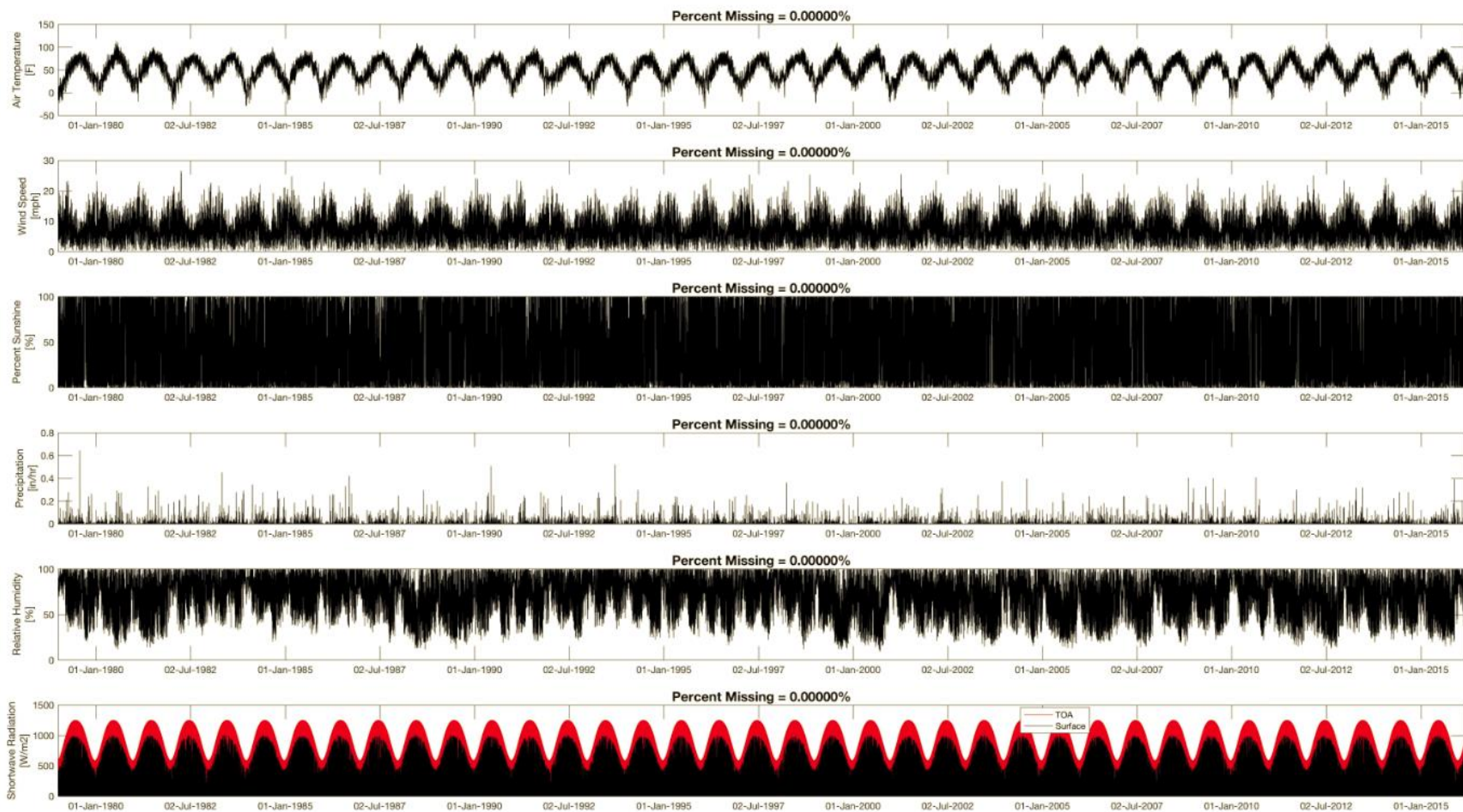


Figure A.5. Climate Location ID: 145867 (Des Moines International Airport)

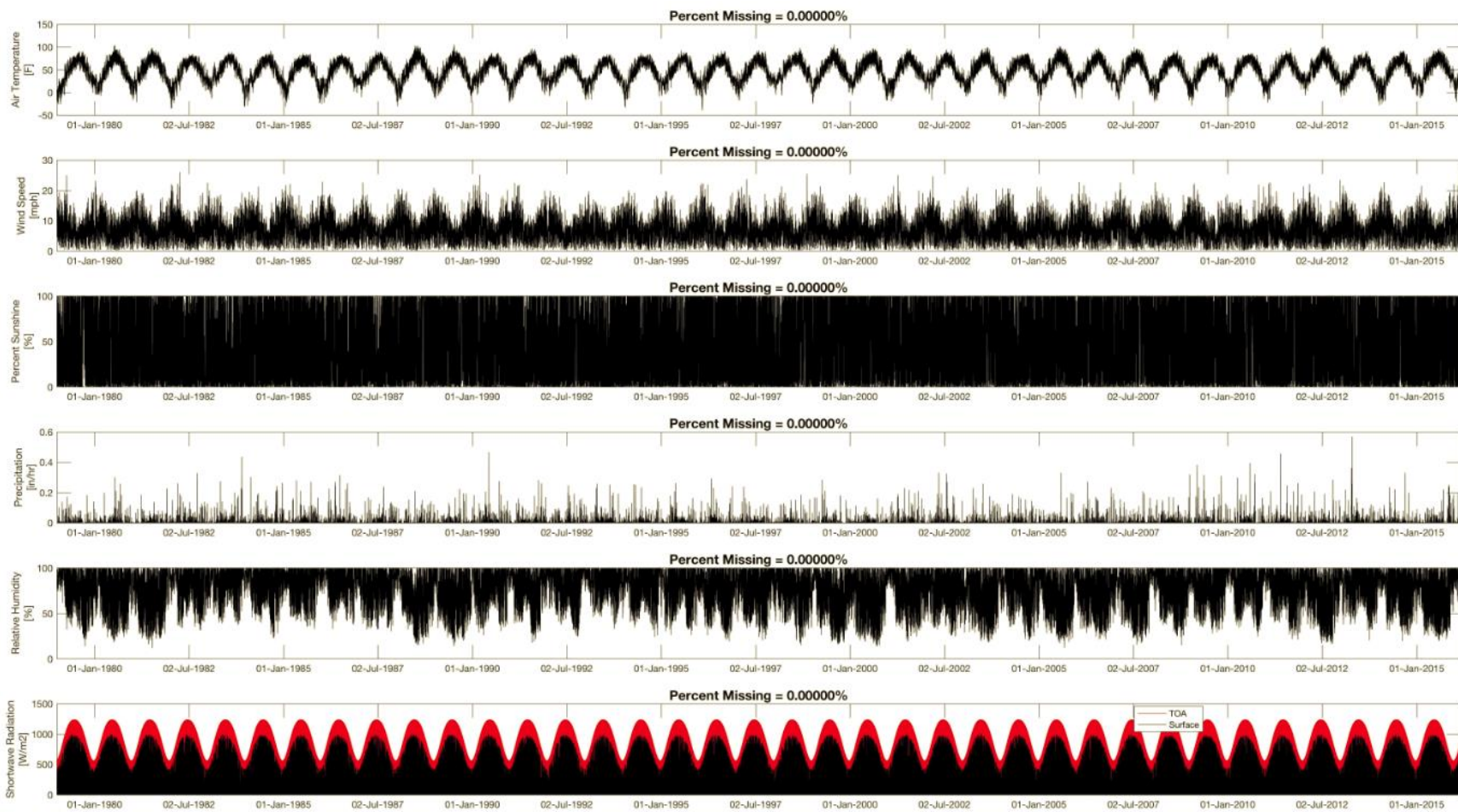


Figure A.6. Climate Location ID: 147024 (Dubuque Regional Airport)

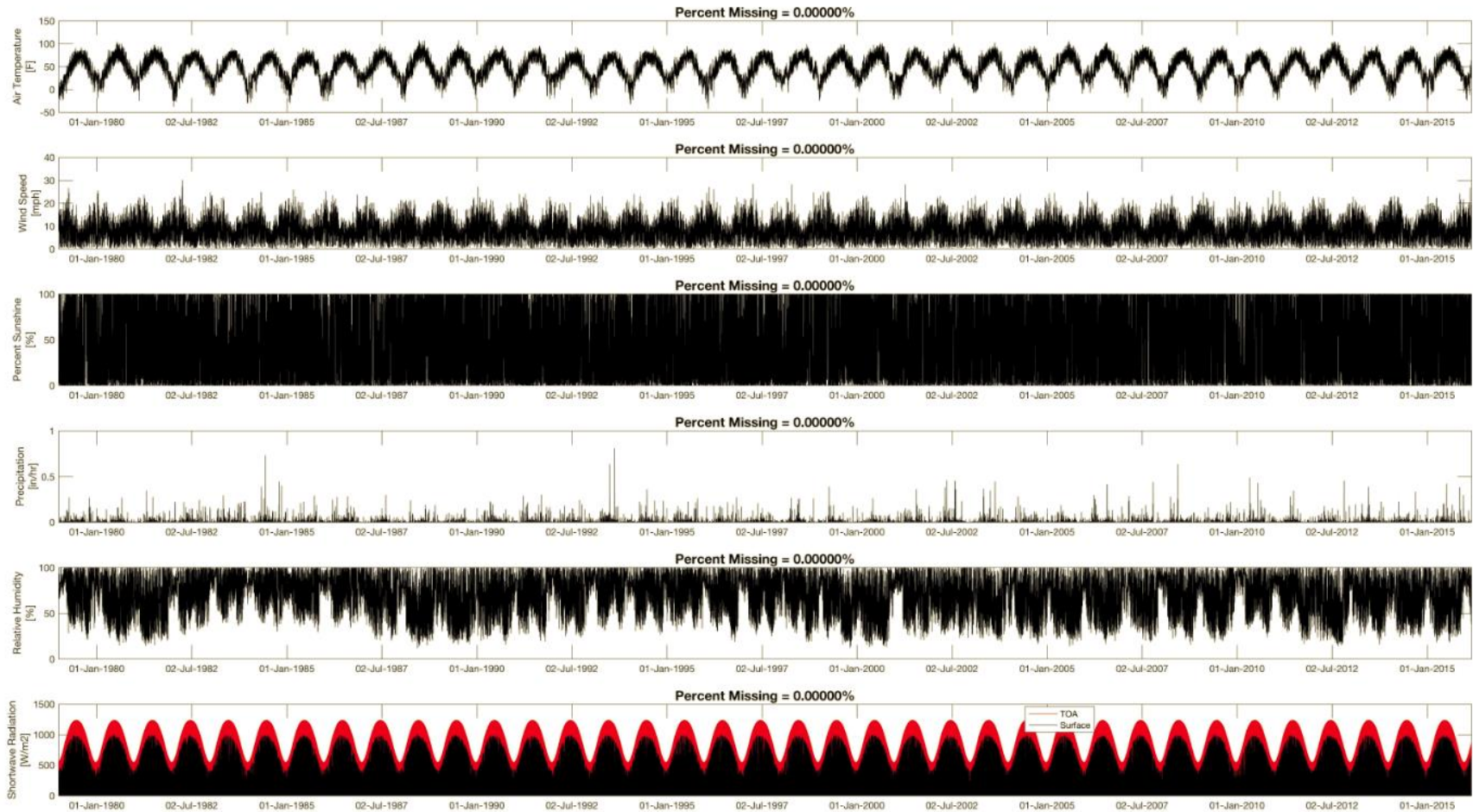


Figure A.7. Climate Location ID: 148169 (Estherville Municipal Airport,

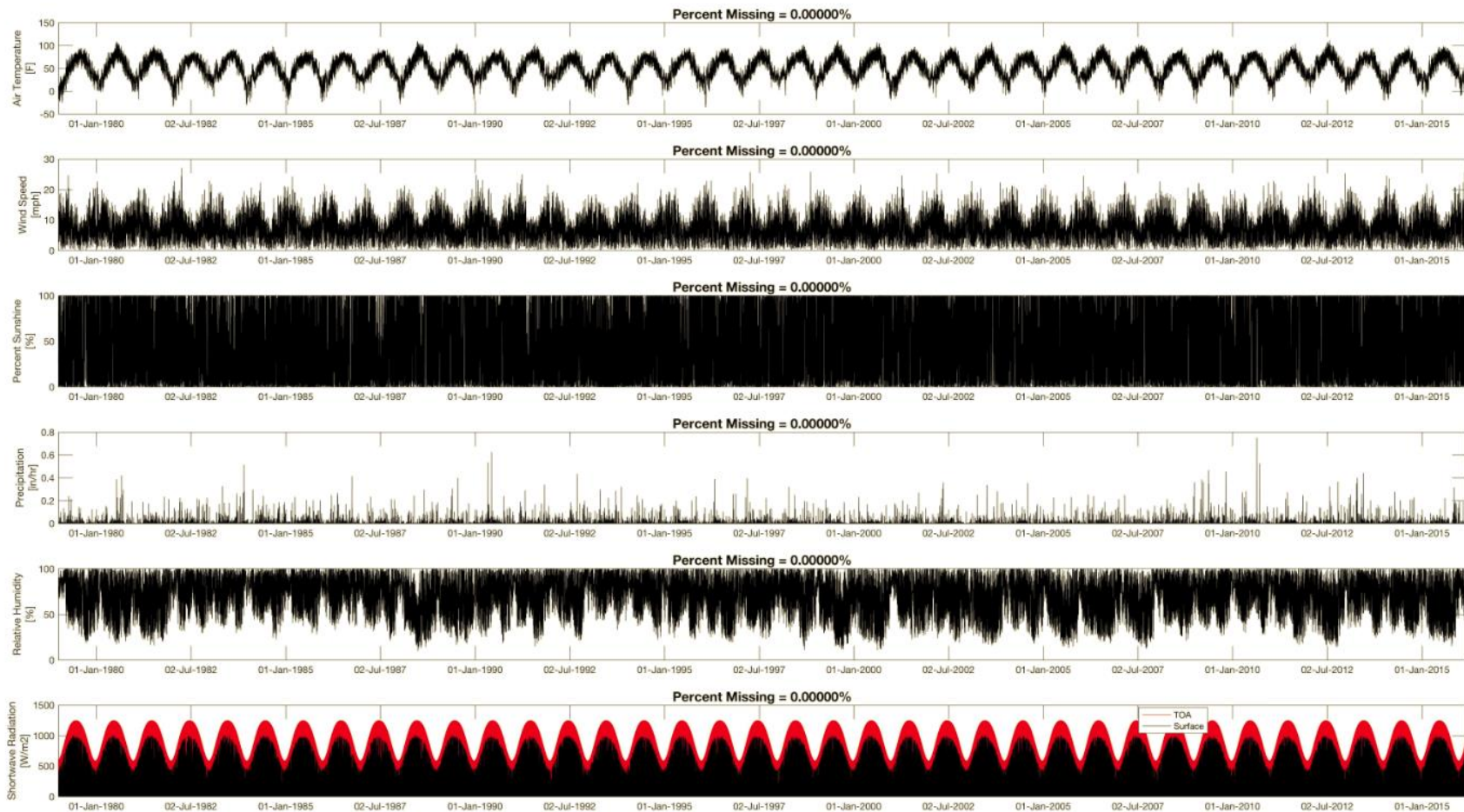


Figure A.8. Climate Location ID: 145871 (Iowa City Municipal Airport)

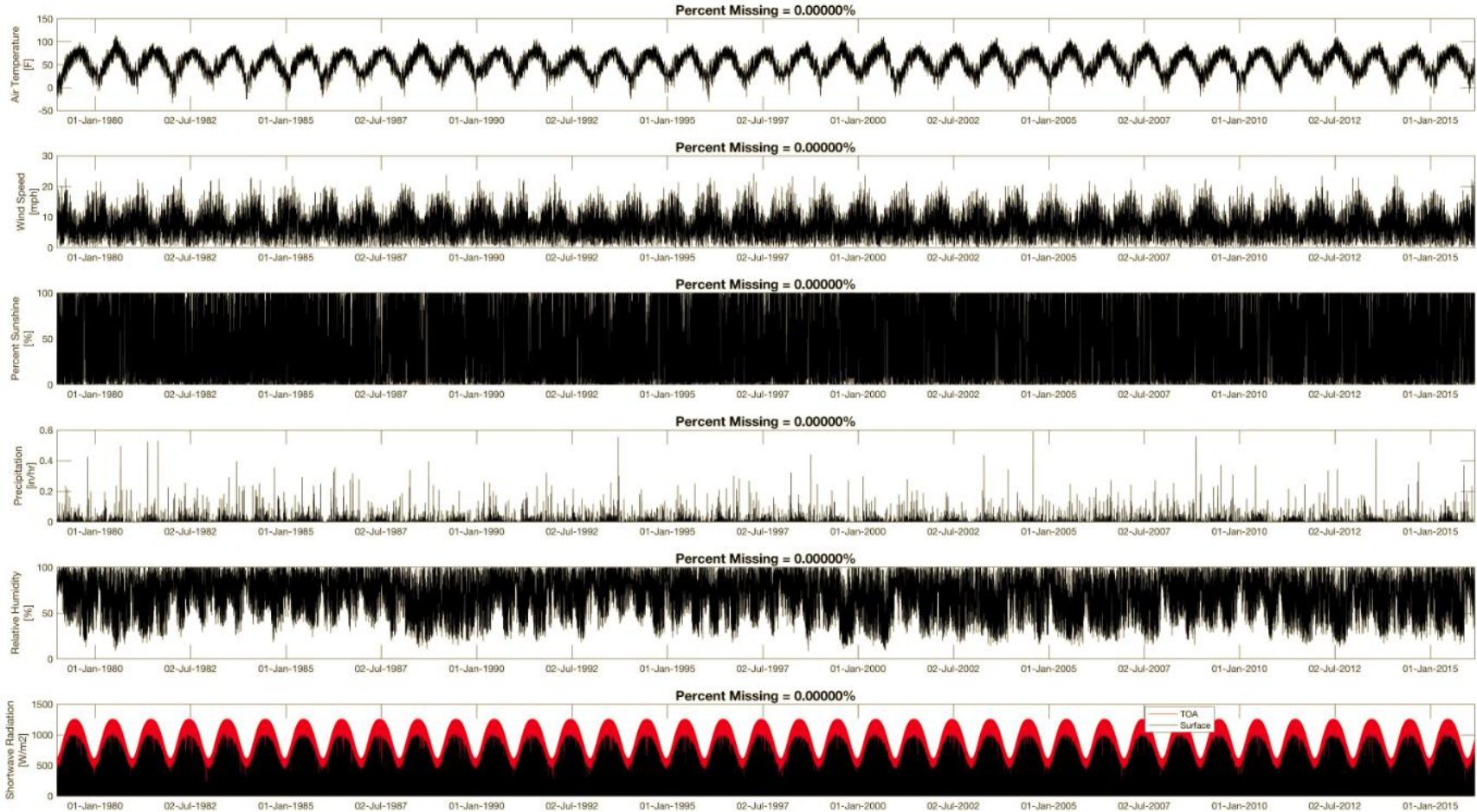


Figure A.9. Climate Location ID: 144715 (Lamoni Municipal Airport)

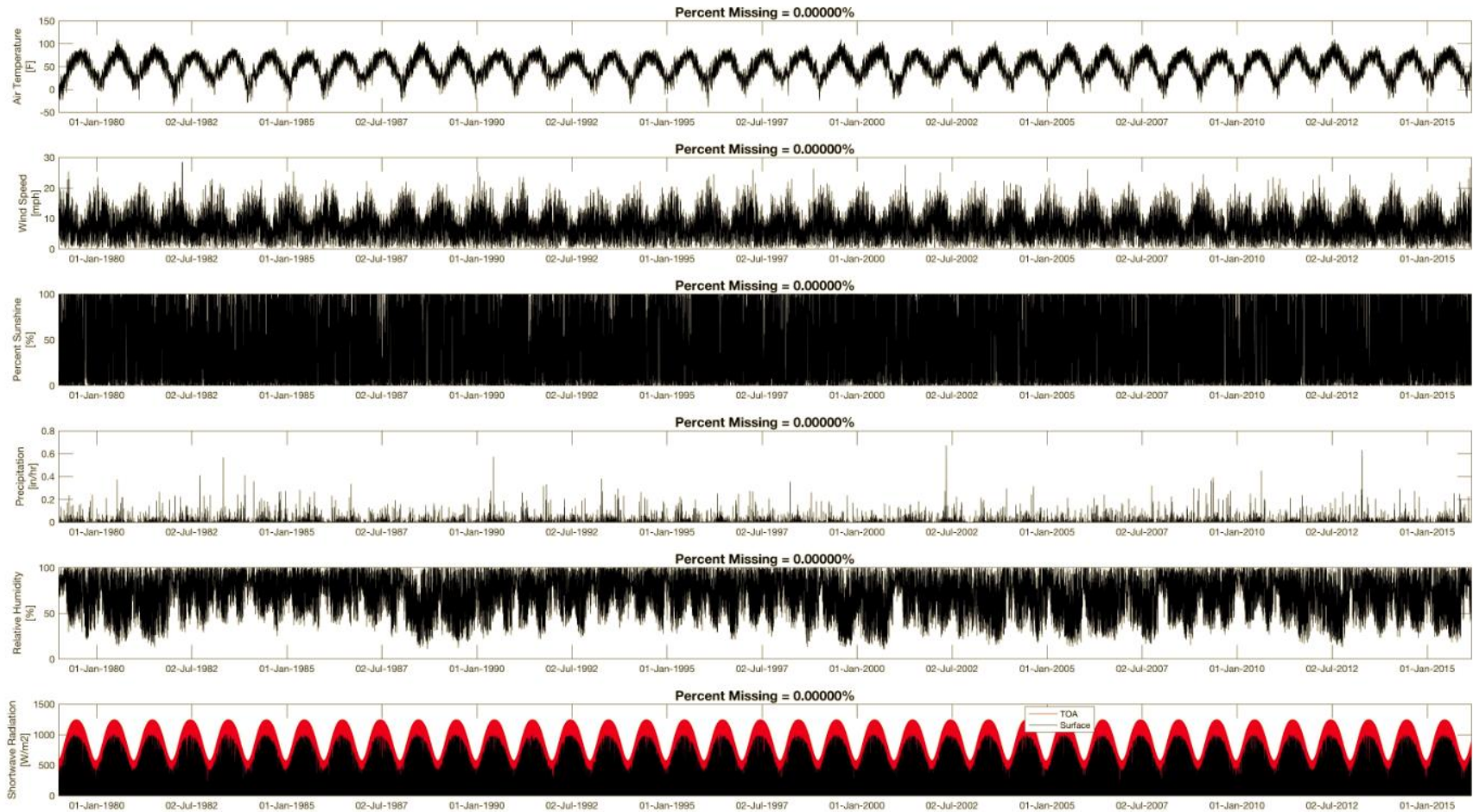


Figure A.10. Climate Location ID: 146444 (Marshalltown Municipal Airport)

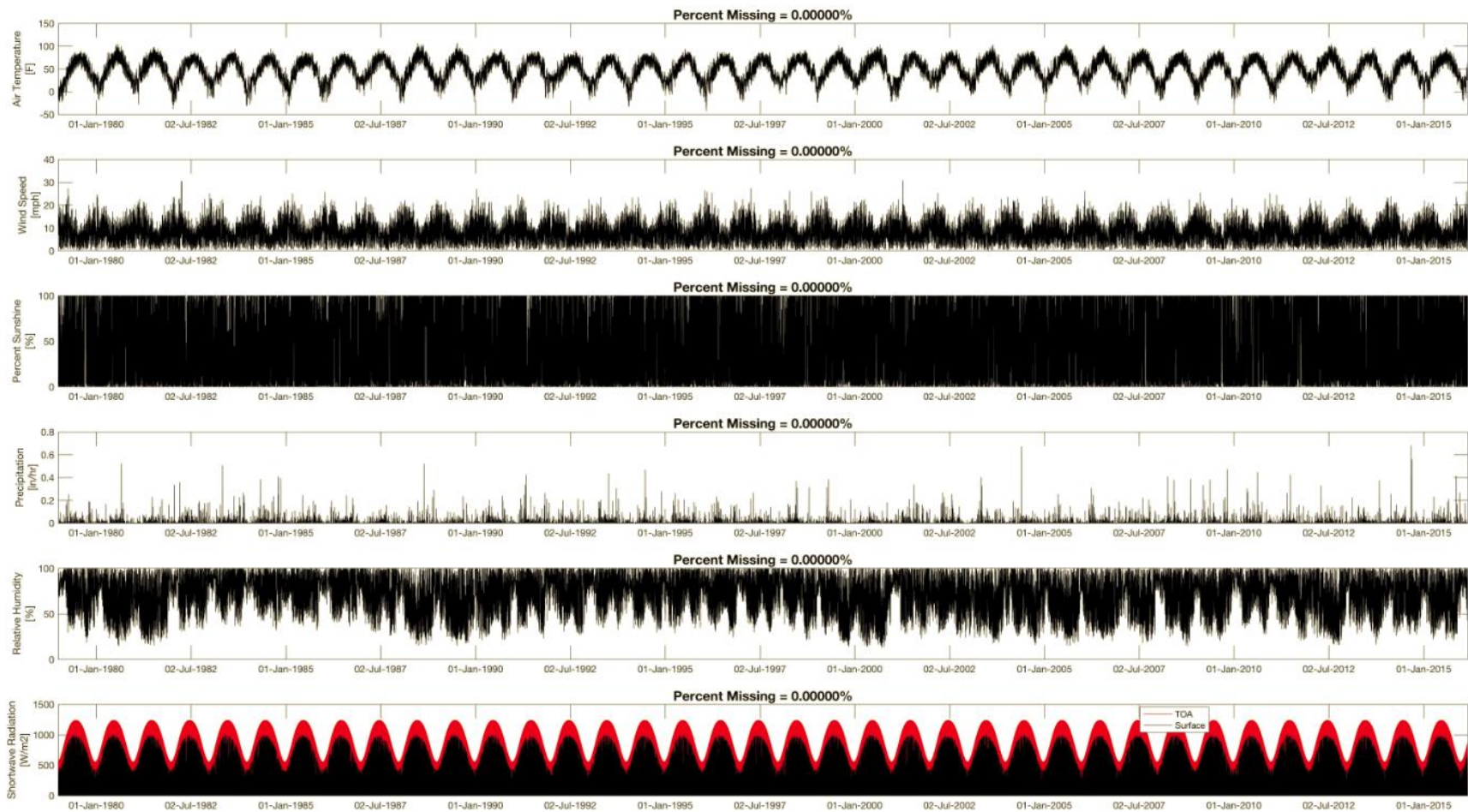


Figure A.11. Climate Location ID: 147596 (Mason City Municipal Airport)

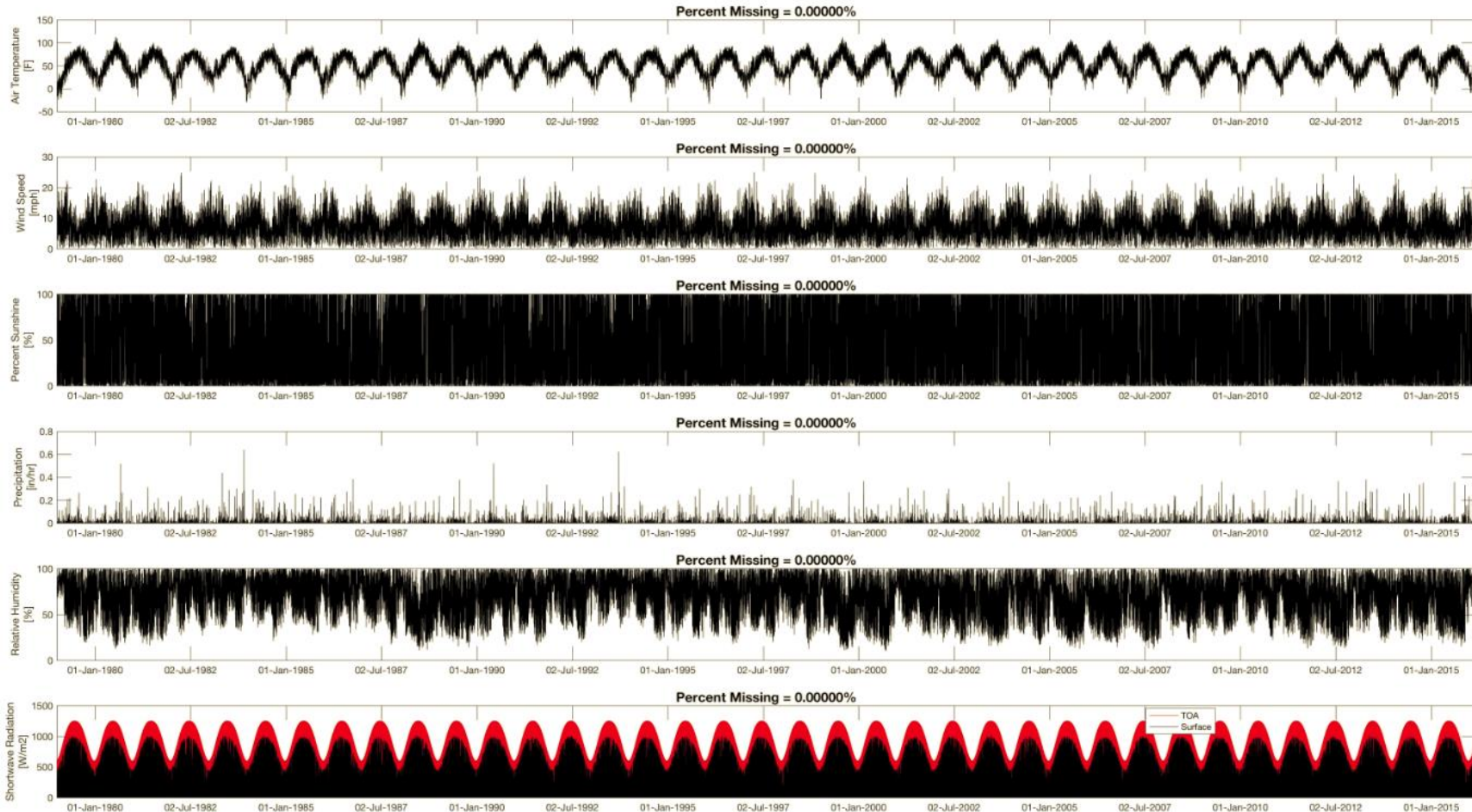


Figure A.12. Climate Location ID: 145293 (Ottumwa Industrial Airport)

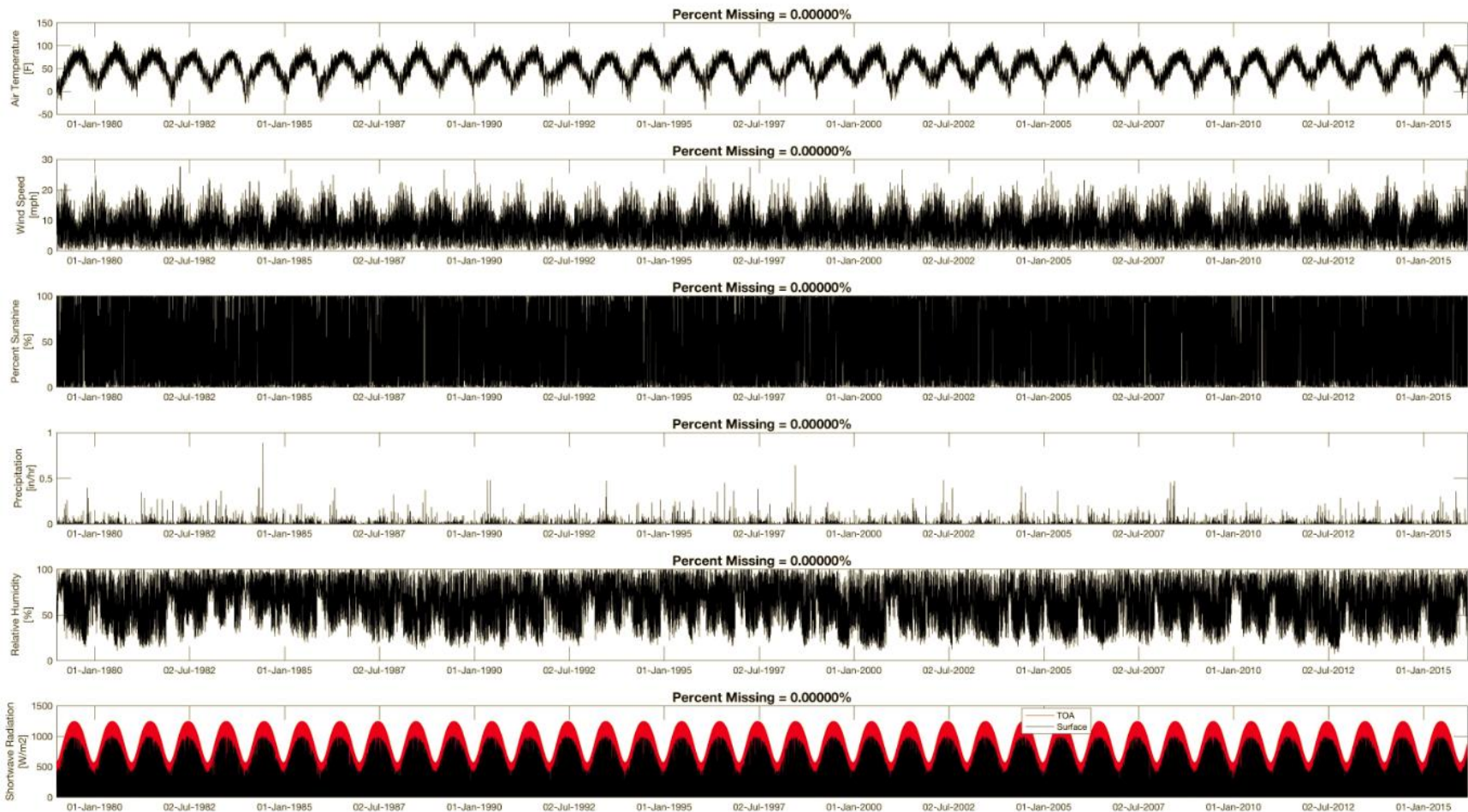


Figure A.13. Climate Location ID: 147015 (Sioux Gateway Airport, Sioux City)

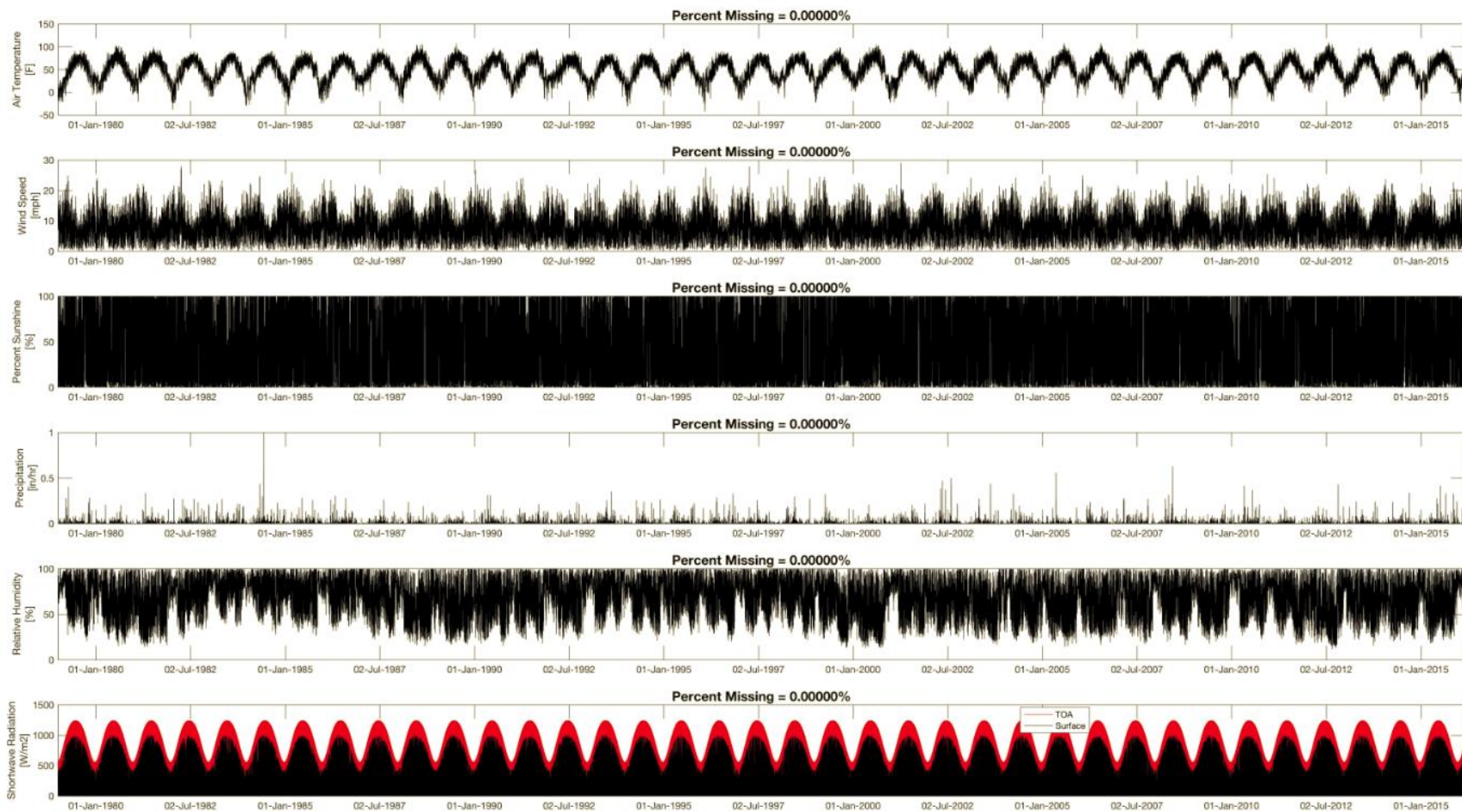


Figure A.14. Climate Location ID: 147593 (Spencer Municipal Airport)

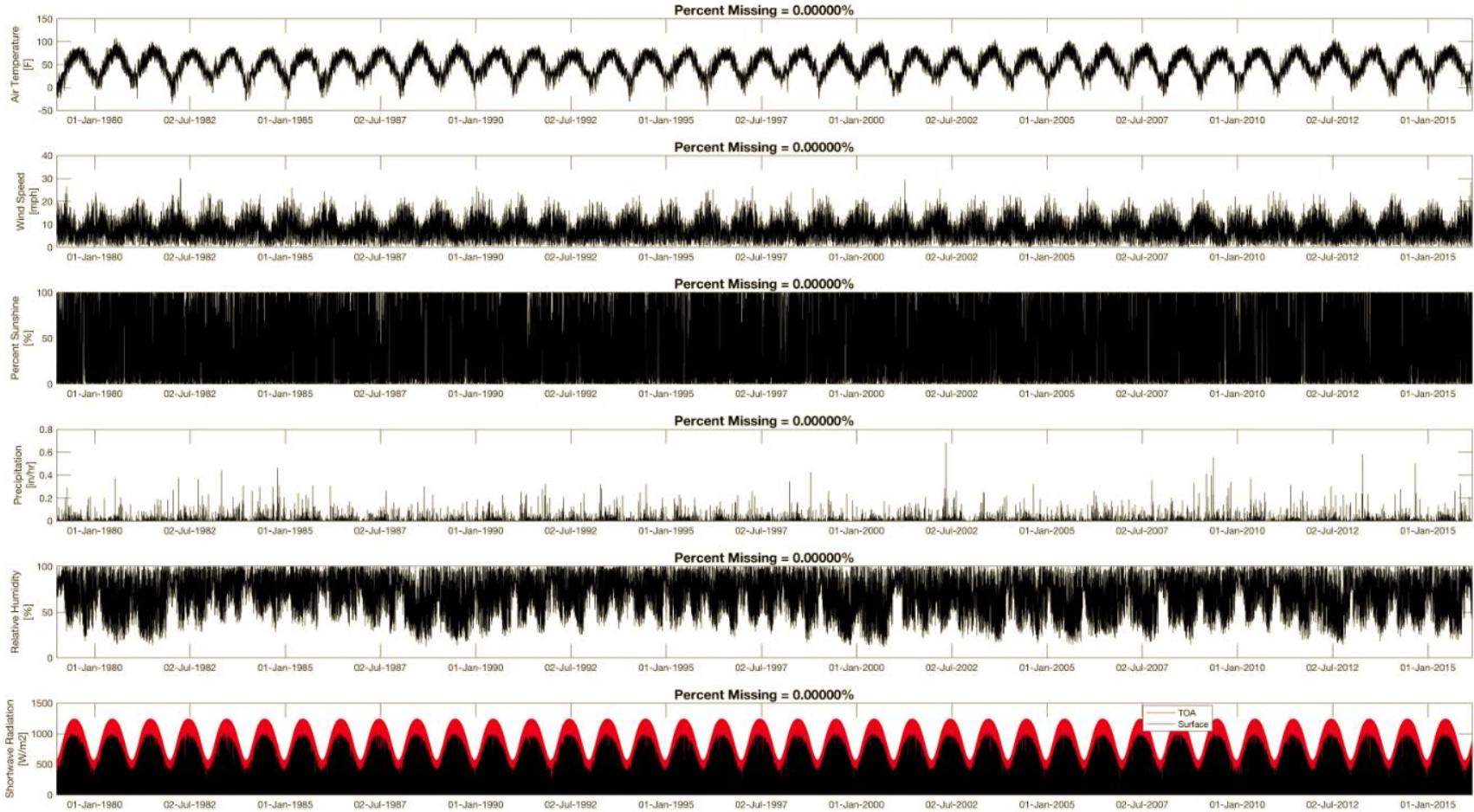


Figure A.15. Climate Location ID: 147021 (Waterloo Municipal Airport)

APPENDIX B: MERRA-2 CLIMATE DATA INPUT CHARTS FOR ALL IOWA LOCATIONS

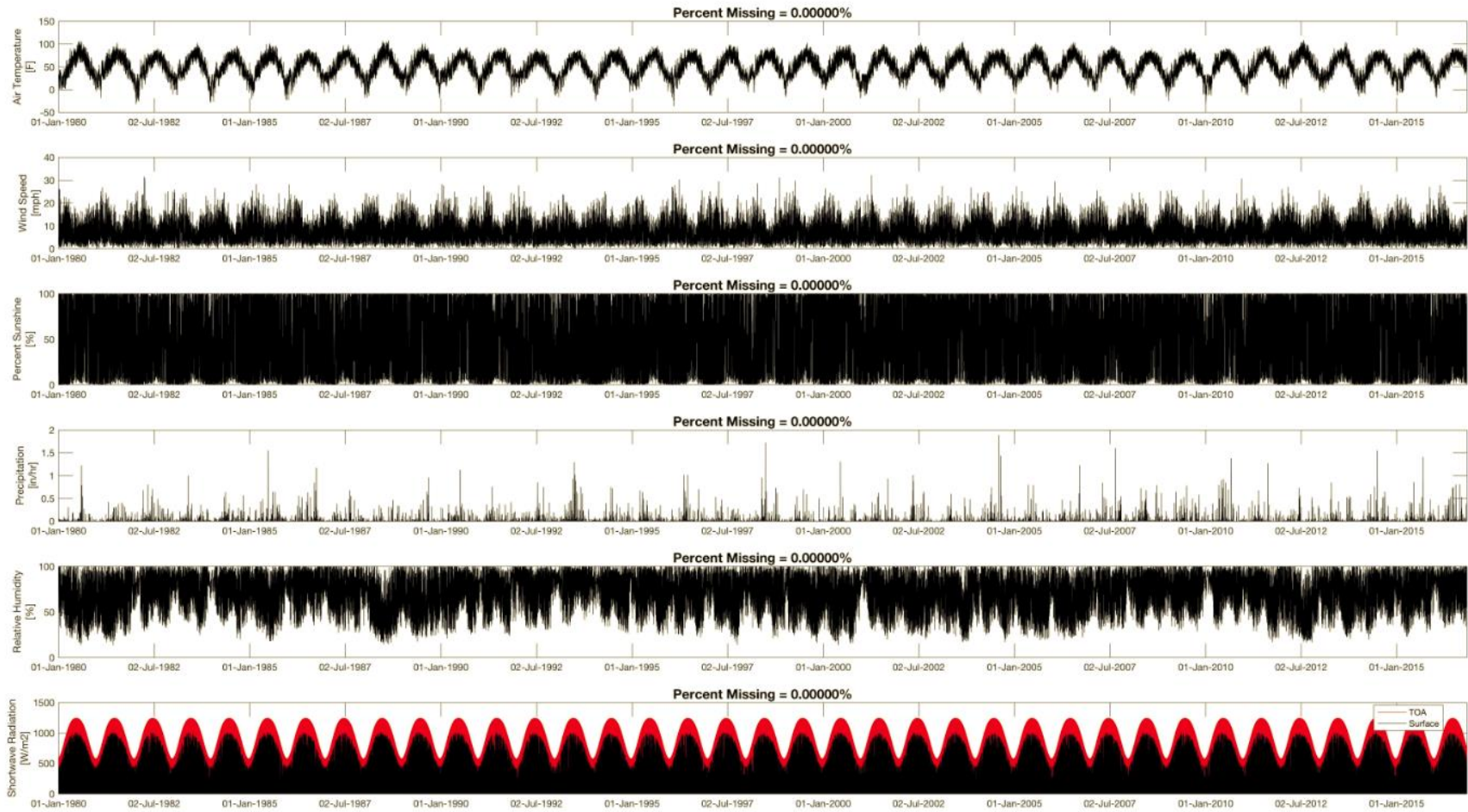


Figure B.1. Climate Location ID: 146443 (Ames Municipal Airport)

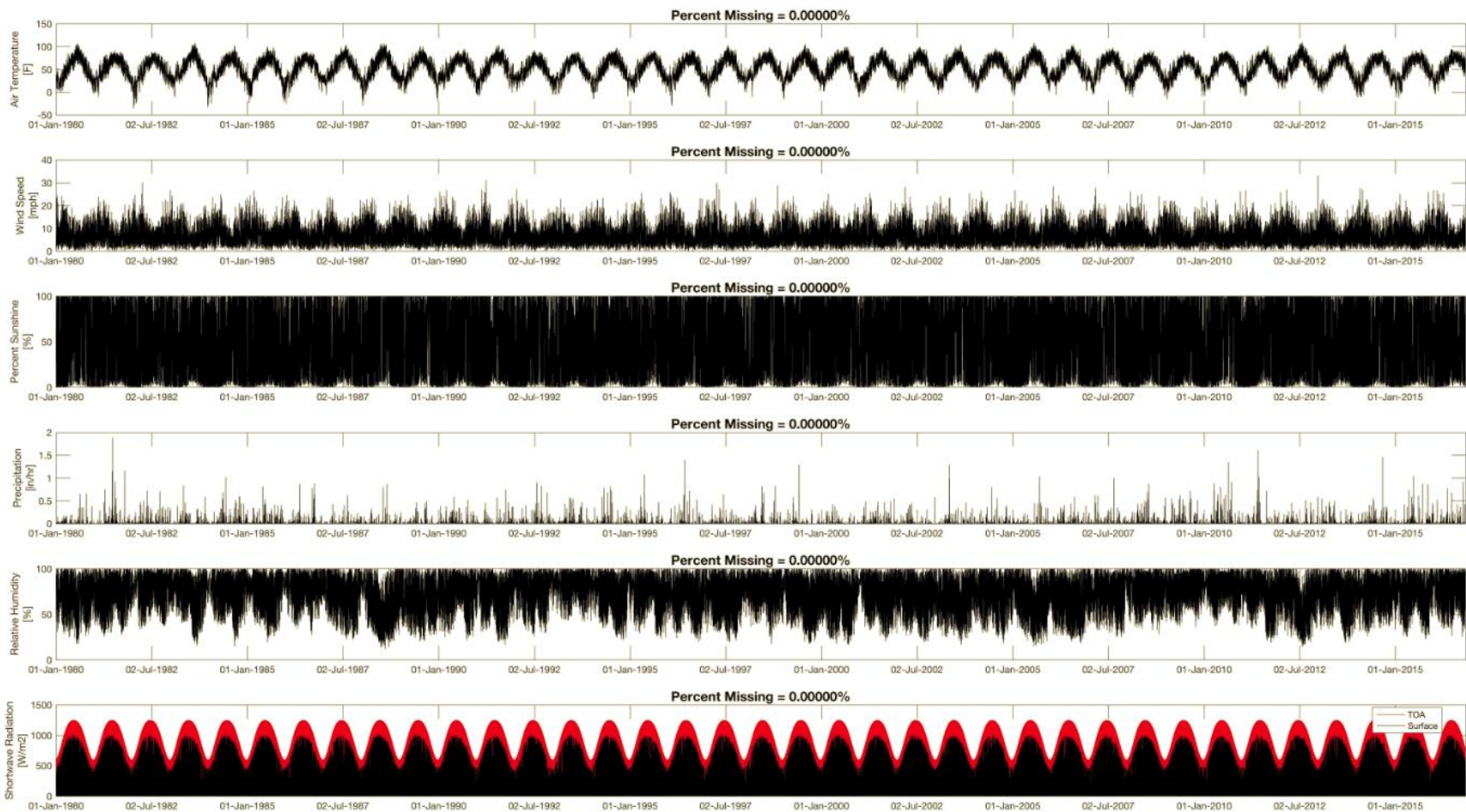


Figure B.2. Climate Location ID: 145295 (Iowa Regional Airport, Burlington)

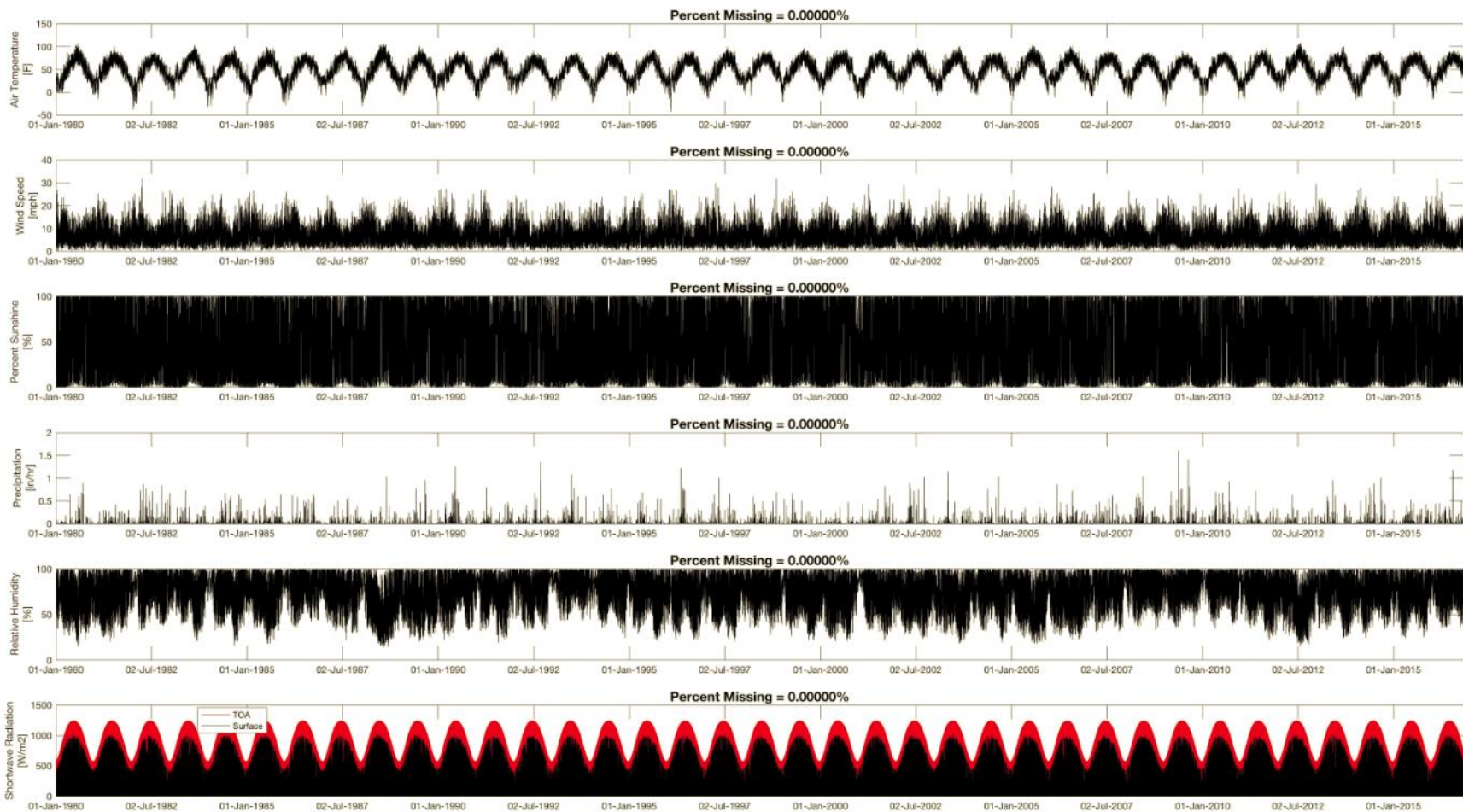


Figure B.3. Climate Location ID: 146446 (Eastern Iowa Airport, Cedar Rapids)

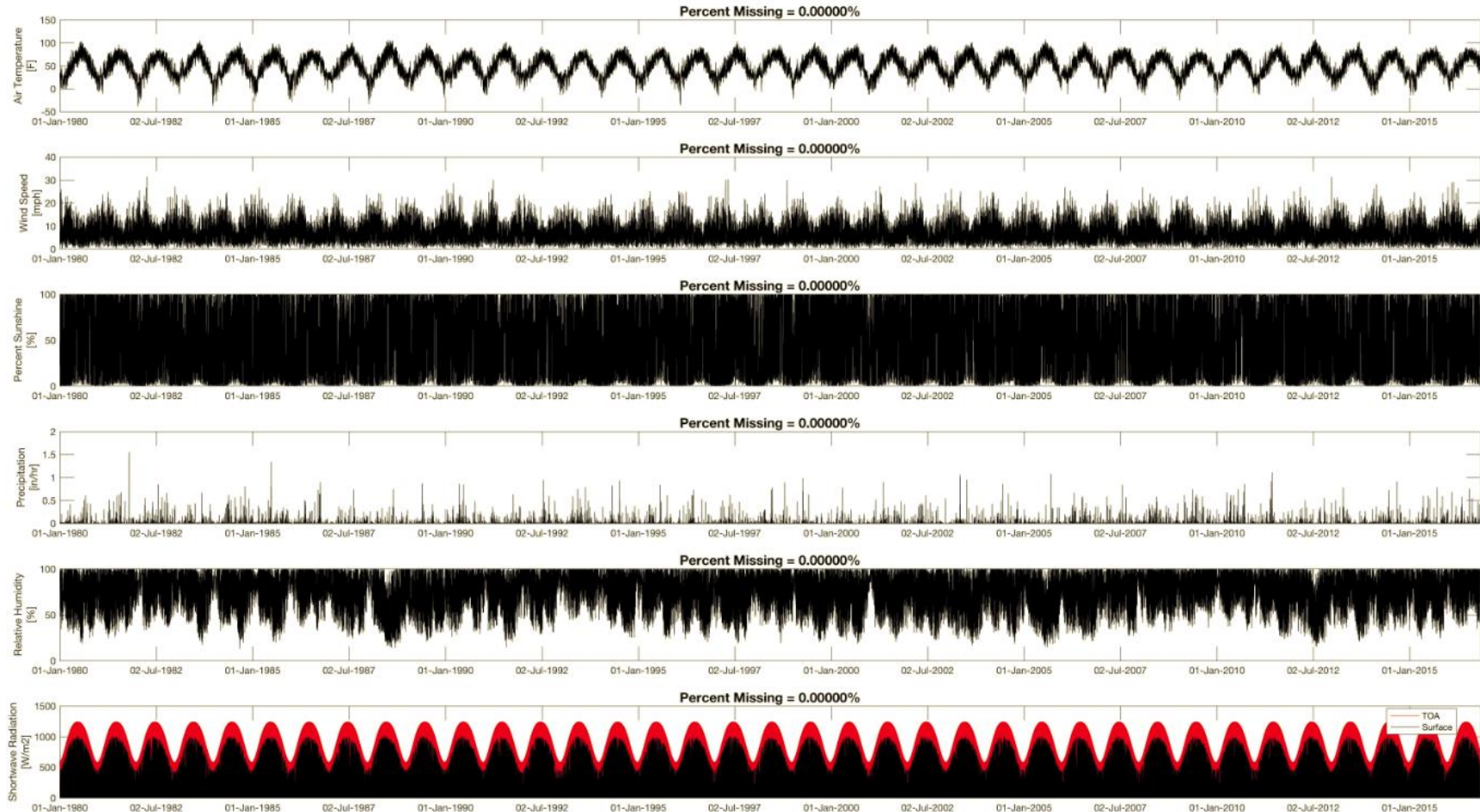


Figure B.4. Climate Location ID: 145872 (Davenport Municipal Airport)

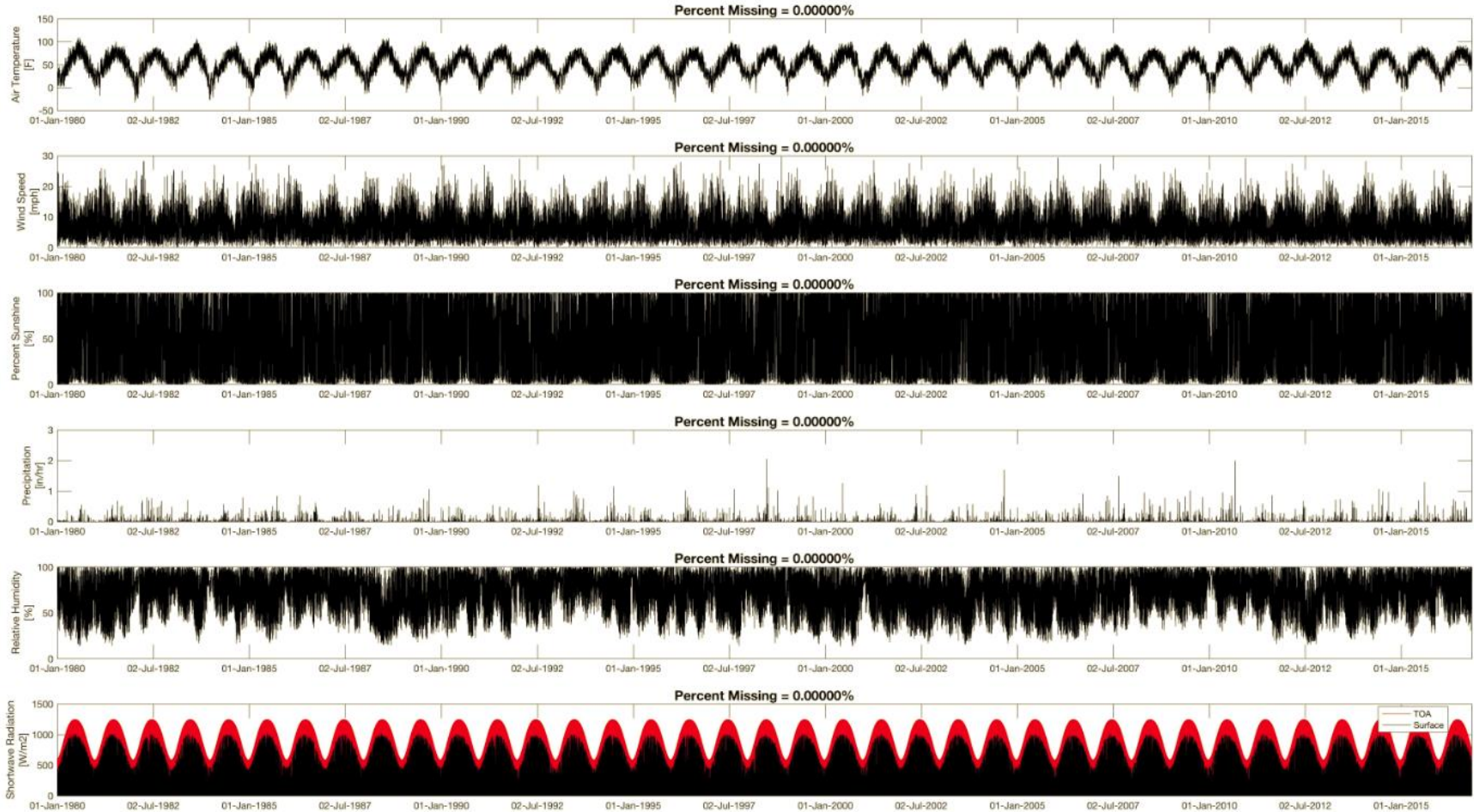


Figure B.5. Climate Location ID: 145867 (Des Moines International Airport)

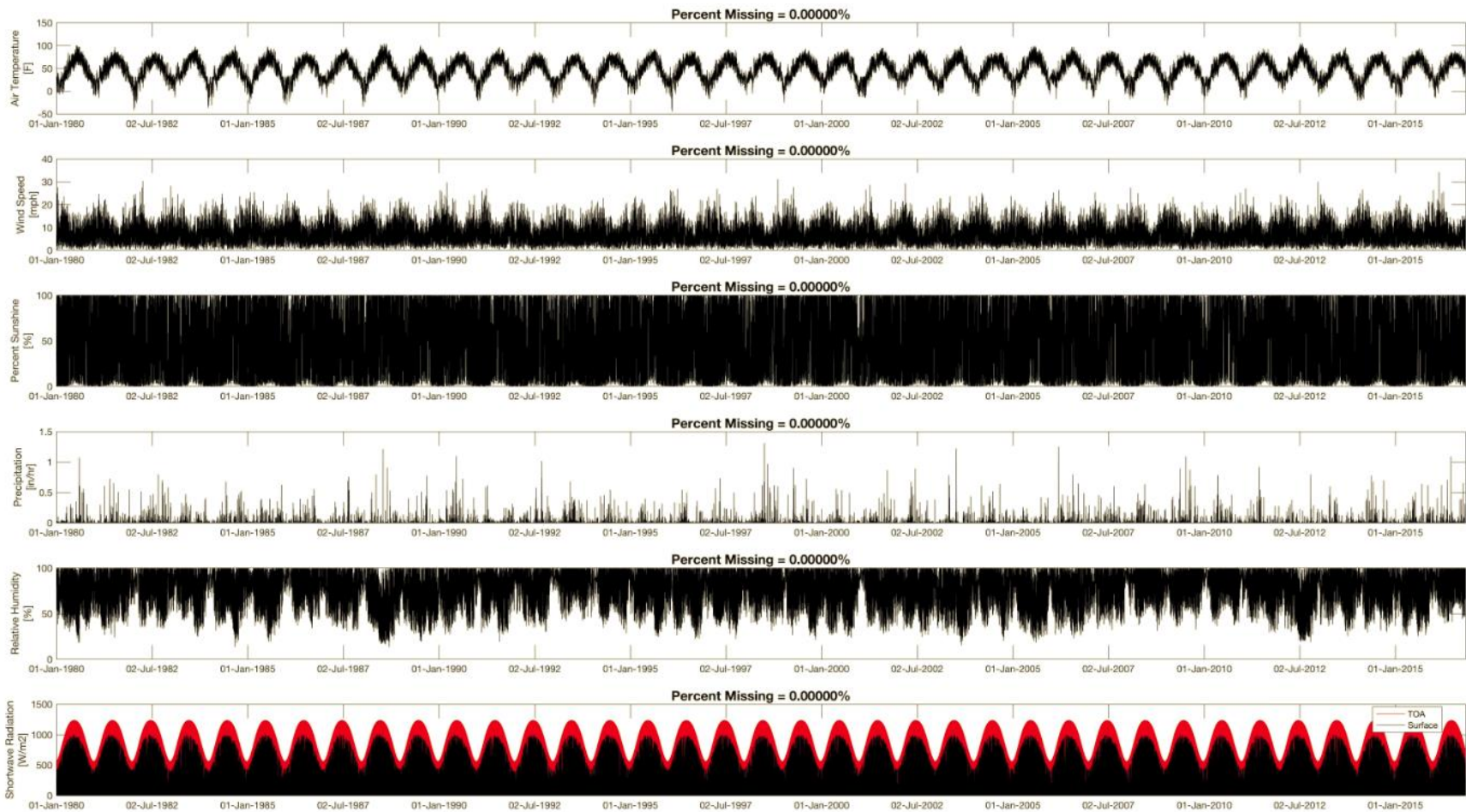


Figure B.6. Climate Location ID: 147024 (Dubuque Regional Airport)

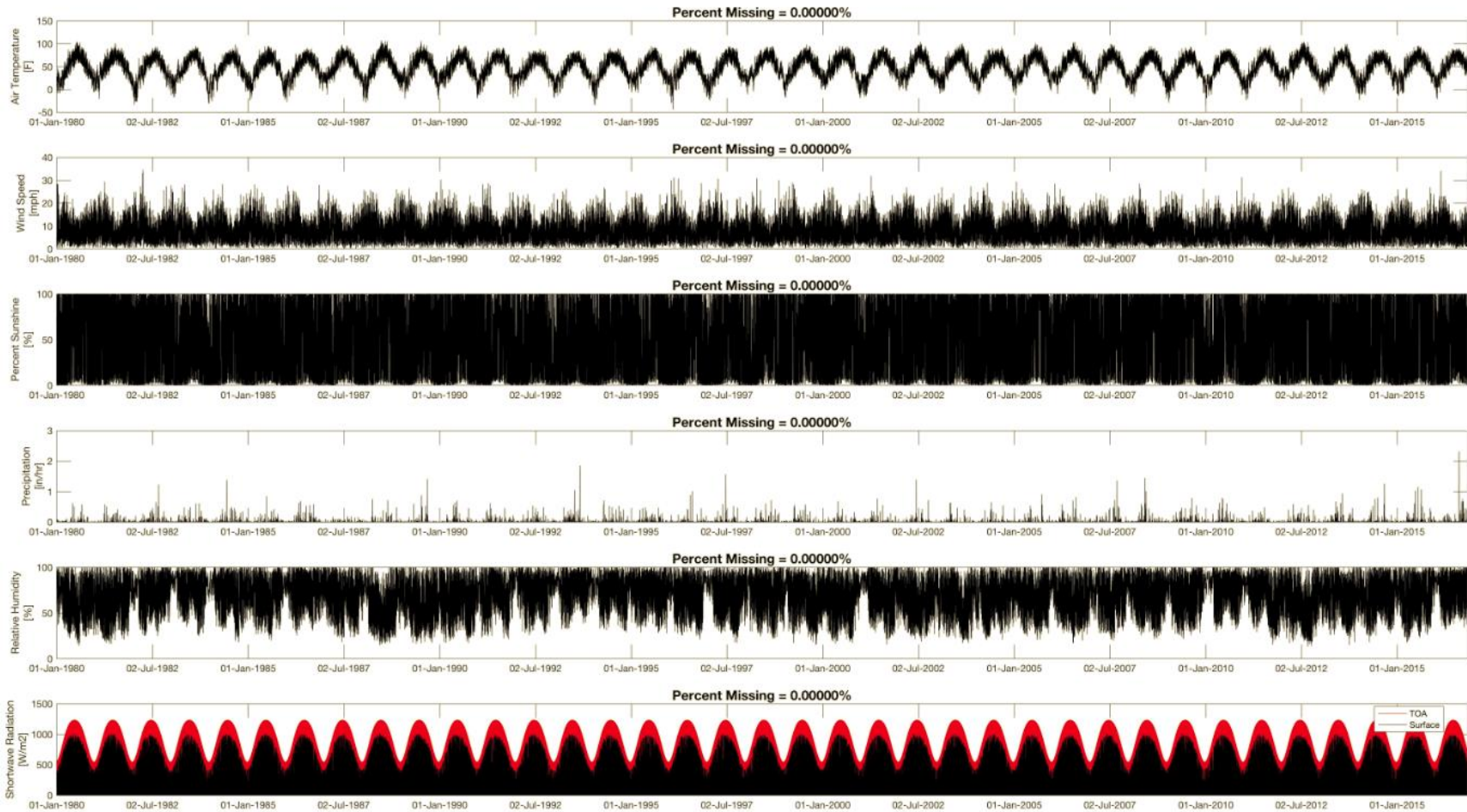


Figure B.7. Climate Location ID: 148169 (Estherville Municipal Airport)

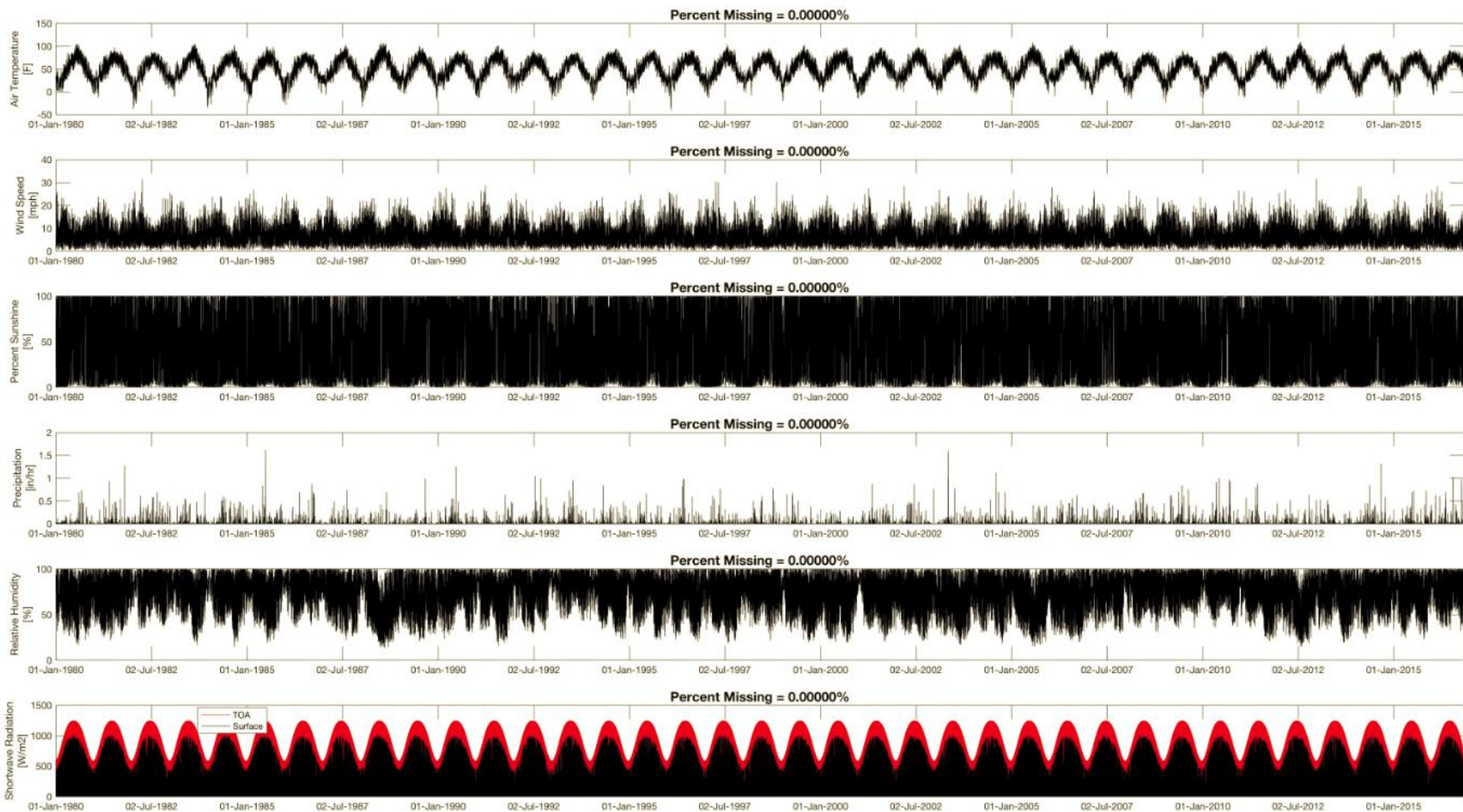


Figure B.8. Climate Location ID: 145871 (Iowa City Municipal Airport)

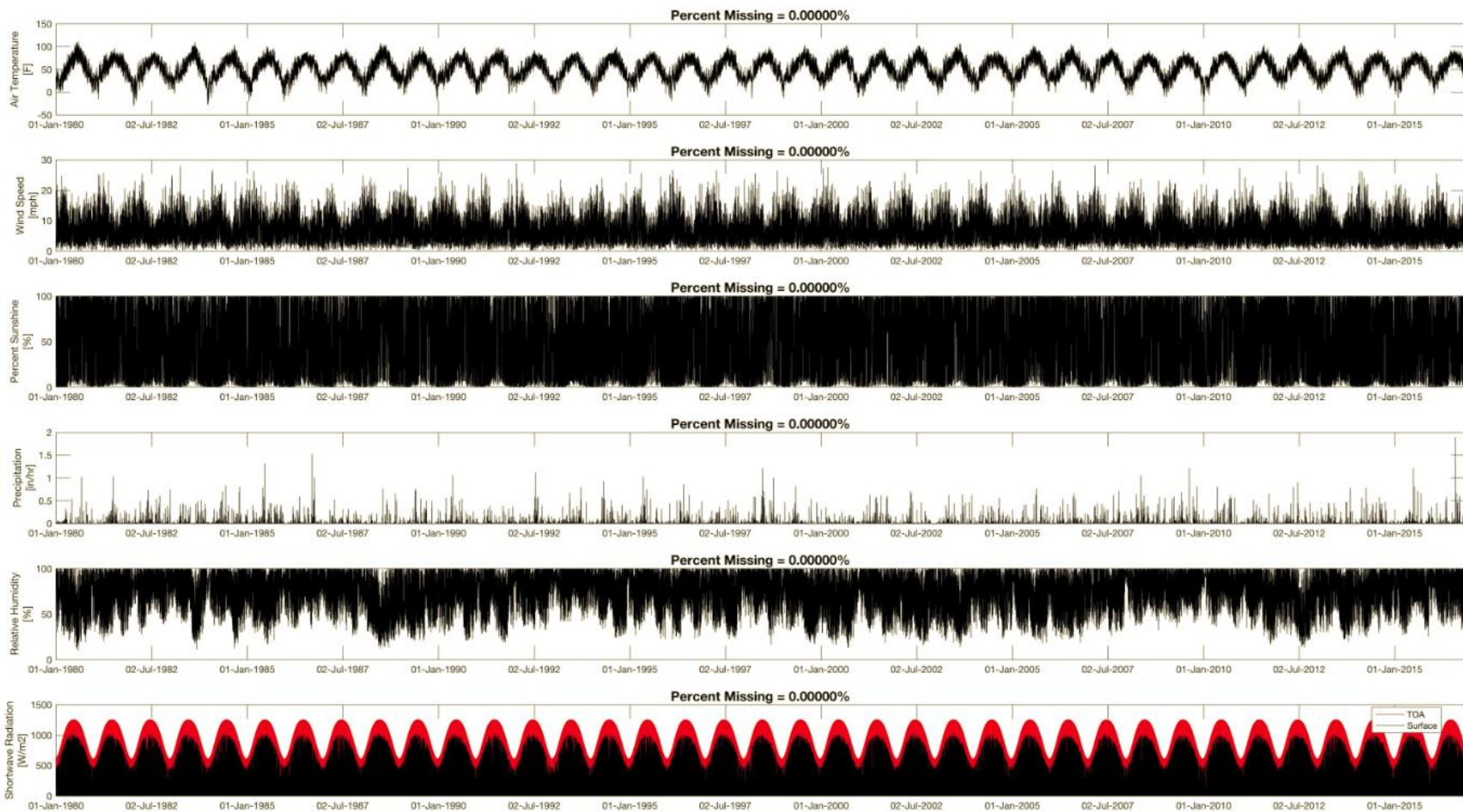


Figure B.9. Climate Location Id: 144715 (Lamoni Municipal Airport)

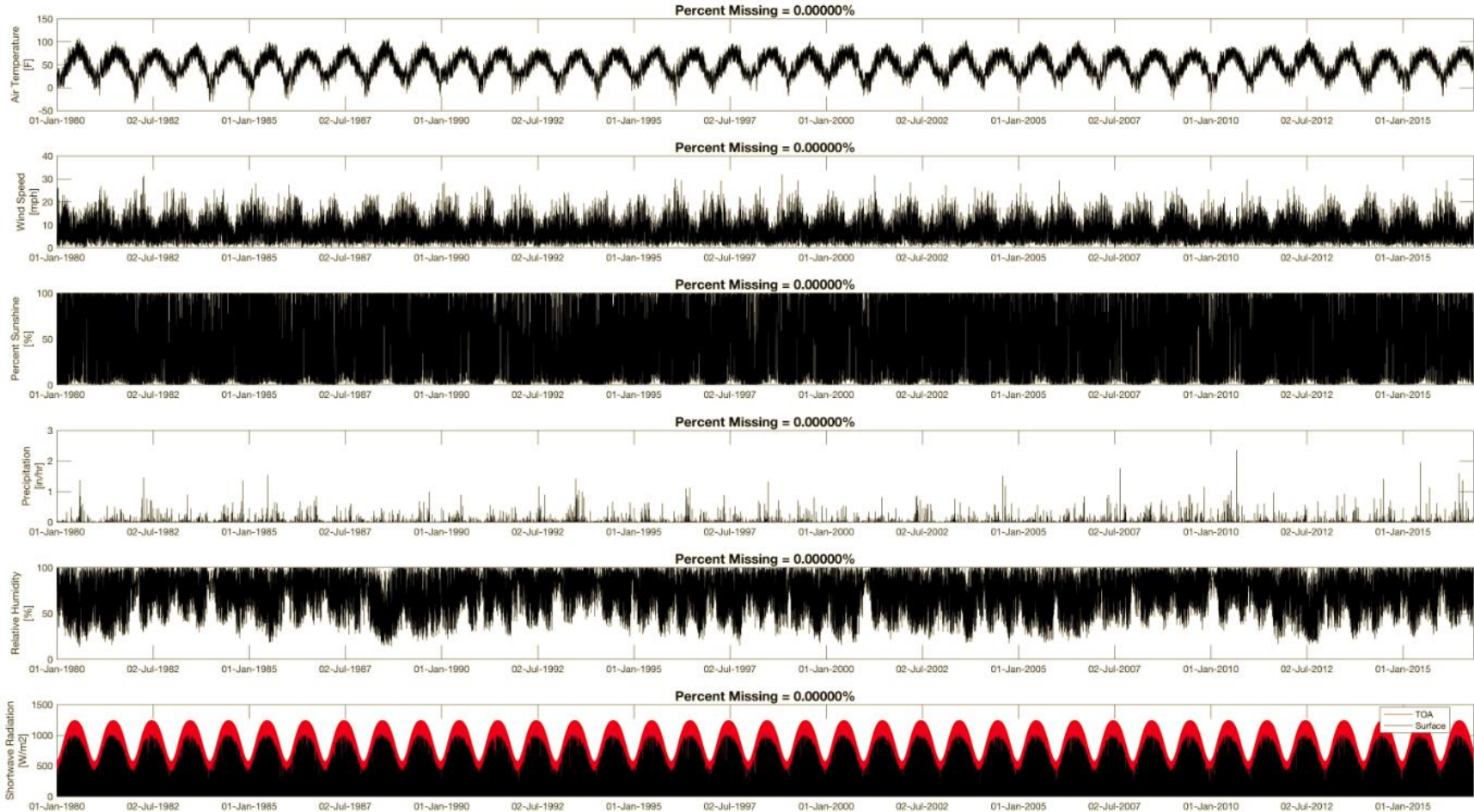


Figure B.10. Climate Location ID: 146444 (Marshalltown Municipal Airport)

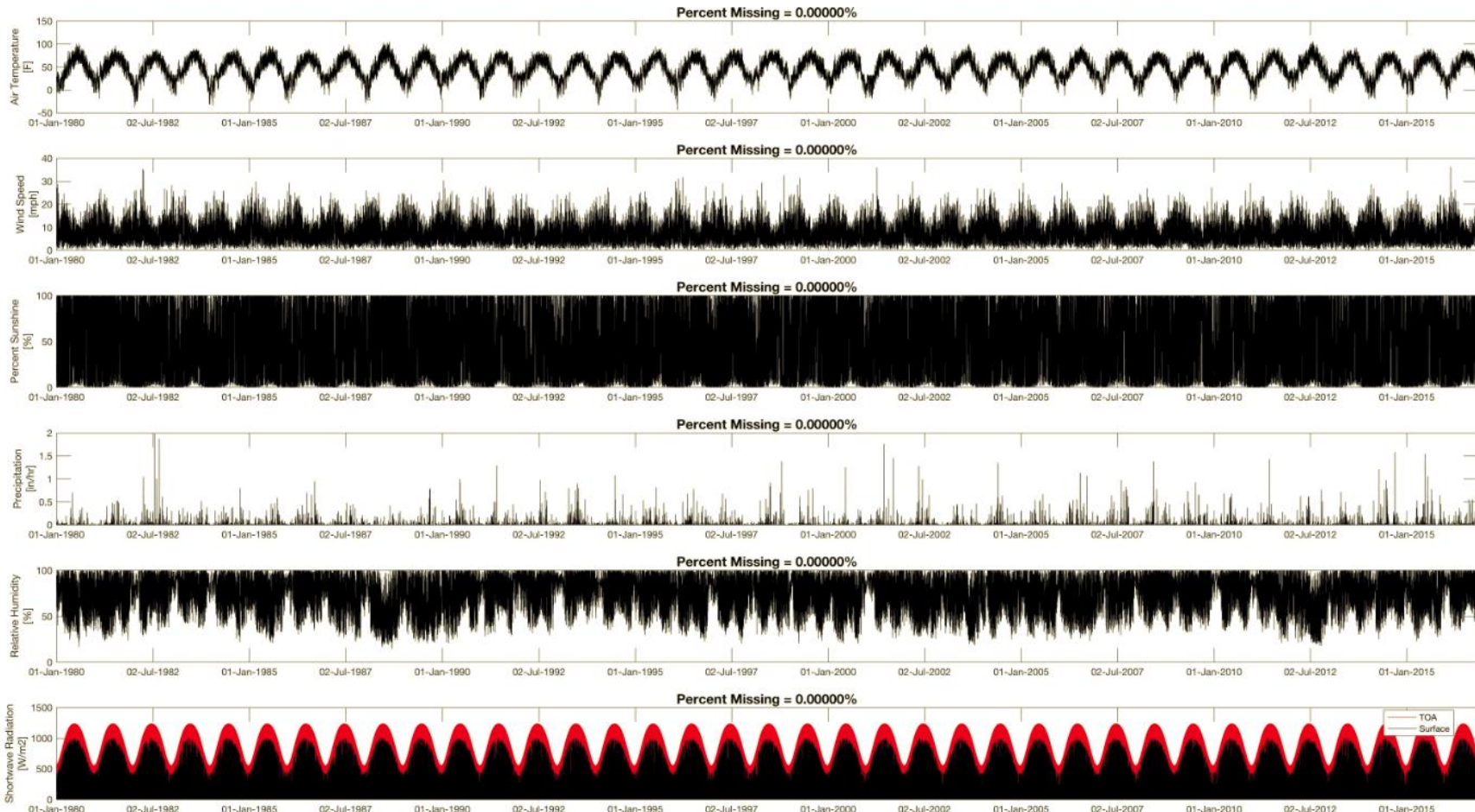


Figure B.11. Climate Location ID: 147596 (Mason City Municipal Airport)

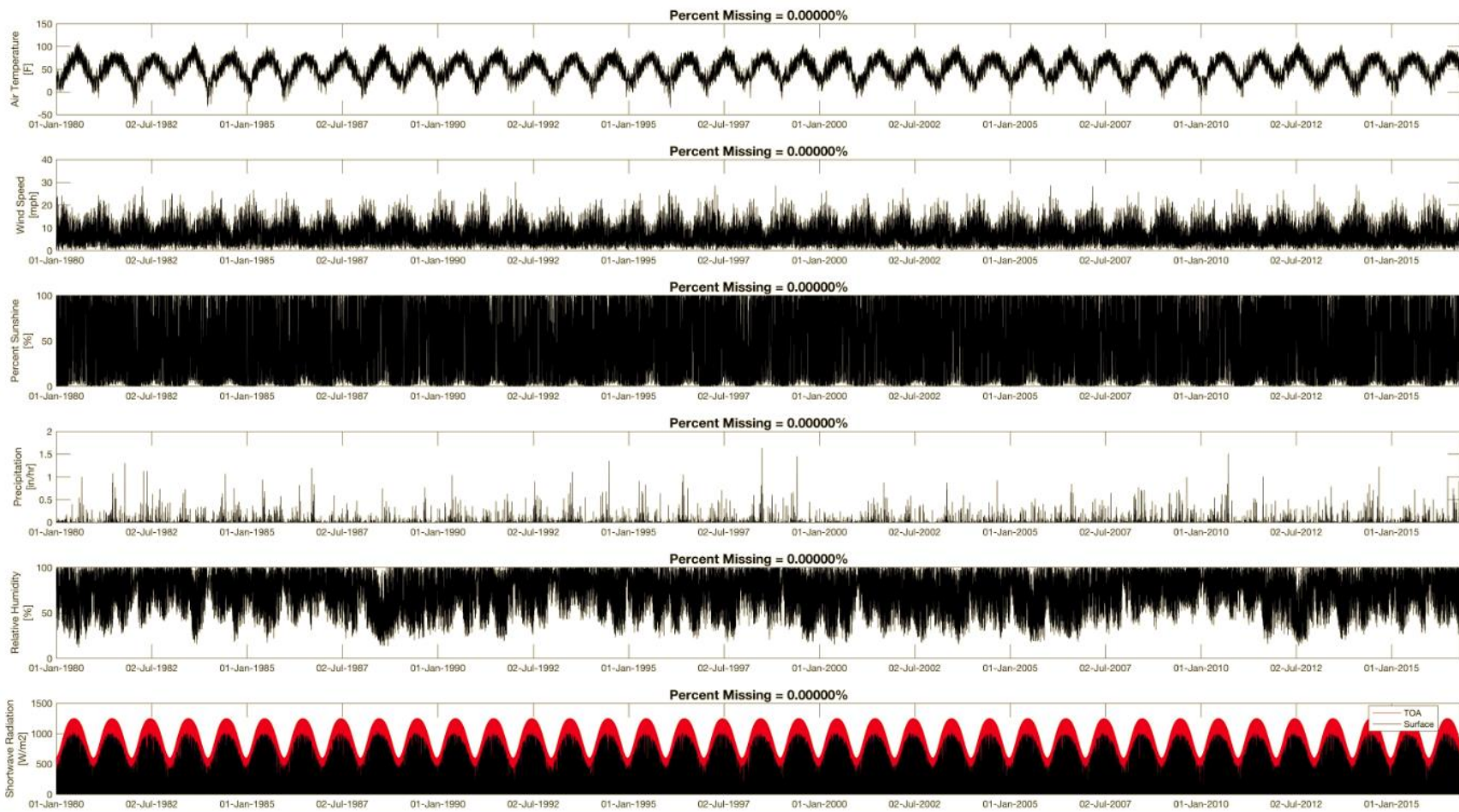


Figure B.12. Climate Location ID: 145293 (Ottumwa Industrial Airport)

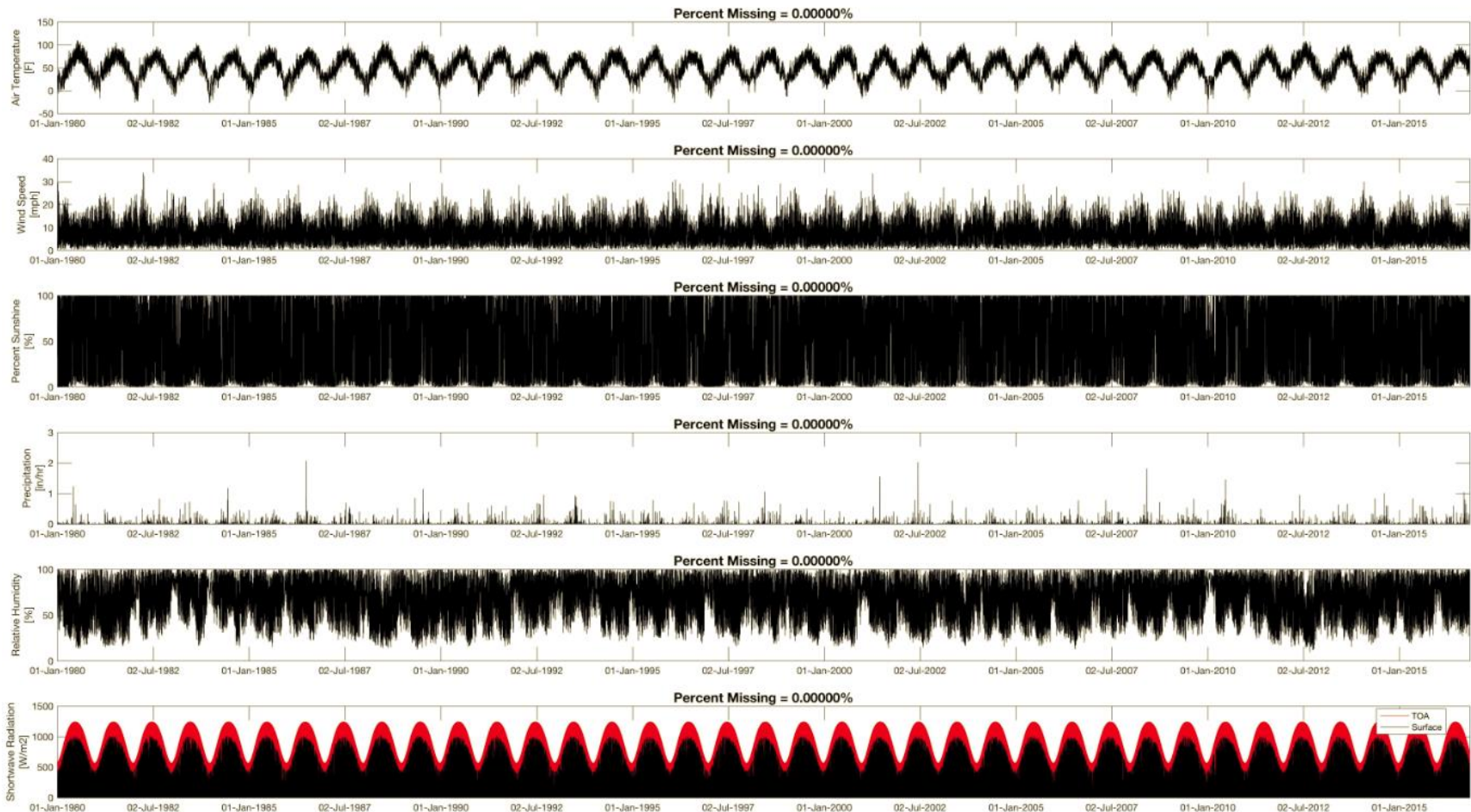


Figure B.13. Climate Location ID: 147015 (Sioux Gateway Airport, Sioux City)

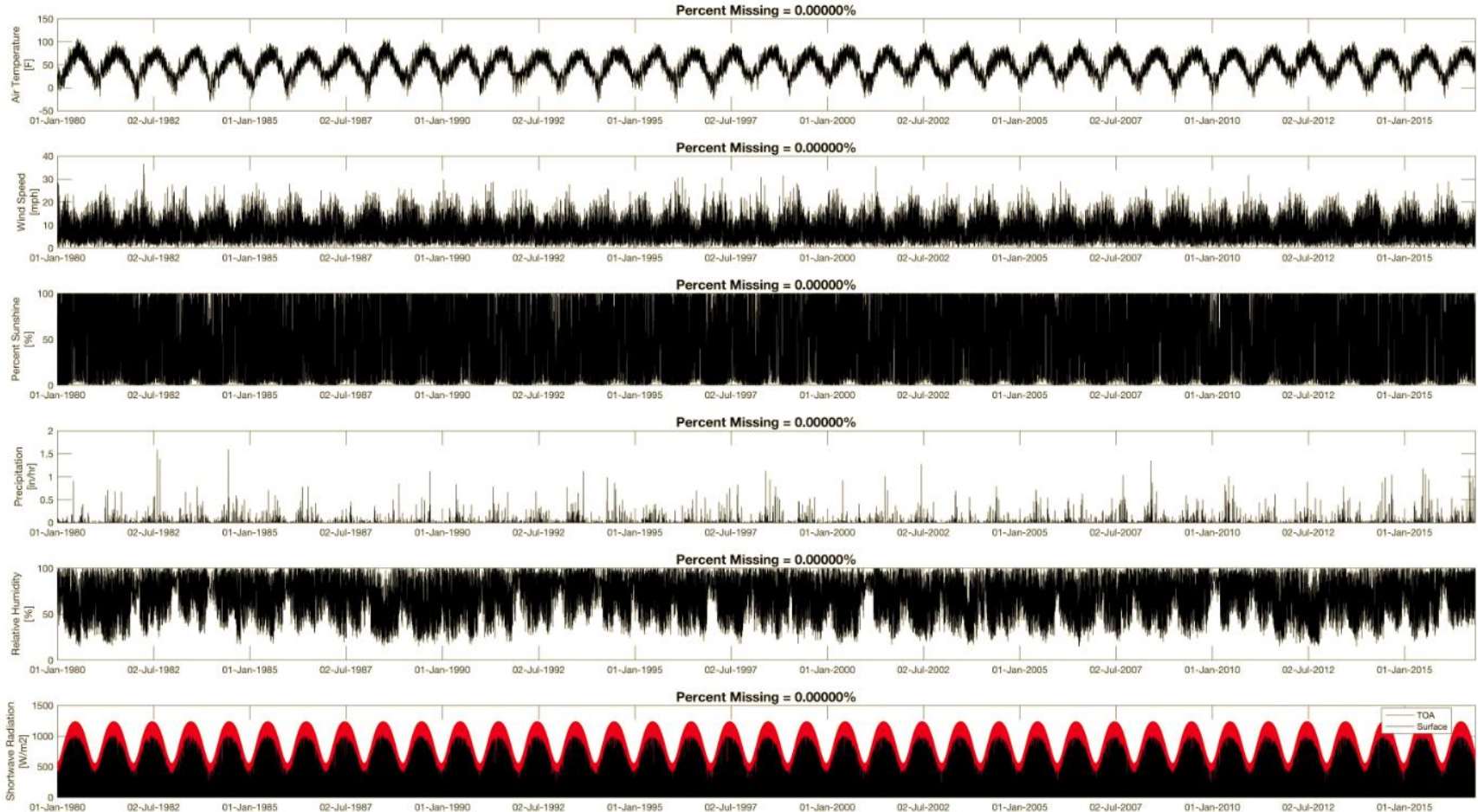


Figure B.14. Climate Location ID: 147593 (Spencer Municipal Airport)

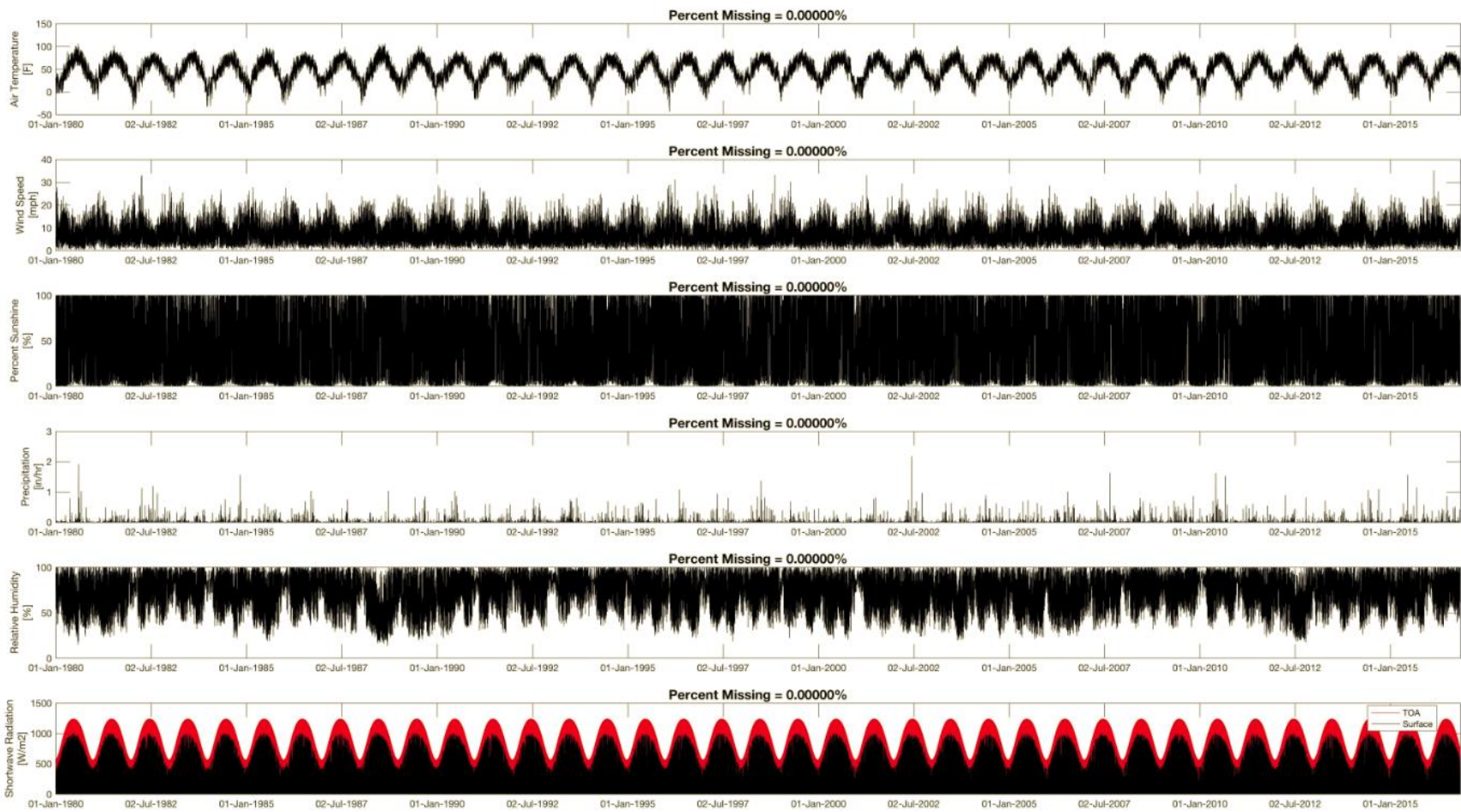


Figure B.15. Climate Location ID: 147021 (Waterloo Municipal Airport)

APPENDIX C: IOWA DOT RECOMMENDED PMED DESIGN INPUTS AND MATERIAL PROPERTIES

New AC Pavement Sections

- A. Performance criteria
 - a. Terminal IRI: 172 in./mi
 - b. AC Top-down fatigue cracking: 2,000 ft/mi
 - c. AC bottom-up fatigue cracking: 25%
 - d. AC thermal cracking: 1,000 ft/mi
 - e. Permanent deformation (Total): 0.75 in.
 - f. Permanent deformation (AC only): 0.25 in.

- B. General information
 - a. Design life: 20 years
 - b. Base/subgrade construction: varies for each pavement (based on PMIS information)
 - c. Pavement construction: varies for each pavement (based on PMIS information)
 - d. Traffic opening month: varies for each pavement (based on PMIS information)
 - e. Initial IRI: varies for each pavement (based on PMIS information) (Default: 63 in./mile)

Note: Default values can be used for b, c, and d above. The values entered will not have any effect on performance prediction outputs. However, for e (Initial IRI), values must match with PMIS data for Iowa specific designs and local calibration analyses.

- C. Traffic information
 - a. Initial two-way AADTT: varies for each pavement (based on PMIS information)
 - b. Number of lanes in design direction: from google map image
 - c. Percent of trucks in design direction: 50%
 - d. Percent of trucks in design lane: 95%
 - e. Operating speed: 60 mph
 - f. Design Lane width: 12 ft
 - g. Other information: Pavement ME recommended (default) values

- D. Climate information
 - a. Location: search for exact location of pavement section that needs to be designed
 - b. Depth of water table: 10 ft

- E. Pavement structure
 - a. Pavement layers: 3-layer (AC/Non-stabilized base/Subgrade)

- F. AC layer properties
 - a. Surface short wave absorptivity: 0.85
 - b. Other information: Pavement ME recommended (default) values

- G. AC layer properties
 - a. Layers thickness: varies for each pavement section
 - b. Unit weight:150
 - c. Thermal conductivity:1
 - d. Heat Capacity:0.23
 - e. Dynamic modulus: Input level 3
 - f. Asphalt binder property varies depending on location
 - i. Northeast: PG 58-28
 - ii. Northwest: PG 64-28
 - iii. Middle-east: PG 58-28
 - iv. Middle-west: PG 64-22
 - v. Southeast: PG 64-22
 - vi. Southwest: PG 64-22
 - g. Other information: Pavement ME recommended (default) values

- H. Non-stabilized base material properties
 - a. Layers thickness: varies for each pavement section
 - b. Type of granular base materials: A-1-a
 - c. Modulus: 35,000 psi
 - d. Other information: Pavement ME recommended (default) values

- I. Subgrade material properties
 - a. Layers thickness: Semi-infinite of subgrade
 - b. Type of subgrade material: A-6
 - c. Modulus: 10,000 psi
 - d. Other information: Pavement ME recommended (default) values

- J. Thermal cracking information: Pavement ME recommended (default) values

New JPCP Sections

- A. Performance criteria
 - a. Terminal IRI: 172 in./mi
 - b. Transverse cracking: 15 %
 - c. Mean joint faulting: 0.12 in.

- B. General information
 - a. Design life: 20 years
 - b. Pavement construction month: varies for each pavement (based on PMIS information)
 - c. Traffic opening month: varies for each pavement (based on PMIS information)
 - d. Initial IRI: varies for each pavement (based on PMIS information) (Default: 63 in./mi)

Note: Default values can be used for b and c above. The values entered will not have any effect on performance prediction outputs. However, for d (initial IRI), values must match with PMIS data for Iowa specific designs and local calibration analyses.

- C. Traffic information
 - a. Initial two-way AADTT: varies for each pavement (based on PMIS information)
 - b. Number of lanes in design direction: from google map image
 - c. Percent of trucks in design direction: 50%
 - d. Percent of trucks in design lane: 95%
 - e. Operating speed: 60 mph
 - f. Design lane width: 12 ft
 - g. Other information: Pavement ME recommended (default) values

- D. Climate information
 - a. Location: search for exact location of pavement section that needs to be designed
 - b. Depth of water table: 10 ft

- E. Pavement structure
 - a. Pavement layers: 3-layer (JPCP/Non-stabilized base/Subgrade)

- F. JPCP design properties
 - a. Surface short wave absorptivity: 0.85
 - b. Joint spacing: 20 ft
 - c. Sealant type: other (including no sealant, liquid, and silicon)
 - d. Doweled transverse joints: True
 - e. Dowel diameter: 1.25 in. to 1.5 in. (based on JPCP thickness)
 - f. Dowel bar spacing: 12 in.
 - g. Shoulder type: google map image
 - h. Edge support: non-widened slab for low and medium traffic/widened slab for high traffic
 - i. Other information: Pavement ME recommended (default) values

- G. PCC material properties
 - a. Layers thickness: varies for each pavement section
 - b. Unit weight: 142.7
 - c. CTE: 5.69 for limestone and 6.86 for quartzite
 - d. Thermal Conductivity: 0.77
 - e. Other information: Pavement ME recommended (default) values

- H. Non-stabilized base material properties
 - a. Layers thickness: varies for each pavement section
 - b. Type of granular base materials: A-1-a
 - c. Modulus: 35,000 psi
 - d. Other information: Pavement ME recommended (default) values

- I. Subgrade material properties
 - a. Layers thickness: Semi-infinite of subgrade
 - b. Type of subgrade material: A-6
 - c. Modulus: 10,000 psi
 - d. Other information: Pavement ME recommended (default) values

AC over JPCP Sections

- A. Performance criteria
 - a. Initial IRI (in./mi): 63
 - b. Terminal IRI (in./mi): 172
 - c. AC top-down fatigue cracking (ft/mi): 2,000
 - d. AC bottom-up fatigue cracking (% lane area): 25
 - e. AC thermal cracking (ft/mi): 1,000
 - f. Permanent deformation - AC only (in): 0.25
 - g. AC total transverse cracking: thermal + reflective (ft/mi): 2,500
 - h. JPCP transverse cracking (percent slabs): 15

- B. General information
 - a. Design life: 20 years
 - b. Base/subgrade construction: varies for each pavement (based on PMIS information)
 - c. Pavement construction: varies for each pavement (based on PMIS information)
 - d. Traffic opening month: varies for each pavement (based on PMIS information)
 - e. Initial IRI: varies for each pavement (based on PMIS information) (Default: 63 in./mi)

Note: Default values can be used for b, c, and d above. The values entered will not have any effect on performance prediction outputs. However, for e (Initial IRI), values must match with PMIS data for Iowa specific designs and local calibration analyses.

- C. Traffic information
 - a. Initial two-way AADTT: varies for each pavement (based on PMIS information)
 - b. Number of lanes in design direction: from google map image
 - c. Percent of trucks in design direction: 50%
 - d. Percent of trucks in design lane: 95%
 - e. Operating speed: 60 mph
 - f. Design Lane width: 12 ft
 - g. Other information: Pavement ME recommended (default) values

- D. JPCP design properties
 - a. Surface short wave absorptivity: 0.85
 - b. Joint spacing: 20 ft
 - c. Sealant type: other (including no sealant, liquid, and silicon)
 - d. Doweled transverse joints: True
 - e. Dowel diameter: 1.25 in. to 1.5 in. (based on JPCP thickness)
 - f. Dowel bar spacing: 12 in.

- g. Shoulder type: google map image
- h. Edge support: non-widened slab for low and medium traffic/widened slab for high traffic
- i. Other information: Pavement ME recommended (default) values

E. JPCP rehabilitation

- a. Slabs distressed/replaced before restoration (%): 0
- b. Slabs repaired/replaced after restoration (%): 0
- c. Transverse joint load transfer efficiency (%): 50

F. Climate information

- a. Location: search for exact location of pavement section that needs to be designed
- b. Depth of water table: 10 ft

G. Pavement structure

- a. Pavement layers: 4 layers (AC/JPCP/Non-stabilized base/Subgrade)

H. AC layer properties

- a. Layers thickness: varies for each pavement section
- b. Unit weight: 150
- c. Thermal conductivity: 1
- d. Heat Capacity: 0.23
- e. Dynamic modulus: Input level 3
- f. Asphalt binder property: varies depending on location
 - i. Northeast: PG 58-28
 - ii. Northwest: PG 64-28
 - iii. Middle-east: PG 58-28
 - iv. Middle-west: PG 64-22
 - v. Southeast: PG 64-22
 - vi. Southwest: PG 64-22
- g. The other information: Pavement ME recommended (default) values

I. PCC material properties

- a. Layers thickness: varies for each pavement section
- b. Unit weight: 142.7
- c. CTE: 5.69 for limestone and 6.86 for quartzite
- d. Thermal Conductivity: 0.77
- e. Other information: Pavement ME recommended (default) values

J. Non-stabilized base material properties

- a. Layers thickness: varies for each pavement section
- b. Type of granular base materials: A-1-a
- c. Modulus: 35,000 psi
- d. The other information: Pavement ME recommended (default) values

K. Subgrade material properties

- a. Layers thickness: Semi-infinite of subgrade
- b. Type of subgrade material: A-6
- c. Modulus: 10,000 psi
- d. The other information: Pavement ME recommended (default) values

APPENDIX D: SUMMARY OF PMED TRANSFER FUNCTIONS FOR PAVEMENT PERFORMANCE PREDICTIONS

New AC and AC over JPCP

Rutting Model: National Calibration Coefficients

Note: ○ Calibration Coefficients	
AC Rutting	
$\frac{\epsilon_p}{\epsilon_r} = k_z \beta_{r1} 10^{k_1 T} k_2 \beta_{r2} N^{k_3 B_{r3}}$ $k_z = (C_1 + C_2 * depth) * 0.328196^{depth}$ $C_1 = -0.1039 * H_{\alpha}^2 + 2.4868 * H_{\alpha} - 17.342$ $C_2 = 0.0172 * H_{\alpha}^2 - 1.7331 * H_{\alpha} + 27.428$ <p>Where: $H_{\alpha c} = total\ AC\ thickness(in)$</p>	$\epsilon_p = plastic\ strain(in/in)$ $\epsilon_r = resilient\ strain(in/in)$ $T = layer\ temperature(^{\circ}F)$ $N = number\ of\ load\ repetitions$
AC Rutting Standard Deviation	0.24 * Pow(RUT,0.8026) + 0.001
AC Layer 1	K1:-2.45 K2:3.01 K3:0.22 Br1:0.4 Br2:0.52 Br3:1.36
Unbound Layer Rutting	
$\delta_a(N) = \beta_s k_1 \epsilon_v h \left(\frac{\epsilon_0}{\epsilon_r} \right) \left e^{-\left(\frac{\rho}{N}\right)^{\beta}} \right $	$\delta_a = permanent\ deformation\ for\ the\ layer$ $N = number\ of\ repetitions$ $\epsilon_v = average\ vertical\ strain(in/in)$ $\epsilon_0, \beta, \rho = material\ properties$ $\epsilon_r = resilient\ strain(in/in)$
Base Rutting	Subgrade Rutting
k1: 0.965 Bs1: 1	k1: 0.675 Bs1: 1
Standard Deviation (BASERUT) 0.1477 * Pow(BASERUT,0.6711) + 0.001	Standard Deviation (BASERUT) 0.1235 * Pow(SUBBRUT,0.5012) + 0.001

Figure D.1. Calibration coefficients of rutting model

Rutting Model: HMA Layer

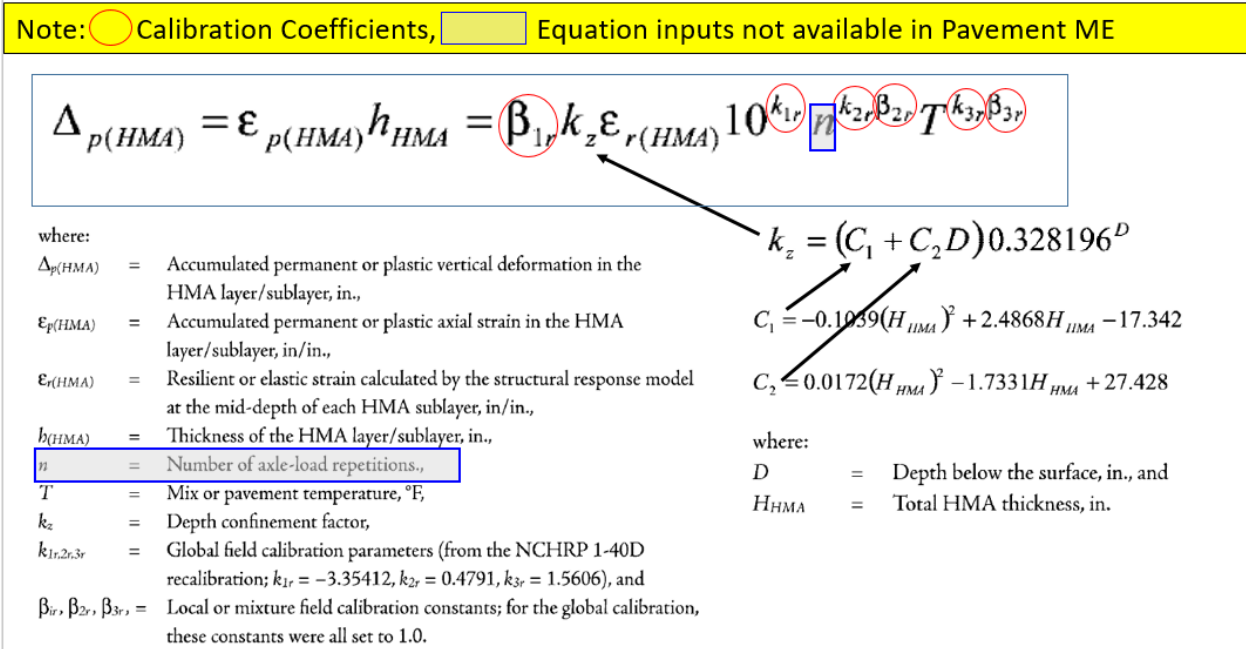


Figure D.2. Transfer function of rutting model: HMA layer

Rutting Model: Subgrade Layer

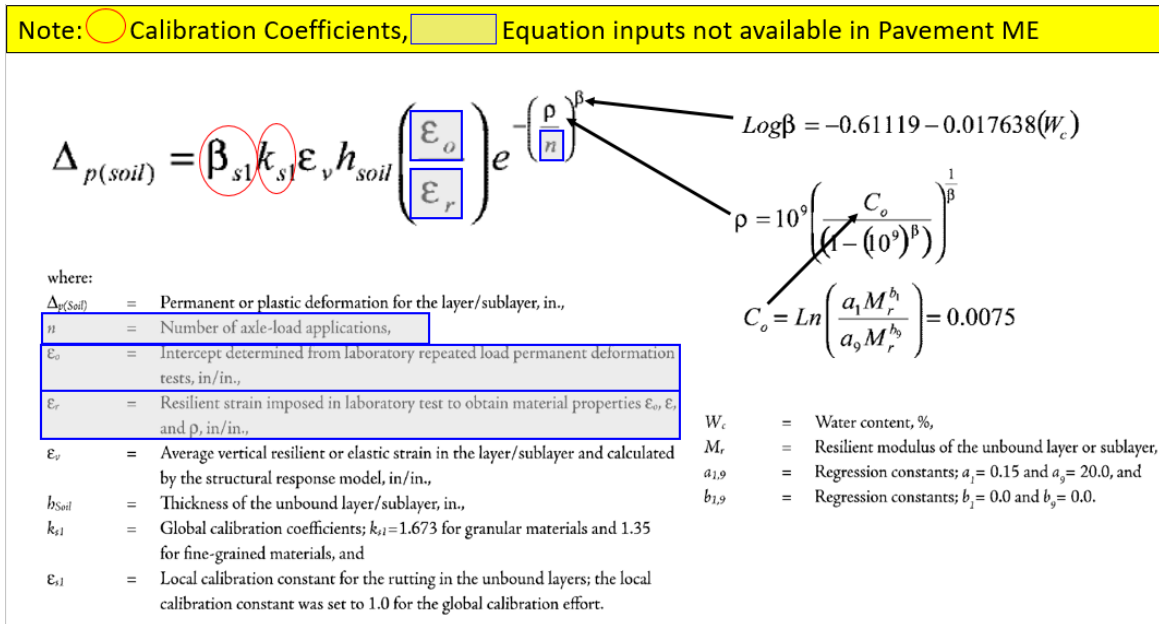


Figure D.3. Transfer function of rutting model: subgrade layer

Fatigue Cracking: National Calibration Coefficients

Note: ○ Calibration Coefficients

• Fatigue Damage

AC Fatigue	
$N_f = 0.00432 * C * \beta_{f3} k_1 \left(\frac{1}{\epsilon_1}\right)^{k_2 \beta_{f2}} \left(\frac{1}{E}\right)^{k_3 \beta_{f3}}$	k1: 3.75
$C = 10^M$	k2: 2.87
$M = 4.84 \left(\frac{V_b}{V_a + V_b} - 0.69\right)$	k3: 1.46
	Bf1: (5.014 * Pow(hac,-3.416)) * 1 + 0
	Bf2: 1.38
	Bf3: 0.88

• Top-down (Longitudinal)

• Bottom-up (Alligator)

AC Top Down Cracking			
$FC_{top} = \left(\frac{C_4}{1 + e^{(C_1 - C_2) \log_{10}(Damage)}}\right) * 10.56$			
c1: 7	c2: 3.5	c3: 0	c4: 1000
AC Cracking Top Standard Deviation			
$200 + 2300 / (1 + \exp(1.072 - 2.1654 * \text{LOG}_{10}(\text{TOP} + 0.0001)))$			

AC Bottom Up Cracking		
$FC = \left(\frac{6000}{1 + e^{(C'_1 + C'_2 C'_2 \log_{10}(D=100))}}\right) * \left(\frac{1}{60}\right)$		
$C'_2 = -2.40874 - 39.748 * (1 + h_{ac})^{-2.856}$		
$C'_1 = -2 * C'_2$		
c1: 1.31	c2: (0.867 + 0.2583 * hac) * 1 + 0	c3: 6000
Bottom up AC Cracking Standard Deviation		
$1.13 + 13 / (1 + \exp(7.57 - 15.5 * \text{LOG}_{10}(\text{BOTTOM} + 0.0001)))$		

Figure D.4. Calibration coefficients of fatigue cracking model

Fatigue Cracking Model: Top Down

Note: ○ Calibration Coefficients, □ Equation inputs not available in Pavement ME

• Fatigue Damage

AC Fatigue	
$N_f = 0.00432 * C * \beta_{f3} k_1 \left(\frac{1}{\epsilon_1}\right)^{k_2 \beta_{f2}} \left(\frac{1}{E}\right)^{k_3 \beta_{f3}}$	k1: 3.75
$C = 10^M$	k2: 2.87
$M = 4.84 \left(\frac{V_b}{V_a + V_b} - 0.69\right)$	k3: 1.46
	Bf1: (5.014 * Pow(hac,-3.416)) * 1 + 0
	Bf2: 1.38
	Bf3: 0.88

where:
 $N_{f(HMA)}$ = Allowable number of axle-load applications for a flexible pavement and HMA overlays.
 ϵ_c = Tensile strain at critical locations and calculated by the structural response model, in./in.
 E_{HMA} = Dynamic modulus of the HMA measured in compression, psi.
 k_1, k_2, k_3 = Global field calibration parameters (from the NCHRP 1-40D re-calibration; $k_1 = 0.007566$, $k_2 = -3.9492$, and $k_3 = -1.281$), and
 $\beta_{f1}, \beta_{f2}, \beta_{f3}$ = Local or mixture specific field calibration constants; for the global calibration effort, these constants were set to 1.0.

• Top-down

$$DI = \sum (\Delta DI)_{j,m,l,p,T} = \sum \left(\frac{n}{N_{f-HMA}} \right)_{j,m,l,p,T} \quad (5-5)$$

where:
 n = Actual number of axle-load applications within a specific time period,
 j = Axle-load interval,
 m = Axle-load type (single, tandem, tridem, quad, or special axle configuration),
 l = Truck type using the truck classification groups included in the MEPDG,
 p = Month, and
 T = Median temperature for the five temperature intervals or quintiles used to subdivide each month, °F.

AC Top Down Cracking			
$FC_{top} = \left(\frac{C_4}{1 + e^{(C_1 - C_2) \log_{10}(Damage)}}\right) * 10.56$			
c1: 7	c2: 3.5	c3: 0	c4: 1000
AC Cracking Top Standard Deviation			
$200 + 2300 / (1 + \exp(1.072 - 2.1654 * \text{LOG}_{10}(\text{TOP} + 0.0001)))$			

Figure D.5. Transfer function of fatigue cracking model: top-down cracking

Fatigue Cracking Model: Bottom-up

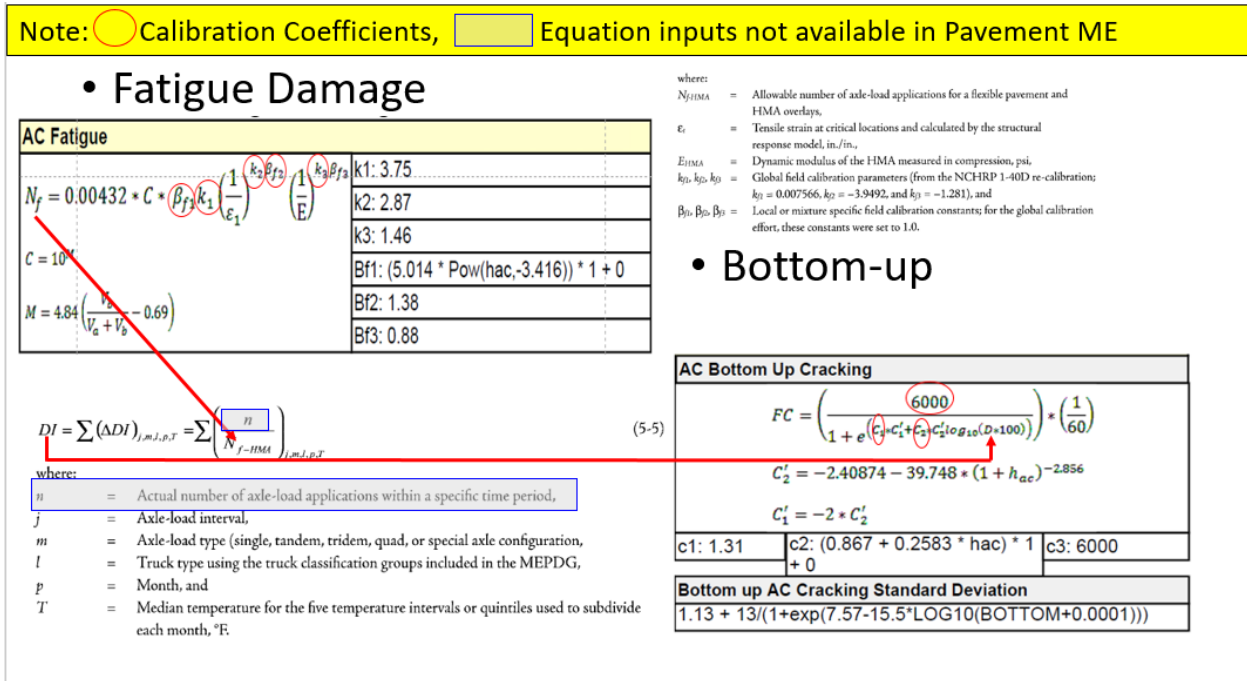


Figure D.6. Transfer function of fatigue cracking model: bottom-up cracking

Thermal Cracking: National Calibration Coefficients

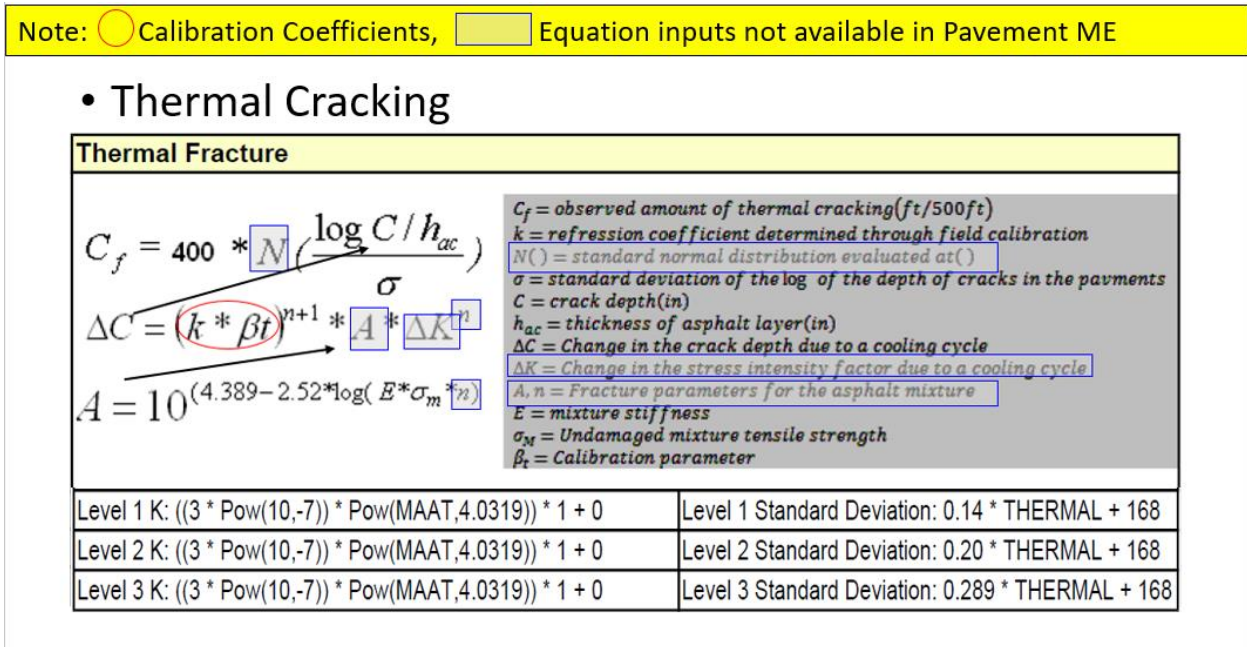


Figure D.7. Calibration coefficients and transfer function of thermal cracking model

International Roughness Index (IRI) Model

Note: ○ Calibration Coefficients

$$IRI = IRI_0 + 0.0150(SF) + 0.400(FC_{Total}) + 0.0080(TC) + 40.0(RD) \quad (5-15a)$$

where:

- IRI_0 = Initial IRI after construction, in./mi,
- SF = Site factor, refer to Eq. 5-15b,
- FC_{Total} = Area of fatigue cracking (combined alligator, longitudinal, and reflection cracking in the wheel path), percent of total lane area. All load related cracks are combined on an area basis—length of cracks is multiplied by 1 ft to convert length into an area basis,
- TC = Length of transverse cracking (including the reflection of transverse cracks in existing HMA pavements), ft/mi, and
- RD = Average rut depth, in.

$$SF = Age[0.02003(PI + 1) + 0.007947(Precip + 1) + 0.000636(FI + 1)]$$

where:

- Age = Pavement age, yr,
- PI = Percent plasticity index of the soil,
- FI = Average annual freezing index, °F days, and
- $Precip$ = Average annual precipitation or rainfall, in.

Figure D.8. Calibration coefficients and transfer function of flexible pavement IRI model

Reflective Cracking Model (AC over JPCP)

Note: ○ Calibration Coefficients

$$\Delta C = k_1 \Delta_{bending} + k_2 \Delta_{shearing} + k_3 \Delta_{thermal}$$

$$\Delta D = \frac{C_1 k_1 \Delta_{bending} + C_2 k_2 \Delta_{shearing} + C_3 k_3 \Delta_{thermal}}{h_{OL}}$$

$$\Delta_{bending} = A(SIF)_B^2$$

$$\Delta_{shearing} = A(SIF)_S^2$$

$$\Delta_{thermal} = A(SIF)_T^2$$

$$D = \sum_{i=1}^N \Delta D$$

$$RCR = \left(\frac{100}{C_4 + e^{(C_5 D)}} \right) * EX_CRK$$

Where

- ΔC = Crack length increment, in
- ΔD = Incremental damage ratio
- $k_1, k_2, k_3, C_1, C_2, C_3, C_4, C_5$ = Calibration factors (local and global)
- $\Delta_{bending}, \Delta_{shearing}, \Delta_{thermal}$ = Crack length increments caused by bending, shearing, and thermal loading
- A, n = HMA material fracture properties
- N = Total number of days
- $(SIF)_B, (SIF)_S, (SIF)_T$ = Stress intensity factors caused by bending, shearing, and thermal loading
- D = Damage ratio
- h_{OL} = Overlay thickness, in
- RCR = Cracks in the underlying layers reflected, %
- EX_CRK = Transverse cracking in underlying pavement layers, ft/mile (transverse cracking)
Alligator cracking in underlying pavement layers, % lane area (alligator cracking)

Figure D.9. Transfer function of reflective cracking model

JPCP

Faulting Model

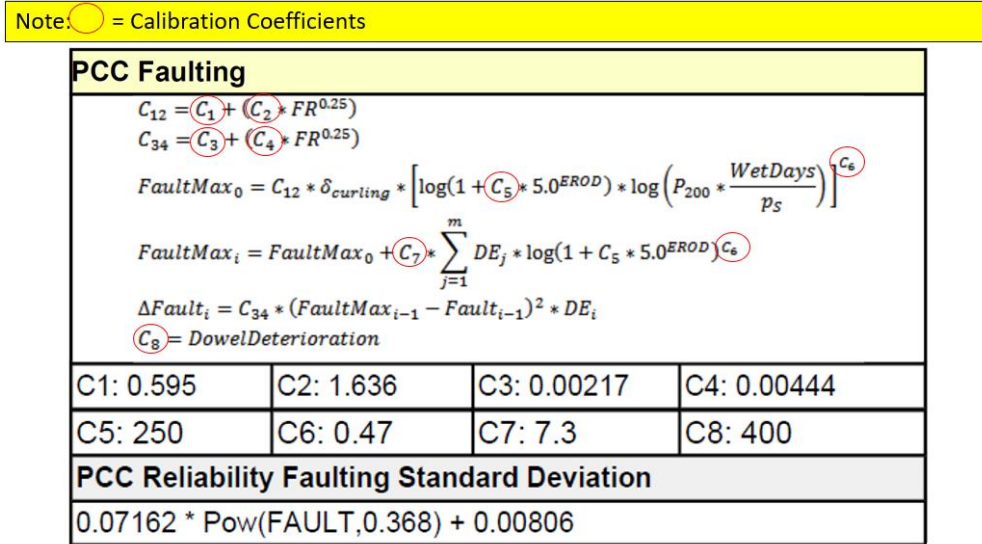


Figure D.10. Calibration coefficients and transfer function of JPCP faulting model

Transverse Cracking Modell

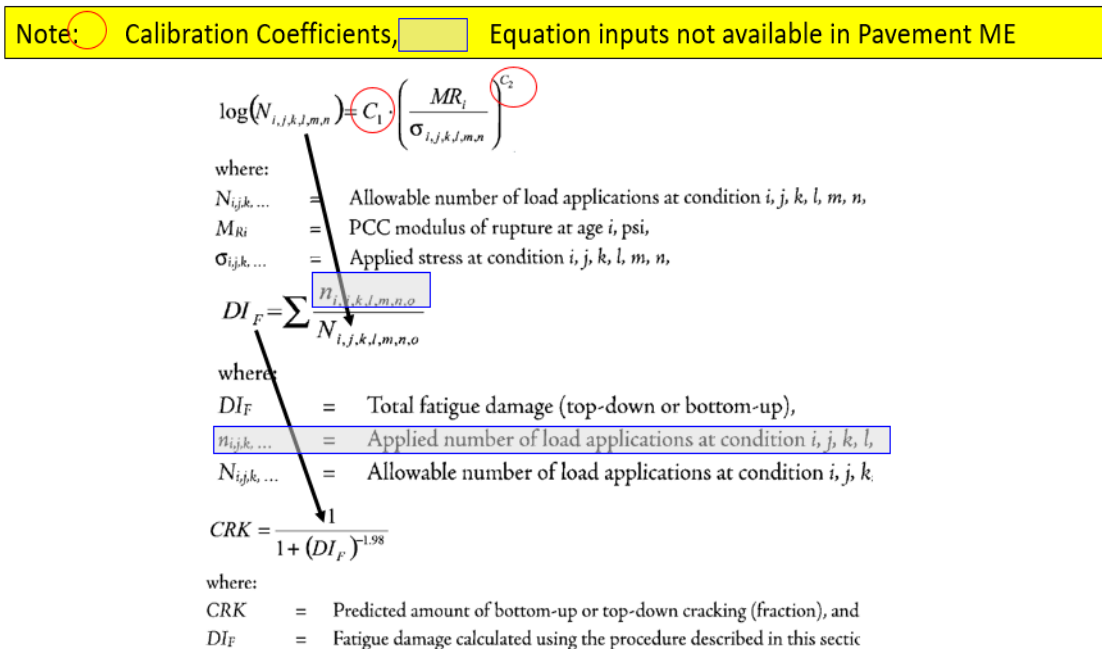


Figure D.11. Transfer function of JPCP transverse cracking model

IRI Model

Note: ○ Calibration Coefficients

$$IRI = IRI_I + C1*CRK + C2*SPALL + C3*TFAULT + C4*SF$$

where:

IRI = Predicted IRI, in./mi,

IRI_I = Initial smoothness measured as IRI, in./mi,

CRK = Percent slabs with transverse cracks (all severities),

$SPALL$ = Percentage of joints with spalling (medium and high severities),

$TFAULT$ = Total joint faulting cumulated per mi, in., and

$$SF = AGE (1 + 0.5556 * FI) (1 + P_{200}) * 10^{-6}$$

where:

AGE = Pavement age, yr,

FI = Freezing index, °F-days, and

P_{200} = Percent subgrade material passing No. 200 sieve.

Figure D.12. Transfer function of JPCP IRI model

APPENDIX E: VALIDATION OF LOCAL CALIBRATION RESULTS FOR INDEPENDENT PAVEMENT SECTIONS

The local calibration coefficients were tested on independent Iowa sections for all of the pavement types. This appendix shows the comparison of field recorded measured data, national calibration results, and local calibration results for all of the individual distresses at different reliabilities.

Flexible/AC Sections

Section 1 – US 52
Construction Year – 1996 (Age 22)
Thickness – 11 inches
AADTT – 317

Distresses	Pavement ME Criteria	PMIS (2018)	NCC (50% reliability)	NCC (92% reliability)	LCC (50% reliability)	LCC (92% reliability)
IRI (in./mi)	172	120.09	122.60	165.80	82.60	112.80
Longitudinal Cracking (ft/mi)	2,000	562	197.21	263.03	212.61	311.82
Alligator Cracking (%)	25	0	0	1.45	0	1.45
Thermal Cracking (ft/mi)	1,000	536.14	1,721.28	2,574.09	175.30	455.53
Total Rutting (in.)	0.75	0.17	0.15	0.20	0.16	0.21

Distresses	NCC (50% reliability)	NCC (92% reliability)	Average % error (NCC)	LCC (50% reliability)	LCC (92% reliability)	Average % error (LCC)
IRI (in./mi)	+2%	+38%	+20%	-31%	-6%	-19%
Longitudinal Cracking (ft/mi)	-65%	-53%	-59%	-62%	-45%	-53%
Alligator Cracking (%)	NA	NA	NA	NA	NA	NA
Thermal Cracking (ft/mi)	+221%	+380%	+301%	-67%	-15%	-41%
Total Rutting (in.)	-12%	+18%	+3%	-6%	+24%	+9%

Section 2 – US 61
Construction Year – 1999 (Age 19)
Thickness – 12.5 inches
AADTT – 1,548

Distresses	Pavement ME Criteria	PMIS (2018)	NCC (50% reliability)	NCC (92% reliability)	LCC (50% reliability)	LCC (92% reliability)
IRI (in./mi)	172	93.35	114.80	156	81.50	111.20
Longitudinal Cracking (ft/mi)	2,000	1,125	216.21	271.56	375.62	451.62
Alligator Cracking (%)	25	0	0	1.45	0	1.45
Thermal Cracking (ft/mi)	1,000	397	1,647.36	2,472.79	149.95	420.79
Total Rutting (in.)	0.75	0.17	0.17	0.23	0.18	0.24

Distresses	NCC (50% reliability)	NCC (92% reliability)	Average % error (NCC)	LCC (50% reliability)	LCC (92% reliability)	Average % error (LCC)
IRI (in./mi)	+23%	+67%	+45%	-13%	+19%	+3%
Longitudinal Cracking (ft/mi)	-81%	-76%	-78%	-67%	-60%	-63%
Alligator Cracking (%)	NA	NA	NA	NA	NA	NA
Thermal Cracking (ft/mi)	+315%	+523%	+419%	-62%	+6%	-28%
Total Rutting (in.)	+0%	+35%	+18%	+6%	+41%	+24%

Rigid/JPCP Sections

Section 1 – US 34
Construction Year – 2000 (Age 18)
Thickness – 11 inches
AADTT – 762

Distresses	Pavement ME Criteria	Measured Data (PMIS)	NCC (50% reliability)	NCC (92% reliability)	LCC (50% reliability)	LCC (92% reliability)
IRI (in./mi)	172	119.65	96.42	136.67	79.46	109.65
JPCP Transverse Slabs (%)	15	11.36	1.55	7.80	0.02	2.18
Mean Joint Faulting (in.)	0.12	0.02	0.03	0.07	0.00	0.02

Distresses	NCC (50% reliability)	NCC (92% reliability)	Average % error (NCC)	LCC (50% reliability)	LCC (92% reliability)	Average % error (LCC)
IRI (in./mi)	-19%	+14%	-3%	-33%	-8%	-21%
JPCP Transverse Slabs (%)	-86%	-31%	-59%	-99%	-80%	-90%
Mean Joint Faulting (in.)	+50%	+250%	+150%	-100%	0%	-50%

Section 2 – I-35
Construction Year – 1999 (Age 19)
Thickness – 12 inches
AADTT – 3,187

Distresses	Pavement ME Criteria	Measured Data (PMIS)	NCC (50% reliability)	NCC (92% reliability)	LCC (50% reliability)	LCC (92% reliability)
IRI (in./mi)	172	129.36	134.45	188.62	80.59	111.31
JPCP Transverse Slabs (%)	15	16.19	5.14	14.06	0.04	2.52
Mean Joint Faulting (in.)	0.12	0.02	0.12	0.17	0.01	0.03

Distresses	NCC (50% reliability)	NCC (92% reliability)	Average % error (NCC)	LCC (50% reliability)	LCC (92% reliability)	Average % error (LCC)
IRI (in./mi)	+4%	+46%	+25%	-37%	-13%	-25%
JPCP Transverse Slabs (%)	-68%	-13%	-41%	-99%	-84%	-92%
Mean Joint Faulting (in.)	+500%	+750%	+625%	-50%	+50%	0%

AC over JPCP Sections

Section 1 – IA 471
 Overlay Year – 1993 (Age 25)
 Thickness – 13 inches
 AADTT – 197

Distresses	Pavement ME Criteria	PMIS (2018)	NCC (50% reliability)	NCC (92% reliability)	LCC (50% reliability)	LCC (92% reliability)
IRI (in./mi)	172	160.87	95.20	130.10	107.30	147.20
Longitudinal Cracking (ft/mi)	2,000	832.36	189.62	411.63	322.61	620.32
Alligator Cracking (%)	25	0	0	1.45	0	1.45
Thermal Cracking (ft/mi)	1,000	1,400.42	1,649	2,112	1,893	2,367
Total Rutting -AC (in.)	0.75	0.10	0.03	0.05	0.01	0.03
Reflective Cracking (ft/mi)	2,500	3,168	1,703	2,198	2,063	2,561

Distresses	NCC (50% reliability)	NCC (92% reliability)	Average % error (NCC)	LCC (50% reliability)	LCC (92% reliability)	Average % error (LCC)
IRI (in./mi)	-41%	-19%	-30%	-33%	-8%	-21%
Longitudinal Cracking (ft/mi)	-77%	-51%	-64%	-61%	-25%	-43%
Alligator Cracking (%)	NA	NA	NA	NA	NA	NA
Thermal Cracking (ft/mi)	+18%	+51%	+34%	+35%	+69%	+52%
Total Rutting -AC (in.)	-70%	-50%	-60%	-90%	-70%	-80%
Reflective Cracking (ft/mi)	-46%	-31%	-38%	-35%	-19%	-27%

Section 2 – US 34
 Overlay Year – 2000 (Age 18)
 Thickness – 12.5 inches
 AADTT – 607

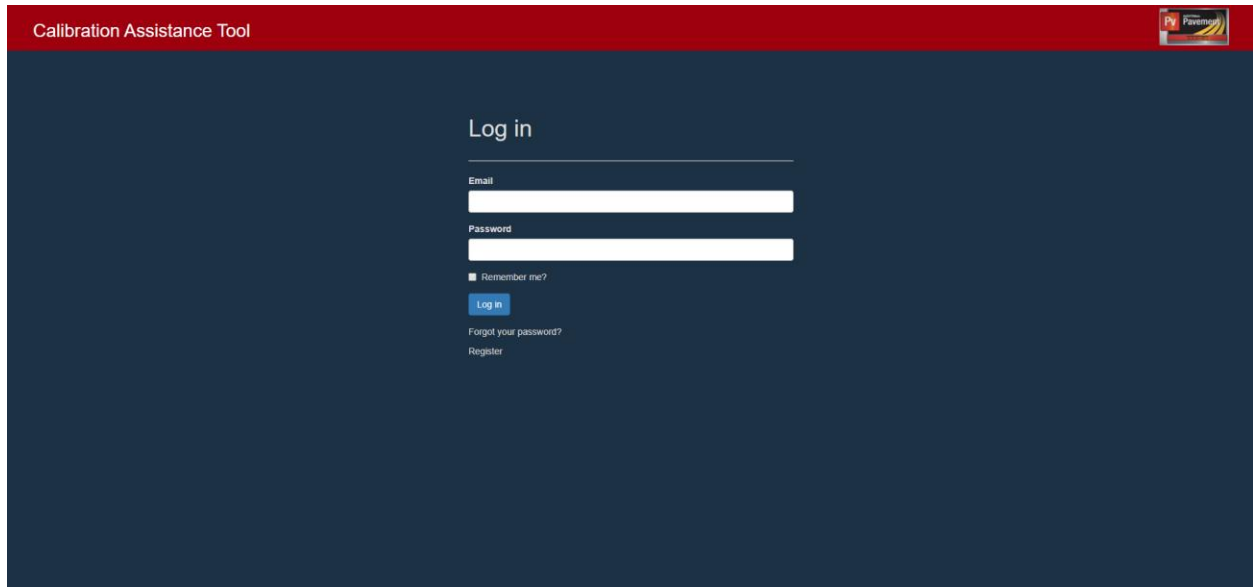
Distresses	Pavement ME Criteria	PMIS (2018)	NCC (50% reliability)	NCC (92% reliability)	LCC (50% reliability)	LCC (92% reliability)
IRI (in./mi)	172	148.65	84.10	115.10	94.70	130.50
Longitudinal Cracking (ft/mi)	2,000	829.62	511.46	742.68	731.45	945.62
Alligator Cracking (%)	25	0	0	1.45	0	1.45
Thermal Cracking (ft/mi)	1,000	1,687.95	1,765	2,242	1,862	2,465
Total Rutting -AC (in.)	0.75	0.11	0.04	0.06	0.02	0.03
Reflective Cracking (ft/mi)	2,500	2,461	1,848	2,564	2,105	2,763

Distresses	NCC (50% reliability)	NCC (92% reliability)	Average % error (NCC)	LCC (50% reliability)	LCC (92% reliability)	Average % error (LCC)
IRI (in./mi)	-43%	-23%	-33%	-36%	-12%	-24%
Longitudinal Cracking (ft/mi)	-38%	-10%	-24%	-12%	+14%	+1%
Alligator Cracking (%)	NA	NA	NA	NA	NA	NA
Thermal Cracking (ft/mi)	+5%	+33%	+19%	+10%	+46%	+28%
Total Rutting -AC (in.)	-64%	-45%	-55%	-82%	-73%	-77%
Reflective Cracking (ft/mi)	-25%	+4%	-10%	-14%	+12%	-1%

APPENDIX F: CALIBRATOR TOOL DEMO FOR LOCAL CALIBRATION

Steps Required

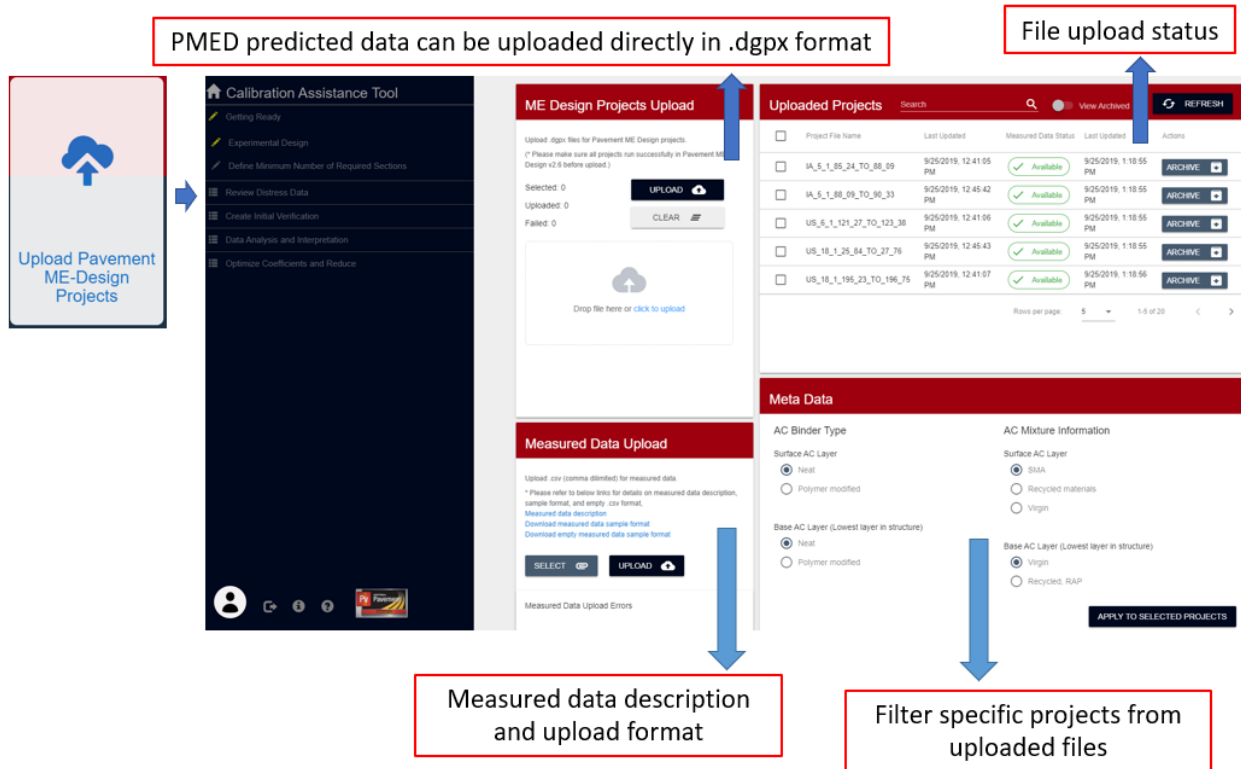
Step 1. Create user account in the web application (<https://pavementmedesign-calibrator.com/CalibratorTest/>).



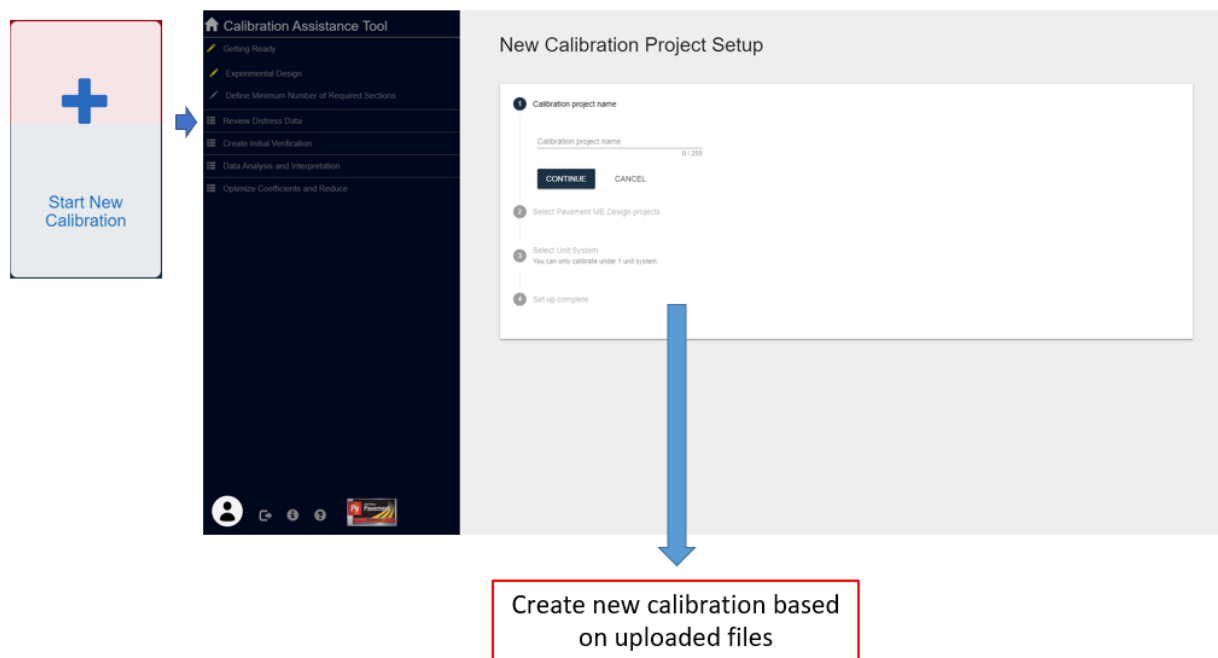
Step 2. Navigate to calibrator homepage.



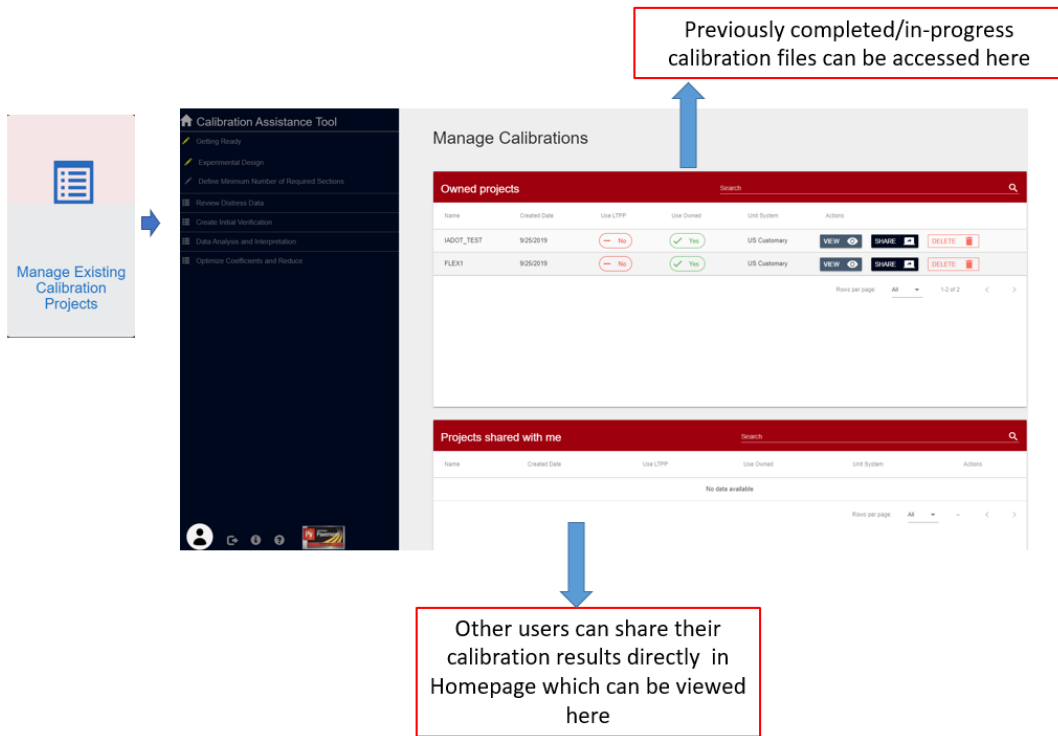
Step 3. Upload .dgp files used for Iowa local calibration study.



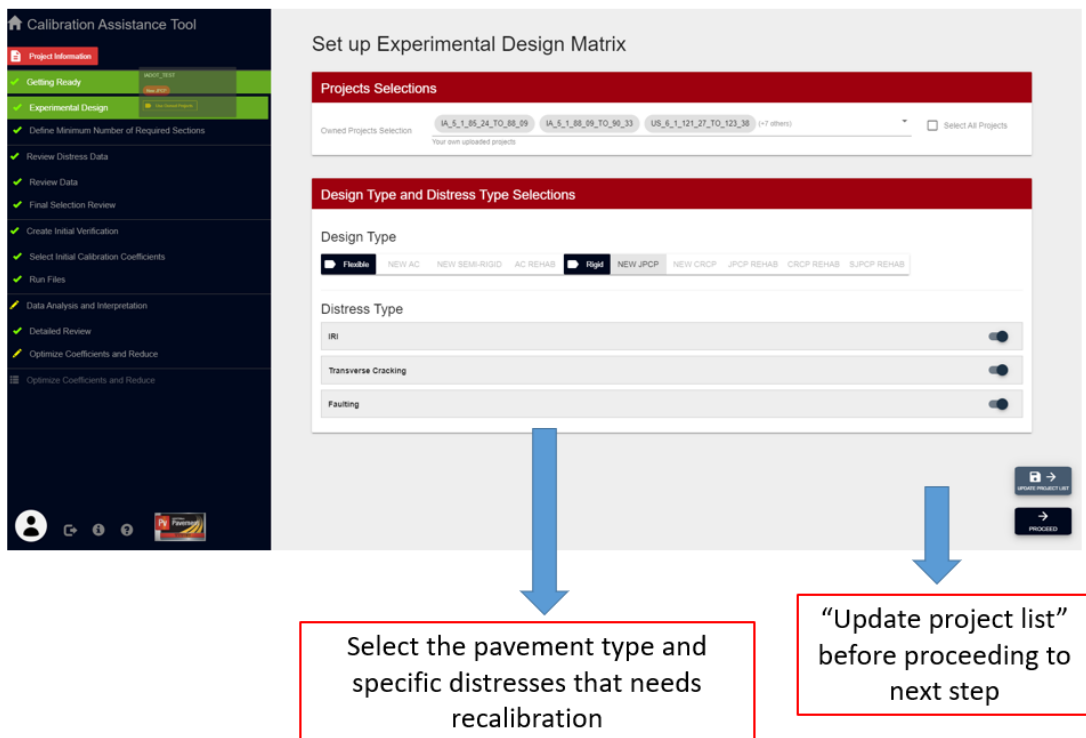
Step 4. Start New Calibration.



Step 5. Manage existing projects if files are previously saved.

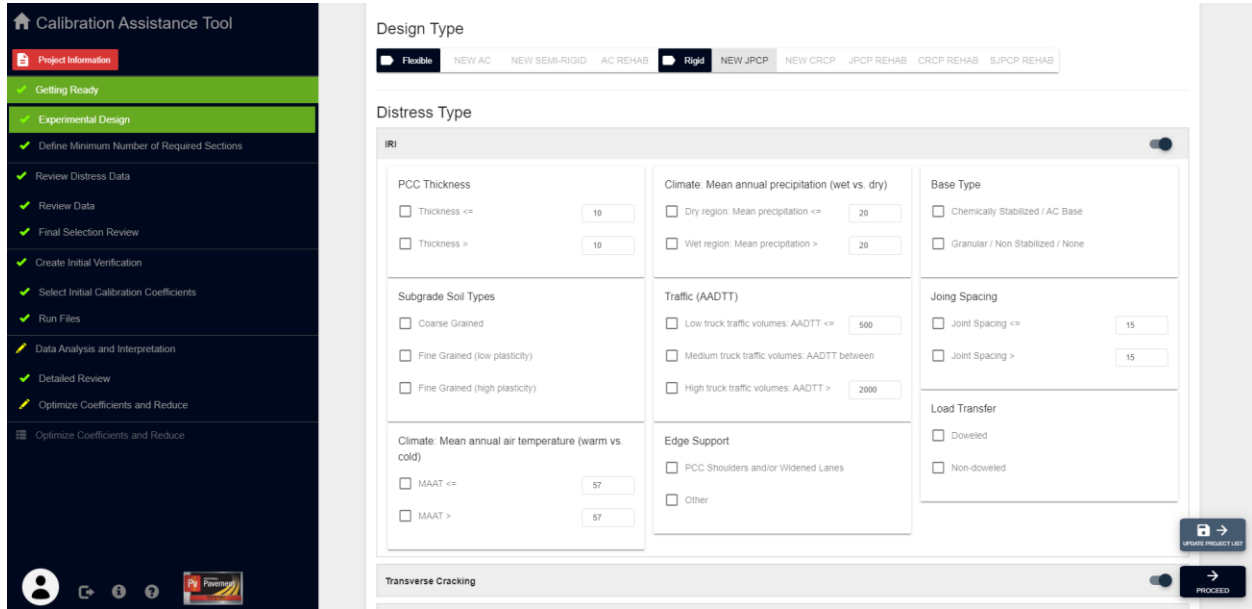


Step 6. Select pavement type and distresses to be locally calibrated.

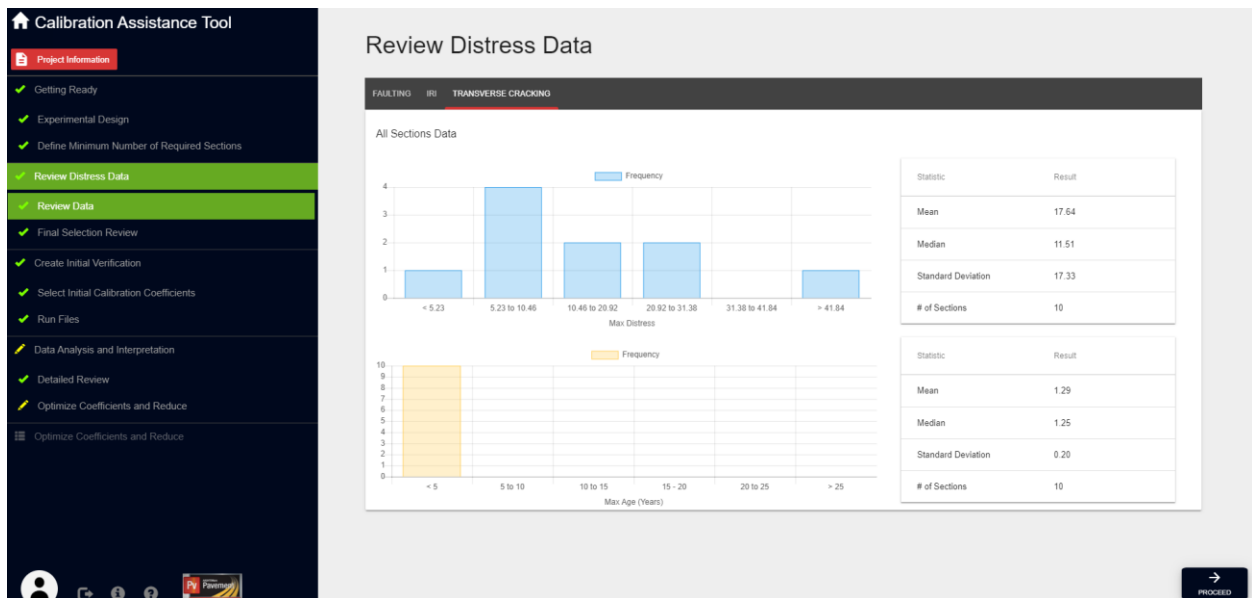


Step 6. Input criteria filter.

Note: Under each distress, the uploaded files can be filtered for recalibration based on general information and design properties. Example: we can specifically select the projects for which the layer thickness is less than 10 inches. We can also input our own thickness as shown above. If we need all sections for analysis, no changes are needed.



Step 7. Statistical summary of inputs from .dgp files.



Step 8. Summary of experimental matrix – traffic, climate and thickness categories of the projects being recalibrated.

The screenshot shows the 'Calibration Assistance Tool' interface. On the left is a sidebar with a checklist of steps. The main area displays an 'Experimental Matrix' table for 'FAULTING IRI TRANSVERSE CRACKING'. The table has columns for 'Thickness' and 'Traffic' (subdivided into '< 500', '500 to 2000', and '> 2000'). The rows are categorized by 'Subgrade Soil' and 'Climate' (Moist and Precipitation). A 'PROCEED' button is visible at the bottom right.

Step 9. Initial verification run. Select calibration coefficients for initial analyses. Only global calibration coefficients are available for now for testing. Additional options to import local calibration coefficients and manual inputs will be added later in future versions.

The screenshot shows the 'Calibration Assistance Tool' interface. On the left is a sidebar with a checklist of steps. The main area is titled 'Set up Initial Verification Run' and contains a 'Select Initial Calibration Coefficients' section. It has radio buttons for 'Global Model Coefficients' (selected), 'Local Calibration Coefficients', 'Import', and 'Manual'. To the right is a table of 'Calibration Coefficients' with columns for 'Coefficient Name' and 'Coefficient Factor'. A 'PROCEED' button is visible at the bottom right.

Coefficient Name	Coefficient Factor
k1	89
k2	103
k3	768
k4	120 + some ---- formula
k1	94
k1	133

Step 10. Run initial calibration files. After everything is set up, click on Run Files. Click on Refresh frequently to check the Run Status. These runs could take hours depending on the number of projects. It won't proceed to the next step unless all runs are completed.

Calibration Assistance Tool

Project Information IADOT_TEST

- ✓ Getting Ready
- ✓ Experimental Design
- ✓ Define Minimum Number of Required Sections
- ✓ Review Distress Data
- ✓ Review Data
- ✓ Final Selection Review
- ✓ Create Initial Verification
- ✓ Select Initial Calibration Coefficients
- ✓ Run Files
- ✓ Data Analysis and Interpretation
- ✓ Detailed Review
- ✓ Optimize Coefficients and Reduce

Optimize Coefficients and Reduce

Run Initial Calibration Files

Project Run Status
REFRESH
RUN FILES

Project File Name	Run Status	Started	Completed	Archived
US_30_2_259_82_TO_263_30	Queued	9/25/2019, 1:05:56 PM	9/25/2019, 1:08:51 PM	No
US_30_2_151_92_TO_156_80	Queued	9/25/2019, 1:02:44 PM	9/25/2019, 1:05:48 PM	No
I_29_1_76_54_TO_90_72	Queued	9/25/2019, 1:12:14 PM	9/25/2019, 1:15:02 PM	No
US_16_1_208_94_TO_211_75	Queued	9/25/2019, 1:02:44 PM	9/25/2019, 1:05:48 PM	No
US_16_1_195_23_TO_196_75	Queued	9/25/2019, 1:05:55 PM	9/25/2019, 1:08:57 PM	No
US_16_1_25_84_TO_27_76	Queued	9/25/2019, 1:09:04 PM	9/25/2019, 1:12:07 PM	No
US_6_1_121_27_TO_123_38	Queued	9/25/2019, 1:12:14 PM	9/25/2019, 1:15:10 PM	No
IA_5_1_88_09_TO_90_33	Queued	9/25/2019, 1:15:17 PM	9/25/2019, 1:18:18 PM	No
IA_5_1_85_24_TO_88_09	Queued	9/25/2019, 1:09:04 PM	9/25/2019, 1:12:08 PM	No
US_30_1_231_41_TO_239_21	Queued	9/25/2019, 1:15:17 PM	9/25/2019, 1:18:19 PM	No

Rows per page: All 1-10 of 10

Step 11. Statistical summary of national calibration results.

Calibration Assistance Tool

Project Information

- ✓ Getting Ready
- ✓ Experimental Design
- ✓ Define Minimum Number of Required Sections
- ✓ Review Distress Data
- ✓ Review Data
- ✓ Final Selection Review
- ✓ Create Initial Verification
- ✓ Select Initial Calibration Coefficients
- ✓ Run Files
- ✓ Data Analysis and Interpretation
- ✓ Detailed Review
- ✓ Optimize Coefficients and Reduce

Optimize Coefficients and Reduce

IRI FATIGUE CRACKING- BOTTOM UP TRANSVERSE CRACKING- THERMAL TOTAL RUTTING

Final Project Selection For Optimization and Validation

US_16_1_212_74_TO_214_39 US_16_2_212_74_TO_214_39 US_216_2_220_29_TO_225_03
 US_216_1_220_29_TO_222_09 US_216_1_225_23_TO_231_19 (+5 others)

Select All Projects

Selected projects will go to optimization and validation run. Validation will be randomly selected when there are more than 10 projects selected.

Binder Types
Neat 1 selected

Total AC Thickness
Thickness <= 5 3 selected

Climate: Mean annual air temperature (warm vs. cold)
MAAT <= 57 2 selected

Traffic (AADTT)
Low truck traffic volumes: AADTT <= 500 3 selected

Subgrade Types
Fine grained (low plasticity) 1 selected

Project ID
US_16_1_212_74_TO_214_39 10 selected

UPDATE FILTERS

Statistic	Result
Bias	-4.87
SEE	0.56
R Squared	0.25
Intercept	64.02
Slope	0.02
n	111
# of Sections	10

Hypothesis Test	p-value
Slope = 1	0.00000
Intercept = 0	0.00000
Pairwise df = 0	0.00089

Time Series

Step 12. Optimization of coefficients – brute force method.

Calibration Assistance Tool

Project Information

- Getting Ready
- Experimental Design
- Define Minimum Number of Required Sections
- Review Distress Data
- Review Data
- Final Selection Review
- Create Initial Verification
- Select Initial Calibration Coefficients
- Run Files
- Data Analysis and Interpretation
- Detailed Review
- Optimize Coefficients and Reduce**
- Optimize Coefficients and Reduce

Coefficients Adjustments

Significant Variables:

Factor name	Global Value	Global Factor	Last Optimized	Coefficients Selection	Min	Max	Increments
AC Rutting BR1	0.4		NA	<input checked="" type="radio"/> Global <input type="radio"/> Last Optimized <input type="radio"/> New Value	0.4	0.4	0
AC Rutting BR2	0.52		NA	<input checked="" type="radio"/> Global <input type="radio"/> Last Optimized <input type="radio"/> New Value	0.52	0.52	0
AC Rutting BR3	1.36		NA	<input checked="" type="radio"/> Global <input type="radio"/> Last Optimized <input type="radio"/> New Value	1.36	1.36	0
Granular Base Rutting BS1	1		NA	<input checked="" type="radio"/> Global <input type="radio"/> Last Optimized <input type="radio"/> New Value	1	1	0
Subgrade Rutting BS1	1		NA	<input checked="" type="radio"/> Global <input type="radio"/> Last Optimized <input type="radio"/> New Value	1	1	0

Rows per page: All 1-5 of 5

RUN OPTIMIZATION **PROCEED**

Step 13. Entering values for optimization. Global Calibration coefficients are available by default. Change the option from Global to New Value as shown above. After inputting all the min, max, and increment values for all of the factors, click on Run Optimization.

Calibration Assistance Tool

Project Information

- Getting Ready
- Experimental Design
- Define Minimum Number of Required Sections
- Review Distress Data
- Review Data
- Final Selection Review
- Create Initial Verification
- Select Initial Calibration Coefficients
- Run Files
- Data Analysis and Interpretation
- Detailed Review
- Optimize Coefficients and Reduce**
- Optimize Coefficients and Reduce

Coefficients Adjustments

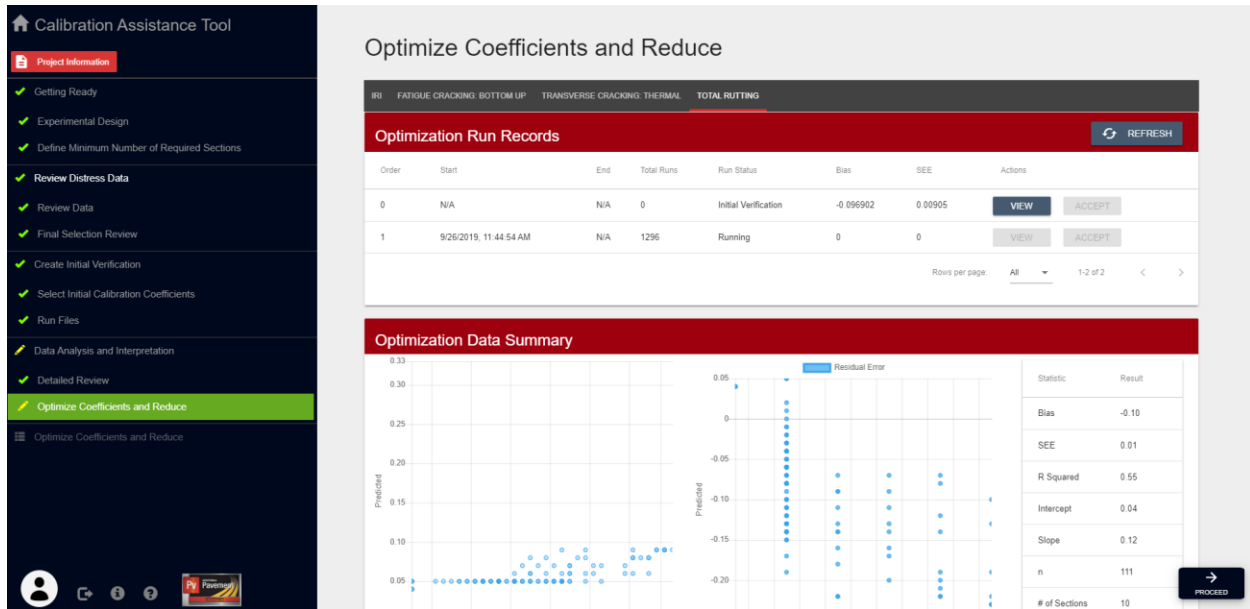
Significant Variables:

Factor name	Global Value	Global Factor	Last Optimized	Coefficients Selection	Min	Max	Increments
AC Rutting BR1	0.4		NA	<input type="radio"/> Global <input type="radio"/> Last Optimized <input checked="" type="radio"/> New Value	0.2	0.6	2
AC Rutting BR2	0.52		NA	<input type="radio"/> Global <input type="radio"/> Last Optimized <input checked="" type="radio"/> New Value	0.52	0.52	0
AC Rutting BR3	1.36		NA	<input type="radio"/> Global <input type="radio"/> Last Optimized <input checked="" type="radio"/> New Value	1.36	1.36	0
Granular Base Rutting BS1	1		NA	<input type="radio"/> Global <input type="radio"/> Last Optimized <input checked="" type="radio"/> New Value	1	1	0
Subgrade Rutting BS1	1		NA	<input type="radio"/> Global <input type="radio"/> Last Optimized <input checked="" type="radio"/> New Value	1	1	0

Rows per page: All 1-5 of 5

RUN OPTIMIZATION **PROCEED**

Step 14. Revised local calibration coefficients.



Advantages of Calibrator Tool

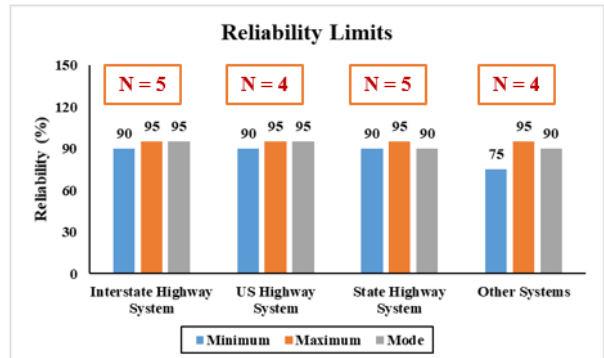
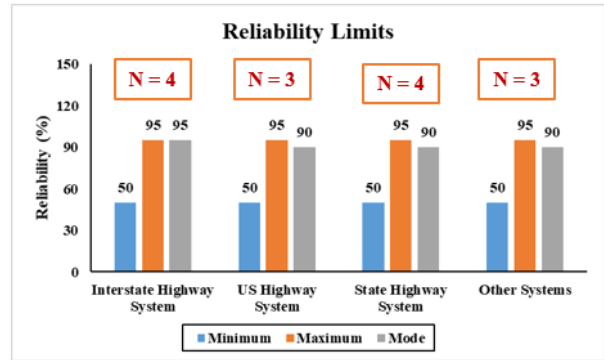
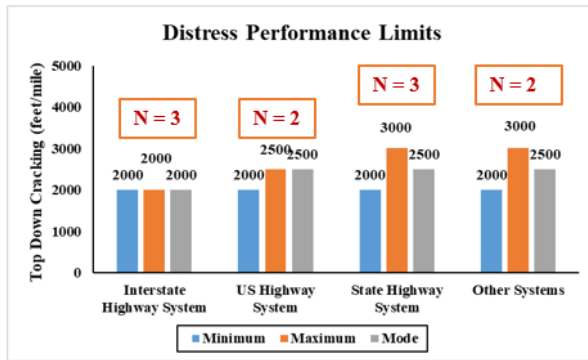
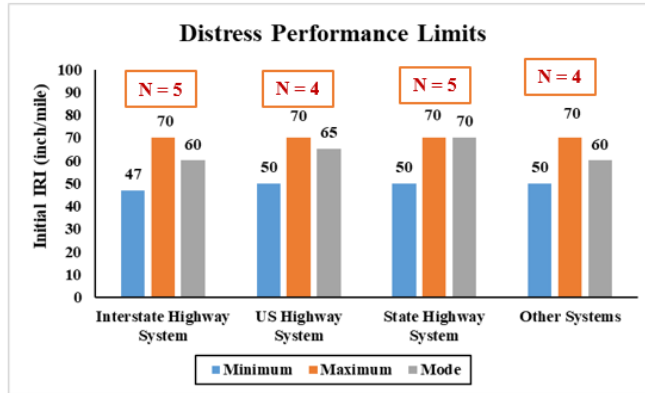
- User friendly
- Saves a lot of time by eliminating data extraction process from PMED files
- Measured versus predicted plots and statistical comparisons automatically generated by the tool
- Multiple projects and pavement types can be created and tested for recalibration at the same time

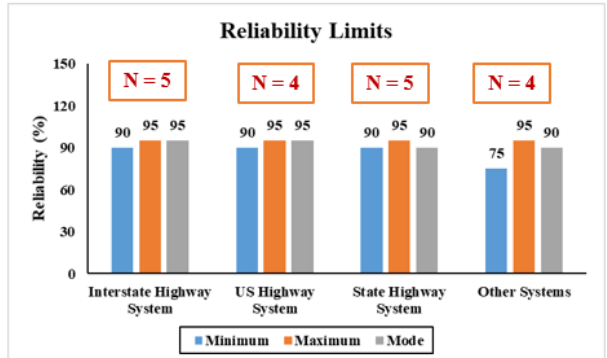
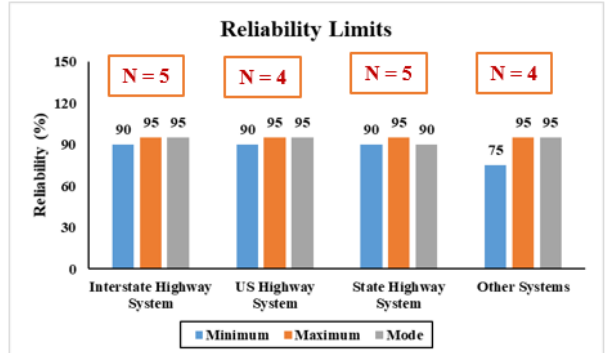
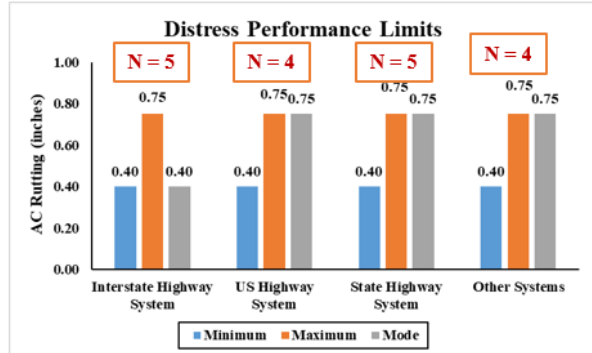
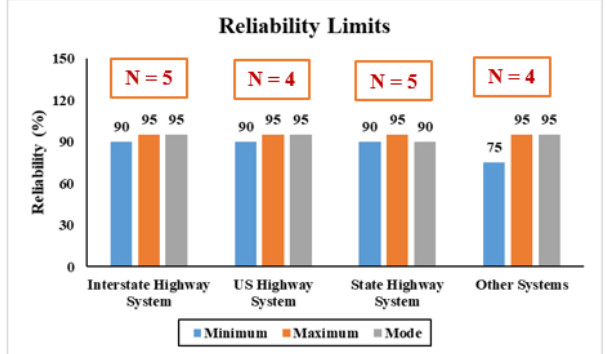
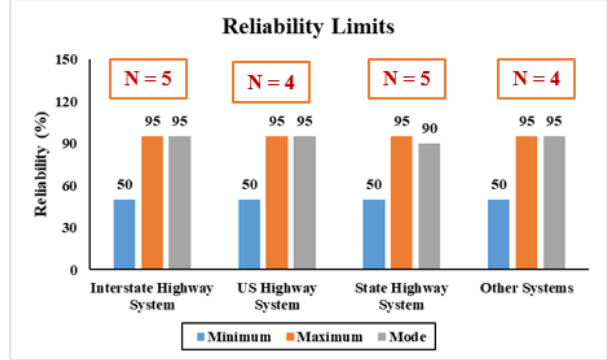
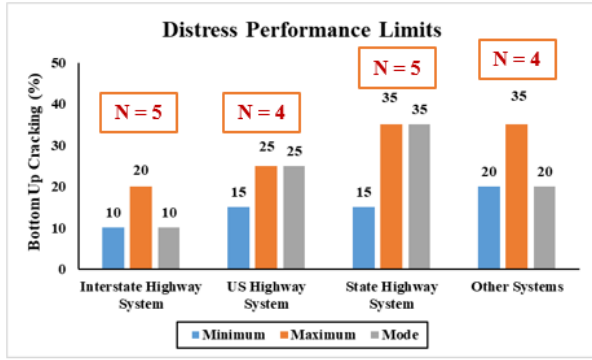
Limitations of Calibrator Tool

- Brute force method is being used for optimizing the coefficients
- Many advanced tools are used in this research study producing robust results compared to brute force method

APPENDIX G: AASHTOWARE PAVEMENT ME DESIGN NATIONAL SURVEY – ADDITIONAL QUESTIONS

Threshold Levels and Design Reliabilities for AC over JPCP





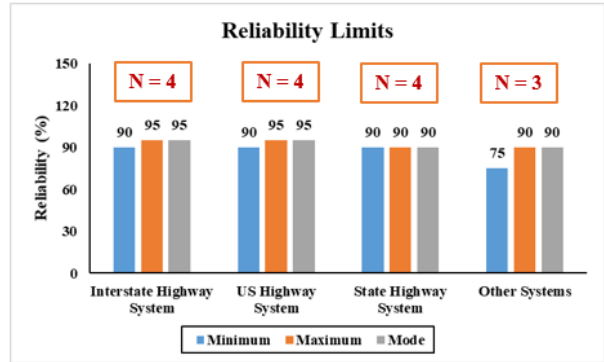


Figure G.1. Summary of survey results for AC over JPCP distresses – design criteria and reliability level

Data Availability for Pavement Designs

Q. Are the following mentioned Pavement ME design data readily available at your agency for any type of pavement?

Are the following mentioned Pavement ME design data readily available at your agency for any type of pavement?			
Input Parameter	Available	Not Available	Requires efforts to obtain
Design Parameters (Thickness of each layer, joint spacing, slab width, dowel size, spacing, etc.)	16	3	6
Pavement Layer Properties	11	4	9
Traffic	15	4	6
Climate	15	6	4

Survey Question	Yes, we collect “reflective cracking distress data only independently from thermal cracking”	No, we collect “reflective and thermal cracking (total transverse cracking)” together	Additional Comments
<p>Does your agency collect “reflective cracking distress data only” independently from thermal cracking? Pavement ME Design software predicts “Total transverse cracking = total reflective cracking + total thermal cracking.” The responses collected from this survey question will help us identify different methods used by the agencies to differentiate different types of cracks.</p>	4	20	<p>1. Most agencies in the SE region do not have significant thermal cracking. – Southeast Cement Promotion Association</p> <p>2. We collect all distress data together using Laser Crack Measuring System (LCMS). We do not get a distinction between the reflective cracking or any new cracking. – Alberta Transportation</p> <p>3. Prior to 2017, we performed manual surveys and only collected a composite cracking value. Starting in 2017, we collect automated data and the cracking is separated by type (e.g., longitudinal, transverse, and alligator). As far as we know, there is no way to determine if a crack is reflective without taking a core directly over the crack. – Arizona DOT</p> <p>4. Our current pavement management system data collection process collects total transverse cracking; however, our study to collect data for local calibration using 64 pavement test sections does include effort to correlate type of crack to causal mechanism. – Mississippi DOT</p>

Survey Question	Yes	No	Additional Comments
Does your agency have any specific methods to differentiate each type of crack collected for recording in Pavement Management Information System (PMIS)?	7	10	<p>1. We are currently transitioning toward the use of LCMS and will have more differentiation between crack type in the future. – South Carolina DOT</p> <p>2. LCMS data collection system collects the following types of data for us: IRI, rutting, wheel path fatigue cracking, longitudinal cracking, transverse (thermal) cracking, miscellaneous cracking, potholes, pick outs, raveling, shoulder cracking, etc. – Alberta Transportation</p> <p>3. Pavement condition data are collected by ARAN/FUGRO that uses their software/algorithm to come up with longitudinal, transverse, and fatigue cracking numbers. – Alaska DOT</p> <p>4. There are three crack types collected during routine network data collection: transverse cracking, load associated cracking (cracking in the wheel path), and non-load associated cracking (everything else). – Alabama DOT</p> <p>5. We have PMS data collection manual (practice) to identify different cracks. – Louisiana DOT</p> <p>6. Our PMS system contains different types of cracks (block, transverse, longitudinal, etc.), but the classifications do not match with Pavement-ME. – Minnesota DOT</p> <p>7. I'm not sure how to answer this question, and we have methods to differentiate cracks, but we don't necessarily collect this data to match the needs of Pavement ME. – Michigan DOT</p> <p>8. Our PMIS relies on observation of where the crack or set of cracks appear at the surface of the pavement. – Mississippi DOT</p> <p>9. FHWA HPMS Guidelines. – Maine DOT</p>

What are the sources of climate data used by your agency for use in AASHTOWare Pavement ME Design Software?	
Climate Data Source	Total Responses
Long Term Pavement Performance (LTPP)	5
Ground Based Weather Station (GBWS)	6
Environmental Sensing Station (ESS)	0
Automated Surface Observing System (ASOS)	1
Automated Weather Station (AWS)	2
Operating Weather Station (OWS)	1
Cooperative Observer Program (COOP)	0
North American Regional Reanalysis (NARR)	10
Modern-Era Retrospective Analysis for Research and Application (MERRA)	16
Others: Road weather information system (RWIS), Western regional climate center	

Survey Question	Yes	No	May be in future	The current availability of climate data is enough for good pavement designs
Has your agency put any efforts into improving/expanding the climate data requirements for pavement designs?	5	14	4	10
Additional Comments:				
1. Years ago, this was done through a university; however, with recent updates to temperature data in Pavement ME, it is unclear if our “corrected” data is better than these new defaults. – North Carolina DOT				
2. Completed research project “Building Accurate Historic and Future Climate MEPDG Input Files for Louisiana DOTD” – Louisiana DOT				
3. MDOT research project conducted to expand stations, add more years, and QA/QC the data. – Michigan DOT				
4. Re-calibrated state weather data in 2018. – Colorado DOT				
5. The following link is to a report for a study the Mississippi DOT funded to obtain better climate data; however, the current plan is to use MERRA rather than the data developed in this study. https://mdot.ms.gov/documents/Research/Reports/Interim%20&%20Final/State%20Study%202023%20Developing%20MEPDG%20Climate%20Data%20Input%20Files%20for%20Mississippi.pdf – Mississippi DOT				

Does your agency keep the soft/electronic copies of the data/records?			
Input Parameter	Available	Not Available	Requires efforts to obtain
Pavement Structures (Type, Design Life and Thickness)	14	3	9
Design and Layer Properties	13	2	11
Traffic	15	3	7
Climate	14	8	3

Local Calibration Approach/Optimization Techniques

Survey Question	Year in which local calibration was last performed	Software version used for local calibration
In which year was local calibration previously performed by your agency and which version of the AASHTOWare Pavement ME Design software was used?	2011 – 1 2015 – 2 2017 – 1 2018 – 2 2019 – 2 2020 – 3	DARWin ME 1.0 – 1 PMED 2.0 – 1 PMED 2.2 – 1 PMED 2.3 – 1 PMED 2.3.1 – 1 PMED 2.5 – 1 PMED 2.5.5 – 2

Survey Question	Yes	No, we use default coefficients in the software	Additional Comments
Does your agency perform local calibration efforts to determine calibration coefficients for AASHTOWare pavement ME designs?	15	4	<p>We are in the process of local calibration now. Hence, the answer is default for threshold values. We have the intention of specifying our own values. In addition, we are in the process of developing a catalog design approach using bottom-up cracking at 0% with the global calibration as a first step. I can explain more if necessary. – South Carolina DOT</p> <p>Being a promotion/technical support group, we aim to use whatever the local agency is doing. However, most agencies in the Southeast are using default calibration at this time. – Southeast Cement Promotion Association</p> <p>We have not done a complete local calibration yet due to limited resources. In most cases, we use default values. We use our own threshold values for different distresses that we have developed in the past. We are working on traffic information at the moment and will be developing some guidelines for the material properties as well. – Alberta Transportation</p> <p>Ongoing efforts to re-calibration. – Louisiana DOT</p> <p>We are in the process of performing our first calibration effort. ARA is helping us with this effort. – Nebraska DOT</p> <p>Two times: once for v2.0 and once for v2.3. – Michigan DOT</p> <p>We first calibrated in 2011 and plan to calibrate again this year. – Arizona DOT</p> <p>Currently in the process. – Maryland DOT</p> <p>We are in the process of collecting data for our first local calibration. – Mississippi DOT</p> <p>Calibration underway. – Maine DOT</p>

Survey Question	Yes	No
Did your agency perform any specific optimization methods to determine calibration coefficients while performing local calibration?	6	11
Optimization Methods: Linear and non-linear optimization, calibrator tool, bootstrapping, MS excel solver, brute force, lingo, sensitivity analysis		

Additional Design Related Questions

Survey Question	Responses
What is the recommended Joint Spacing (ft) for JPCP in your state?	Minimum – 12 ft Maximum – 20 ft Mean – 16 ft (23 ft) Mode – 15 ft (23 responses)

Survey Question	Yes	No	Maximum Width (Responses)
Does your agency use Widened Slab for JPCP?	18	5	Minimum – 13 ft Maximum – 16 ft Mean – 14 ft (17 responses) Mode – 14 ft (17 responses)

Survey Question	Yes	No	Maximum Width (Responses)
Does your agency use Tied PCC Shoulders?	19	4	Minimum – 10 ft Maximum – 12 ft Mean – 11 ft (11 responses) Mode – 10 ft (11 responses)

APPENDIX H: PMED INPUTS FOR RELIABILITY AND THICKNESS DETERMINATION TASK

New AC Pavement Sections

- A. Performance criteria
 - a. Terminal IRI: Interstate (160 in./mi); US, State, and Others (200 in./mi)
 - b. AC Top-down fatigue cracking: 2,000ft/mi (PMED Default for all highway systems)
 - c. AC bottom-up fatigue cracking: Interstate (10%); US (20%); State and Others (35%)
 - d. AC thermal cracking: Interstate (500 ft/mi); US, State, and Others (700 ft/mi)
 - e. Permanent deformation (Total): Interstate (0.40 in.); US (0.50 in.); State and Others (0.65 in.)
 - f. Permanent deformation (AC only): 0.25 in. (PMED Default)

- B. General information
 - a. Design life: 20 years
 - b. Base/subgrade construction: PMED Default
 - c. Pavement construction: 1998
 - d. Traffic opening month: 1999
 - e. Initial IRI: 72 in./mi

- C. Traffic information
 - a. Initial two-way AADTT: Interstate (24,041), US (4,884), State (844), and Others (200)
 - b. Number of lanes in design direction: 2
 - c. Percent of trucks in design direction: 50%
 - d. Percent of trucks in design lane: 95%
 - e. Operating speed: 70 mph for Interstate; 60 mph for US, State, and Others
 - f. Design Lane width: 12 ft
 - g. The other information: Pavement ME recommended (default) values

- D. Climate information
 - a. Location: Mason City
 - b. Depth of water table: 10 ft

- E. Pavement structure
 - a. Pavement layers: 3-layer (AC/Non-stabilized base/Subgrade)

- F. AC layer properties
 - a. Surface short wave absorptivity: 0.85
 - b. The other information: Pavement ME recommended (default) values

- G. AC layer properties
 - a. Layers thickness: Varied 4 in. to 12 in.
 - b. Unit weight: 150

- c. Thermal conductivity:1
- d. Heat Capacity:0.23
- e. Dynamic modulus: Input level 3
- f. Asphalt binder property: PG 64-28
- g. The other information: Pavement ME recommended (default) values

H. Non-stabilized base material properties

- a. Layers thickness: 10 in.
- b. Type of granular base materials: A-1-a
- c. Modulus: 35,000 psi
- d. The other information: Pavement ME recommended (default) values

I. Subgrade material properties

- a. Layers thickness: Semi-infinite of subgrade
- b. Type of subgrade material: A-6
- c. Modulus: 10,000 psi
- d. The other information: Pavement ME recommended (default) values

New JPCP Sections

A. Performance criteria

- a. Terminal IRI: Interstate (160 in./mi); US, State and Others (200 in./mi)
- b. Transverse cracking: Interstate (10%); US (15%); State and Others (20%)
- c. Mean joint faulting: Interstate (0.15 in.); US (0.20 in.); State and Others (0.25 in.)

B. General information

- a. Design life: 20 years
- b. Pavement construction month: 1998
- c. Traffic opening month: 1999
- d. Initial IRI: 63 in./mi

C. Traffic information

- a. Initial two-way AADTT: Interstate (29,298), US (6,604), State (1,840) and Others (412)
- b. Number of lanes in design direction: 2
- c. Percent of trucks in design direction: 50%
- d. Percent of trucks in design lane: 95%
- e. Operating speed: 70 mph for Interstate; 60 mph for US, State and Others.
- f. Design lane width: 12 ft
- g. The other information: Pavement ME recommended (default) values

D. Climate information

- a. Location: Mason City
- b. Depth of water table: 10 ft

- E. Pavement structure
 - a. Pavement layers: 3-layer (JPCP/Non-stabilized base/Subgrade)

- F. JPCP design properties
 - a. Surface short wave absorptivity: 0.85
 - b. Joint spacing: 20 ft
 - c. Sealant type: other (including no sealant, liquid, and silicon)
 - d. Doweled transverse joints: True
 - e. Dowel diameter: 1.25 in. to 1.5 in. (based on JPCP thickness)
 - f. Dowel bar spacing: 12 in.
 - g. Shoulder type: google map image
 - h. Edge support: non widened slab for low and medium traffic/widened slab for high traffic
 - i. The other information: Pavement ME recommended (default) values

- G. PCC material properties
 - a. Layers thickness: Varied 4 in. to 12 in.
 - b. Unit weight: 142.7
 - c. CTE: 5.69
 - d. Thermal Conductivity: 0.77
 - e. Other information: Pavement ME recommended (default) values

- H. Non-stabilized base material properties
 - a. Layers thickness: varies for each pavement section
 - b. Type of granular base materials: A-1-a
 - c. Modulus: 35,000 psi
 - d. The other information: Pavement ME recommended (default) values

- I. Subgrade material properties
 - a. Layers thickness: Semi-infinite of subgrade
 - b. Type of subgrade material: A-6
 - c. Modulus: 10,000 psi
 - d. The other information: Pavement ME recommended (default) values

AADTT Considerations

Road Classification	Level of Traffic – Manual of Practice	AC – Two Way AADTT Considered	JPCP – Two Way AADTT Considered
Interstate	More than 5,000	24,041	29,298
US	2,000 to 5,000	4,884	6,604
State	500 to 2,000	844	1,840
Others	Less than 500	200	412

APPENDIX I. LIST OF PROJECT DATA FILES WITH DESCRIPTIONS

Folder Name	File Types	Description
AASHTOWare Pavement ME National Survey Results	PDF	Individual responses received from state highway agencies
Webinars	PPT	Presentations on summary from Pavement ME Design Webinar
Iowa DOT PMED Inputs	Word	Design inputs and material properties recommended by Iowa DOT for local calibration
PMIS Database and Calibration	PPT, Word, Excel, MATLAB, Python, R Studio	Latest updated PMIS database for sections selected for local calibration and individual section summary, Complete spreadsheets showing local calibration process, Python-MATLAB-R Studio codes used to optimize the local calibration coefficients
Reflective Cracking Sensitivity Analysis	Excel, Word, PPT	Complete documents related to performing sensitivity analysis of reflective cracking model
BCOA_SJPCP Sensitivity Analysis	Excel, Python, Word	Complete documents related to performing sensitivity analysis of SJPCP/AC model
Climate Task Files TAC Meeting	Dgpx, hcd, Excel, Word, PPT PDF, PPT	Complete documents related to performing four-way comparisons for climate study along with latest hcd files from MERRA-2 Documents related to or presented during TAC meetings
Final Project Report	PPT	Complete summary and results of the project in single presentation

**THE INSTITUTE FOR TRANSPORTATION IS THE FOCAL POINT FOR TRANSPORTATION
AT IOWA STATE UNIVERSITY.**

InTrans centers and programs perform transportation research and provide technology transfer services for government agencies and private companies;

InTrans contributes to Iowa State University and the College of Engineering's educational programs for transportation students and provides K–12 outreach; and

InTrans conducts local, regional, and national transportation services and continuing education programs.



**IOWA STATE
UNIVERSITY**

Visit InTrans.iastate.edu for color pdfs of this and other research reports.